

# **Discovery and Optimization of 1,3,5-trisubstituted Pyrazolines as Potent and Highly Selective Allosteric Inhibitors of PKC $\zeta$**

Dissertation

zur Erlangung des Grades  
des Doktors der Naturwissenschaften  
der Naturwissenschaftlich-Technischen Fakultät III  
Chemie, Pharmazie, Bio- und Werkstoffwissenschaften  
der Universität des Saarlandes

von

Master-Pharmazeut  
Mohammad Abdel-Halim Abdel-Naby Abdel-Latif  
Saarbrücken  
2013

Tag des Kolloquiums : 13.08.2013

Dekan	Prof. Dr. Volkhard Helms
Berichterstatter:	Prof. Dr. Rolf W. Hartmann
	Prof. Dr. Ashraf H. Abadi
Vorsitzender:	Prof. Dr. Claus Jakob
Akad. Mitarbeiterin:	Dr. Sonja Keßler

Diese Arbeit entstand unter der Anleitung von Prof. Dr. R.W. Hartmann in der Fachrichtung 8.2 Pharmazeutische und Medizinische Chemie der Naturwissenschaftlich- Technischen Fakultät III der Universität des Saarlandes von Juni 2010 bis Juli 2013.

## Acknowledgment

All my gratitude is to **Allah** (Arabic name of God), to Whom goes all my thanks and appreciation, and to Whom I owe the courage and strength to complete this thesis.

I am indebted to Prof. Rolf W. Hartmann for giving me the honor to be a member of his great research group and accepting me as a PhD student in Saarland University under his kind supervision. Thanks for offering me such a wonderful atmosphere to learn and to work as well. Thanks for providing me with the lab space as well as all the required facilities and materials.

My endless appreciation goes to Prof. Ashraf H. Abadi, Professor of Pharmaceutical Chemistry and Dean, Faculty of Pharmacy and Biotechnology, The German University in Cairo, for partly suggesting the point of the research and for his continuous support along my Master and PhD work. Thanks for the constructive supervision, enthusiasm, inspiration and for being always available as well as giving me a lot from his precious time to solve all the problems. Thanks for the continuous efforts finding a source for financial support. Thanks for recommending to work in Professor Hartmann's group and to be a PhD student in Saarland. I will be always grateful for his support in all levels.

Deep thanks are due to Dr. Matthias Engel, Saarland University, for suggesting the kinase biological target and guiding the modifications in chemistry and biology throughout the whole project until the current results were reached. Thanks for the great help in the writing of the scientific papers. I am really grateful for his great efforts in teaching me the concept and the biological assays and for always being there with help, guidance and endless support scientifically and personally. Thanks to his working group members namely Wolfgang Fröhner, Christian Schmitt, Nadja Weber and Tamara Paul for their great help and kind assistance.

I would like to thank Prof. Frank M. Boeckler, University of Tuebingen, and Prof. Gary A. Piazza, Mitchell Cancer Institute, USA, for their help in the Mdm2 binding assay and the cell growth inhibition assays.

I would like to thank Dr. Joseph Zapp for the NMR measurements, Dr. Stefan Boettcher for running the mass spectrometry, Martina Schwarz, Katrin Schmitt and Lothar Jager for executive and technical assistance.

My special thanks to my dear colleague Mostafa Hamed for his help and for his nice companionship through the whole PhD work in Germany and Egypt. Thanks to Ahmed Saad for the great help and support.

I am greatly thankful to all my colleagues in the Pharmaceutical Chemistry Department, the German University in Cairo for the emotional support, comradely, and encouragement during the completion of this work specially, Dr. Rasha El-Nashar, Amal Yassin, Noura Riad, Mohamed Salah, Menna Hammam, Noha Osman, Heba Wagdy, Amal Ali, Dalia Sherif, Mohammad Weam and Nora Ayman.

I would like to thank my wife and my children whose dedication, understanding, love and persistent confidence in me has taken the load off my shoulder.

Lastly, and most importantly, I wish to thank my parents. They raised me, supported me, taught me, loved me and gave me a lot. To them I dedicate this thesis.

Mohammad Abdel-Halim Abdel-Naby Abel-latif

## Abbreviations

Å	angstrom
ADP	adenosine 5'-diphosphate
AHR	airway hyperreactivity
AKT	protein Kinase B
aPKC	atypical protein kinase C
Arg (R)	arginine
Asp (D)	aspartic acid
ATP	adenosine 5'-triphosphate
Bcl-X <sub>L</sub>	B-cell lymphoma-extralarge
BCR	B cell receptor
BCs	B cells
cAMP	cyclic AMP (adenosine 3',5'-cyclic monophosphate)
CBP	CREB binding protein
CC	column chromatography
cGMP	cyclic GMP (guanosine 3',5'-cyclic monophosphate)
ConA	concanavalin A
COPD	chronic obstructive pulmonary disease
cPKC	conventional or classical protein kinase C
DAG	diacylglycerol
DDQ	2,3-dichloro-5,6-dicyano-1,4-benzoquinone
DMEM	Dulbecco's modified Eagle's medium
DMF	dimethylformamide
DMSO	dimethyl sulphoxide
DNA	deoxyribonucleic acid
DTT	dithiothreitol
EGF	epidermal growth factor
ERK	extracellular signal-regulated kinases
ESI	electrospray ionization
FA	fluorescence anisotropy
FBS	fetal bovine serum
FCS	fetal calf serum
FP	fluorescent peptide
GLP	G9A-like protein
Glu (E)	glutamic acid
Gly (G)	glycine
GSK3	glycogen synthase kinase-3
GST	glutathione-S-transferase
HBA	hydrogen bond acceptor
HBD	hydrogen bond donor
Hdm2	human double minute 2
HEK293	human embryonic kidney-293
His (H)	histidine
HM	hydrophobic motif
Hz	hertz
IC <sub>50</sub>	half maximal inhibitory concentration

---

IFN- $\gamma$	interferon- $\gamma$
IGF	insulin-like growth factor
I $\kappa$ B	inhibitor of nuclear factor- $\kappa$ B
IKK	inhibitor of nuclear factor- $\kappa$ B kinase
IL-1	interleukin-1
IL-10	interleukin-10
IL-13	interleukin-13
IL-1b	interleukin-1b
IL-4	interleukin-4
IL-5	interleukin-5
IL-6	interleukin-6
iNOS	inducible nitric oxide synthase
Jak1	Janus kinase-1
$K_m$	Michaelis constant
KO	knock out
Leu (L)	leucine
LPS	lipopolysaccharide
Lys (K)	lysine
MAPK	mitogen-activated protein kinase
Mdm2	murine double minute 2
MEK	mitogen-activated protein kinase kinase
MEKK	mitogen-activated protein kinase kinase kinase
MEP	molecular electrostatic potentials
MHz	megahertz
MSK1	mitogen and stress-activated protein kinase
mTORC2	mammalian target of rapamycin complex 2
MTT	3-(4,5-dimethylthiazol-2-yl)-2,5-diphenyltetrazolium bromide
ND	not determined
NF- $\kappa$ B	nuclear factor- $\kappa$ B
NKT cells	natural killer T cells
nM	nanomolar
NMR	nuclear magnetic resonance
NO	nitric oxide
nPKC	novel protein kinase C
OVA	ovalbumin
p62	sequestosome-1
Par-4	prostate androgen responsive-4
Par-6	partitioning-defective protein-6
PB1	Phox/Bem 1
PDB	protein data bank
PDK1	phosphoinositide-dependent kinase-1
PH domain	Pleckstrin homology domain
Phe (F)	phenylalanine
PI3K	phosphoinositide 3-kinase
PIF pocket	docking site for PIFtide and other hydrophobic motif sequences (PIFtide: Peptide encompassing the hydrophobic motif sequence of PRK2)
PKA	protein kinase A
PKC	protein kinase C

---

PKG	protein kinase G
PPI	pseudosubstrate inhibitor
ppm	parts per million
PRK2	PKC-related protein kinase 2
PS	pseudosubstrate
RSK	ribosomal s6 kinase
SAR	structure activity relationship
SCCHN	squamous cell carcinomas of the head and neck
Ser (S)	serine
SETD6	SET domain-containing protein 6
SGK	serum-and glucocorticoid-induced protein kinase
STAT6	signal transducer and activator of transcription
TCR	T-cell receptor
Th1	T helper 1
Th2	T helper 2
Thr (T)	Threonine
TNF $\alpha$	tumor necrosis factor- $\alpha$
Tris	Tris (hydroxymethyl)aminomethane
Trp (W)	tryptophan
Tyr (Y)	tyrosine
Val (V)	valine
WT	wild type
Xaa	any amino acid
$\mu$ M	micromolar

## Abstract

The atypical PKC $\zeta$  is a promising therapeutic target in inflammatory diseases and B cell lymphoma. Therefore, there is an increasing need to develop selective inhibitors for this enzyme without affecting the closely related PKC family members. Allosteric inhibitors were found to be an effective tool in achieving this aim. Optimization yielded the 1,3,5-trisubstituted pyrazoline scaffold which proved to be rich in modifiable sites, all acting as hot spots for improving binding affinity. The phenolic group at the 5-phenyl was essential for activity. The presence of a lipophilic substituent at the 1-phenyl was important for high potency. The 3-position was tolerant for diverse types of substituents, acting as a means to optimize polarity and physicochemical characteristics. A methyl group at the 4-position of the pyrazoline increased the potency, and was reported to enhance pyrazoline's chemical stability. The optimized compounds showed two orders of magnitude improvement in the cell free assay potency and more than 10 times increase in cellular potency in U937 cells. The compounds showed high selectivity for PKC $\zeta$  vs. the closely related PKC $\iota$  and other PKCs, and were most likely targeting the PIF-pocket. Since the pyrazoline scaffold showed shape complementarity also to the p53-Mdm2 interaction site, the ability to compete this other protein-protein interaction was tested. However, the compounds which showed potent growth inhibition in cells failed to show activity in the binding assay.

## Zusammenfassung

Die atypische PKC $\zeta$  ist ein vielversprechendes Target bei Entzündungserkrankungen und B-Zell-Lymphomen. Daher besteht ein Bedarf, selektive Inhibitoren dieses Enzyms zu entwickeln, welche eng verwandte PKC-Isoformen nicht hemmen. Allosterische Hemmstoffe stellten gute Ansatzpunkte zum Erreichen dieses Zieles dar. Eine Optimierung führte zu 1,3,5-trisubstituierten Pyrazolinen, die an vielen Positionen vorteilhaft modifiziert werden konnten, was jeweils in einer effektiven Erhöhung der Bindungsaffinität resultierte. Der Phenolrest in der 5-Position war dabei essentiell für die biologische Aktivität. Ebenso war die Anwesenheit eines lipophilen Substituenten am 1-Phenylrest wichtig für eine hohe Potenz. An der 3-Position wurden verschiedene Arten von Substituenten toleriert, so dass hier die Polarität der Verbindungen und weitere physikochemische Eigenschaften optimiert werden konnten. Eine Methylgruppe an der 4-Position des Pyrazolins erhöhte die Wirkstärke zusätzlich und wurde zugleich als stabilisierend auf die chemische Stabilität beschrieben. Die optimierten Hemmstoffe zeigten eine um zwei Größenordnungen höhere Potenz im zellfreien Assay und eine 10-fach bessere Wirksamkeit im U937-Zellassay als die Ausgangsverbindungen. Die Verbindungen besaßen eine hohe Selektivität für PKC $\zeta$  gegenüber der stark homologen PKC $\iota$  und weiteren PKC-Isoenzymen, und griffen wahrscheinlich an der PIF-Tasche an. Da das Pyrazolingerüst auch eine Formkomplementarität zur p53-Mdm2-Interaktionsstelle aufwies, wurde die Fähigkeit, diese andere Protein-Protein-Interaktion zu kompetitieren, getestet. Für diejenigen Verbindungen, die eine potente Hemmung des Zellwachstums zeigten, konnte jedoch keine Aktivität im Bindungsassay nachgewiesen werden.

# Table of Content

<b>1</b>	<b>General Introduction .....</b>	<b>1</b>
1.1	Kinases and Protein Phosphorylation .....	1
1.1.1	<i>Regulation of Enzyme Activity by Phosphorylation.....</i>	<i>1</i>
1.1.2	<i>Protein kinase structure.....</i>	<i>2</i>
1.1.3	<i>AGC Kinases.....</i>	<i>2</i>
1.1.3.1	PKCs .....	3
1.1.3.1.1	Classification of PKCs .....	3
1.1.3.1.2	Regulation of PKCs.....	5
1.1.3.1.2.1	Activation/regulation of aPKCs: .....	5
1.2	Physiological Importance of PKC $\zeta$ .....	7
1.2.1	<i>Relevance of PKC<math>\zeta</math> in Immunology and Inflammation.....</i>	<i>7</i>
1.2.1.1	PKC $\zeta$ and NF- $\kappa$ B Signaling.....	7
1.2.1.2	Role of PKC $\zeta$ in Secondary Lymphoid Organ Maturation and B Cell Differentiation, Activation and Survival.....	9
1.2.1.3	PKC $\zeta$ and T helper cells differentiation.....	10
1.2.1.4	PKC $\zeta$ in Asthma.....	10
1.2.1.5	PKC $\zeta$ and Liver Inflammation.....	12
1.2.2	<i>PKC<math>\zeta</math> in Cancer .....</i>	<i>13</i>
1.3	Protein Kinases as Drug Targets.....	15
1.3.1	<i>Classification of Kinase Inhibitors .....</i>	<i>15</i>
1.3.1.1	Advantages of Allosteric Inhibitors .....	16
1.3.2	<i>PIF Pocket as an Allosteric Site to Modulate AGC Kinases Activity.....</i>	<i>16</i>
1.3.2.1	Discovery and Physiological Function .....	16
1.3.2.2	Molecular Interactions of the Natural HM Peptide Ligands.....	18
1.3.2.3	Allosteric Mechanism by the PIF Pocket.....	19
1.3.2.3.1	Role of the $\alpha$ C-helix in Allosteric Control through the PIF Pocket.....	19

---

1.3.2.4	Targeting the PIF Pocket with Small Molecule Ligands to Inhibit the Activity of AGC Kinases .....	21
1.3.2.4.1	Discovery of First Allosteric PKC $\zeta$ Inhibitors .....	22
1.3.2.4.2	Other Reported Inhibitors for PKC $\zeta$ .....	24
1.4	Exploration of the Pyrazoline Scaffold in Other Protein-Protein Interaction Targets as Exemplified by the p53-Mdm2 Interaction.....	26
1.4.1	<i>The Tumor Suppressor p53</i> .....	26
1.4.2	<i>p53-Mdm2 Interactions</i> .....	26
1.4.3	<i>Some Small Molecule Non-peptide Inhibitors of p53-Mdm2 Interaction</i> .....	27
<b>2</b>	<b>Scientific goal</b> .....	<b>30</b>
<b>3</b>	<b>Results</b> .....	<b>32</b>
3.1	Discovery and Optimization of 1,3,5-trisubstituted Pyrazolines as Potent and Highly Selective Allosteric Inhibitors of PKC $\zeta$ .....	32
3.2	Trisubstituted and Tetrasubstituted Pyrazolines as a Novel Class of Cell-growth Inhibitors in Tumor Cells with Wild Type p53 .....	104
<b>4</b>	<b>Discussion, Conclusion and Outlook</b> .....	<b>132</b>
<b>5</b>	<b>References</b> .....	<b>137</b>

# 1 General Introduction

## 1.1 Kinases and Protein Phosphorylation

Protein phosphorylation is a post-translational modification that regulates most cellular activities. It is a specific enzymatic reaction in which one protein serves as a substrate for protein kinases, namely phosphotransferases, that catalyze the transfer of the  $\gamma$ -phosphate of ATP to an acceptor amino acid in the protein substrate.<sup>1,2</sup>

In eukaryotes, proteins are either phosphorylated on serine/threonine residues or on tyrosine residues. Thus, protein kinases can be considered broadly to be Ser/Thr kinases or Tyr kinases, or in some instances, dual-specificity kinases when they phosphorylate Ser/Thr as well as tyrosine residues.<sup>1</sup> For regulation of enzyme activity, the phosphorylation of serine and threonine residues is the most important. Analysis of the human genome showed that there are 518 protein kinases (1.7% of the proteins encoded).

### 1.1.1 Regulation of Enzyme Activity by Phosphorylation

Phosphorylation of enzymes and proteins by specific protein kinases is the most wide spread mechanism for the regulation of enzyme activity; it represents a flexible and reversible means of regulation and plays a critical role in signal transduction where the added phosphate group can be removed by one of the phosphatases, allowing different specificities to be used in the forward and reverse reactions. The biological processes may be switched on or off to meet different demands.<sup>2</sup>

The added phosphate group can form an extensive network of hydrogen bonds which can link different parts of a poly peptide chain, in addition to its ability to make electrostatic interactions especially with arginine residues hence attracting a cluster of positively charged amino acid side chains. Both types of interactions are important for control of protein function on phosphorylation through induction of large to small scale allosteric conformational changes. Sometimes the introduced phosphate affects the enzyme activity solely by its electrostatic effect without apparent change in enzyme conformation, where an attached phosphate group can form part of a structure that is directly recognized by binding sites of other proteins.<sup>1,2</sup>

Phosphorylation results in a number of diverse responses in different proteins, for example, it may result in the activation or inhibition of enzyme activity or, as mentioned above, it can create a protein recognition site for another protein. Each of these events allows a phosphorylated protein to signal downstream proteins initiating a cascade of reactions.<sup>3</sup>

### 1.1.2 Protein kinase structure

Protein kinases share a common catalytic domain with highly conserved architecture but they have a variety of different regulatory mechanisms. The kinase may be present as a single domain or it may be covalently linked to other regulatory domains. The fold of the catalytic kinase domain, comprising about 300 amino acid residues, consists of a smaller N-terminal lobe of about 80 residues (the small lobe) with the conserved regulatory helix  $\alpha C$  and about 200 residues C-terminal large lobe. The two lobes are linked by a hinge region. The protein substrate binding site faces the ATP-binding site between the small and the large lobes. The ATP-binding site is a conserved site in all protein kinases.<sup>4,5</sup>

The active site contains a number of highly conserved motifs that are essential for catalytic activity. Key catalytic motifs include the ATP/Mg<sup>2+</sup> binding motifs and the activation loop. A large number of kinases are activated by phosphorylation of the activation loop, which is typically disordered in its inactive state but assumes a stable structure in its phosphorylated active state.

In most of the AGC kinases, the C-terminal folds back onto the catalytic domain and ends in the hydrophobic motif (HM), where it binds a particular hydrophobic pocket in the small lobe termed the "PIF pocket" which will be discussed later in more details.<sup>6</sup> Figure 1 shows a cartoon representation for PKA highlighting most of the described elements.

### 1.1.3 AGC Kinases

The AGC kinase family is a subgroup of Ser/Thr protein kinases including cAMP-dependent protein kinase (PKA), cGMP-dependent protein kinase (PKG) and protein kinase C (PKC)(reviewed in <sup>6</sup>). It includes 60 of the 518 human protein kinases, of which 42 possess functional domains, other than the kinase core, which are involved in regulating kinase activity and localization.

Activation of many AGC kinases involves phosphorylation of two highly conserved regulatory motifs namely the activation loop, which is located in the catalytic domain (in the C-lobe), and the hydrophobic motif (HM) found in a non-catalytic region following the kinase domain. Additionally, several AGC kinases need another important phosphorylation of a further site that promotes their integrity, which is termed the "turn motif".

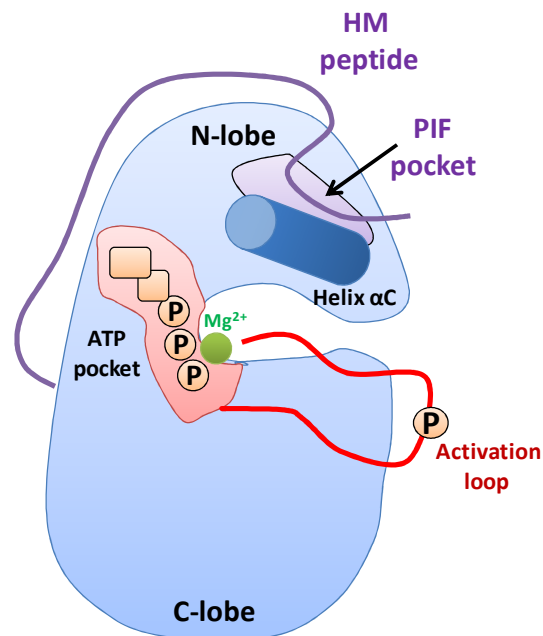


Figure 1: Cartoon representation of protein kinase A (PKA). Some of the critical components of the kinase active site: the activation loop, helix  $\alpha C$ , ATP, magnesium ion. The C-terminal HM peptide and PIF pocket are also shown. (Adapted from <sup>7</sup>).

### 1.1.3.1 PKCs

The protein kinase C (PKC) family (reviewed in <sup>8</sup>) represents around 2% of the human kinome. There are 10 mammalian PKCs sharing a highly conserved catalytic domain, carrying motifs required for ATP/substrate binding and catalysis, in addition to a more divergent regulatory domain at the N-terminus. Both the catalytic and regulatory domains are linked through more variable hinge regions.

PKCs regulatory domains contain an auto-inhibitory isoform-specific sequence called pseudosubstrate domain which contains an alanine instead of the serine/threonine phosphoacceptor site, but otherwise resembles a PKC substrate. The regulatory domain usually contains C1 and C2 domains, which are structural domains that influence the sensitivity of each PKC to different stimuli as well as their function and mechanism of regulation.

#### 1.1.3.1.1 Classification of PKCs

Based on the structural differences found in their regulatory domains, PKCs can be classified into three distinct subgroups (shown in Figure 2-A): the conventional or classical PKCs (cPKCs), the novel PKCs (nPKCs) and the atypical PKCs (aPKCs).

## Introduction

- 1) The cPKCs comprise PKC $\alpha$ , PKC $\beta$ I, PKC $\beta$ II and PKC $\gamma$ . They have a conserved C1 domain that contains a double zinc finger and a pocket that binds diacylglycerol (DAG) and phospholipids. They also contain a C2 domain which has a binding site for calcium, rendering this subfamily sensitive to calcium.
- 2) The nPKCs comprise PKC $\delta$ , PKC $\epsilon$ , PKC $\eta$ , and PKC $\theta$ . Similar to the cPKCs, the novel PKCs are activated by DAG and phospholipids, but they are calcium independent as their C2 domain lacks the critical calcium-coordinating acidic residues.

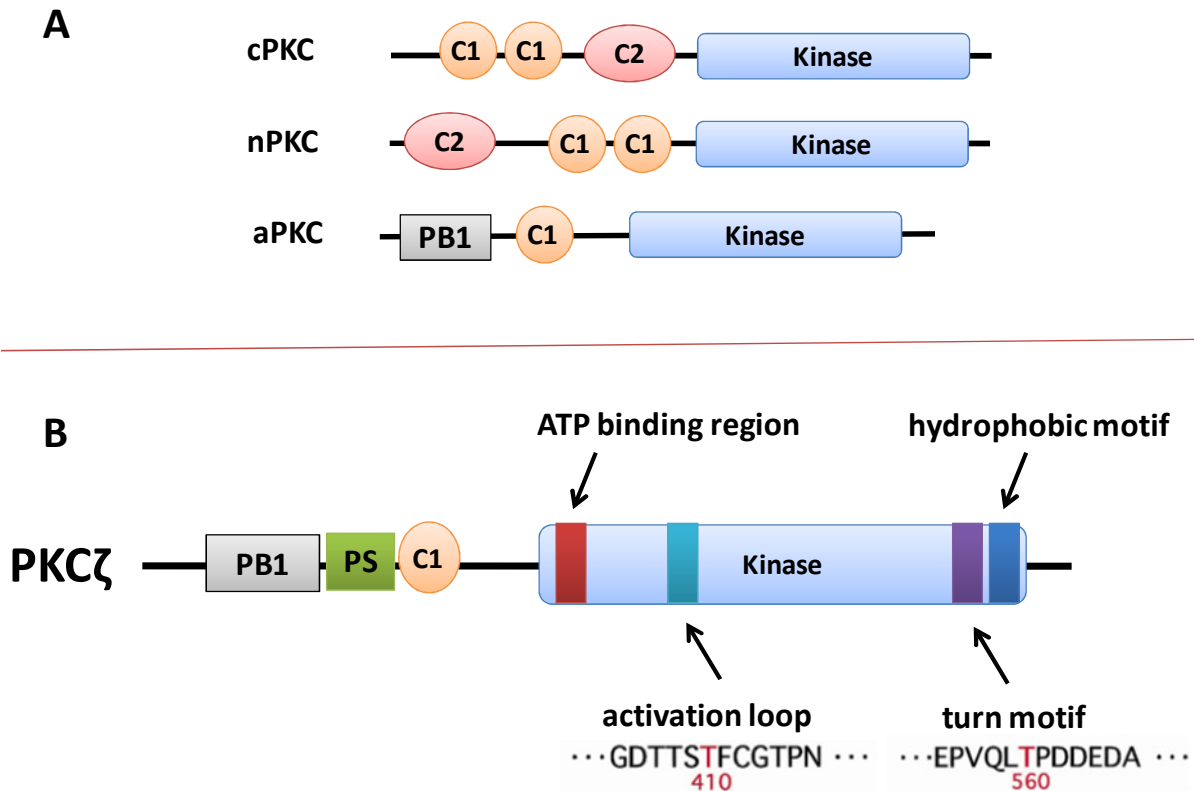


Figure 2: (A) Structure of the PKC family. Schematic representation of the different PKC subfamilies and their domain structural organization. The PKC family is divided into three structurally and functionally distinct subgroups according to their regulatory domains: the classical isoforms (cPKC), novel isoforms (nPKC) and atypical isoforms (aPKC). Conserved region 1 (C1) confers binding to diacylglycerol and phospholipids, and C2 senses calcium. PB1 (Phox / Bem domain 1) is specific for aPKC and acts as a dimerization domain (adapted from<sup>9</sup>). (B) Detailed schematic representation of domain structure of the aPKC $\zeta$ . PKC $\zeta$  consists of a PB1 domain in the N-terminus, a pseudosubstrate (PS), a C1 domain, and a Ser/Thr kinase domain in the C terminus. The kinase domain includes an ATP-binding region, an activation loop, a turn motif, and a hydrophobic motif. Thr410 in the activation loop is phosphorylated by PDK1. Thr560 in the turn motif is the phosphorylation site. (Adapted from<sup>10</sup>).

- 3) The aPKCs include PKC $\zeta$  and PKC $\iota$  (also known as PKC $\lambda$  in mice). They are insensitive to calcium due to the lack of a C2 domain and insensitive to DAG as they have an

## Introduction

---

atypical C1 domain with only a single zinc-finger structure. At the N-terminus, they have a distinct structural domain called Phox/Bem 1 (PB1) that is unique for this PKC subfamily; it is a protein-protein interaction domain that mediates interactions with other PB1-containing scaffolding proteins thus links them as a network. Figure 2-B shows a schematic representation of the domain structure of PKC $\zeta$ .

### 1.1.3.1.2 Regulation of PKCs

During the inactive state, PKC is auto-inhibited by its pseudosubstrate, which blocks the substrate-binding pocket located in the kinase domain.<sup>11</sup> As mentioned before with many AGC kinases, to attain an active state, phosphorylation of the kinase domain has to take place on three (cPKCs and nPKCs) or two (aPKCs) Ser or Thr sites to stabilize the active kinase conformation. While cPKCs and nPKCs are phosphorylated on their turn motif, hydrophobic motif peptide and activation loop, aPKCs do not require HM phosphorylation as will be explained later. Two upstream kinases seem to be required for this process. The first one is phosphoinositide-dependent kinase-1 (PDK1) to phosphorylate the activation loop in the kinase domain,<sup>12</sup> where this phosphorylation requires docking of the phosphorylated HM peptide from the substrate kinase to the PIF pocket of PDK1.<sup>13</sup> The other kinase is the mammalian target of rapamycin 2 complex (mTORC2), which controls phosphorylation of the turn motif and hydrophobic sites in the C-terminal tails of these kinases.

In the case of aPKCs, there is an acidic phosphomimetic Asp or Glu which is present in the HM peptide instead of a phosphorylatable Ser or Thr. This acidic residue can replace the phosphate (of HM-phosphate) in its interaction with the PIF pocket of PDK1, escaping the requirement for the hydrophobic site phosphorylation.<sup>13, 14</sup> After the PKC gets the required two/three required phosphorylations, the kinase becomes only active after lipid second messenger or allosteric stimulation to release the pseudosubstrate peptide from the active site and reach the fully active state.<sup>6</sup>

As this thesis is concerned with the aPKC $\zeta$ , its activation and regulation will be discussed in more details as follows.

#### 1.1.3.1.2.1 Activation/regulation of aPKCs:

- 1) Activation by lipids: where, unlike the cPKCs and nPKCs, aPKCs cannot be activated by DAG or Ca<sup>2+</sup>, rather they have been suggested to respond to other lipids such as phosphatidylinositols, phosphatidic acid, arachidonic acid, and ceramide (reviewed in <sup>15</sup> and <sup>9</sup>). However, it is unclear whether some of these effects are physiologically relevant.
- 2) Regulation through interaction with specific binding partners: an important mechanism to modulate activation and give spatial and temporal specificity:

## **Introduction**

---

- Par-4, which is found to bind the zinc-finger at the C1 domain of the aPKCs, inhibiting their enzymatic activity.<sup>16</sup> Par-4 is considered a specific inhibitor of aPKCs.
- Adapters, which bind the PB1 domain affecting localization but not the enzymatic activity of the aPKCs: PB1 is a modular scaffold domain, which can be involved in polar heterodimeric interactions.<sup>17</sup> In addition to the aPKCs, PB1 domains exist in adapter/scaffold proteins (such as p62 and Par-6), and also in other kinases of the mitogen-activated protein kinase (MAPK) family, including MEK5 $\alpha$  and MEKK3. p62 and Par-6 are selective adapters for the aPKCs.<sup>18, 19</sup> Par-6 has been shown to be crucial to the control of cell polarity and, through its PB1 domain, to allocate the aPKCs specifically in polarity-related functions. On the other hand, the p62/aPKC signaling platform plays a critical role in NF- $\kappa$ B activation.<sup>20</sup> It is not a substrate and does not seem to significantly affect the intrinsic kinase activity of the aPKCs.<sup>19</sup>

Thus, the formation of aPKC complexes with different adapters, scaffold proteins, and regulators such as Par-6, p62, and Par-4 serves to confer specificity and plasticity to the actions of these kinases and to establish a signaling network. However, the factors that determine which complex is formed at a given time remain to be identified.<sup>9</sup>

# 1.2 Physiological Importance of PKC $\zeta$

## 1.2.1 Relevance of PKC $\zeta$ in Immunology and Inflammation

### 1.2.1.1 PKC $\zeta$ and NF- $\kappa$ B Signaling

The transcription factor NF- $\kappa$ B is critical in a number of cell functions including growth, survival and key inflammatory and immune responses. Uncontrolled activation of NF- $\kappa$ B can induce cancer development, autoimmune, and chronic inflammatory diseases as a result of exacerbated lymphocyte function.<sup>21</sup>

The most classical form of NF- $\kappa$ B is a heterodimer of p50 and p65 (RelA), which is sequestered in the cytosol by the inhibitory protein I $\kappa$ B $\alpha$  preventing its nuclear translocation. Upon cell activation by tumor necrosis factor- $\alpha$  (TNF $\alpha$ ) or interleukin-1 (IL-1), I $\kappa$ B $\alpha$  is phosphorylated, which triggers its ubiquitination and subsequent degradation through the proteasome. This serves to release NF- $\kappa$ B, which translocates to the nucleus, where, in collaboration with coactivator proteins, it stimulates the transcription of its target genes. The kinase responsible for the signal-induced phosphorylation of I $\kappa$ B is a heterodimer of three subunits: two catalytic subunits (IKK $\alpha$  and IKK $\beta$ ) and a regulatory subunit termed IKK $\gamma$ . The IKK complex can be activated by direct phosphorylation of the  $\beta$  subunit by a putative IKK kinase, as shown Figure 3 (reviewed in <sup>22</sup>).

PKC $\zeta$  was shown to play a significant role in NF- $\kappa$ B activation at two different levels, IKK activation and NF- $\kappa$ B transcriptional activity:

1. PKC $\zeta$  has IKK kinase function. In the lung where PKC $\zeta$  is abundantly expressed, it is required for IKK activation in response to TNF $\alpha$ , IL-1b, or lipopolysaccharide (LPS), as shown in Figure 3.<sup>23</sup>
2. Phosphorylation of Ser311 in the RelA subunit is a fine control of NF- $\kappa$ B transcriptional activity. As mentioned earlier, NF- $\kappa$ B is initially controlled by an all-or-nothing nuclear translocation pathway. Fine tuning is required as NF- $\kappa$ B regulates the expression of a large number of genes, thus mechanisms need to be in place to fine-tune the process. PKC $\zeta$  represents one of the most important fine controls, where PKC $\zeta$ -mediated phosphorylation of RelA regulates transcription.<sup>24</sup> PKC $\zeta$  is found to phosphorylate Ser311 on the RelA subunit of NF- $\kappa$ B, which has been shown to be required for full NF- $\kappa$ B transcriptional activity *in vivo* and in cell culture experiments.<sup>23</sup> Under basal conditions, RelA is methylated at Lys310 by the methyl transferase SETD6, promoting recruitment of GLP protein which, along with its partner G9a, promotes methylation of histones leading to

## Introduction

closed chromatin and inhibited transcription of  $\kappa$ B-dependent genes. After activation of cells by TNF, PKC $\zeta$  phosphorylates Ser311, leading to release of GLP, demethylation of Lys310 and recruitment of the transcriptional coactivator CBP to the phosphorylated RelA, which promotes acetylation of Lys310 and of histones, which, together with their diminished methylation, resulting in enhanced transcription.<sup>9, 25</sup> This way, both acetylation and methylation have been shown to have a functional interplay with phosphorylation to fine-tune NF- $\kappa$ B transcriptional activation. The role of PKC $\zeta$  in NF- $\kappa$ B dependent genes transcription is summarized in Figure 4.

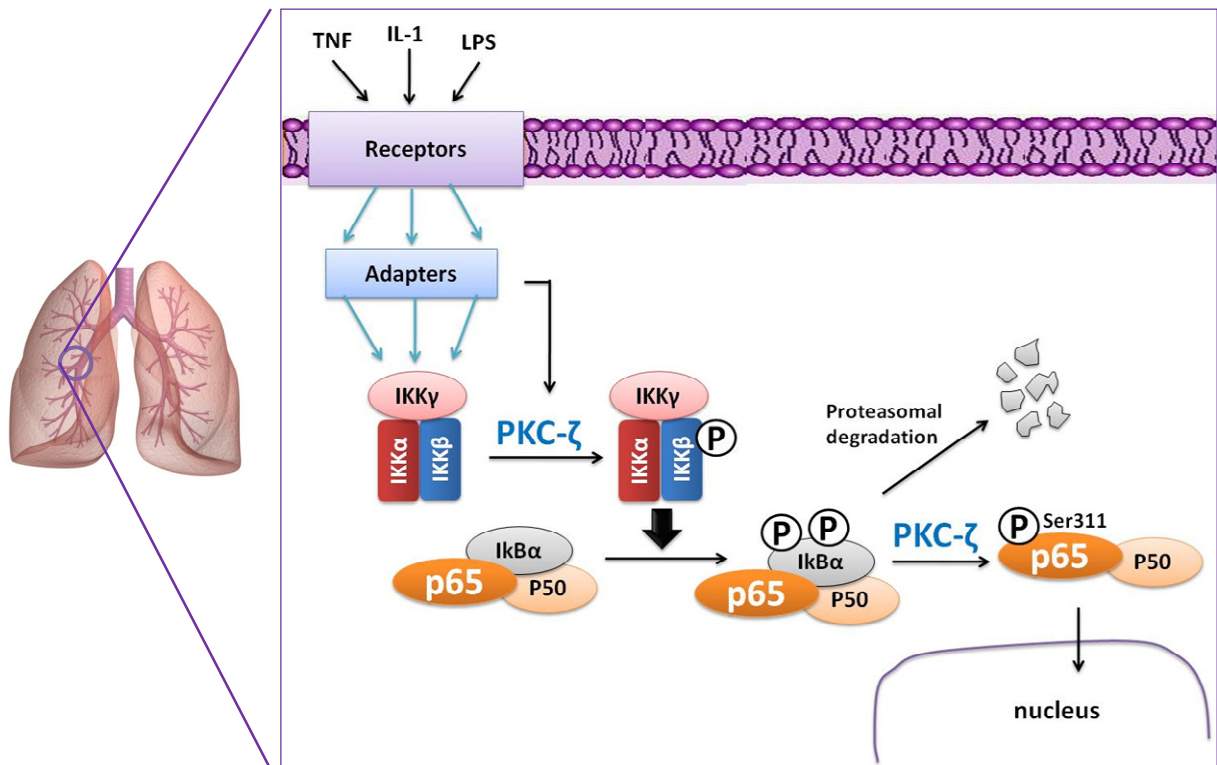


Figure 3: NF- $\kappa$ B activation and possible roles for PKC $\zeta$ . The binding of different ligands to their respective receptors in the plasma membrane triggers the recruitment of specific adapters for each receptor which orchestrate the formation of a signalosome complex that is constituted of two catalytic (IKK $\alpha$  and IKK $\beta$ ) and one regulatory subunit (IKK $\gamma$ ). In the lungs, PKC $\zeta$  act as an IKK kinase leading to activation of the complex. This complex in turn phosphorylates I $\kappa$ B, that is subsequently ubiquitinated and degraded through the proteasome system, releasing NF- $\kappa$ B (the most classical components of which are p65-p50 heterodimers) to translocate to the nucleus and interact with elements in the promoter of inflammatory and survival genes harboring  $\kappa$ B-elements in their promoters. The second role for PKC $\zeta$  in Ser311 phosphorylation will be discussed in the next figure with more details. (Adapted from<sup>9</sup>).

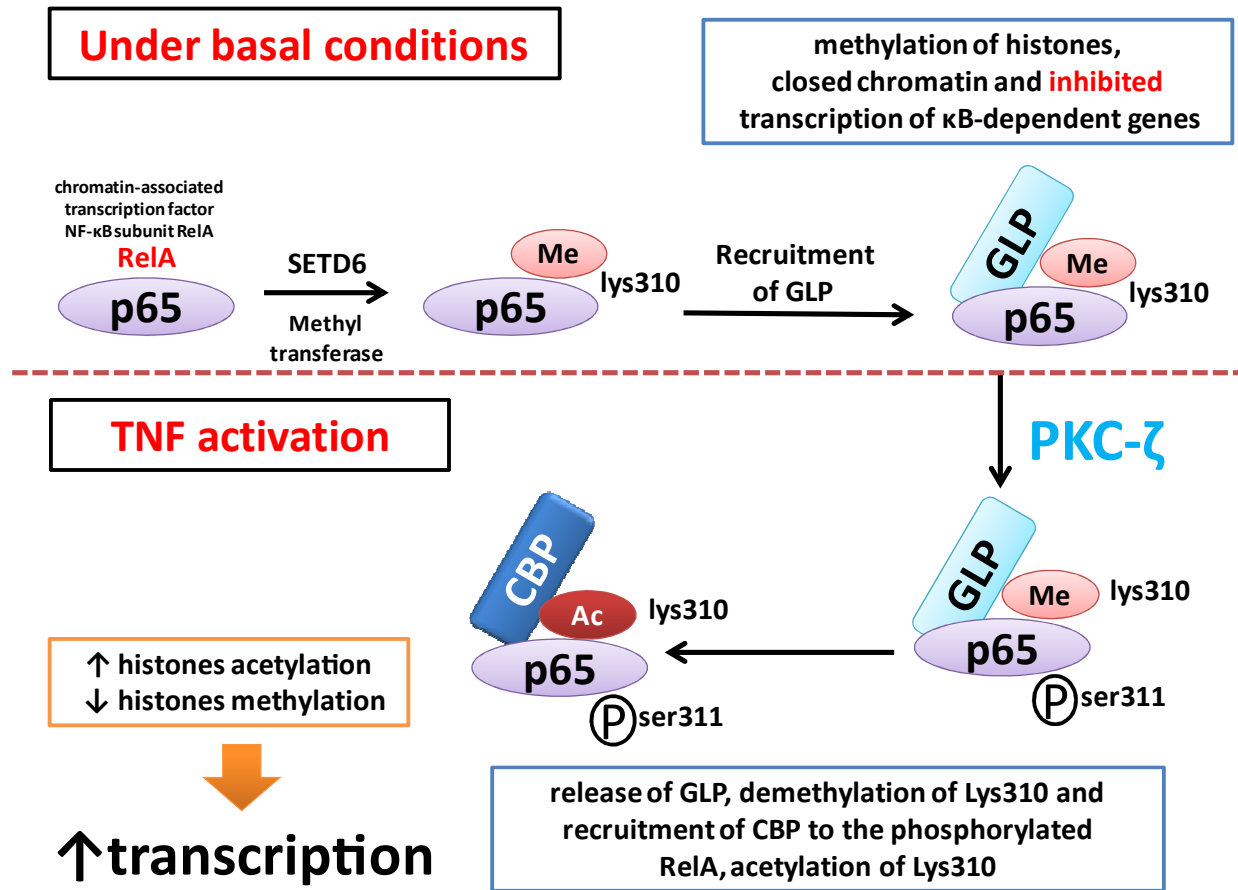


Figure 4: PKC $\zeta$ -mediated phosphorylation of RelA and its regulation of NF- $\kappa$ B transcriptional activity. (Adapted from <sup>24</sup>).

### 1.2.1.2 Role of PKC $\zeta$ in Secondary Lymphoid Organ Maturation and B Cell Differentiation, Activation and Survival

In PKC $\zeta$  deficient mice, the formation and maturation of secondary lymphoid organs (Peyer's patches and spleen) is altered during the first weeks after birth. However, most of these defects are overcome in adult animals indicating that PKC $\zeta$  could have an important role in B cell maturation in young animals which can be compensated by other molecules in adult mice.<sup>23</sup>

PKC $\zeta$  is required for an optimal survival rate, cell cycle entry, and proliferation after B cell receptor (BCR) stimulation in adult animals.<sup>26</sup> It was found that PKC $\zeta$  mediates B cell proliferation and survival by activation of the extracellular signal-regulated kinase (ERK) pathway. Even more importantly, after B cell receptor stimulation, PKC $\zeta$  induces the transcription of I $\kappa$ B and other NF- $\kappa$ B-dependent genes, such as IL-6 or Bcl-X<sub>L</sub> which are

## Introduction

---

impotent for B cell survival. Although PKC $\zeta$  is an important mediator of the NF- $\kappa$ B pathway as previously discussed, the activation and nuclear translocation of this transcription factor is not inhibited in BCs in PKC $\zeta$ -deficient mice.<sup>26</sup> The role of PKC $\zeta$  in B cell development is summarized in Figure 5-A.

### 1.2.1.3 PKC $\zeta$ and T helper cells differentiation

PKC $\zeta$  is essential for the development and differentiation of naïve T cells into Th2 cells. PKC $\zeta$ -deficient CD4+ T cells which are differentiated *in vitro* under Th2 polarizing conditions secrete low levels of Th2-related cytokines IL-4, IL-5, IL-10 and IL-13, compared to the amount of cytokines released by CD4+ T cells from wild type mice.<sup>27</sup> In PKC $\zeta$ -deficient mouse, the T-dependent humoral immune responses are very faint; these mice are not able to mount a proper humoral response against T-dependent antigens. The nuclear translocation of RelA was impaired in PKC $\zeta$ -deficient cells.<sup>27</sup> However, the role of PKC $\zeta$  is not restricted to NF- $\kappa$ B activation during Th2 differentiation, but rather PKC $\zeta$  has a more fundamental role in this process by playing a pivotal function in IL-4 signaling, which, along with signals arising from the T-cell receptor (TCR), is essential for the activation of the Th2 differentiation program.<sup>27</sup> Stat6 phosphorylation in response to IL-4 stimulation was impaired even in mature undifferentiated PKC $\zeta$ -deficient T cells. It was found that PKC $\zeta$  directly interacts with and phosphorylates Jak1 in response to IL-4 stimulation, which is important for the activation of the Jak1/Stat6 pathway *in vitro* and *in vivo*.<sup>28</sup> The role of PKC $\zeta$  in Th2 cell differentiation is summarized in Figure 5-B.

On the other hand, Th1 differentiation from PKC $\zeta$ -deficient naïve CD4+ T cells appears not to be affected in this function, as the release of the typical Th1-associated cytokine IFN-gamma is not affected by the lack of PKC $\zeta$ .

### 1.2.1.4 PKC $\zeta$ in Asthma

Asthma is a disease of chronic airway inflammation in which Th2 cells play a critical role (reviewed in<sup>29</sup> and<sup>30</sup>). Thus, CD4+ T cells producing Th2 cytokines play a prominent role in the lungs of asthmatic subjects, particularly because IL-4 and IL-13 enhance immunoglobulin E (IgE) production, IL-4, IL-9 and IL-10 enhance mast cell growth, IL-5 enhances eosinophil accumulation, and IL-9 and IL-13 directly enhance mucus hypersecretion and airway hyperreactivity (AHR).<sup>29, 30</sup> PKC $\zeta$  can be considered as an important key player in asthma based on these previously mentioned findings:

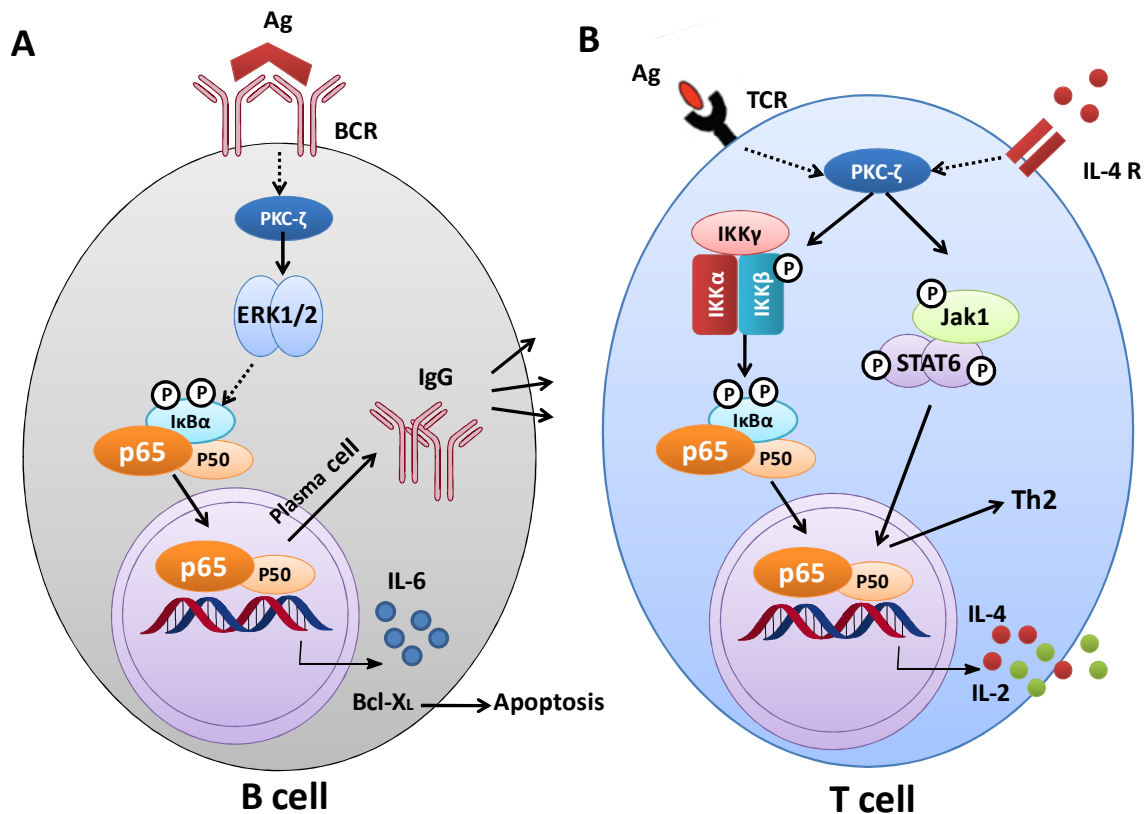


Figure 5: PKC $\zeta$  in signaling pathways leading to lymphocyte activation and/or differentiation. (A) Signaling through B cell antigen receptor (BCR) in B-lymphocytes. PKC $\zeta$  is required for the activation of ERK after antigen challenge and is necessary for I $\kappa$ B transcription. The transcription of NF- $\kappa$ B-dependent genes IL-6 and Bcl-X<sub>L</sub>, and the secretion of T-dependent immunoglobulins depend on PKC $\zeta$ -mediated signaling. (B) Signaling pathways in T lymphocytes. After antigen presentation, downstream signaling through T cell receptor (TCR) takes place. PKC $\zeta$  is important for IKK activation and NF- $\kappa$ B nuclear translocation. Signaling through IL-4 receptor (IL-4R) requires PKC $\zeta$  to fully activate Jak1/Stat6 pathway and therefore to promote Th2 differentiation. (Adapted from <sup>31</sup>).

- 1) In lung tissue, PKC $\zeta$  is abundantly expressed and was found to be required for both IKK and NF- $\kappa$ B phosphorylation in response to TNF $\alpha$ , IL-1b, or LPS.<sup>23</sup>
- 2) PKC $\zeta$  is a critical modulator of the Th2 response and acts as an important player in the Jak1/Stat6 signaling cascade involved in the activation through IL-4.

Accordingly, PKC $\zeta$  can be a potentially relevant target in treatment of asthma. In Th2 cells with PKC $\zeta$  deficiency, IL-4 is significantly reduced in addition to the synthesis of three other Th2 cytokines namely IL-5, IL-10, and IL-13.<sup>27</sup> Moreover, loss of PKC $\zeta$  inhibited allergic airway disease in ovalbumin (OVA) mouse model and reduced allergic response to the OVA challenge, where mucus production was not observed in lung sections. In addition, IL-4, IL-5, IL-13 and eotaxin supernatant levels, which were dramatically increased in OVA-challenged WT mice, were severely reduced in similarly treated PKC $\zeta$  deficient mice.<sup>27</sup>

## Introduction

---

In a previous study using a mouse model, blockade of PKC $\zeta$  signals by instillation of pseudosubstrate inhibitor (PPI) showed that PPI alleviates allergen-specific Th2 response and asthmatic manifestations. Inhibition of PKC $\zeta$  was shown to decrease IL-5 and IL-13 levels in bronchoalveolar lavage fluid to approximately 20% of the control levels and also caused a marked drop in the level of TNF- $\alpha$ . In addition, serum OVA-specific IgE level and *ex vivo* IL-4, IL-5 and IL-13 production by peribronchial lymph node cells were also considerably lower in PPI-treated mice.<sup>32</sup>

Morin et al. recently studied the role of PKC $\zeta$  in airway hyper responsiveness using an *in vitro* model of TNF $\alpha$ -treated human bronchi and an *in vivo* guinea pig model of chronic asthma. PKC $\zeta$ -specific inhibition produced a significant increase in isoproterenol sensitivity in TNF $\alpha$ -treated bronchi and OVA-sensitized guinea pig bronchi. An enhanced expression of PKC $\zeta$  was ascertained in the *in vivo* model of allergic asthma and was delineated in TNF $\alpha$ -treated bronchi when compared with an untreated control, where there was an observed increase in bronchi Ca<sup>2+</sup> sensitivity which was reversed upon treatment with the Myr-PKC $\zeta$ -peptide inhibitor.<sup>33</sup> PKC $\zeta$  is also found to be largely involved in eosinophil migration in asthma, although its specific intracellular targets remain undefined.<sup>34</sup> Additionally, some studies reported PKC $\zeta$  to mediate lung inflammation in response to cigarette smoking.<sup>35</sup> Altogether, these data can validate PKC $\zeta$  as therapeutic target in asthma and lung inflammation.

However, the validity of using PPI to study PKC $\zeta$  should be studied due to the possible reactivity with PKC $\iota$  or other PKCs which also have essential roles in Th2 function. Nevertheless, the PPI results are consistent with the findings from PKC $\zeta$ -knockout mice studies.

Furthermore, the evidence that PKC $\zeta$  is heavily expressed in lung extracts under resting conditions is consistent with this kinase's putative role in other pulmonary diseases, including chronic obstructive pulmonary disease (COPD) and lung cancer.<sup>36</sup>

### 1.2.1.5 PKC $\zeta$ and Liver Inflammation

T cell-mediated immune responses play important roles in the pathogenesis of a variety of human liver disorders including autoimmune liver disease, viral hepatitis, and alcoholic liver disease (<sup>37</sup> and references there in).

In T-cell-mediated hepatitis, T cells release IL-4 which targets NKT cells and hepatocytes leading to the production of IL-5 and eotaxin-1 respectively, both of which are important mediators in the control of eosinophil infiltration and liver injury in ConA-induced hepatitis, a well-established model to study T cell-mediated hepatitis (Figure 6).

Based on its previously mentioned role in IL-4 signaling, PKC $\zeta$  is also important player in T-cell-induced hepatitis, therefore in PKC $\zeta$ -KO mice with ConA-induced hepatitis, synthesis

## Introduction

of IL-5 and eotaxin-1 was reduced with a consequent reduction in liver injury.<sup>28</sup> Moreover, the loss of Par-4 (a -ve regulator for PKC $\zeta$ ) in Par-4-KO mice injected with ConA exacerbates the appearance of liver necrosis.<sup>28</sup>

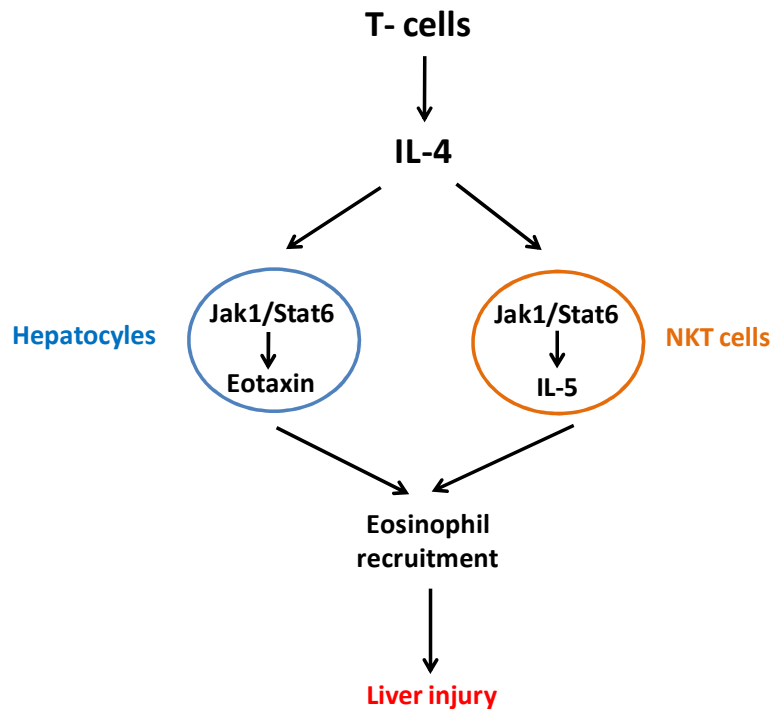


Figure 6: Mechanism of liver injury activated by IL-4. IL-4 activates Jak1/Stat6 in hepatocytes to produce eotaxin, and triggers IL-5 production by natural killer T cells (NKT). Both mediators promote liver eosinophil recruitment and damage. (Copied from <sup>36</sup>).

### 1.2.2 PKC $\zeta$ in Cancer

PKC $\zeta$  was reported to mediate several key steps in tumor progression including cell proliferation, survival, cell migration and angiogenesis. In cancer-specific cell models, PKC $\zeta$  is required for EGF (epidermal growth factor)-induced migration of human breast and lung cancer cells.<sup>38,39</sup> PKC $\zeta$  is involved in the control of glioblastoma cell migration and invasion by regulating the cytoskeleton rearrangement, cell adhesion and matrix metalloproteinase-9 expression.<sup>40</sup>

PKC $\zeta$  was shown to be highly expressed in head and neck tumors. Inhibition of PKC $\zeta$  was shown to reduce proliferation and viability of squamous cell carcinomas of the head and neck (SCCHN) as it reduced EGFR-mediated MAPK signaling and DNA synthesis. In addition, PKC $\zeta$  inhibition was found to potentiate the action of other growth inhibitors in SCCHN.<sup>41</sup> PKC $\zeta$  may also have an important role in angiogenesis in renal cell carcinoma.<sup>42</sup> A recent report

## **Introduction**

---

suggested a role for the nuclear PKC $\zeta$  fraction in sustaining intracellular tumor pathways that allow cancer cells to become drug-resistant, which suggests that selective inhibition of nuclear PKC $\zeta$  can restore the effectiveness of chemotherapeutic agents in chemo-resistant cancer cells.<sup>43</sup>

Inhibition of PKC $\zeta$  activity in U937 human leukemic cells *in vitro* and *in vivo* (in *nude* mice) was found to sensitize tumor cells to chemotherapeutic drug-induced cytotoxic activity.<sup>44</sup> Moreover, PKC $\zeta$  was found to be highly expressed in follicular B cell lymphoma and other lymphoma cells compared to normal B cells. It was reported to be a target for the anticancer antibody rituximab in follicular B cell lymphoma.<sup>45</sup> In addition, PKC $\zeta$  may be a possible therapeutic target in Mantle cell lymphoma.<sup>46</sup>

### 1.3 Protein Kinases as Drug Targets

Since protein phosphorylation controls a diverse range of cellular and pathogenic processes, even subtle changes in protein kinase activity can lead to a wide variety of diseases including cancer, inflammatory disorders, diabetes, neurodegeneration and central nervous system diseases. This pivotal role has made protein kinases an important and tractable therapeutic class for drug discovery.<sup>47</sup>

Currently, there are 12 US Food and Drug Administration-approved protein kinase inhibitors for various cancer indications,<sup>48</sup> whereas other therapeutic areas are yet strongly under-represented. One reason for this focus on cancer, although not the only one, is that many kinase inhibitors exhibit off-target effects because of poor selectivity. While multi-targeted agents (also called “group selective”) are often considered more efficient than selective inhibitors for oncology patients with possibly acceptable adverse effects,<sup>49, 50</sup> an accumulation of side-effects due to unwanted off-target inhibition must be avoided in non-life-threatening diseases. The major reason for the difficulty in optimizing the selectivity of kinase inhibitors is that they are mainly directed to the ATP-binding pocket, which is highly conserved in all 518 kinases of the human kinome.<sup>47</sup>

These off-target side effects of protein kinase inhibitors have diverted efforts from targeting the ATP-binding pocket in order to produce inhibitors that have the potential to be more kinase specific. The specificity in targeting particular protein kinases may be achieved more readily by targeting more remote sites away from the highly conserved ATP binding pocket.<sup>47</sup>

#### 1.3.1 Classification of Kinase Inhibitors

- 1) Type I inhibitors: bind to the highly conserved ATP binding pocket in the kinase’s active conformation.<sup>51</sup> These compounds represent the vast majority of ATP-competitive inhibitors. It is also to be noted that these inhibitors must ultimately target the kinase with high affinity to compete with the high intracellular concentrations of ATP, however they sometimes do not discriminate between the ATP-binding sites conserved in protein kinases and other ATP-binding proteins.<sup>52</sup>
- 2) Type II inhibitors: bind to an inactive conformation occurring in certain kinases thus prevent kinase activation. They use the ATP binding cleft and an adjacent hydrophobic pocket created by the activation loop which is accessible only when the Phe side-chain of the conserved DFG motif moves out of the hydrophobic pocket.
- 3) Type III inhibitors: allosteric inhibitors which target allosteric or regulatory sites in the protein kinase. This class of inhibitors is more promising to achieve selectivity because

such inhibitors exploit binding sites and regulatory mechanisms that are unique to a particular kinase.<sup>5</sup> It is worth mentioning that the typical allosteric effectors are those that regulate the catalytic activity by binding to a region distant from the active site. This, however, should not be confused with modulators that can partly bind to the active site like type II inhibitors.<sup>53</sup>

### 1.3.1.1 Advantages of Allosteric Inhibitors

- 1) Higher selectivity, even permitting targeting kinases which were not previously considered as druggable.
- 2) Escape from the crowded patent space around ATP-binding site-directed inhibitors due to novel chemical entities targeting new binding sites.
- 3) No increase in  $IC_{50}$ s in cellular compared to cell-free assays (in general, for kinases with relatively high ATP-binding affinities ( $K_m = 1\text{--}20\ \mu\text{M}$ ), it was proven to be difficult to develop ATP-competitive inhibitors with sufficient selectivity and cellular activity).<sup>54</sup>
- 4) Allosteric inhibitors may cause sustained inactivation for the target kinase in cellular environment even after the washout of the inhibitor as some allosteric inhibitors can promote activation loop dephosphorylation.<sup>53</sup> This finding is verified by our allosteric inhibitors as will be discussed later in this thesis. ATP competitive inhibitors can rather stabilize the active conformation by protecting the phosphorylated residues from phosphatase action, as exemplified by an ATP-competitive inhibitor of PKC,<sup>55</sup> or in some cases increase phosphorylation of the target kinase as in the case of PKB/AKT. It was found that treatment of cells with active site inhibitors increased the steady state levels of phosphorylated AKT.<sup>56</sup> Such undesirable effects can make ATP competitive inhibitors completely ineffective *in vivo*, since the target kinase would respond with an increased activity after wash-out of the inhibitor.<sup>53</sup>

## 1.3.2 PIF Pocket as an Allosteric Site to Modulate AGC Kinases Activity

### 1.3.2.1 Discovery and Physiological Function

The PIF-binding pocket is a conserved regulatory element located on the small lobe of the kinase domain and is present in all of the members of the AGC kinase family. It was first described in phosphoinositide-dependent kinase-1 (PDK1)<sup>13</sup> based on the similarity to the intramolecular docking site of the C-terminal peptide FSEFCOOH in protein kinase A (PKA),<sup>57</sup> where in all X-ray-structures of active PKA, the PIF pocket is occupied by this C-terminal

## Introduction

hydrophobic motif (HM) peptide. The HM peptide FSEF-COOH at the C-terminal end of PKA is the shortest HM sequence found. In several other AGC kinases, the motif is extended to Phe-Xaa-Xaa-Phe-Ser/Thr-Tyr/Phe, in which the Ser/Thr is the phosphorylated residue.<sup>13</sup> PDK1 was found to lack the HM peptide; its PIF pocket serves as a transient intermolecular docking site for the C-terminal HM motifs of other substrate AGC kinases which need activation loop phosphorylation by PDK1 to be fully active (Figure 7). This interaction of HM peptides from various substrate kinases with PDK1 PIF pocket is essential for its complete catalytic activity.<sup>13,58</sup> An exception to this is the PKB family, which are activated by PDK1 via a different mechanism depending on the PH domains of both PDK1 and PKB. Based on this finding, the PIF pocket was characterized as an allosteric site on PDK1 catalytic domain which transduces signals from interacting ligands to the active site.

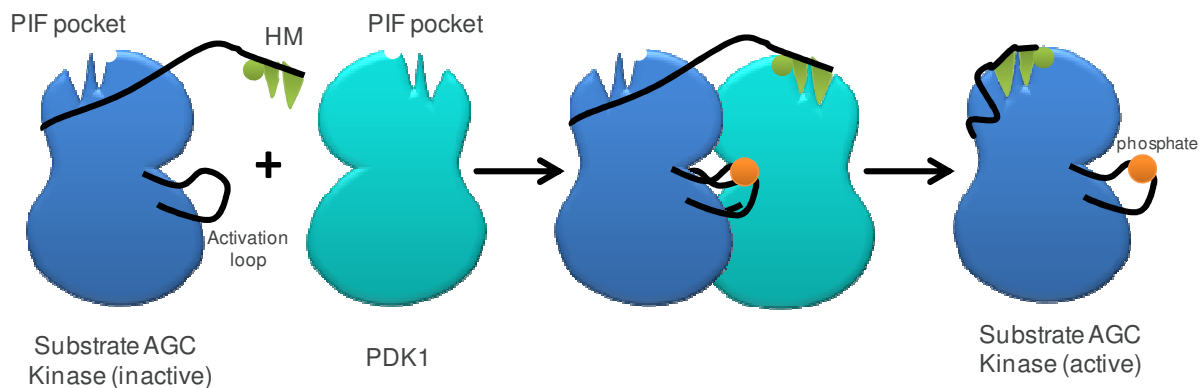


Figure 7: Physiological role of the PIF pocket in PDK1. Recognition and phosphorylation of the substrate AGC kinases (except PKB) depend on a transient intermolecular docking interaction involving the HM of substrate AGC kinase and PIF pocket of PDK1. (Adapted from<sup>53</sup>).

The HM peptide derived from the PKC-related protein kinase 2 (PRK2), the PRK2-Interacting Fragment peptide “PIFtide”, was found to have the strongest affinity and activating potency on PDK1, hence the name of the receptor site – the PIF pocket- on PDK1.<sup>59</sup>

In most HM peptides, there is a serine or threonine residue C-terminal to the FXXF motif which is phosphorylated by another kinase (mostly mTORC2). This HM phosphorylation turns the inactive AGC kinase into a PDK1 substrate as the negatively charged phosphate exhibits an essential docking interaction with the PIF pocket.<sup>59</sup> However, in some AGC kinases like PKC $\zeta$ ,  $\iota$  and PRK, an aspartate or glutamate residue is found instead of the phospho Ser/Thr residue which is able to mimic its interaction with the PIF pocket, thus abolishing the need for a “priming” kinase for the HM motif phosphorylation. The binding of HM and the HM-phosphate to the PIF pocket acts in concert to stabilize the active structure of the kinase.<sup>60, 61</sup>

## Introduction

After binding to PDK1, the substrate kinase is phosphorylated by PDK1 at the activation loop which triggers the release of the substrate kinase, causing the free the HM peptide to fold back and bind intramolecularly to its own PIF pocket. This interaction is probably enforced because the prior T-loop phosphorylation promotes the formation of a functioning PIF pocket through the stabilization of the  $\alpha$ C-helix, as will be mentioned later. Thus, the active enzyme conformation is fully stabilized and ready to phosphorylate downstream substrates dependent on further regulatory mechanisms (Figure 7).<sup>59</sup>

### 1.3.2.2 Molecular Interactions of the Natural HM Peptide Ligands

There are two major forces which drive the affinity of the natural ligand HM peptides towards the PIF pocket: hydrophobic and Van der Waals interactions by the two phenyl rings from the FXXF motif, and ionic and hydrogen-bond interactions mediated by a negatively charged residue C-terminal to the FXXF motif and by the peptide backbone respectively.<sup>53</sup> The intramolecular interactions by the HM peptide with the PIF pocket of PKC  $\beta$ II is shown in Figure 8.

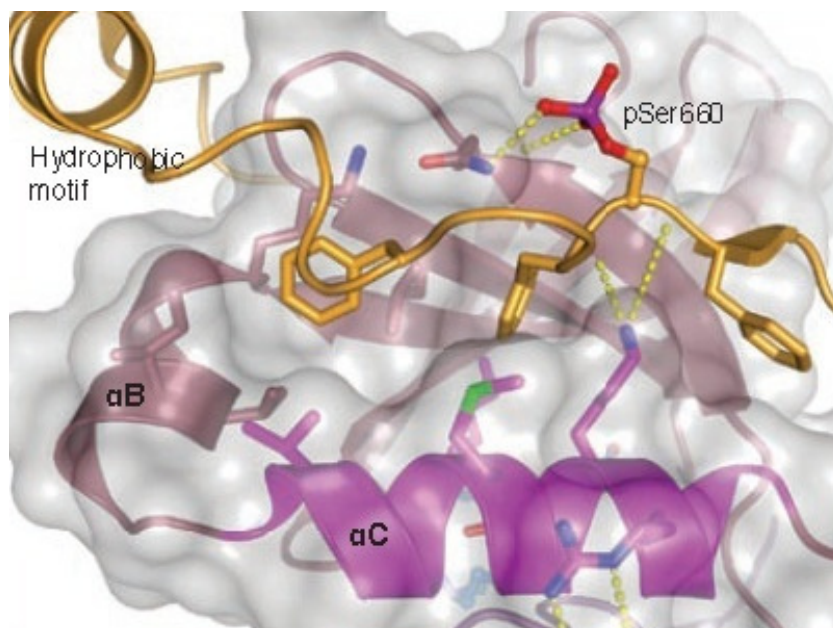


Figure 8: The intramolecular binding of HM peptide to the PIF pocket in PKC $\beta$ II (PDB 2I0E). The hydrophobic motif FEGFSF in PKC $\beta$ II is comprised of residues 656-661, shown in golden yellow. The hydrophobic motif is phosphorylated at Ser660. The three aromatic side chains of the hydrophobic motif, Phe656, Phe659, and Phe661, form lipophilic interactions with helices  $\alpha$ B and  $\alpha$ C, and strands  $\beta$ 4 and  $\beta$ 5, shown in purple (the framing elements of the PIF pocket). Several hydrogen bonds are anchoring the hydrophobic motif to helix  $\alpha$ C and strand  $\beta$ 4. For example, the backbone carbonyl of Phe659 is hydrogen bonded to the side chain of Lys391 of helix  $\alpha$ C, while the phosphate of Ser660 is hydrogen bonded to the conserved Gln411 on strand  $\beta$ 4 (from the crystal structure of PKC $\beta$ II bound to a competitive inhibitor of ATP).<sup>62</sup> The Figure is copied from <sup>6</sup>.

### 1.3.2.3 Allosteric Mechanism by the PIF Pocket

The PIF pocket is considered as an allosteric site that can modulate the kinase catalytic activity. It has been previously shown that the binding of the PIF pocket ligand activators in PDK1 produces local changes at the PIF binding pocket, as well as allosteric changes at the ATP binding site and the activation loop.<sup>63</sup> Furthermore, the activity states of PIF pocket and ATP-binding site are intimately coupled as has been shown by the co-crystal structure of the type II inhibitor MP7 with PDK1 (PDB ID: 3NAX).<sup>64</sup> As a result of this conformational linkage, the allosteric interaction between the two sites is mutual. So, it can be reasoned that compounds stabilizing such non active PIF pocket shapes will also induce catalytically inactive conformations in the ATP-binding site of PDK1.<sup>53</sup>

#### 1.3.2.3.1 Role of the $\alpha$ C-helix in Allosteric Control through the PIF Pocket

The crystal structure of PDK1 revealed the PIF pocket as a shallow, 5Å deep surface pocket with a hydrophobic center and polar surrounding residues. The most important secondary elements framing the PIF pocket are the  $\beta$ -sheets 4 and 5, a short  $\alpha$ B-helix and the  $\alpha$ C-helix (the same elements are shown for PKC $\beta$ II PIF pocket in Figure 8).<sup>60</sup>

The  $\alpha$ C-helix plays the most crucial role in allosteric regulation of AGC kinase activity as it provides a structural link between the PIF pocket and the phosphorylated T-loop Ser/Thr residue.<sup>61,65</sup> The binding of the HM peptide to the PIF pocket induces a disordered-to-ordered transition of the  $\alpha$ C-helix, which promotes the interaction of a basic  $\alpha$ C-helix residue with the activation loop phosphate in some AGC kinases for example Arg129 in PDK1, as shown in Figure 9-A. Vice versa, T-loop phosphorylation favors the formation and stabilization of an intact  $\alpha$ C-helix and hence the formation of the PIF pocket, which has been demonstrated in the case of PKB.<sup>65</sup> In this way, both formation of the  $\alpha$ C-helix and T-loop phosphorylation mutually stabilize the kinase in its active state, mediated by electrostatic interaction of the two elements.

However in the crystal structure of some AGC kinases like PKC $\beta$ II (PDB 2I0E), this direct interaction between the activation loop phosphate and the  $\alpha$ C helix basic residue is missing. Instead, the activation loop phosphate on Thr500 (PKC $\beta$ II numbering) forms an ion pair with Arg465 of the catalytic loop and Lys489 of the activation loop. This correctly orients Glu490 of the activation loop for hydrogen bonding to Arg392 of the  $\alpha$ C-helix. In turn, this rearrangement orients the  $\alpha$ C-helix in an optimum position to aid the catalysis (Figure 9-B).<sup>62</sup>

## Introduction

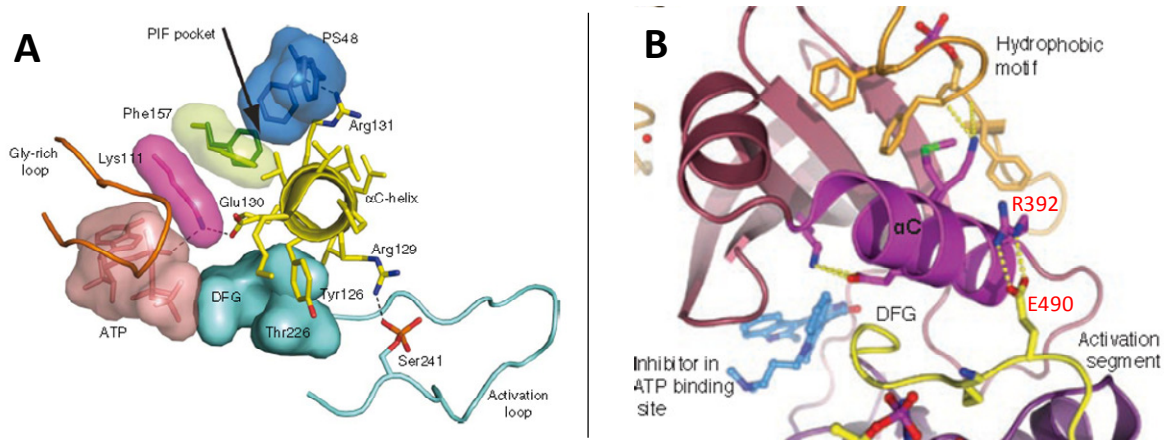


Figure 9: Interactions mediated by the  $\alpha$ C-helix. (A) The PIF pocket and its link to the kinase's active site: the figure shows the allosteric activator PS48 bound to PIF pocket of PDK1. There are two important interactions mediated by PIF pocket through the  $\alpha$ C-helix to affect the structural elements that regulate kinase activity. The first interaction is made by Arg129 from the  $\alpha$ C-helix with activation loop phosphate, while the second one is through Glu130 with Lys111, which directly interacts with ATP phosphates. Both interactions are promoted by binding of the natural HM peptide or ligand activators to the PIF pocket.<sup>63</sup> (B) From the crystal structure of PKC $\beta$ II bound to a competitive inhibitor of ATP: intramolecular docking of HM peptide to PIF pocket is shown, where the activation loop phosphate is not in direct interaction with the  $\alpha$ C-helix. However, Glu490 from the activation loop interacts with Arg392 from the  $\alpha$ C-helix.<sup>62</sup>

Additionally, the  $\alpha$ C-helix can form a highly conserved salt bridge between a glutamate residue from the  $\alpha$ C-helix (Glu130 in PDK1) and a lysine residue (Lys111 in PDK1) in the active site (also shown in Figure 9-A).<sup>60,63</sup> This Lys can directly interact with and correctly positions the phosphates from ATP for catalysis. Based on its crucial role, disturbance of the  $\alpha$ C-helix is inevitably accompanied by inhibition of the kinase catalytic activity. Considerably, inactive structures of the AGC kinases PKB/AKT,<sup>65,66</sup> MSK1,<sup>67</sup> and RSK2<sup>68</sup> exhibit a completely disturbed PIF pocket; two of its lining walls, the conserved  $\alpha$ C- and  $\alpha$ B-helices, are either disordered or replaced by an unusual  $\beta$ -sheet. Thus, changes in the HM/PIF pocket are accompanied by inactive conformations of key residues in the ATP-binding pocket and of the T-loop.<sup>53</sup> Some of the putative effects expected from PIF pocket-directed allosteric inhibitors are shown in Figure 10.

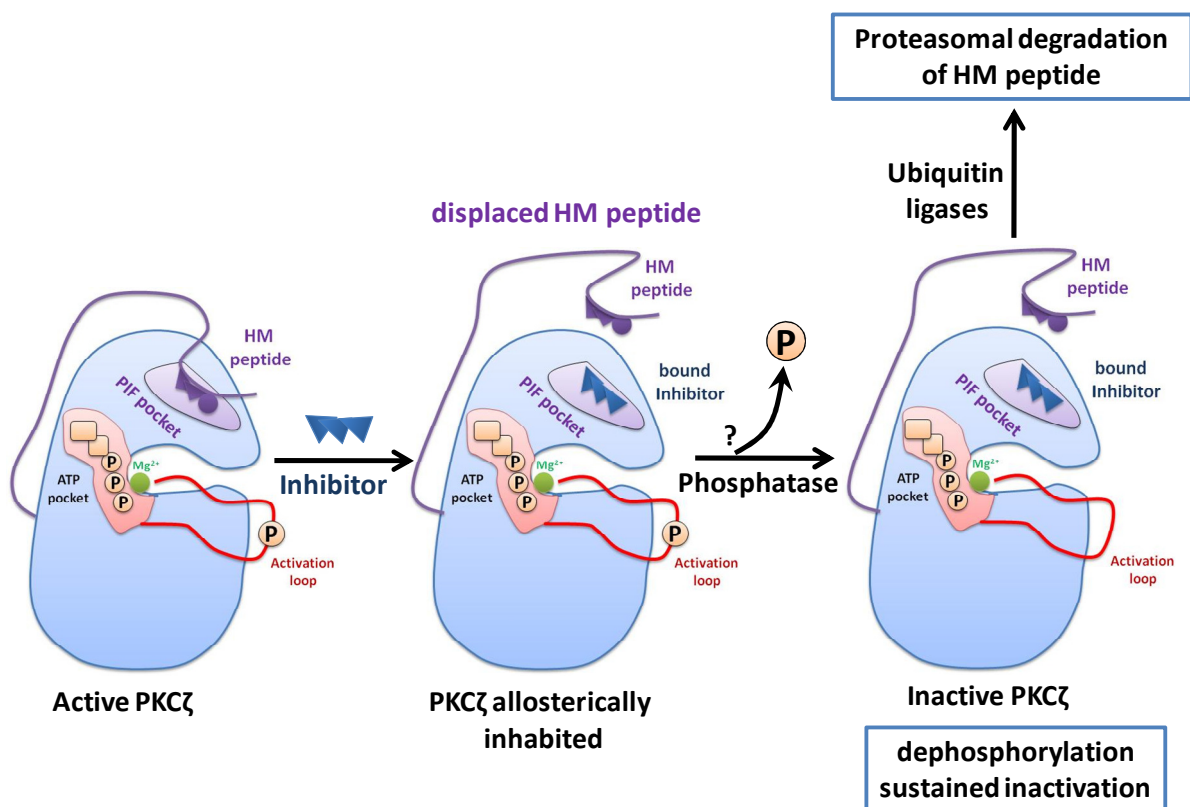


Figure 10: Proposed mechanism of action of allosteric inhibitors binding to the PIF pocket of AGC kinases e.g. PKC $\zeta$ . Intramolecular binding of the HM peptide to the PIF pocket stabilizes the kinase active conformation. The allosteric inhibitor binds to the PIF pocket leading to displacement of the HM peptide. Allosteric inhibitors can promote dephosphorylation at the activation loop and thus sustained inactivation of PKC. In addition, displaced peptide extension might be recognized as a misfolded element by ubiquitin ligases, promoting increased degradation by the proteasome. (Adapted from <sup>53</sup>).

### 1.3.2.4 Targeting the PIF Pocket with Small Molecule Ligands to Inhibit the Activity of AGC Kinases

Being an allosteric site which can regulate the kinase activity, the PIF-binding pocket may offer a great advantage over the ATP pocket as a drug target, where the PIF-binding pocket shows a lower degree of sequence conservation in comparison to the highly conserved ATP-binding site. In particular, the amino acids surrounding the hydrophobic groove, being within reach of small molecules, are only moderately conserved thus offering the possibility to develop more selective compounds compared to the possibility using ATP-competitive strategies. Targeting the PIF pocket could be an option even in case of closely related kinase isoforms such as the PKC family, which was considered not druggable by the currently available design strategies targeting the ATP binding pocket since no isoform-selective kinase inhibitors have

been obtained so far. It is important to note that a sequence alignment of the PKC isoforms reveals a much lower degree of conservation in the regulatory PIF pocket. This difference can even be shown in case of the most closely related  $\alpha$ PKC isoforms  $\zeta$  and  $\iota$ , which enabled us to develop potent and highly selective isoform inhibitors towards PKC $\zeta$ , as will be presented later in this thesis.

Through continuous research work, the PIF pocket was shown to transduce activation or inhibition by small molecule modulators. The first efforts to develop PIF pocket ligands were directed to PDK1 PIF pocket, yielding the discovery and development of compounds that are PDK1 activators and protein-protein interaction inhibitors.<sup>58,63,69,70</sup> These ligands prevent the docking of the HM peptide to the PIF pocket of PDK1, thus inhibiting the phosphorylation and activation of all substrate AGC kinases except PKB/AKT. On the other hand, targeting the PIF pocket by small molecule inhibitors was only successful towards the atypical PKC $\zeta$ ,<sup>71, 72</sup> the target of interest in this thesis.

### 1.3.2.4.1 Discovery of First Allosteric PKC $\zeta$ Inhibitors

The development of the first allosteric PKC $\zeta$  inhibitors started when two 3-phenylglutaric acid monoanilides, which are weak inhibitors of the atypical PKC $\zeta$ , were discovered during routine screening of hits previously identified as weak PDK1 activators against a panel of related AGC kinases (compounds A and B, Figure 11).<sup>72</sup> Potency optimization was achieved via bioisosteric replacement of the amide function involving cyclization to the benzimidazole analogs to yield 4-benzimidazolyl-3-phenylbutanoic acid analogues. The new scaffold showed increased potency as inhibitors of full-length PKC $\zeta$ , highlighting that these more drug-like aryl moieties such as benzoheterocycles can be tolerated by subregions of the mostly hydrophobic PIF pocket.

Several 4-benzimidazolyl-3-phenylbutanoic acid analogues were synthesized and tested for their inhibitory activity against full-length PKC $\zeta$ . The results showed that the benzimidazole ring can have large substituents such as 5-iodine and 5-phenyl with increase in potency, thus demonstrating the high structural plasticity of the PIF pocket (cf. compounds 1q and 1y in Figure 11). Furthermore, a potential halogen bond of the iodine in the 5-iodobenzimidazole derivatives (as in 1q) was indicated by the SARs. This halogen bond is probably engaging the 5-iodo substituent with the backbone carbonyls and/or the His289 imino nitrogen. Thus, 1q was identified to be the most potent compound of the series, shown in Figure 11 ( $IC_{50}$  of the racemate = 18  $\mu$ M).

The enhancing effect of halogen substitutions at the aryl rings was coherent with SARs observed with PDK1 activators<sup>69, 73</sup> and in agreement with our results for the triarylpyrazolines which will be shown later in this thesis. In addition, the PIF pocket in PKC $\zeta$  can tolerate even longer alkyl chains at the phenyl ring (cf. compound 1x in Figure 11).

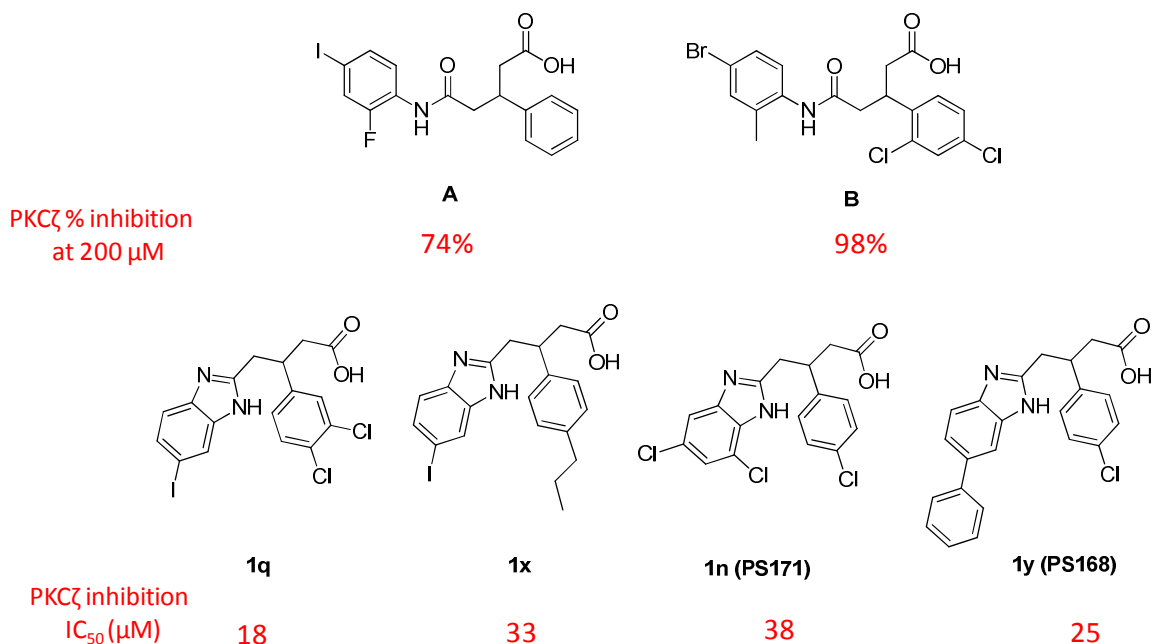


Figure 11: Allosteric inhibitors targeting the PIF pocket of PKCζ.

Targeting the PIF pocket was confirmed by several lines of experimental evidence:

- (i) Several compounds of the series which are active PKCζ inhibitors (e.g. 1x and 1y) were able to show moderate activation of PDK1 by about 3 fold at 50 μM.
- (ii) Binding of 1n (PS171 in <sup>71</sup>) to the PDK1-PIF pocket was confirmed by co-crystallography (PDB ID: 4A07).<sup>71</sup>
- (iii) When compounds 1n and 1y (PS168 in <sup>71</sup>) were tested against PKCζ mutated at residues central to the PIF pocket (PKCζ-Val297Leu and PKCζ-Leu328Phe), they totally lost their inhibitory potency.<sup>71</sup>

Selectivity testing showed that, unlike the more potent compound 1q, compounds 1x, 1n and 1y were highly selective inhibitors of PKCζ, without affecting PKCι (the most closely related isoform). Further testing with PKCζ mutants suggested that the natural replacement of Phe321 in PKCι by Leu328 in PKCζ was responsible for the PKCζ specificity of 1n (PS171) and 1y (PS168).<sup>71</sup> Luciferase reporter gene assay, which monitors the PKCζ-mediated coactivation of NF-κB in U937 cells, confirmed the cellular inhibitory activity toward PKCζ since many 4-benzimidazolyl-3-phenylbutanoic acid analogs efficiently suppressed the activity of NF-κB after induction by TNF-α.

Two important observations were made:

- (i) There was a close correlation between the cell-free and cellular inhibition potencies, indicating that PKC $\zeta$  was targeted in both cases.
- (ii) No loss of potency occurred in the cell compared with that of the cell-free assay.<sup>72</sup> Beside the greater selectivity, another advantage over ATP-competitive compounds is being unaffected by the high intracellular ATP concentration that can cause up to a 100-fold increase of IC<sub>50</sub>s in case of ATP-competitive compounds.<sup>74</sup>

Another important result of this study was the fact that the same compounds that caused activation of PDK1 by binding to the PIF pocket triggered inhibition of another AGC kinase.

### 1.3.2.4.2 Other Reported Inhibitors for PKC $\zeta$

A limited number of compounds were reported as PKC $\zeta$  inhibitors, all of which have limited selectivity in particular towards the most closely related isoform, PKC $\iota$ , for instance, hydroxyphenyl-1-benzopyran-4-ones, represented by compounds 1, 2 and 3 in ref.<sup>75</sup>. A second example is PKC $\zeta$ I257.3 (*N*-(4-((dimethylamino)methyl)benzyl)-1*H*-pyrrole-2-carboxamide) with an IC<sub>50</sub> of 28  $\mu$ M against PKC $\zeta$ .<sup>76</sup> In addition, the 2-(6-phenylindazolyl)-benzimidazole derivative (compound 9 in ref.<sup>77</sup>) was reported by Trujillo et al. as a potent PKC $\zeta$  inhibitor with an IC<sub>50</sub> of 5.2 nM. It also showed good selectivity versus other PKC isoforms but with less than 10-fold selectivity towards PKC $\iota$ . Moreover, several kinases from less related families were significantly inhibited.<sup>77</sup>

Another inhibitor is CRT0066854, a thieno[2,3-*d*]pyrimidine-based chemical inhibitor of aPKCs. The compound is about 4-fold more potent against PKC $\iota$  than PKC $\zeta$ , where the measured IC<sub>50</sub> values for full-length PKC $\zeta$  and PKC $\iota$  were 639 nM and 132 nM respectively. The compound showed significant cross reactivity with PRK2 and CDK5.<sup>78</sup> Another recent report described a series of 2-amino-3-carboxy-4-phenylthiophenes as non-competitive aPKCs inhibitors, where the most potent compound showed an IC<sub>50</sub> of 0.8 and 0.9  $\mu$ M vs. PKC $\zeta$  and PKC $\iota$  respectively (compound 30 in ref.<sup>79</sup>). Although the compounds lacked aPKC isoform selectivity and showed moderate activity in the cell free assay, the compounds showed high activity in cellular assays approaching a single digit nM range which suggests the need for further biological testing to exclude off-target interactions.<sup>79,80</sup> All the structures of the aforementioned inhibitors are shown in Figure 12.

## Introduction

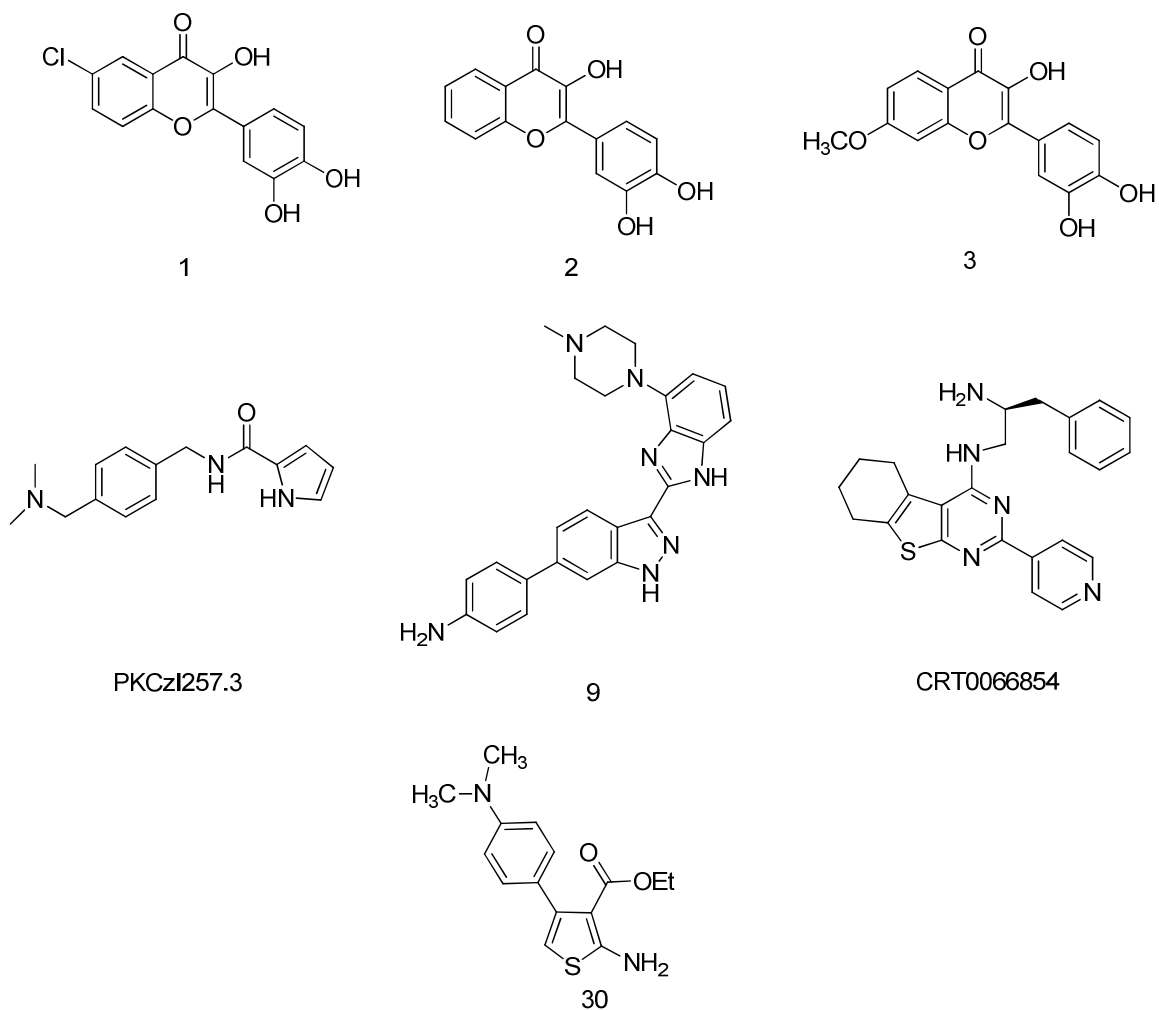


Figure 12 : Other PKC $\zeta$  inhibitors. Compounds 1-3 are the hydroxyphenyl-1-benzopyran-4-ones in ref.<sup>75</sup>. Compound 9 is a 2-(6-phenylindazolyl)-benzimidazole derivative (ref.<sup>77</sup>). Compound 30 is a 2-amino-3-carboxy-4-phenylthiophene derivative, the most potent compound in ref.<sup>79</sup>.

# 1.4 Exploration of the Pyrazoline Scaffold in Other Protein-Protein Interaction Targets as Exemplified by the p53-Mdm2 Interaction

## 1.4.1 The Tumor Suppressor p53

The tumor suppressor p53, known as “the guardian of the genome”, is a transcription factor that plays a crucial role in the regulation of DNA repair, cell cycle and apoptosis.<sup>81-83</sup> Its activity is important to the health and survival of tissues, as it suppresses the growth of defective cells such as tumor cells and prevents damaged cells from multiplying and passing their mutated genes to the next generation. Accordingly, p53 is found to be functionally inactivated by mutation or deletion in about 50% of human cancers.<sup>84</sup> The murine double minute 2 (Mdm2; Hdm2 in humans) oncoprotein is a cellular inhibitor of p53 that can bind the trans-activation domain of p53 and down regulate its ability to activate transcription.

Mdm2 inhibits the activity of p53 through several ways; it prevents p53 from interaction with other proteins, exports p53 out of the nucleus away from nuclear DNA, and promotes p53 proteasomal degradation through its E3 ubiquitin ligase activity.<sup>85, 86</sup>

In cancers with wild type p53, its function was found to be effectively inhibited by Mdm2. The imbalance of the Mdm2/p53 activities can lead to malignant transformation of normal cells, where over-expression of Mdm2 promotes cells growth and tumorigenesis.<sup>87</sup> Mdm2 was found to be amplified in 7% of human cancers when 28 different types of human cancers in nearly 4,000 human tumor samples were analyzed.<sup>88</sup>

## 1.4.2 p53-Mdm2 Interactions

The high-resolution crystal structures of human Mdm2 complexed with the transactivation domain of p53, residues 15–29 (PDB code 1YCR),<sup>89</sup> showed that the p53-Mdm2 interaction is mediated by a well-defined hydrophobic surface pocket in Mdm2 and three key hydrophobic residues in p53, namely Phe19, Trp23, and Leu26 (Figure 13). All the three amino acids undergo multiple van der Waals contacts with the surrounding Mdm2 receptor amino acids, while Trp23 forms an additional hydrogen-bond with the backbone carbonyl of Leu54 in Mdm2. These three amino acid residues can be imagined to act as three fingers which insert themselves into three complementary pockets on the Mdm2 surface. The relative compactness of Mdm2 binding pocket made it appear possible to design non-peptide, drug-like small-molecule

## Introduction

inhibitors to prevent this interaction and act as a tool to reactivate p53 in cells with wild type p53.<sup>90</sup>

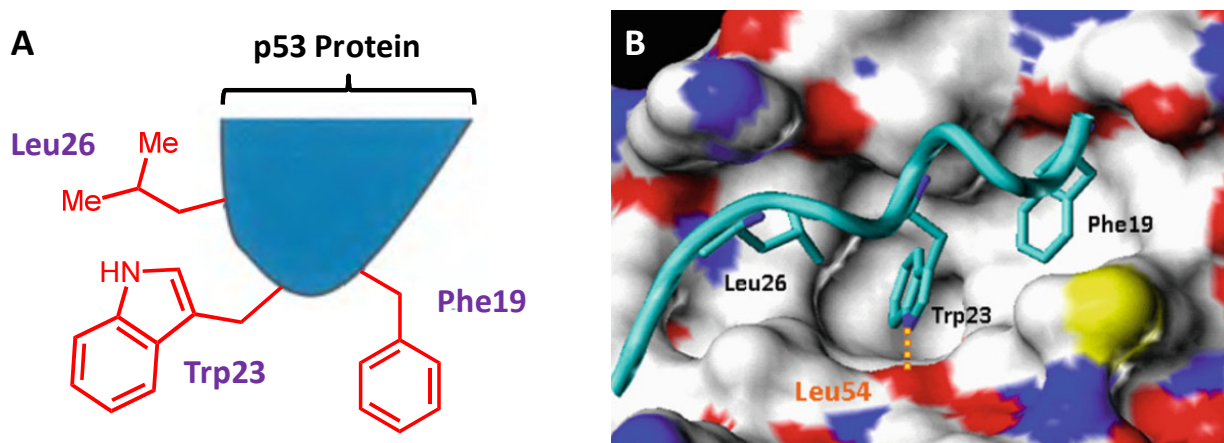


Figure 13: The p53–Mdm2 interaction. (A) The hotspot triad made up of Leu26, Trp23 and Phe19 in P53, these three amino acid residues are acting as three fingers which insert into three complementary pockets on the Mdm2 surface (copied from <sup>91</sup>). (B) p53 (blue) bound to Mdm2, p53's hot spots (Leu26, Trp23 and Phe19) can be seen as sticks buried deep in the Mdm2 pocket. The hydrogen-bond formed between Trp23 and Mdm2's backbone carbonyl of Leu54 can be seen as an orange dashed line. (Copied from <sup>90</sup>).

### 1.4.3 Some Small Molecule Non-peptide Inhibitors of p53-Mdm2 Interaction

Owing to the critical inhibitory function of Mdm2 on p53, blocking the interaction between Mdm2 and p53 has been anticipated to be a potential cancer therapeutic approach. It was proposed that by mimicking the three key hydrophobic residues in p53, non-peptide small-molecule inhibitors can achieve high affinities to Mdm2 and displace p53 from its complex with Mdm2.

Nutlins are among the first potent and specific Mdm2 inhibitors. They were discovered by Vassilev and co-workers at Hoffman-La Roche.<sup>92</sup> Nutlins were discovered by high-throughput screening of a diverse library of synthetic compounds. They have a *cis*-imidazoline core structure; both nutlin-1 and nutlin-2 were tested as racemate while nutlin-3a is an active enantiomer (Figure 15). Nutlins 1, 2 and 3a are able to disrupt the p53-Mdm2 interaction with IC<sub>50</sub> values of 0.26, 0.14 and 0.09  $\mu$ M, respectively.

The crystal structure of Mdm2 complexed with nutlin-2 (PDB code: 1RV1) shows that nutlin-2 is able to mimic the interactions of the p53 peptide (Figure 14). In nutlin-2, one of the bromophenyl groups interacts with the Trp23 pocket, the other interacts with the Leu26 pocket, and the ethoxy side chain targets the Phe19 pocket. The backbone of the imidazoline scaffold

## Introduction

mimics the  $\alpha$ -helix of p53. It is to be noted that, nutlin-2 does not make a H-bond similar to the one between Trp23 indole NH in p53 and the backbone carbonyl group of Leu54 in Mdm2.

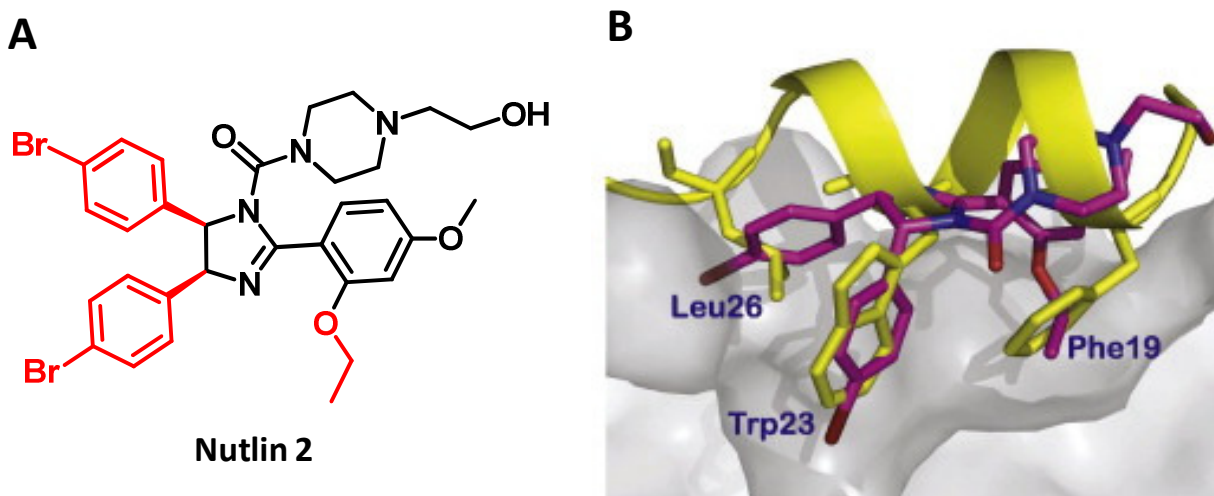
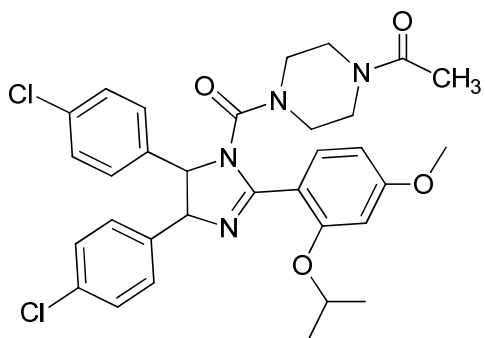


Figure 14: Interactions of Nutlin-2 with Mdm2. (A) The three lipophilic parts in nutlin-2 which mimic the hotspot triad of p53 are highlighted in red. (B) The overlay of nutlin-2 (PDB code: 1RV1) and p53 trans-activation domain peptide (PDB code: 1YCR) on the Mdm2 surface. Nutlin-2 and p53 peptide are colored in magenta and yellow respectively. (Copied from <sup>93</sup>)

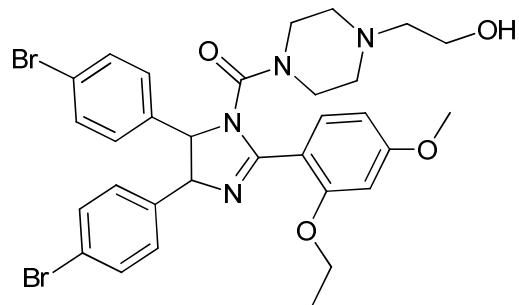
Grasberger et al. discovered benzodiazepinedione-based Mdm2 inhibitors using high throughput screening of combinatorial libraries.<sup>94</sup> The benzodiazepinedione compound 1 (in reference <sup>94</sup>) showed a  $K_i$  of 80 nM in the fluorescent peptide displacement (FP) assay (structure is shown in Figure 15). Extensive modifications have been made on spirooxindoles by Ding et al. employing a structure-based *de novo* design strategy.<sup>95, 96</sup> MI-147 was reported as one of the most potent of this class of compounds, with a  $K_i$  of 0.6 nM in an FP-based competitive binding assay.<sup>97</sup> All the structures are shown in Figure 15.

## Introduction

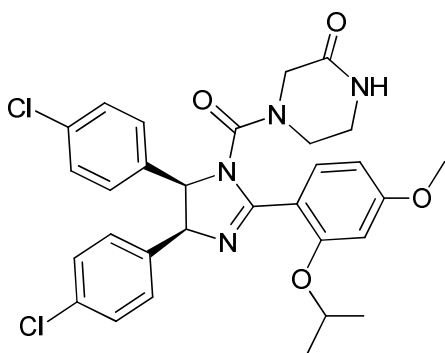
---



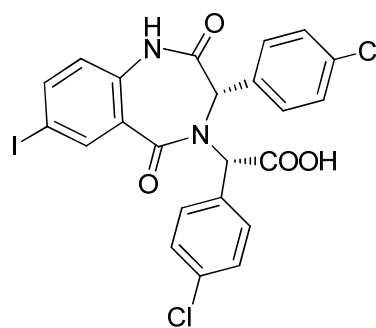
Nutlin-1



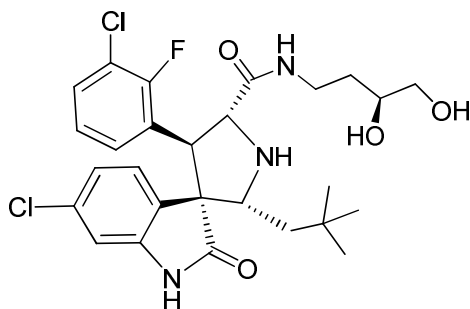
Nutlin-2



Nutlin-3a



compound 1



MI-147

Figure 15: Small molecule inhibitors of p53-Mdm2 interaction.

## 2 Scientific goal

The  $\alpha$ PKC $\zeta$  was reported to play an important role in NF- $\kappa$ B signaling, B cell development and Th2 cell differentiation. In addition, PKC $\zeta$  was found to be abundantly expressed in lung and liver tissues. These findings suggested that PKC $\zeta$  is a possible target in the treatment of bronchial asthma, liver inflammation and autoimmune diseases. Moreover, several reports suggested PKC $\zeta$  inhibition as a strategy to suppress some types of cancers like B cell lymphoma.

However, no potent isoform selective inhibitors for PKC $\zeta$  vs. its closely related isoform PKC $\iota$  have been discovered to date. In our study, we aimed at developing a selective class of PKC $\zeta$  inhibitors that can offer a pharmacological tool for further cellular and disease model studies to validate PKC $\zeta$  as a possible therapeutic target. Selective inhibitors are also required to address the possible adverse effects resulting from PKC $\zeta$  inhibition especially on glucose uptake following to insulin action.

The use of ATP-competitive type I inhibitors is a less promising approach due to the highly conserved sequence of the ATP binding pocket in PKC family and generally in all protein kinases. To overcome this, we directed our efforts to the PIF pocket which was previously reported as an allosteric site to modulate kinase activity in AGC kinases. In normal physiological conditions, the PIF pocket is bound to the C-terminal HM peptide contributing to the stabilization of the kinase in its fully active conformation. Therefore, disrupting this protein-protein interaction by small molecule non-peptide inhibitors was the major aim behind our efforts to achieve the required inhibition.

We decided to start the modifications based on the previously reported 4-benzimidazolyl-3-phenylbutanoic acids, PIF pocket directed allosteric PKC $\zeta$  inhibitors to finally reach more potent and selective inhibitors having pyrazoline scaffold as will be illustrated in chapter 3.1.

Furthermore, we aimed at testing the pyrazoline scaffold as a possible inhibitor for the p53-Mdm2 interaction as another type of protein-protein interaction since p53 binding pocket on Mdm2/Hdm2 partially resembles the PIF pocket regarding shape and physicochemical properties. The displacement of the p53 from its binding to Mdm2 using small molecule non-peptide inhibitors is a proven strategy to induce apoptosis in cancer cells with wild type p53.

The pyrazoline scaffold is a rigid scaffold with favorable synthetic tractability. Consequently, it seemed reasonable that we introduce it into such type of protein-protein interaction pockets which need a highly modifiable synthetic scaffold to reach the desired activity and selectivity, since many “hot spots” in protein-protein interaction sites are

## **Scientific goal**

---

characterized by a hydrophobic groove. We proposed that the pyrazoline core can mimic the  $\alpha$ -helix of p53's trans-activation domain and can furnish versatile 1-, 3- and 5- lipophilic substituents to mimic the hot spot triad of p53 (Leu26, Trp23 and Phe19) which interact with Mdm2. This proposal was supported by structural overlay of the planned tri- and tetra-substituted pyrazolines (energy minimized form) with the closely similar, previously reported *cis*-imidzoline inhibitor, nutlin-2, as appearing in its crystal structure with Mdm2 (as will be shown in chapter 3.2).

## 3 Results

### 3.1 Discovery and Optimization of 1,3,5-trisubstituted Pyrazolines as Potent and Highly Selective Allosteric Inhibitors of PKC $\zeta$

A major part of this chapter is submitted to the Journal of Medicinal Chemistry

#### ABSTRACT

There is increasing evidence that the atypical protein kinase C (PKC)  $\zeta$  might be a therapeutic target in pulmonary and hepatic inflammatory diseases. However, targeting the highly conserved ATP-binding pocket in the catalytic domain held little promise to achieve selective inhibition. In the present study, we introduce 1,3,5-trisubstituted pyrazolines as potent and selective allosteric PKC $\zeta$  inhibitors. The rigid scaffold offered many sites for modification, all acting as hot spots for improving activity and displaying sharp structure-activity relationships. Targeting of PKC $\zeta$  in cells was confirmed by reporter gene and transfection assays. The strongly reduced cell-free and cellular activities towards a PIF-pocket mutant of PKC $\zeta$  suggested that the inhibitors most likely bound to the PIF-pocket on the kinase catalytic domain. Thus, using a rigidification strategy and by establishing and optimizing multiple molecular interactions with the binding site, we were able to significantly improve the potency of the previously reported PKC $\zeta$  inhibitors.

#### INTRODUCTION

The Protein kinase C (PKC) family comprises the classical (cPKC $\alpha$ ,  $\beta$ I,  $\beta$ II, and  $\gamma$ ), novel (nPKC $\delta$ ,  $\epsilon$ ,  $\eta$ , and  $\theta$ ), and atypical (aPKC $\zeta$  and  $\lambda$ /I) isoenzymes, based on their biochemical requirements for activation. Only cPKCs respond to calcium, whereas both cPKCs and nPKCs are sensitive to phorbol esters and the lipid second messenger diacylglycerol (DAG). Finally, PKC $\zeta$  and PKC $\iota$  (termed  $\lambda$  in the mouse) were named atypical because they do not respond to the above agents but might be activated by some lipids, such as phosphatidylinositols and ceramide (reviewed in <sup>1</sup>). In addition, aPKC activity is regulated by protein interaction partners that also provide the required temporal and spatial specificity, including the inhibitory protein Par-4 and the adapter protein p62.<sup>2,3</sup>

Both atypical PKCs share a high degree of identity (84%) in the catalytic domain, and are less conserved in the N-terminal regulatory PB1 and C1 domains (53% identical). Although both

## Results

---

enzymes are similarly regulated and activated, not all of their biological functions are redundant (see<sup>3</sup> for a recent review). PKC $\zeta$  knockout mice appeared grossly normal; only the formation and maturation of secondary lymphoid organs was altered during the first weeks after birth, however, most of these defects were overcome in adult animals.<sup>4</sup> These findings suggested that targeting PKC $\zeta$  with specific inhibitors might not cause harmful toxic effects. On the other hand, knockout of the PKC $\iota$  gene was lethal in early embryonic development.<sup>5</sup> With respect to the PKC $\zeta$  biological function, knockout studies revealed that PKC $\zeta$  was essential for the development and differentiation of B cells and Th2 cells.<sup>6</sup> As a consequence, PKC $\zeta$ -deficient mice developed only a mild form of concanavalin A-induced hepatitis,<sup>7</sup> with a dramatic decrease in leukocyte infiltration and liver apoptosis.<sup>8</sup> Since Th2 responses critically mediate humoral immunity against extracellular pathogens and in allergic reactions, OVA-induced allergic airway inflammation was also strongly reduced in PKC $\zeta$ -deficient mice.<sup>6</sup>

On the molecular level, PKC $\zeta$  mediates B cell proliferation and survival by activation of the extracellular signal-regulated kinase (ERK) pathway.<sup>9-11</sup> Even more importantly, after B cell receptor stimulation, PKC $\zeta$  induces the transcription of I $\kappa$ B and other NF- $\kappa$ B-dependent genes, such as IL-6 or Bcl-X<sub>L</sub>.<sup>4, 11</sup> The activation of the transcriptional activity of NF- $\kappa$ B is one of the key functions of PKC $\zeta$  in autoimmune and chronic inflammatory diseases because it can lead to exacerbated lymphocyte activities.<sup>12</sup> PKC $\zeta$  phosphorylates Ser311 on the RelA subunit of NF- $\kappa$ B,<sup>13</sup> which has been shown to be required for full NF- $\kappa$ B transcriptional activity *in vivo* and in cell culture experiments.<sup>4</sup> Numerous transfection experiments using kinase-defective dominant-negative mutants, overexpression studies and anti-sense experiments further supported a role for the PKC $\zeta$  in the control of NF- $\kappa$ B activation.<sup>14-19</sup> Another important consequence of the Ser311 phosphorylation by PKC $\zeta$  was demonstrated by Levy et al.: it triggered displacement of the histone methyltransferase GLP from RelA, which abrogated the GLP-mediated methylation of histone H3, thus finally enabling NF- $\kappa$ B to become transcriptionally active.<sup>20</sup> In addition, a rather cell type specific function as an IKK kinase was demonstrated for PKC $\zeta$  in the lung, exerting additional control on the NF- $\kappa$ B activation in these tissues, but not in fibroblasts or T cells.<sup>4,6,8,13</sup>

In the lung tissue where the kinase is abundantly expressed, PKC $\zeta$  was required for both IKK and NF- $\kappa$ B activation in response to TNF $\alpha$ , IL-1b, or LPS.<sup>4</sup> Contrastingly, in naïve T cells, PKC $\zeta$  was not involved in NF- $\kappa$ B activation but was rather found to be essential for the efficient activation of Jak1 and the subsequent phosphorylation and nuclear translocation of Stat6.<sup>6</sup> As a consequence, PKC $\zeta$ -deficient naïve CD4+ T cells were not able to differentiate into Th2 cells and secreted low levels of the Th2-related cytokines, IL-4, IL-5, IL-10, and IL-13.<sup>6</sup> Similarly, PKC $\zeta$  interacted with and phosphorylated Jak1 in the mouse liver and in IL-4-stimulated fibroblasts, and PKC $\zeta$  activity was required for Stat6 activation.<sup>8</sup> Altogether, these studies established a central role of PKC $\zeta$  in the IL-4/Stat6 pathway.

The identified function of PKC $\zeta$  in the IL-4 signaling might also be relevant in the T-cell-mediated fulminant hepatitis, which had been discovered using the concanavalin A (ConA)

## Results

---

model.<sup>21</sup> In this model, PKC $\zeta$ -deficient mice showed impaired NF- $\kappa$ B activation in the liver, which should have resulted in impaired survival. Nevertheless, the mice showed reduced damage to the liver and a healthier state than their wild type littermates.<sup>8</sup> It was found that some major effects brought about by the loss of PKC $\zeta$  was the reduced induction of serum IL-5 and liver eotaxin which are two important mediators of liver damage.<sup>8</sup>

Besides its direct implication in the control of transcription factors such as NF- $\kappa$ B and Stat6, PKC $\zeta$  was recently reported to be involved in the regulation of gene expression at the epigenetic level as well; it was found to physically interact with and phosphorylate DNA methyltransferase 1, resulting in a reduced activity of this enzyme.<sup>22</sup> In agreement with this observation, down-regulation of PKC $\zeta$  signalling was identified as a potential mechanism by which very low density lipoproteins might silence pro-inflammatory genes in macrophage-like THP-1 cells, an effect which is known to be mediated by *de novo* DNA methylation.<sup>23</sup>

The other atypical PKC, PKC $\iota$ , was demonstrated to act as an oncogene in lung cancer, colon carcinoma and other types of solid tumors (reviewed in<sup>24</sup>). In a recent study, specific inhibition of PKC $\iota$  in the liver led to normalization of glucose and triglyceride levels *in vivo*,<sup>25</sup> thus potentially expanding the scope for selective PKC $\iota$  inhibitors to the metabolic syndrome and to insulin-resistant states of obesity.

As a potential adverse side effect of PKC $\zeta$  inhibitors, impairment of the insulin-dependent glucose uptake might be considered, because PKC $\zeta$  was also demonstrated to play an important role in the phosphorylation and activation of the glucose transporter GLUT-4.<sup>26, 27</sup> However, all of these findings were derived from experiments in rats or mice, whereas in humans, PKC $\iota$  and not  $\zeta$  appears to be the major aPKC expressed in skeletal muscle.<sup>28</sup> Thus, PKC $\zeta$ -selective inhibitors might not suppress glucose uptake in human muscle tissue. Alternatively, tissue-specific drug delivery might be a viable approach to reduce potential side effects.

In summary, an increasing body of evidence suggests that PKC $\zeta$  might be suited as a pharmacological target in allergic asthma of the lung and in liver inflammation. Up to now, drug development efforts towards this target were rather limited. Given the high similarity of the ten PKC isoforms in their ATP-binding sites, traditional approaches using ATP-competitive inhibitor strategies did not appear very promising because of the difficulty of obtaining selective inhibitors.<sup>29</sup> Hence, only a few small molecule compounds were reported as PKC $\zeta$  inhibitors, but all with limited selectivity in particular against the most closely related isoform, PKC $\iota$ , including hydroxyphenyl-1-benzopyran-4-ones<sup>30</sup> and PKCzI257.3 (*N*-(4-((dimethylamino)methyl)benzyl)-1*H*-pyrrole-2-carboxamide).<sup>31</sup> A 2-(6-phenylindazolyl)-benzimidazole derivative was reported as a potent PKC $\zeta$  inhibitor which was less active toward PKC $\iota$ , however, several kinases from less related families were significantly inhibited.<sup>32</sup> Most recently, CRT0066854, a thieno[2,3-*d*]pyrimidine-based chemical inhibitor of aPKCs was reported. However, the compound was

## Results

---

about four-fold more potent against PKC $\iota$  than PKC $\zeta$ . In addition, it showed significant cross reactivity with PRK2 and CDK5.<sup>33</sup> Titchenell et al. reported a series of non-ATP competitive aPKC inhibitors with an unidentified binding site, exhibiting IC<sub>50</sub>s in the low  $\mu$ M range.<sup>34, 35</sup> While these 2-amino-3-carboxy-4-phenylthiophenes showed remarkable selectivity against other PKC families, they inhibited both aPKC $\iota$  and - $\zeta$  with equal potency. However, it remains to be shown whether the more than three orders of magnitude higher activity of the compound series in cell-based *vs.* cell-free assays is due to inhibition of intracellular aPKCs or other mechanisms.<sup>35</sup>

Inhibitors with a true allosteric mode of action are generally believed to be more selective, because they are targeting less conserved, often subtype-specific regulatory sites. However, they often display only moderate affinities.<sup>36</sup> Recently, the first allosteric inhibitors of a PKC isoenzyme which bind to the so-called PIF-pocket (also named the hydrophobic motif (HM) pocket) of PKC $\zeta$  were reported.<sup>37</sup> These 4-benzimidazolyl-3-phenylbutanoic acids exhibited a remarkable selectivity even against the most closely related isoform, PKC $\iota$ , however the potency (IC<sub>50</sub> = 18  $\mu$ M for compound A, Figure 1) required optimization. Of note, the first efforts to develop PIF pocket ligands were directed to PDK1 PIF pocket, yielding the discovery and development of compounds that are PDK1 activators and protein-protein interaction inhibitors.<sup>38-42</sup>

In the present study, we describe the design, synthesis and optimization of tri- and tetra-substituted pyrazoline derivatives as novel allosteric inhibitors of PKC $\zeta$ . Several compounds potently inhibited the purified, recombinant enzyme and blocked PKC $\zeta$ -dependent signalling in U937 cells. Furthermore, we demonstrate that the pyrazoline core is a versatile scaffold which allows independent fine-tuning of all substituents to optimize potency, physicochemical properties and stability.

## RESULTS AND DISCUSSION

### CHEMISTRY

**Design concept.** The previously published allosteric inhibitors of PKC $\zeta$  contained three flexible bonds connecting the essential aromatic rings (Figure 1), which were thought to bind to the two hydrophobic grooves of the PIF-pocket.<sup>37</sup> Therefore, rigidification of the molecule offered great potential to enhance the binding affinity. Since the presence of a carboxyl function was another potential shortcoming with respect to cell permeability, we also envisaged its replacement by a H-bond acceptor function, which would potentially interact with Lys301 of

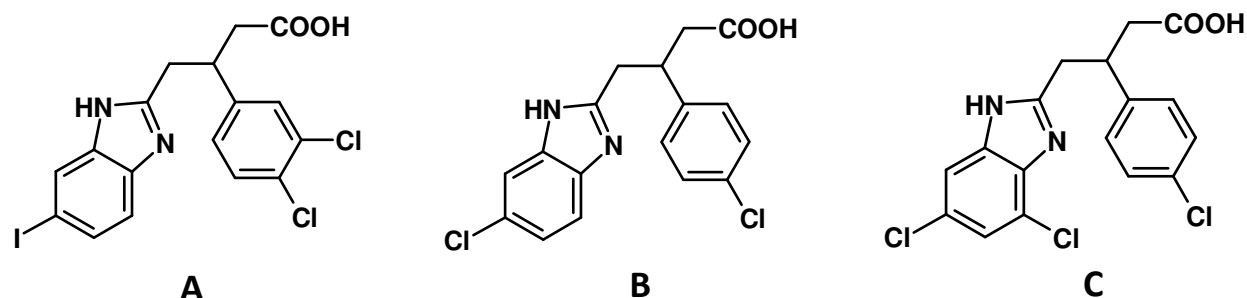


**Figure 1.** Structures of the previously published allosteric inhibitors of PKC $\zeta$ . (The original codes in ref.<sup>37</sup> were **A**, 1q; **B**, 1a; **C**, 1n).

PKC $\zeta$  instead of the carboxylate. Interestingly, some of the published allosteric PKC $\zeta$  inhibitors (e.g. those depicted in Figure 1, **B** and **C**) were found to be allosteric activators of PDK1 as well, suggesting that the shapes of the PIF-pockets in active PDK1 and inactive PKC $\zeta$  may share some similarities. Moreover, since the binding modes of **B** and **C** in the PIF-pocket of PDK1 were elucidated after cocrystallography (superimposed in Figure 2A, PDB codes 4A06 and 4A07, respectively), we reasoned that the bound conformations of the small molecules could serve as templates for the design of rigidified analogues. Thus our preferred strategy was to fix the relative positions of the two aromatic moieties of **B** and **C** as observed in the cocrystal with PDK1. Such a conformation was compatible as well with binding to the PIF-pocket of the active PKC $\iota$  catalytic domain (PDB code: 3A8X), which displayed a very similar shape.

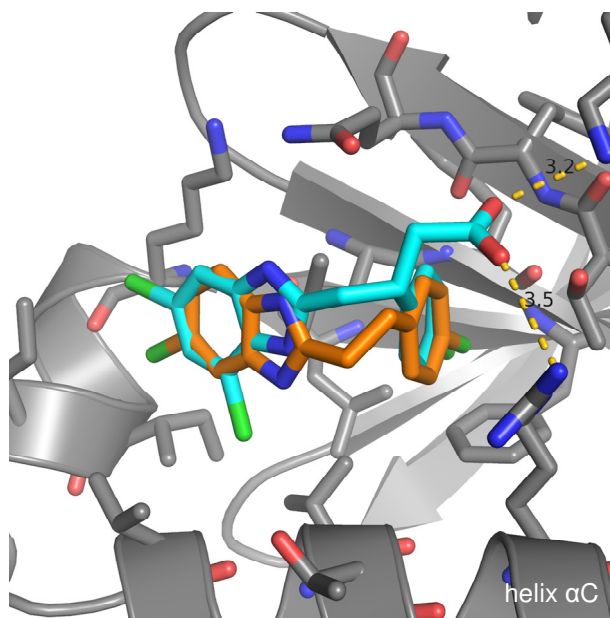


**Figure 2 (A)** Superimposed binding modes of **B** (orange) and **C** (cyan) (cf. Figure 1) in the PIF-pocket of PDK1 (PDB codes 4A06 and 4A07, respectively). For compound **C**, ionic interactions with two PIF-pocket residues were identified (distances are given in angstrom), whereas the carboxyl side chain of **B** was not resolved. The conformation of the less substituted compound **B** was used as a template for ligand design.

## Results

The defined requirements were met by utilizing pyrazoline ring as a central core furnished with two aromatic rings in the 1- and 5-positions (see superimposition in Figure 2B). The presence of an  $sp^3$  hybridized atom at one of the connection positions seemed important to conserve the dihedral angle enclosed by the single bonds linked to the aromatic rings in the PIF-pocket-bound B. Furthermore, the pyrazoline system was synthetically accessible by a three component reaction, allowing introduction of three different substituents at positions 1, 3 and 5. This flexible synthetic approach provided the possibility to optimize all three positions independently using a diverse range of substituted phenyls or other moieties.

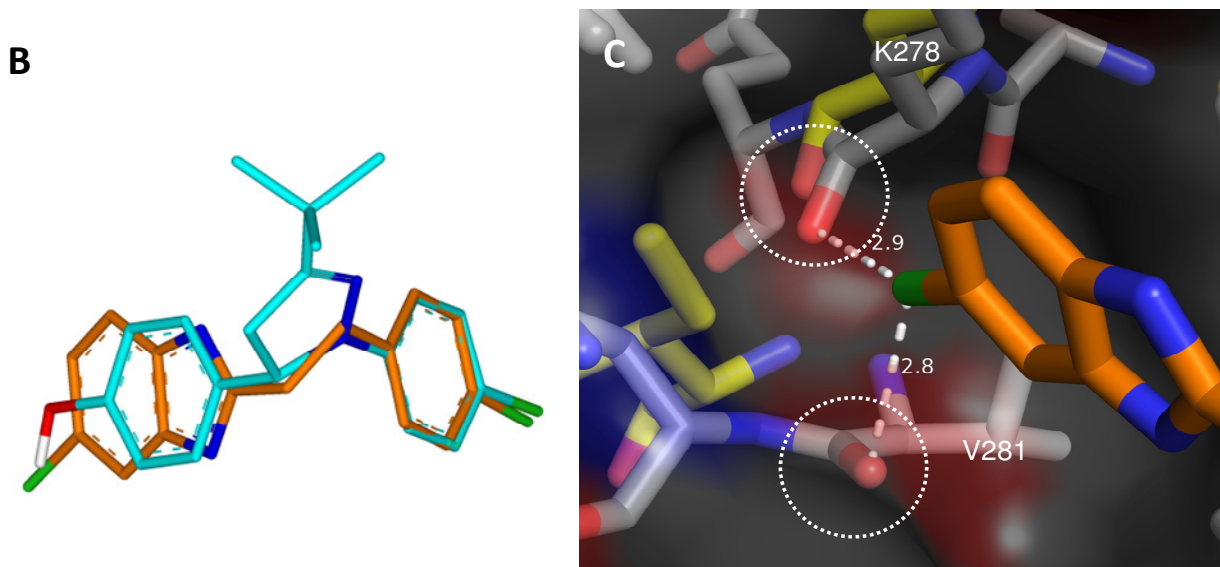


Figure 2 (B) Pyrazoline prototype compound 1a superimposed with the 3D structure of B in the cocrystal-bound conformation (taken from PDB entry 4A06) (C) Two carbonyl functions are available for H-bonding in the PIF-pocket of atypical PKC $\iota$ . The cocrystal structure of PDK1 with compound B (orange) bound in the PIF-pocket (PDB code: 4A06, yellow residues) was superimposed with the crystal structure of the atypical PKC $\iota$  (PDB code: 3A8X, grey residues), the most closely related isoform of PKC $\zeta$ . The benzimidazole ring (orange) denotes the putative position of B in the superimposed PIF-subpocket of PKC $\iota$ . Two backbone carbonyl groups derived from PKC $\iota$  Lys278 and Val281, respectively (circled), are sequestered into the PIF-subpocket, and would be in a close distance (indicated in angstrom) to the 5'-chlorine of the benzimidazole if a similar binding mode was assumed. In contrast, the carbonyl equivalent to that of Lys278 in PDK1 is less available (upper circle, yellow residue).

**Synthesis.** The synthesis of the target compounds was carried out in two steps. In the first step, a Claisen-Schmidt condensation was carried out between aromatic aldehydes and pinacolone or acetophenone analogues, using 10% aq. KOH as a catalyst in methanol, in order to afford the required enones. In the second step, these enones were reacted to give the desired pyrazolines using the previously reported regioselective synthesis of 1,3,5-triarylpyrazolines.<sup>43</sup> This was accomplished via enone-arylhydrazine hydrochloride condensation reaction under an inert atmosphere using DMF as solvent while heating for 5 hours at 85°C (Schemes 1,2 and 3).

## Results

In our early trials, *p*-hydroxybenzaldehyde was used in an attempt to obtain the essential *p*-hydroxy group on the phenyl enone derivatives. Unfortunately, the phenoxide anion, which was generated due to the strong alkaline reaction conditions, both hindered the reaction and reduced the yield dramatically. Hence, we decided to use methoxy or ethoxybenzaldehyde derivatives, which afforded the respective enones in a very high yield; the final compounds were then obtained after deprotection using  $\text{BBr}_3$  in dichloromethane at  $-78^\circ\text{C}$  (Scheme 2, step iii).

In an attempt to test the effect of other substituents at the 5-phenyl, *t*-butoxybenzaldehyde was used to get the enone **E1** (Figure 3), which was then reacted with 4-chlorophenylhydrazine hydrochloride to yield compound **D**. Surprisingly, compound **1a** was the major product obtained while compound **D** was obtained in a very low yield. This clearly suggested that the *t*-butyl ether group was spontaneously cleaved to give the corresponding *p*-hydroxyl group under the reaction conditions used. This fact was confirmed by comparing  $^1\text{H-NMR}$  and  $^{13}\text{C-NMR}$  spectra of both **E1** and **1a**. The concomitant cleavage was observed throughout the 33 reactions shown in Scheme 1, thus providing a short and facile pathway for obtaining 5-(4-hydroxy phenyl) pyrazolines in a good yield, eliminating the need for deprotection and ether cleavage by  $\text{BBr}_3$ .

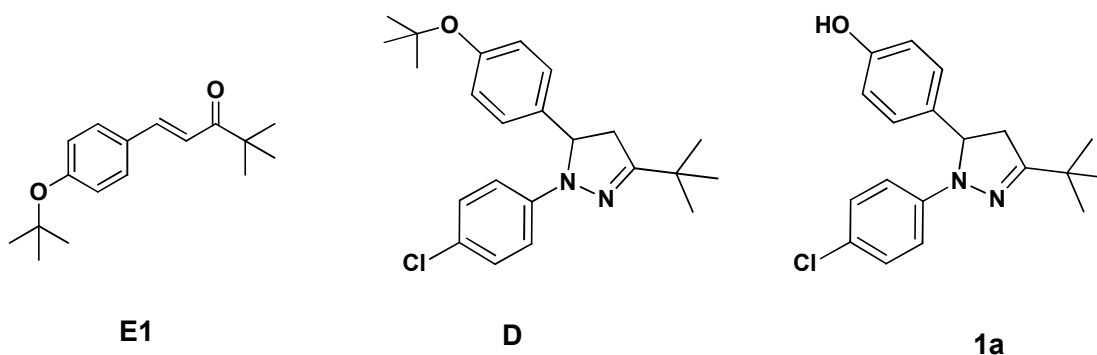


**Figure 3.** Structure of the enone intermediate **E1** which yielded **1a** after reacting with *p*-chlorophenyl hydrazine, via a spontaneous ether cleavage of **D**.

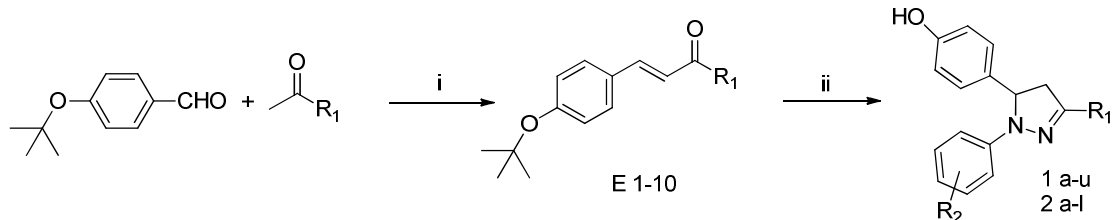
The aniline derivatives were obtained in a very good yield by synthesizing the respective nitro derivatives followed by reduction using  $\text{SnCl}_2 \cdot 2\text{H}_2\text{O}$  in refluxing methanol (Scheme 3). To introduce a methyl group at position 4 of the pyrazoline derivative **3h**, deprotonation of the acidic methylene group with LDA at  $-78^\circ\text{C}$  was done to give the respective anion which was instantly trapped with methyl iodide to afford the methyl-substituted pyrazoline derivative **8**.<sup>43</sup> This compound was then deprotected using  $\text{BBr}_3$  to give compound **9** (Scheme 4). Oxidation of the pyrazoline ring in **3e** to the corresponding pyrazole **10** was achieved using DDQ in refluxing benzene followed by deprotection using  $\text{BBr}_3$  to afford compound **11** (Scheme 5).

It is worth mentioning that the use of the arylhydrazine as hydrochloride salt rather than the free base was of great importance to increase the yield of the cyclization reaction and to reduce the reaction side products. In addition to this, one equivalent amount of HCl was added to the

## Results

reaction medium in order to improve the yield especially when enones containing basic moieties, like pyridine or aniline as in **E8** and **E10**, respectively, were used.

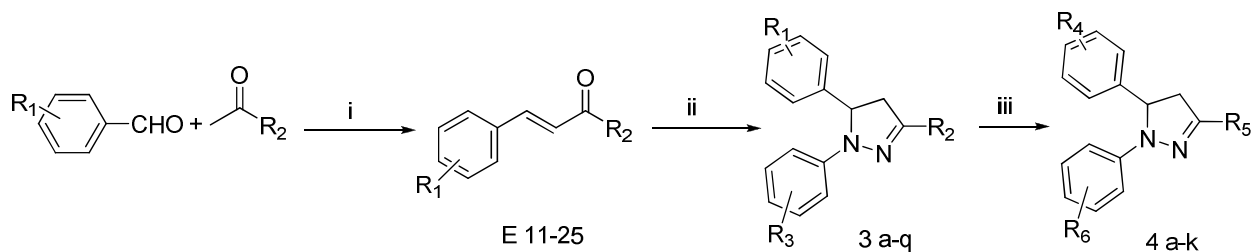
### Scheme 1



Reagents and conditions: (i) 10% KOH, MeOH, ice cooling then room temperature, overnight; (ii) 1.5 equiv Ar-NH-NH<sub>2</sub>·HCl, DMF, 85 °C, 5h.

No.	E	R1	R2	No.	E	R1	R2
<b>1a</b>	1	<i>t</i> -Bu	4-Cl	<b>1r</b>	1	<i>t</i> -Bu	3-chloro-4-fluoro
<b>1b</b>	1	<i>t</i> -Bu	4-F	<b>1s</b>	1	<i>t</i> -Bu	3,4-difluoro
<b>1c</b>	1	<i>t</i> -Bu	4-Br	<b>1t</b>	1	<i>t</i> -Bu	2,3,4-trifluoro
<b>1d</b>	1	<i>t</i> -Bu	4-CF <sub>3</sub>	<b>1u</b>	1	<i>t</i> -Bu	4-H
<b>1e</b>	1	<i>t</i> -Bu	4-CH <sub>3</sub>	<b>2a</b>	2	phenyl	4-Cl
<b>1f</b>	1	<i>t</i> -Bu	4-isopropyl	<b>2b</b>	2	phenyl	3-Cl
<b>1g</b>	1	<i>t</i> -Bu	4-COOH	<b>2c</b>	3	2-hydroxyphenyl	4-Cl
<b>1h</b>	1	<i>t</i> -Bu	3-Cl	<b>2d</b>	4	2-methoxyphenyl	4-Cl
<b>1i</b>	1	<i>t</i> -Bu	3-F	<b>2e</b>	5	2-ethoxyphenyl	4-Cl
<b>1j</b>	1	<i>t</i> -Bu	3-CF <sub>3</sub>	<b>2f</b>	6	2-chlorophenyl	4-Cl
<b>1k</b>	1	<i>t</i> -Bu	3-CH <sub>3</sub>	<b>2g</b>	7	thiophen-2-yl	4-Cl
<b>1l</b>	1	<i>t</i> -Bu	2-Cl	<b>2h</b>	7	thiophen-2-yl	4-Br
<b>1m</b>	1	<i>t</i> -Bu	2-F	<b>2i</b>	7	thiophen-2-yl	4-CF <sub>3</sub>
<b>1n</b>	1	<i>t</i> -Bu	2,4-dichloro	<b>2j</b>	8	pyridin-2-yl	3-Cl
<b>1o</b>	1	<i>t</i> -Bu	2,4-difluoro	<b>2k</b>	9	pyrrol-2-yl	3-Cl
<b>1p</b>	1	<i>t</i> -Bu	2,4-dimethyl	<b>2l</b>	10	4-aminophenyl	4-Cl
<b>1q</b>	1	<i>t</i> -Bu	2,6-dichloro				

### Scheme 2



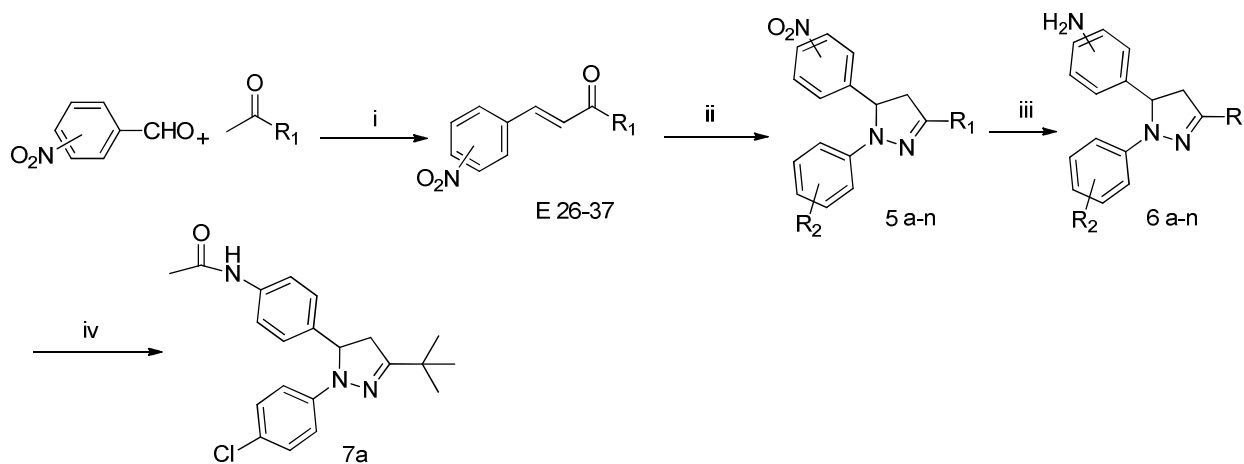
Reagents and conditions: (i) 10% KOH, MeOH, ice cooling then room temperature, overnight; (ii) 1.5 equiv Ar-NH-NH<sub>2</sub>·HCl, DMF, 85 °C, 5h; (iii) 3-9 equiv BBr<sub>3</sub>, CH<sub>2</sub>Cl<sub>2</sub>, -78 °C then room temperature, 20h.

3/4	E	R1	R2	R3	R4	R5	R6
<b>a</b>	11	3-OMe	<i>t</i> -Bu	4-Cl	3-OH	<i>t</i> -Bu	4-Cl
<b>b</b>	12	4-OMe	<i>t</i> -Bu	4-OMe	4-OH	<i>t</i> -Bu	4-OH
<b>c</b>	13	4-Cl	<i>t</i> -Bu	4-OMe	4-Cl	<i>t</i> -Bu	4-OH
<b>d</b>	14	3-F,4-OMe	<i>t</i> -Bu	4-Cl	3-F,4-OH	<i>t</i> -Bu	4-Cl

## Results

e	15	3-Cl,4-OMe	<i>t</i> -Bu	4-Cl	3-Cl,4-OH	<i>t</i> -Bu	4-Cl
f	16	4-F,3-OMe	<i>t</i> -Bu	3-Cl	4-F,3-OH	<i>t</i> -Bu	3-Cl
g	17	3,4-dimethoxy	2-methoxyphenyl	4-Cl	3,4-dihydroxy	2-hydroxyphenyl	4-Cl
h	18	3-F,4-OMe	2-methoxyphenyl	3-Cl	3-F,4-OH	2-hydroxyphenyl	3-Cl
i	19	3,5-difluoro-4-OEt	2-methoxyphenyl	3-Cl	3,5-difluoro-4-OH	2-hydroxyphenyl	3-Cl
j	20	2,3-difluoro-4-OMe	2-methoxyphenyl	3-Cl	2,3-difluoro-4-OH	2-hydroxyphenyl	3-Cl
k	21	3-F,4-OMe	2,4-dimethoxyphenyl	3-Cl	3-F,4-OH	2,4-dihydroxyphenyl	3-Cl
l	22	4-F	<i>t</i> -Bu	4-Cl	-	-	-
m	13	4-Cl	<i>t</i> -Bu	4-Cl	-	-	-
n	23	4-Br	<i>t</i> -Bu	4-Cl	-	-	-
o	24	4-CN	<i>t</i> -Bu	4-Cl	-	-	-
p	25	4-OMe	phenyl	4-Cl	-	-	-
q	-	4-OH	Me	4-Cl	-	-	-

Scheme 3

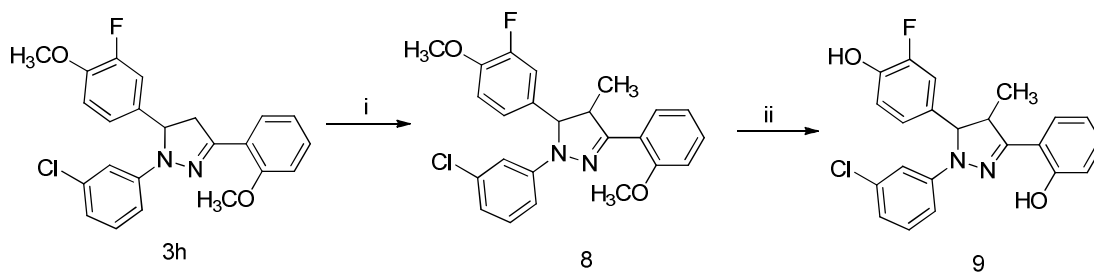


Reagents and conditions: (i) 10% KOH, MeOH, ice cooling then room temperature, overnight; (ii) 1.5 equiv Ar-NH-NH<sub>2</sub>·HCl, DMF, 85 °C, 5h; (iii) 5 equiv SnCl<sub>2</sub>·2H<sub>2</sub>O, MeOH, reflux, 2h; (iv) 1.5 equiv CH<sub>3</sub>COCl, acetone, ice cooling, 2h.

5/6	E	NO <sub>2</sub> /NH <sub>2</sub> position	R1	R2
a	26	4	<i>t</i> -Bu	4-Cl
b	26	4	<i>t</i> -Bu	2,4-difluoro
c	26	4	<i>t</i> -Bu	3-Cl
d	27	3	<i>t</i> -Bu	4-Cl
e	28	4	cyclopropyl	3-Cl
f	29	4	1-methylcyclopropyl	3-Cl
g	30	4	cyclohexyl	4-Cl
h	31	4	thiophen-2-yl	3-Cl
i	32	4	furan-2-yl	3-Cl
j	33	4	2-chlorophenyl	3-Cl
K	34	4	2-trifluoromethylphenyl	3-Cl
l	35	4	2-methylphenyl	3-Cl
m	36	4	2-methoxyphenyl	3-Cl
n	37	4	benzo[d][1,3]dioxol-5-yl	3-Cl

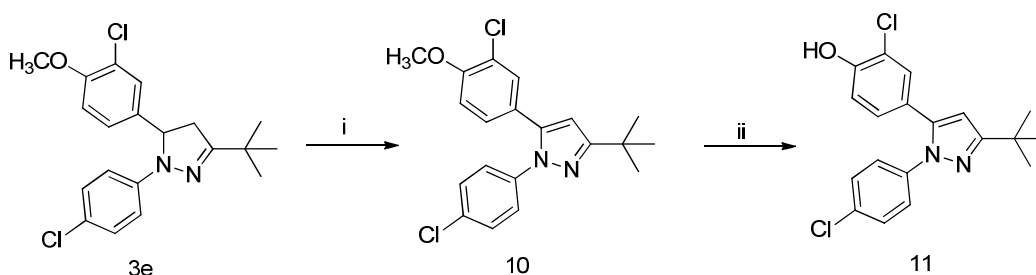
## Results

### Scheme 4



Reagents and conditions: (i) 1.5 equiv LDA, 1.5 equiv MeI, THF,  $-78^{\circ}\text{C}$  then room temperature, 20h; (ii) 6 equiv  $\text{BBr}_3$ ,  $\text{CH}_2\text{Cl}_2$ ,  $-78^{\circ}\text{C}$  then room temperature, 20h.

### Scheme 5



Reagents and conditions: (i) 1.5 equiv DDQ, benzene, reflux, 5h; (ii) 3 equiv  $\text{BBr}_3$ ,  $\text{CH}_2\text{Cl}_2$ ,  $-78^{\circ}\text{C}$  then room temperature, 20h.

## BIOLOGICAL ACTIVITY

### Structure-Activity Relationships (SARs) in the Cell-Free Assay

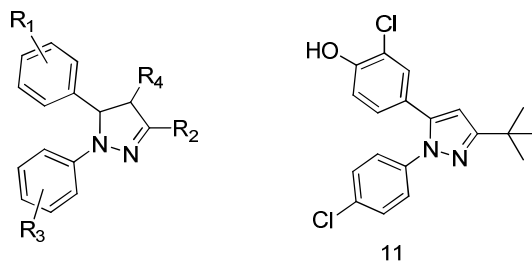
To test the suitability of the scaffold, some initial pyrazoline compounds were synthesized containing, on the one hand, *p*-halogen-substituted phenyl rings like in the previous PIF-pocket-directed compounds. On the other hand, a phenol was introduced to potentially exploit specific features identified in the PIF-pocket of  $\text{PKC}\zeta$ , which were potentially conserved in  $\text{PKC}\zeta$  as well. The  $\text{PKC}\zeta$  PIF-pocket exposed two backbone carbonyl groups that could be targeted by H-bonds, derived from Val281 and Lys278 (Figure 2C). Given the high structural similarity among the atypical PKCs in the catalytic domain, it was expected that the corresponding carbonyl functions are also present in  $\text{PKC}\zeta$ . On the contrary, both carbonyls in the equivalent PDK1 PIF-subpocket are considerably less or not accessible.

All the initially synthesized compounds were screened against recombinant, full length  $\text{PKC}\zeta$  at a concentration of  $62.5\ \mu\text{M}$ ; for compounds showing more than 75% inhibition, the  $\text{IC}_{50}$

## Results

was determined (Table 1). Then at a later stage, favorable features identified with the first compound series were combined. With respect to the determined IC<sub>50</sub>s, it should be noted that the inhibition at compound concentrations lower than 0.2 μM could not be accurately measured, because this was equal to the concentration of the PKCζ protein in the assay.

**Table 1.** Inhibition of recombinant PKCζ and the NF-κB pathway in cells



Cpd No.	R1	R2	R3	R4	Cell free assay		NF-κB reporter gene assay (U937 cells)	
					% inhibition at 62.5 μM <sup>a</sup>	IC <sub>50</sub> (μM) <sup>a</sup>	% inhibition at 5 μM <sup>a</sup>	IC <sub>50</sub> (μM) <sup>a</sup>
1a	4-OH	<i>t</i> -Bu	4-Cl	H	91.5	10.7	75.1	3.2
1b	4-OH	<i>t</i> -Bu	4-F	H	95.5	9.4	63.8	ND <sup>a</sup>
1c	4-OH	<i>t</i> -Bu	4-Br	H	93.2	11.4	58.4	ND
1d	4-OH	<i>t</i> -Bu	4-CF <sub>3</sub>	H	94.2	8.8	ND <sup>b</sup>	ND
1e	4-OH	<i>t</i> -Bu	4-CH <sub>3</sub>	H	88.8	12.6	62.9	ND
1f	4-OH	<i>t</i> -Bu	4-isopropyl	H	54.9	ND	ND <sup>b</sup>	ND
1g	4-OH	<i>t</i> -Bu	4-COOH	H	47.9	ND	40.7	ND
1h	4-OH	<i>t</i> -Bu	3-Cl	H	96.8	5.2	64.6	ND
1i	4-OH	<i>t</i> -Bu	3-F	H	98.1	2.2	73.5	ND
1j	4-OH	<i>t</i> -Bu	3-CF <sub>3</sub>	H	96.1	2.7	89.7	2.7
1k	4-OH	<i>t</i> -Bu	3-CH <sub>3</sub>	H	91.7	3.5	73.7	ND
1l	4-OH	<i>t</i> -Bu	2-Cl	H	57.1	ND	23.5	ND
1m	4-OH	<i>t</i> -Bu	2-F	H	57.6	ND	48.7	ND
1n	4-OH	<i>t</i> -Bu	2,4-dichloro	H	71.0	ND	50.2	ND
1o	4-OH	<i>t</i> -Bu	2,4-difluoro	H	68.0	ND	51.8	ND
1p	4-OH	<i>t</i> -Bu	2,4-dimethyl	H	59.9	ND	41.5	ND
1q	4-OH	<i>t</i> -Bu	2,6-dichloro	H	65.5	ND	12.3	ND
1r	4-OH	<i>t</i> -Bu	3-chloro-4-fluoro	H	98.8	0.9	92.0	1.9
1s	4-OH	<i>t</i> -Bu	3,4-difluoro	H	97.8	0.5	90.1	0.9
1t	4-OH	<i>t</i> -Bu	2,3,4-trifluoro	H	91.7	0.7	84.2	3.1
1u	4-OH	<i>t</i> -Bu	4-H	H	84.3	28.8	38.5	ND
2a	4-OH	phenyl	4-Cl	H	95.6	3.5	50.8	ND
2b	4-OH	phenyl	3-Cl	H	90.5	2.1	42.2	ND
2c	4-OH	2-hydroxyphenyl	4-Cl	H	92.0	1.5	68.2	ND
2d	4-OH	2-methoxyphenyl	4-Cl	H	68.4	ND	26.5	ND
2e	4-OH	2-ethoxyphenyl	4-Cl	H	42.8	ND	48.2	ND
2f	4-OH	2-chlorophenyl	4-Cl	H	90.8	12.7	38.7	ND
2g	4-OH	thiophen-2-yl	4-Cl	H	97.0	0.6	52.8	ND
2h	4-OH	thiophen-2-yl	4-Br	H	95.2	0.5	64.2	ND
2i	4-OH	thiophen-2-yl	4-CF <sub>3</sub>	H	99.4	0.4	76.3	2.9
2j	4-OH	pyridin-2-yl	3-Cl	H	82.2	6.2	70.2	ND
2k	4-OH	pyrrol-2-yl	3-Cl	H	63.0 <sup>c</sup>	0.5	54.1	ND
2l	4-OH	4-aminophenyl	4-Cl	H	98.0	5.4	42.3	ND
3l	4-F	<i>t</i> -Bu	4-Cl	H	0	ND	3.7	ND
3m	4-Cl	<i>t</i> -Bu	4-Cl	H	11.8	ND	5.5	ND
3n	4-Br	<i>t</i> -Bu	4-Cl	H	39.0	ND	9.3	ND
3o	4-CN	<i>t</i> -Bu	4-Cl	H	20.7	ND	20.1	ND
3p	4-OMe	phenyl	4-Cl	H	21.1	ND	2.9	ND
3q	4-OH	Me	4-Cl	H	58.8	ND	50.8	ND
4a	3-OH	<i>t</i> -Bu	4-Cl	H	95.6	5.3	89.9	2.0
4b	4-OH	<i>t</i> -Bu	4-OH	H	40.9	ND	35.0	ND
4c	4-Cl	<i>t</i> -Bu	4-OH	H	72.2	ND	37.3	ND
4d	3-F,4-OH	<i>t</i> -Bu	4-Cl	H	98.5	3.8	95	3.7

## Results

<b>4e</b>	3-Cl,4-OH	<i>t</i> -Bu	4-Cl	H	94.5	0.7	85	2.9
<b>4f</b>	4-F,3-OH	<i>t</i> -Bu	3-Cl	H	75.0 <sup>c</sup>	0.3	92.8	2.5
<b>4g</b>	3,4-dihydroxy	2-hydroxyphenyl	4-Cl	H	89.7 <sup>c</sup>	<0.1	62.0	ND
<b>4h</b>	3-F,4-OH	2-hydroxyphenyl	3-Cl	H	64.7 <sup>c</sup>	2.9	71.7	ND
<b>4i</b>	3,5-difluoro-4-OH	2-hydroxyphenyl	3-Cl	H	62.0 <sup>d</sup>	11.1	75.1	2.5
<b>4j</b>	2,3-difluoro-4-OH	2-hydroxyphenyl	3-Cl	H	69.4 <sup>d</sup>	6.6	81.7	1.4
<b>4k</b>	3-F,4-OH	2,4-dihydroxyphenyl	3-Cl	H	89.0 <sup>c</sup>	<0.1	87.4	1.1
<b>5a</b>	4-NO <sub>2</sub>	<i>t</i> -Bu	4-Cl	H	0	ND	5.9	ND
<b>6a</b>	4-NH <sub>2</sub>	<i>t</i> -Bu	4-Cl	H	19.0	ND	22.7	ND
<b>6b</b>	4-NH <sub>2</sub>	<i>t</i> -Bu	2,4-difluoro	H	52.3	ND	23.5	ND
<b>6c</b>	4-NH <sub>2</sub>	<i>t</i> -Bu	3-Cl	H	53.6	ND	42.3	ND
<b>6d</b>	3-NH <sub>2</sub>	<i>t</i> -Bu	4-Cl	H	18.7	ND	21.9	ND
<b>6e</b>	4-NH <sub>2</sub>	cyclopropyl	3-Cl	H	57.4	ND	24.5	ND
<b>6f</b>	4-NH <sub>2</sub>	1-methylcyclopropyl	3-Cl	H	55.6	ND	47.7	ND
<b>6g</b>	4-NH <sub>2</sub>	cyclohexyl	4-Cl	H	9.1	ND	30.9	ND
<b>6h</b>	4-NH <sub>2</sub>	thiophen-2-yl	3-Cl	H	33.0	ND	44.9	ND
<b>6i</b>	4-NH <sub>2</sub>	furan-2-yl	3-Cl	H	48.1	ND	26.1	ND
<b>6j</b>	4-NH <sub>2</sub>	2-chlorophenyl	3-Cl	H	1.3	ND	24.4	ND
<b>6k</b>	4-NH <sub>2</sub>	2-trifluoromethylphenyl	3-Cl	H	24.0	ND	50.8	ND
<b>6l</b>	4-NH <sub>2</sub>	2-methylphenyl	3-Cl	H	30.0	ND	31.3	ND
<b>6m</b>	4-NH <sub>2</sub>	2-methoxyphenyl	3-Cl	H	28.3	ND	28.2	ND
<b>6n</b>	4-NH <sub>2</sub>	benzo[d][1,3]dioxol-5-yl	3-Cl	H	38.0	ND	22.2	ND
<b>7a</b>	4-NHCOCH <sub>3</sub>	<i>t</i> -Bu	4-Cl	H	45.1	ND	25.5	ND
<b>9</b>	3-F,4-OH	2-hydroxyphenyl	3-Cl	CH <sub>3</sub>	81.8 <sup>c</sup>	0.72	73.0	ND
<b>11</b>	-	-	-	-	54.0 <sup>d</sup>	17.4	93.0	3.0
<b>A</b>	-	-	-	-	54.6 <sup>d</sup>	15.9	6.4	ND

<sup>a</sup>Values are mean values of at least two experiments; standard deviation <15%; <sup>b</sup>compounds were toxic in the MTT assay (Supplementary Table S3); <sup>c</sup>% inhibition is shown at 10  $\mu$ M; <sup>d</sup>% inhibition is shown at 20  $\mu$ M; ND: not determined

While the *p*-halogen-substituted prototype compounds (at both the 1- and 5-phenyl) showed only little activity towards the purified enzyme (**3m-n**), **1a** inhibited PKC $\zeta$  by more than 90% (Table 1). The IC<sub>50</sub> was determined to be 10.7  $\mu$ M, thus showing somewhat higher activity than the most potent compound from the previous series of allosteric PKC $\zeta$  inhibitors, compound **A** (named **1q** in <sup>37</sup>), for which we determined an IC<sub>50</sub> of 15.9  $\mu$ M. This value was close to the previously reported IC<sub>50</sub> for this compound (18  $\mu$ M).<sup>37</sup>

Using the hit compound **1a** as a template, numerous sites of modification around the pyrazoline ring system were explored, as described in the following.

### The 5-phenyl

As observed already in the initial screening, the phenolic OH at the *para*-position of **1a** was found to be essential for activity; like chlorine and bromine, fluorine could not successfully replace this OH either (compound **3l**). Next, we tested several H-bond acceptor (HBA) functions, including the lipophilic and electron-withdrawing nitro function as well as the more hydrophilic cyano group (compounds **5a** and **3o** respectively), which, however, completely abolished the inhibitory activity. Replacing the phenolic OH in compound **2a** by a methoxy function (compound **3p**) resulted in an almost inactive compound as well. Altogether, these findings indicated that the crucial role of the hydroxyl function came from its H-bond donating ability. In the light of these results, the amino group was conceivable as a possible bioisostere. Therefore, we synthesized a series of aniline derivatives including compounds **6a-n**. Surprisingly, none of these aromatic amine compounds showed an activity comparable to that of the hit **1a**, giving

## Results

---

clear indication that the primary amine function cannot replace the hydroxyl in its interaction with the target amino acid(s). Shifting the amino function to the *meta*-position (compound **6c**) did not recover the potency either. The largely reduced activity might be attributed to the lower  $\delta+$  character of the amine hydrogen atoms or to the slightly different spatial orientation of the aromatic amine. To increase the H-bond donor (HBD) capacity of the amino function, the amino group in compound **6a** was acetylated to yield the acetamido analogue of **1a** (compound **7a**). This modification recovered some of the activity compared with **6a**, but the potency was still considerably lower than that of **1a**, suggesting that the acetyl moiety was not well tolerated by the PIF-subpocket.

Compound **4a**, a positional isomer of **1a**, in which the hydroxyl group is shifted to the *meta*-position, was synthesized to investigate the optimal position of the hydroxyl group. This modification led to a modest increase of activity by roughly 2 fold, suggesting that a more efficient hydrogen bonding might occur from the *meta*-position. In compounds synthesized later, after optimization at other positions, it was therefore logic to include a compound with a 3,4-dihydroxy function (catechol derivative) to test if this might further improve the potency by establishing a bidentate H-bond interaction with the putative carbonyl oxygen, or by targeting even two different carbonyl functions. Indeed, compound **4g** showed a more than 15 fold increase in activity when compared to the 4-hydroxy congener **2c**.

To further increase the potency through fine-tuning at the phenol ring, we decided to synthesize compounds **4d** and **4e** bearing an additional *m*-fluoro or *m*-chloro substituent adjacent to the essential 4-hydroxyl group. Both halogens triggered superior activity; while the additional *m*-fluoro increased the potency about 3 fold, the *m*-chloro led to a dramatic increase in activity by more than 15 fold. This beneficial effect of the neighboring halogen substitution can be attributed to two major effects: firstly, the electron withdrawing effect, particularly of the fluorine, increased the partial positive charge on the hydroxyl hydrogen, thus enhancing the strength of the hydrogen bond. Secondly, the presence of the halogen at the aromatic ring restored its lipophilicity, thus increasing the entropy of binding to the rather hydrophobic pocket. Obviously, the second effect prevailed as indicated by the larger impact of the chlorine. As another potential benefit, this *meta*-halogen substitution was also expected to improve the stability of the hydroxyl group towards metabolic phase II conjugation reactions which might be important for *in vivo* activity.<sup>44, 45</sup>

### The 1-phenyl

To test the importance of the halogen substitution, we synthesized compound **1u** which lacked the 4-chloro of **1a**. The higher  $IC_{50}$  showed that the 4-chloro is important for activity, which was consistent with the previous observation with PIF-pocket-directed PKC $\zeta$  inhibitors, in which ring substitutions with halogens or alkyl had a large impact on the potency and possibly also on the selectivity.<sup>37</sup> Several compounds bearing various lipophilic electron withdrawing

## Results

---

substituents, comprising 4-fluoro, 4-bromo and 4-trifluoromethyl, were prepared (compounds **1b-d**, respectively). All of them showed inhibitory activity comparable with that of the 4-chloro analogue, and this finding was consistent with the result obtained for compounds **2g-i** also substituted with 4-chloro, 4-bromo and 4-trifluoromethyl at the 1-phenyl ring, respectively (further discussed below). Interestingly, replacing the 4-chloro in **1a** by 4-methyl (compound **1e**) kept the activity at a similar level, suggesting that mainly the lipophilic character of the 4-substituent rather than its electronegativity is the important factor for the improvement of the activity. This was confirmed by synthesizing compounds **1g** and **4b** with polar hydrophilic substituents (4-carboxy and 4-hydroxy, respectively). The presence of such polar groups was obviously deleterious to the activity, in agreement with their putative binding to the entirely hydrophobic subpocket 2 lacking any accessible HBD/HBA function (Figure 4, binding model). However, sensitivity to steric hindrance at the 4-position of this aromatic ring with regard to potency was found, as replacing the 4-methyl in compound **1e** by a bulkier branched alkyl like isopropyl (compound **1f**) significantly decreased the activity.

Moving the lipophilic substituent from *para*- to the *meta*-position brought this group in an even better position for interaction with the pocket; this was evident from compounds **1h-k**, substituted by *m*-chloro, *m*-fluoro, *m*-trifluoromethyl and *m*-methyl, respectively, which showed about two- to four times higher potencies than the corresponding *p*-substituted analogues (**1a-b** and **1d-e**). The finding that both the *para*- and the *meta*-substitution had a boosting effect prompted us to synthesize some hybrid compounds with 3,4-disubstitutions. Interestingly, compounds **1r** with 3-chloro-4-fluoro, and **1s** with 3,4-difluoro substituents were among the most active compounds with submicromolar IC<sub>50</sub>s, indicating at least additive effects of the lipophilic substituents at these two positions. On the other hand, lipophilic substitution of the *ortho*-position as in the case of compounds **1l** (*o*-chloro) and **1m** (*o*-fluoro) dramatically reduced the activity when compared to the corresponding *meta*-substituted analogues. This unfavorable effect of the *ortho*-substitution was also confirmed by the di-substituted analogues **1n** (2,4-dichloro), **1o** (2,4-difluoro), **1p** (2,4-dimethyl), and **1q** (2,6-dichloro). This was unexpected since it was assumed that the *ortho* effect would actually stabilize the biologically active conformation and hence increase the binding affinity. It could be speculated that a steric clash of the *ortho*-substituent with the border of the hydrophobic subpocket might hinder binding of the compounds, or might push away the helix alpha-C, thus impairing the putative H-bond interaction of the pyrazoline imine with the helix residue Lys301 (cf. Figure 2A; Arg131 is equivalent to Lys301 in PKC $\zeta$ ).

However, in compound **1t** with 2,3,4-trifluoro substitution, the effect of the *ortho*-fluoro on activity was minimal, maintaining a submicromolar IC<sub>50</sub> similar to the potent 3,4-difluoro analogue (compound **1s**). In **1t**, favorable synergistic effects of the *para*- and *meta*-fluorine substitution seemed to outbalance the adverse effect observed with the isolated *ortho*-

## Results

---

substitution. Such favorable interaction could potentially be explained by dipole–dipole interactions with the peptide backbone from Leu328 of the  $\beta$ -sheet bordering subpocket 2.

### Substituent at position 3

To explore the relative importance of the bulky *t*-butyl substituent in hit compound **1a**, we started the modifications by contracting it to a methyl group (compound **3q**). Rather unexpectedly, this modification caused a considerable drop of activity. This result was not anticipated because the third substituent of the pyrazoline core was not expected to bind to the PIF-pocket, rather the binding model predicted that it would point outside the pocket. Nevertheless, the favorable effect of the *t*-butyl group on the affinity could be explained based on the binding model. Firstly, the strong positive inductive effect of the *t*-butyl might be propagated via the conjugated double bond, thus increasing the electron density and hence the H-bond acceptor strength of the pyrazoline nitrogen. However, an even more important, parallel effect of the bulky *t*-butyl group might be the shielding of this potential H-bond with the pyrazoline nitrogen from water molecules. This might be particularly relevant here in the case of a highly water accessible surface pocket, where H-bonds are strongly competed and weakened by water molecules. Schmidtke et al. showed that shielding such a H-bond by an ethyl “lid” provided by the ligand created a more lipophilic binding groove which significantly stabilized and enhanced the H-bond interaction.<sup>46</sup> In the future, this concept might receive broad attention especially in the growing field of protein-protein interaction inhibitors, even though it might not seem logic at first sight to introduce a (bulky) lipophilic residue at a water exposed position.

Replacing the *t*-butyl by unsubstituted phenyl increased the activity about 3 times (compounds **2a-b**), which might be explained by additional interactions exerted by the aromatic  $\pi$ -electrons, such as CH- $\pi$  or cation- $\pi$  interactions. Interestingly, it was previously reported that such a cation- $\pi$  interaction effectively enhanced the binding affinity of a ligand by up to 8 kJ/mol at a fully solvent exposed binding site, proving that such an interaction is not attenuated by hydration effects.<sup>47</sup> It might thus successfully substitute H-bond interactions in cases where the binding site cannot be protected from water molecules.

A further two fold increase in activity was achieved by substituting this phenyl with a hydroxyl group at the *o*-position (compound **2c**) which might be at least partially attributed to the mesomeric enhancement of the  $\pi$ -electron system. In addition, calculations of the lowest energy conformer of **2c** (Supplementary Figure S1) suggested that the hydroxyl group forms an intramolecular H-bond with the pyrazoline nitrogen, thus fixing the phenyl ring in a favorable position, also resulting in a smaller entropic penalty upon ligand binding. Furthermore, the hydroxyl oxygen is potentially available as an alternative HBA for Lys301 (see Figure 4, binding model). In contrast, the loss of this conformational constraint in the methoxy- and ethoxy-substituted analogues (**2d** and **2e**, respectively) was accompanied by a gradual decrease of the

## Results

---

potency. As could be confirmed by *ab initio* calculations, the ether oxygen in these compounds was preferably pointing to the opposite side due to electrostatic repulsion with the pyrazoline nitrogen.

Substitution of the 4-position with an amino group (**2l**) did not increase the activity compared to the unsubstituted phenyl, apparently contradicting the presumed cation- $\pi$  interaction. However, a closer inspection of the calculated electrostatic potential surface (Supplementary Figure S1) revealed that the strong electron donating effect of the amino function slightly increased the electron density even at the *p*-hydroxy on the 5-phenyl, thus negatively affecting the H-bond donor strength. The same effect was also observed in the case of the 2-methoxy and ethoxy substituents, but not with the 2-hydroxyl analogue **2c** or the unsubstituted analogue **2a**, providing another explanation for the substantially decreased activity of the two alkoxy derivatives.

Replacing this 2-hydroxyl by a lipophilic, electron-withdrawing group like chlorine led to more than eight fold reduction in potency (compound **2f**), also corroborating that a higher electron density was favorable for the activity.

Next, some heteroaryl rings were introduced instead of the phenyl in compounds **2a-b**, starting with a mildly basic heterocycle like 2-pyridyl (compound **2j**) which would improve the physicochemical properties and could potentially offer its nitrogen as HBA. However, the activity was reduced by about three fold compared with that of **2b**, indicating that an electron-poor heterocycle was inferior to phenyl. Moreover, the pyridine nitrogen apparently could not replace the pyrazoline imine as HBA, which might be due to electrostatic repulsion between the lone pairs of the nitrogen atoms, forcing the pyridine nitrogen to rotate to a position opposite to the imine (Supplementary Figure S1). On the other hand, the thiophene ring in compounds **2g-i** caused remarkable increase in activity by more than six fold when compared with the unsubstituted phenyl analogue (compare **2g** with **2a**). A similar improvement was observed with the pyrrole analogue **2k**. The higher potency conferred by the five-membered heterocycles compared with the phenyl might be attributed to the higher electron polarizability of these ring systems, enabling superior Van der Waals and  $\pi$ -electron-dependent interactions.

In summary, the SARs were fully consistent with a cation- $\pi$  interaction, as the  $\pi$ -electron density highly correlated with the potency – with the only exception of **2l**, as discussed above.

As can be concluded from the SARs, the electronic properties and bulkiness of the substituents in position 3 allow the adjustment of the electron density and water accessibility of the pyrazoline nitrogen, respectively, but can also slightly influence the H-bond donor capacity of the essential hydroxyl function. Aromatic systems could serve as  $\pi$ -electron donors to Lys301 in addition. Furthermore, since the 3-position of the pyrazoline ring tended to be very tolerant with respect to a variety of substituents like bulky alkyls, hydroxylated phenyl, and heteroaryl

## Results

rings, it was identified as a key position for the optimization of the physicochemical properties such as water solubility and logP.

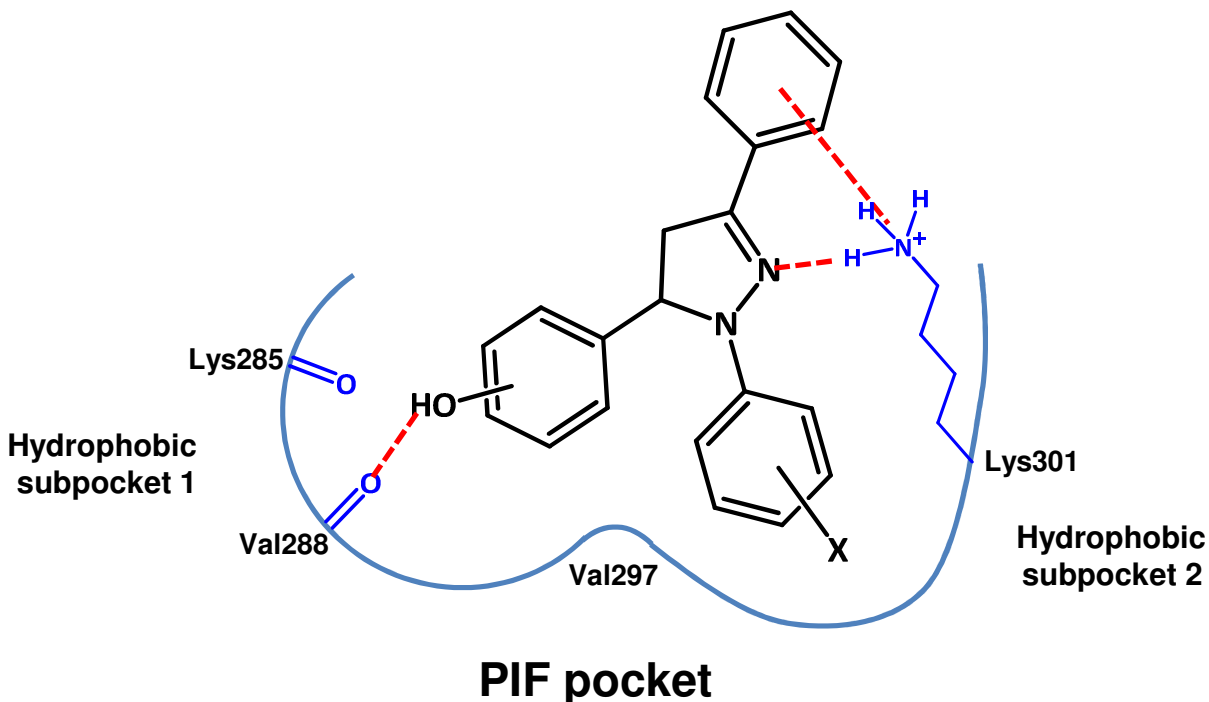


**Figure 4.** Model for the hypothetical interaction of the triphenylpyrazoline analogues based on the SAR. Given the high homology to the crystallized PKC $\zeta$  isoform, the PIF-pocket of PKC $\zeta$  can be assumed to feature two mostly hydrophobic subpockets which accommodate the two phenyl rings (1-phenyl and 5-phenyl). The essential hydroxyl function is thought to interact with the backbone carbonyl of Lys285 or Val288 (Lys278 and Val281, respectively, in PKC $\zeta$ , cf. Figure 2C), thus determining the binding orientation. The 1-phenyl ring binds to the merely hydrophobic subpocket 2. For the potential interaction with Lys301, both the imine nitrogen and the phenyl  $\pi$ -electrons are within appropriate distances.

Finally, the proposed binding model (Figure 4) also was confirmed by synthesizing the inverted analogue of **1a** in which the substituents of the two aromatic rings were reversed (compound **4c**). This inversion resulted in a less active compound, suggesting that the imine nitrogen interaction might be lost if the phenol ring still binds to the same position as with **1a**, thus accounting for the drop of potency. In contrast, the alternative binding mode with the phenol ring docking to the other subpocket was unlikely bearing in mind the huge loss of activity observed with the bisphenol compound **4b**.

### Some combined favorable features and further modifications.

In order to further enhance the binding affinity, it was straightforward to combine some of the favorable modifications identified in the compounds described above. For instance, while the *t*-butyl was kept at position 3 of the pyrazoline, the essential phenolic OH was shifted to *m*-position, combined with an adjacent *p*-fluoro substituent, and a 3-chloro substituent was placed at the 1-phenyl. The resulting compound **4f** proved to be one of the most potent compounds, with an IC<sub>50</sub> of 0.3 μM. In addition, four compounds were prepared (**4h-k**) in which we employed the 2-hydroxyphenyl at position 3 of the pyrazoline as it had augmented the activity before (compound **2c**). As another beneficial effect, we expected a reduction of the logP, while the *ortho*-hydroxyl should be rather protected from phase II conjugation.<sup>48</sup> We first combined this moiety with the 3-fluoro-4-hydroxyphenyl at the 5-position of pyrazoline (**4h**). However, in this case the fluorine did not increase the activity like it was observed before with the 3-*t*-butyl analogue **4d**. In compounds **4i-j**, we added a second fluorine compared with compound **4h**, to yield a difluoro-substitution adjacent to the essential *p*-hydroxyl group at the 4-phenyl residue. Unexpectedly, in compound **4i** this second fluorine in 5-position of the phenyl caused a more than 4 fold decrease in activity compared with **4h**, while in **4j** the second fluorine in *o*-position still reduced the activity by half. Although this di-fluoro substitution in the vicinity of the essential phenolic OH was expected to increase its HBD ability, it decreases at the same time the electron density on the aromatic ring, which might have attenuated putative Van der Waals and CH-π interactions with the aliphatic PIF-pocket residues.

In compound **4k**, an additional 4-hydroxyl group was introduced to the 3-phenyl. Compared with **4h**, this additional OH caused a dramatic increase in activity by more than 29-fold, yielding one of the most potent compounds of the present series. This order of magnitude corresponded to an affinity gain of more than 8.5 kJ/mol as estimated based on the IC<sub>50</sub>s, suggesting that the *p*-hydroxyl could be involved in a potential H-bond with the target site, too.

### Introduction of a fourth alkyl substituent at position 4 of the pyrazoline

Afterwards we decided to test the effect of introducing a fourth small alkyl substituent like methyl at position 4 of the pyrazoline core. Hence, we prepared compound **9** as the 4-methyl analogue of compound **4h**. Interestingly, this 4-methyl led to more than four fold increase in activity compared with compound **4h**, which could be explained either by additional hydrophobic interactions or by the effect of this 4-substitution on the relative orientation of the neighboring groups arising from the pyrazoline core, or by a combination of both effects. It is worth mentioning that alkylation of 1,3,5-trisubstituted pyrazolines at position 4 was reported to increase the chemical stability of the ring towards oxidation to the corresponding pyrazole.<sup>43</sup>

## Results

### Core ring planarity

To test the effect of core planarity (pyrazoline vs. pyrazole), the pyrazole derivative compound **11** was prepared by oxidation of compound **4e**. Switching to the planar pyrazole system caused more than 24 fold drop in activity confirming the importance of the tetrahedral  $sp^3$  hybridized atom (C5) to conserve the dihedral angle enclosed by 1- and 5-phenyl for the biologically active conformation. Moreover, this finding was in agreement with a non ATP-competitive binding mechanism of the pyrazolines, because if the ATP-binding pocket was the target site, conversion to the flat pyrazole ring system should have rather increased the binding affinity. Indeed, trisubstituted pyrazole compounds were reported to be potent ATP-competitive inhibitors of several serine/threonine kinases.<sup>49-52</sup>

### Selectivity and proof of the allosteric mechanism

We screened **1a** and most of the active compounds which showed  $IC_{50}$ s below 10  $\mu$ M for their ability to inhibit the most closely related isoform, PKC $\iota$  (Table 2).

**Table 2.** Inhibition of PKC $\iota$  at 20  $\mu$ M<sup>a</sup>

Cpd No.	PKC $\iota$ % inhibition at 20 $\mu$ M	Cpd No.	PKC $\iota$ % inhibition at 20 $\mu$ M	Cpd No.	PKC $\iota$ % inhibition at 20 $\mu$ M
<b>1a</b>	0	<b>2a</b>	31.6	<b>4a</b>	17.4
<b>1h</b>	43.5	<b>2b</b>	45.5	<b>4d</b>	29.7
<b>1i</b>	19.3	<b>2c</b>	13.4	<b>4e</b>	0
<b>1j</b>	17.0	<b>2h</b>	21.4	<b>4g</b>	44.1
<b>1k</b>	13.9	<b>2i</b>	45.9	<b>4h</b>	25.2
<b>1r</b>	31.6	<b>2j</b>	24.1	<b>4i</b>	45.2
<b>1s</b>	23.7	<b>2k</b>	20.3	<b>4j</b>	39.2
<b>1t</b>	7.8	<b>2l</b>	38.7	<b>9</b>	23.1

<sup>a</sup>Values are mean values of at least two experiments; standard deviation <15%.

Remarkably, **1a** did not show any inhibition even at 40  $\mu$ M, and all the compounds which had shown submicromolar  $IC_{50}$ s towards PKC $\zeta$  did not exhibit appreciable inhibition of PKC $\iota$  at 20  $\mu$ M, indicating that these compounds were highly selective for PKC $\zeta$ . In addition, this finding strongly argued for a non-ATP-competitive mechanism, since the ATP binding sites of both atypical PKCs are lined by almost identical residues, rendering such a degree of selectivity for ATP-pocket-directed compounds rather unlikely. On the other hand, the PIF-pocket in PKC $\iota$  can be regarded as a kind of PKC $\zeta$  PIF-pocket mutant which differs in only two amino acid residues (Leu328 is Phe and His289 is Asn in PKC $\iota$ , respectively).<sup>53</sup> This difference in the PIF-pocket might account for the lack of activity against PKC $\iota$ , suggesting that our compounds were targeting the PIF-pocket in PKC $\zeta$ . It is worth mentioning that even single mutation of Leu328 in PKC $\zeta$  into Phe was enough to abolish the inhibitory activity of the previously published inhibitor compound **C** (PS171 in ref<sup>53</sup>). Furthermore, compound **4f**, the most potent compound among the *t*-Bu analogues was screened against all PKC isoforms and some of the related AGC kinases. Interestingly, **4f** did not show inhibition for all of the tested kinases and only gave weak inhibition for SGK1 by about 20% (Supplementary Table S4). Again, this selectivity for PKC $\zeta$

## Results

vs. other PKC isoform can be explained by the bulkier Phe residue present in the PIF pocket of all PKCs which is replaced by smaller Leu in PKC $\zeta$ .

Consistent with this assumption, a more direct evidence for the allosteric mechanism and targeting of the PIF-pocket was obtained by testing the inhibitory potency of **1a** and three of the more potent congeners (**2c**, **2h** and **4e**) towards PKC $\zeta$  mutated at a residue central to the PIF-pocket (PKC $\zeta$ [Val297Leu]) (Table 3). The inhibitory potencies of compounds **1a**, **2c**, and **2h** were reduced by a factor of more than two, while for compound **4e**, we noticed a more than 20 fold increase of the IC<sub>50</sub> against the mutant. The latter finding might be explained by a steric clash of the *m*-chloro with the larger Leu297 residue in the mutated PIF-pocket, and was in agreement with the proposed binding model (cf. Figure 4).

**Table 3.** Inhibition of PKC $\zeta$  [Val297Leu] vs. PKC $\zeta$  [wt]<sup>a</sup>

Cpd No.	IC <sub>50</sub> ( $\mu$ M),PKC $\zeta$ [Val297Leu]	IC <sub>50</sub> ( $\mu$ M),PKC $\zeta$ [wt]	Relative potency (wt vs. mutant)
<b>1a</b>	26.7	10.7	2.5
<b>2c</b>	3.1	1.5	2.1
<b>2h</b>	1.0	0.5	2.0
<b>4e</b>	14.8	0.7	20.8

<sup>a</sup>Values are mean values of at least two experiments; standard deviation <15%.

To further investigate the non-ATP competitive mechanism, we performed reporter dye assays using SYPRO Orange, a dye that is known to change fluorescence dramatically when it binds to hydrophobic patches of proteins, thus being applicable as a conformational sensor (Figure 5).<sup>54</sup> Our results suggested that compounds **1a**, **2i** and **4f** as well as the previously published allosteric inhibitor **A** could induce the exposure of hydrophobic regions in the protein, to which the dye bound, thereby increasing its fluorescence. In contrast, the ATP-competitive PKC inhibitor Ro31-822055 did not trigger this effect. It is likely that the allosteric inhibitors stabilize an inactive protein conformation which renders hydrophobic residues accessible for the reporter dye.

In addition, HEK293 cell transfection experiments using PKC $\zeta$  wild type and [Val297Leu] mutant expression plasmids were performed, to investigate whether the compounds would cause a persistent inactivation of the target kinase. After transfection, the cells were treated with the allosteric inhibitor **4f** and the ATP-competitive compound Ro31-8220, respectively, in serum-free medium. After stimulation of the PI3/PDK1 signaling pathway by IGF-I, the recombinant proteins were isolated from the cells and the enzymatic activity was measured after extensive washing. We found that treatment of the cells with **4f** reduced the specific activity of the isolated wild type PKC $\zeta$  in a concentration-dependent manner (Figure 6). This suggested that the conformational change for which we provided evidence in the SYPRO Orange binding experiment was also induced in the cellular environment, which might have triggered persistent deactivation by cellular regulatory mechanisms, e.g. dephosphorylation.

## Results

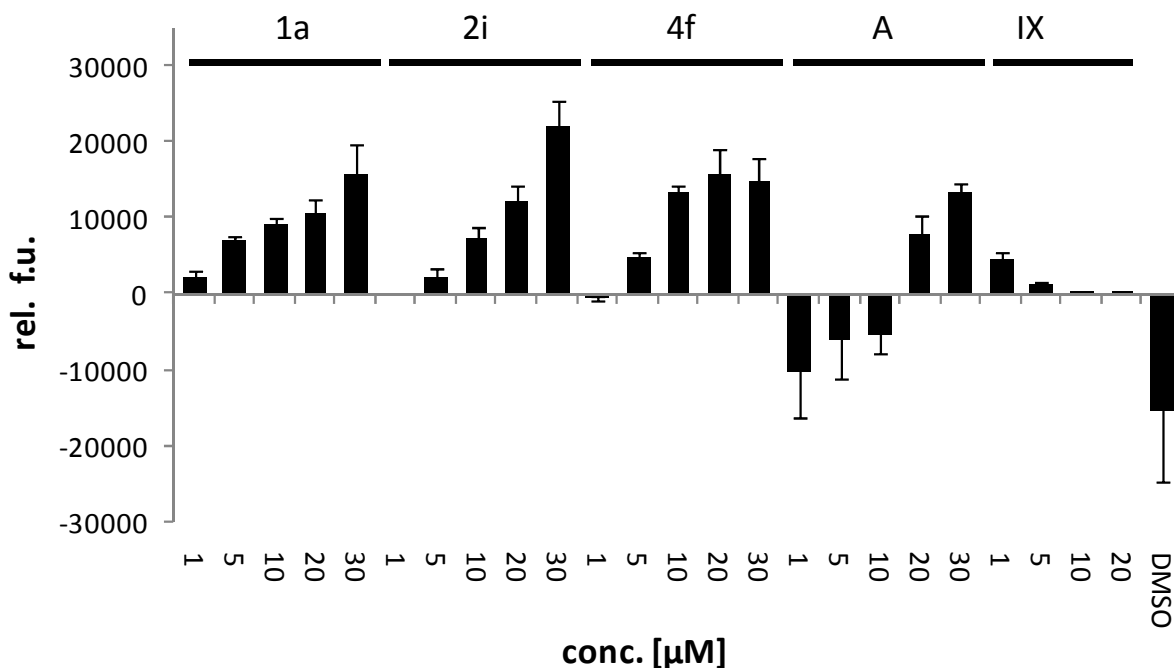


**Figure 5.** Allosteric inhibitors of PKC $\zeta$  increase the exposure of hydrophobic patches. The fluorescence of the indicator dye SYPRO Orange was measured in the presence of recombinant PKC $\zeta$  (0.5  $\mu$ M) and different concentrations of some pyrazoline compounds (**1a**, **2i**, **4f**), the previously published allosteric inhibitor **A**, the ATP-competitive inhibitor Ro31-8220 (**IX**), or DMSO as a control. From each plotted value, the respective fluorescence intensity obtained with the identical mixture but in the absence of PKC $\zeta$  protein was subtracted. All reaction mixtures were incubated for 4 min at 37°C before measurement. The data shown are representative for a set of three independent experiments which gave essentially the same results. Indicated are the relative fluorescence units with standard deviations.

Such a mechanism was observed earlier with allosteric inhibitors and type II inhibitors which shift the intracellular equilibrium toward inactive conformations of the target kinases, thereby promoting dephosphorylation, as exemplified for a type II inhibitor of PDK1.<sup>56</sup> In contrast, the enzymatic activity of the PKC $\zeta$  protein isolated from the Ro31-8220-treated cells was not significantly altered compared to the DMSO-treated control. Ro31-8220 was chosen for this transfection experiment because it is more selective for PKCs than staurosporine and does not inhibit PI3-kinase/PDK1-dependent signaling,<sup>57</sup> which might have artificially blocked the potential intracellular re-phosphorylation and activation of the recombinant enzyme by PDK1 during IGF-I stimulation. In addition, Ro31-8220 was reported to effectively inhibit PKC $\zeta$  and  $\eta$  in transfected cells at concentrations of 2-3  $\mu$ M.<sup>58, 59</sup>

In order to prove that the sustained reduction of the PKC $\zeta$  activity was specifically dependent on the PIF-pocket, the same experiment was performed in parallel using the PKC $\zeta$ [Val297Leu] mutant expression plasmid. Indeed, treatment of the transfected cells with **4f**

## Results

did not affect the specific activity of the mutant PKC $\zeta$  relative to the DMSO-treated control samples, demonstrating that deactivation of the kinase required an intact PIF-pocket.

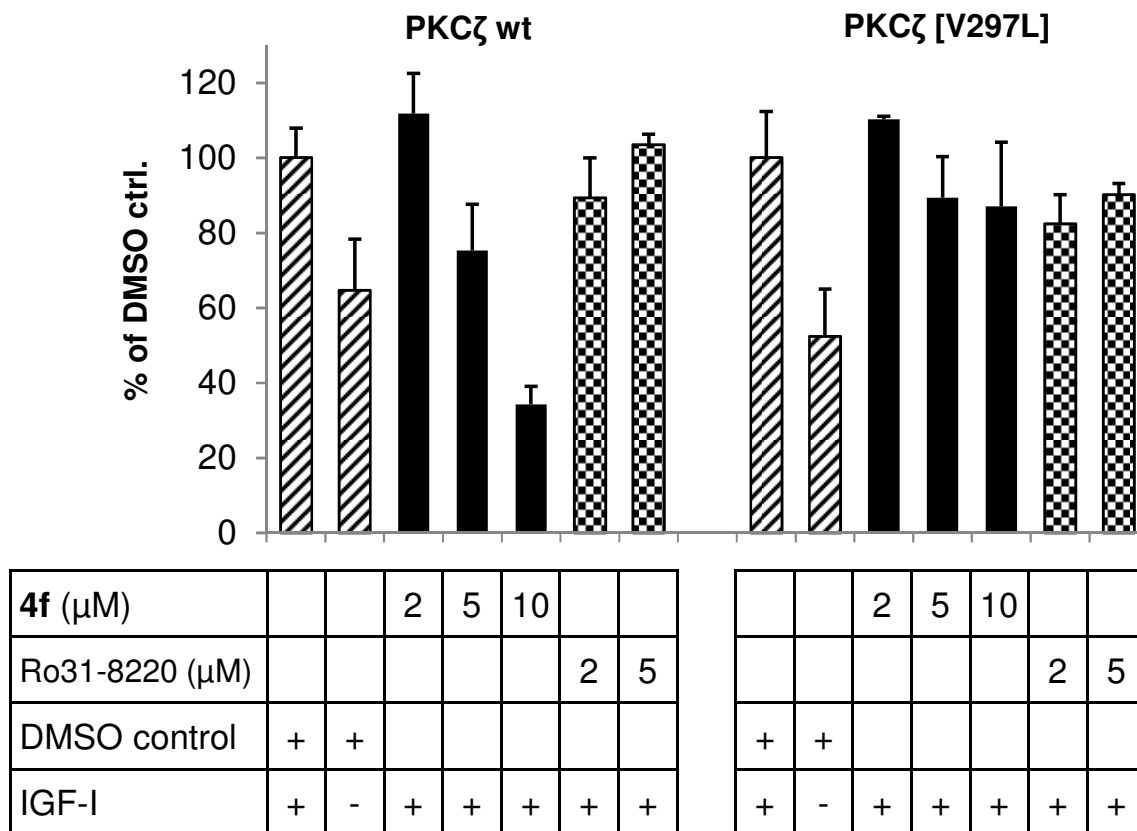


**Figure 6.** Compound **4f** induces deactivation of PKC $\zeta$  in cells. HEK293 cells were transfected with GST-PKC $\zeta$  wild type and [Val297Leu] mutant expression plasmids, and incubated with **4f**, the bisindolylmaleimide Ro31-8220 or DMSO, respectively, for 6h in serum-free medium. After stimulation with IGF-I for 30 min, the cells were lysed and the recombinant proteins pulled down using glutathione agarose. The purified PKC $\zeta$  was eluted from the beads using glutathione and the enzymatic activity was measured in a phosphorylation assay. All treatments were done in triplicates; shown are the representative values of two independently performed experiments.

In summary, this experiment showed that the allosteric inhibitors of PKC $\zeta$  might offer an additional advantage over ATP-competitive inhibitors under *in vivo* conditions which might have implications on the efficacy, future studies will show whether there is even a persistent inactivation caused by allosteric inhibitors of PKC $\zeta$ , because deactivation of PKC $\zeta$  is likely to persist after washout of the inhibitor in the conditions of the experiment. Altogether, our experimental data strongly corroborated that the binding site of the allosteric PKC $\zeta$  inhibitors was the PIF-pocket.

Cellular Effects on the NF- $\kappa$ B Signaling Pathway

To analyze cellular effects on the NF- $\kappa$ B signaling pathway, the U937 cell line was chosen, where PKC $\zeta$  is strongly expressed and is essential for the NF- $\kappa$ B activation.<sup>15,60</sup> Transfections were performed using a reporter gene plasmid expressing luciferase under control of NF- $\kappa$ B response elements to monitor PKC $\zeta$ -induced effects on NF- $\kappa$ B activation (the principle of assay is illustrated in Figure 7). All the compounds were tested in the reporter gene assay at a 5  $\mu$ M concentration, and the IC<sub>50</sub> was determined for compounds showing 75% inhibition or higher (Table 1).

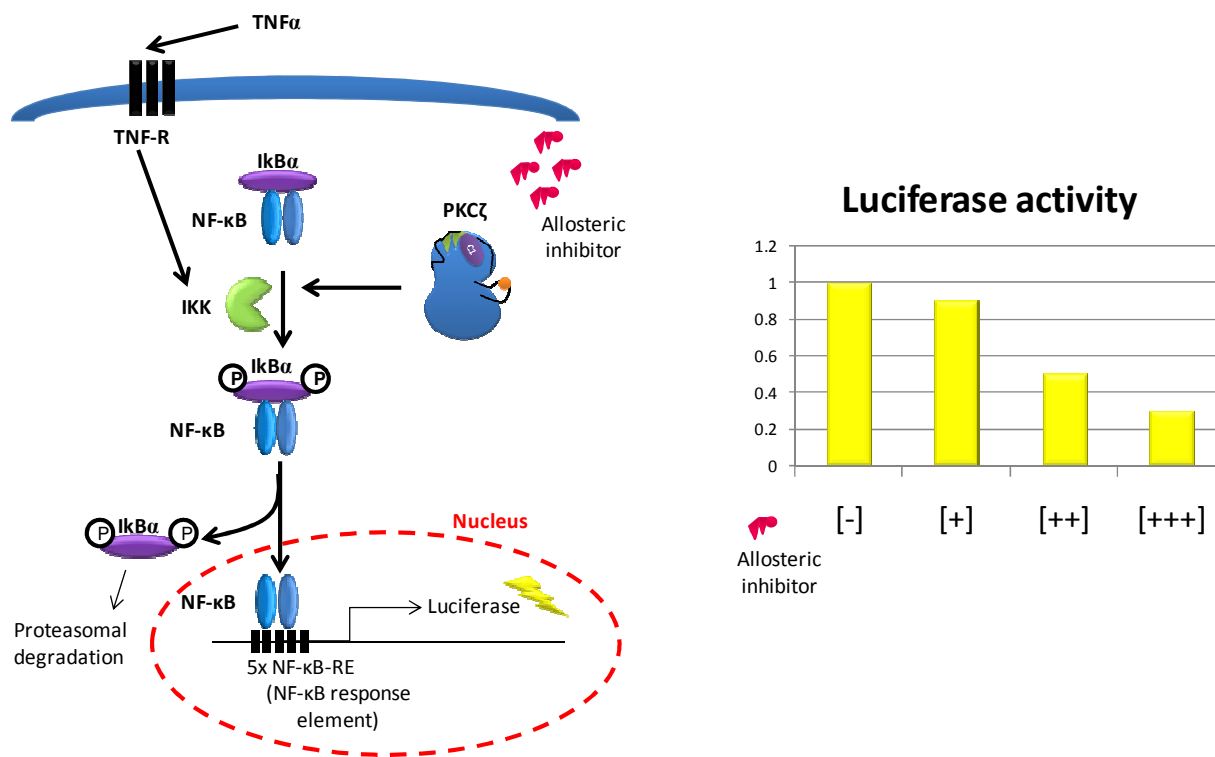


Figure 7: Reporter gene assay in U937 cells. Inhibition of PKC $\zeta$  in U937 cells transfected with a reporter gene plasmid expressing luciferase under control of NF- $\kappa$ B response elements is correlated with the inhibition of the produced luminescence in response to TNF $\alpha$ .

From the very beginning, we verified that the hit compound **1a** was effective in this cell-based assay. We found that **1a** was able to disrupt the NF- $\kappa$ B activation cascade as monitored by the reporter enzyme with an IC<sub>50</sub> of 3.2  $\mu$ M (Table 1). Initially, we checked whether the inhibition of another kinase known to participate in the activation of NF- $\kappa$ B could have been responsible for the observed effect. Hence, **1a** was tested towards all kinases associated with the TNF Receptor-1 signaling complex, whose composition in U937 cells had been elucidated.<sup>61</sup> It was found that **1a** did not inhibit any of the purified kinases at a concentration of 10  $\mu$ M (Table S1, Supporting information).

## Results

---

We then analyzed whether there was a correlation between the compounds' potencies in cellular and cell-free conditions. To this end, the compounds were grouped into high, moderate and low activity categories according to their potencies to inhibit purified PKC $\zeta$  (see Table S2, Supporting Information). Then the Wilcoxon's signed rank test was applied by pair-wise comparison of the corresponding cellular potencies. It was found that compounds with low potency towards the purified PKC $\zeta$  also displayed a significantly lower inhibition of the NF- $\kappa$ B activation than compounds showing a moderate ( $P=0.002$ ) or a strong inhibition ( $P=0.00017$ ) of the purified PKC $\zeta$ . The degree of significance was somewhat lower when comparing the groups with moderate and high inhibition of PKC $\zeta$  in the cell free assay ( $P=0.0273$ ). However, the latter significance was obtained only after excluding the compounds with plain 3-aryl and hetero aryl moieties from the analysis, all of which had uniformly impaired the cellular activity of the compounds when compared to the 3-*t*-butyl analogues (see below). Altogether, the statistical significance corroborated that PKC $\zeta$  was also the intracellular target of the pyrazoline compounds, consistent with our data from the HEK293 cell transfection experiment.

As already anticipated by the statistical analysis, many structural modifications caused the same trend both for the cell-free and the cellular potencies (Table 1). In particular, the phenolic OH at the 1-phenyl was essential for PKC $\zeta$  cellular inhibitory activity as well, since all compounds lacking the phenolic OH were inactive (cf. compounds **3l-p** and **5a**). Similarly, the aniline derivatives **6a-d** and **6h** were all less active than their respective phenolic analogues.

Compound **1s** with 3,4-difluoro-substitution at the 1-phenyl was the most active compound in cells with an IC<sub>50</sub> of 0.9  $\mu$ M. It could be noticed that introduction of multiple fluorine atoms at the 1-phenyl was an effective means to enhance the cellular potency (compounds **1s**, **1j**, **2i** and **1t**).

Unlike in the cell-free assay, it was clearly observed that the plain aryl and heteroaryls at position 3 of the pyrazoline were not a superior replacement for the *t*-Bu group of **1a**, since compounds **2a-b**, **2g-h** and **2j-k** showed equal or worse inhibition of the reporter gene activity when compared with their *t*-butyl analogues **1a** and **1g**. This could be possibly explained by an increased non-specific binding of the multi-aryl ring system to other cellular proteins. However, increasing the polarity of the 3-phenyl, e.g. by *ortho*-hydroxylation, resulted in higher cellular potency when compared to the plain phenyl (compounds **2c**, **4h-j**), with the best activity achieved by a 2,4-dihydroxy-substitution in **4k**. This compound was among the two most potent compounds in the cell free assay and displayed the second highest cellular activity with an IC<sub>50</sub> of 1.1  $\mu$ M.

Unexpectedly, the pyrazole analogue **11** was equally active to its respective pyrazoline **4e**, which might be attributed to off-target interactions as the cell-free assay data showed a huge reduction of PKC $\zeta$  inhibition. In addition, the methyl-substitution at position 4 of the pyrazoline (compound **9**) did not add to the activity in cells. The higher lipophilicity of compound **9** might

## Results

have decreased the cellular availability due to reduced solubility in the assay medium and/or increased non-specific interaction (the additional methyl group in compound **9** raised the calculated logP by 0.35 to 0.57 units, depending on the calculation method used). Probably for the same reason, we noted that for the more potent compounds, the cellular assay conditions seemed to level the potencies. However, the two most active compounds in cells were found among the most potent submicromolar inhibitors in the cell free assay (compounds **1s** and **4k**). Importantly, we were able to improve the cellular potency of the previously reported allosteric PKC $\zeta$  inhibitors by more than one order of magnitude.

### Inhibition of NO formation in RAW 264.7 macrophage cells.

PKC $\zeta$  was reported to be essential for the NF- $\kappa$ B pathway activation in RAW cells.<sup>62</sup> In the same cell line NF- $\kappa$ B activation was required to induce transcription of inducible nitric oxide synthase (iNOS) after LPS stimulation.<sup>63</sup> Hence, iNOS is one of the enzymes that are transcriptionally co-regulated by PKC $\zeta$  signaling pathway; accordingly, our allosteric PKC $\zeta$  inhibitors were expected to suppress the induction of iNOS and to reduce the release of its specific enzymatic product, nitric oxide (NO), in the cell culture medium (the principle of the assay is shown in Figure 8). Indeed, we found that several of our most potent compounds (**4f**, **2h** and **2i**, see Table 4) but not two analogues which were inactive or less active against purified PKC $\zeta$  (**1l** and **1u**) were effectively suppressing the production of NO after LPS stimulation (Table 4) in the low  $\mu$ M range. Furthermore, the hit compound **1a** also triggered iNOS suppression but at a somewhat lower extent than **4f**, **2h** and **2i**, consistent with its less potent inhibition of PKC $\zeta$ . Curcumin, a known inhibitor of iNOS induction<sup>64</sup> was tested in parallel as a positive control (Table 4).

**Table 4.** Inhibition of iNOS induction in RAW 264.7 macrophage cells

Cpd No.	% inhibition at 7.5 $\mu$ M <sup>a</sup>	IC <sub>50</sub> ( $\mu$ M) <sup>a</sup>
1l	26	ND
1u	32	ND
1a	50	7.5
4f	74	4.6
2h	65	3.4
2i	69	2.4
Curcumin	97	0.8

<sup>a</sup>Values are mean values of at least four experiments; standard deviation  $\leq$ 10%.

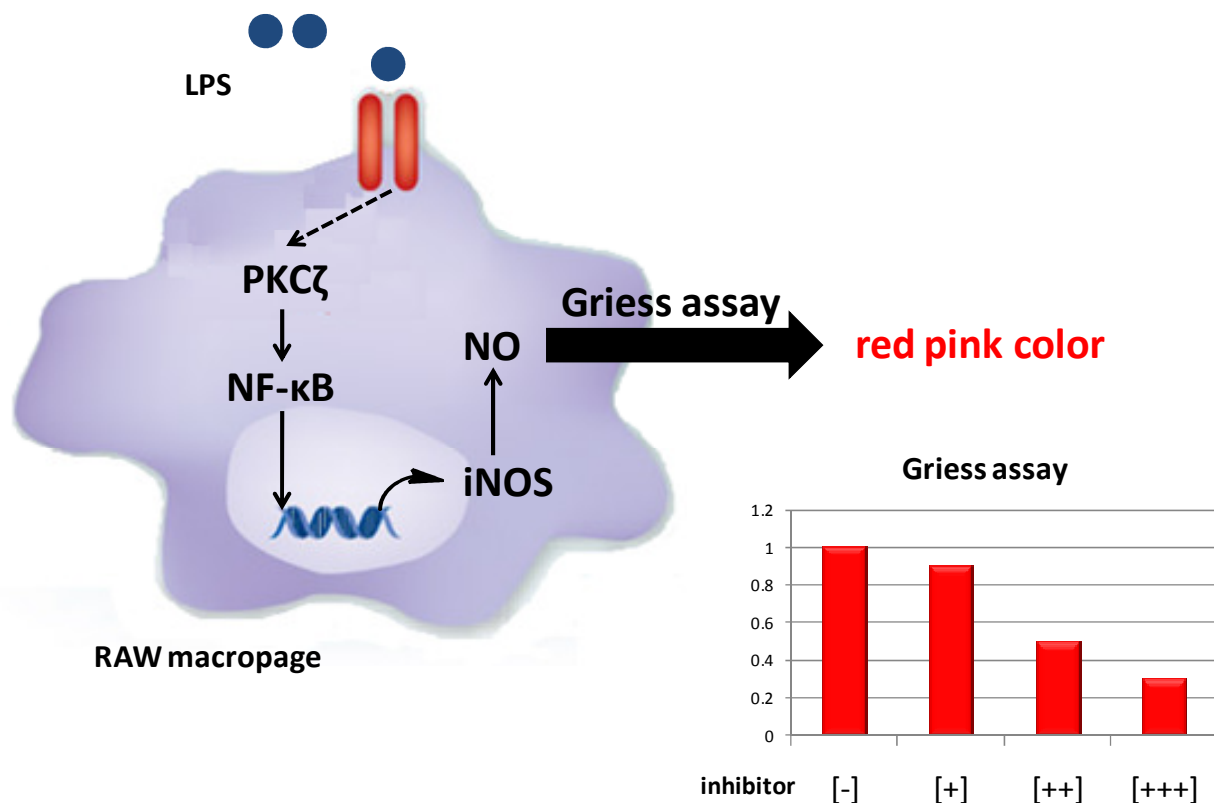


Figure 8: Inhibition of PKC $\zeta$  in RAW cells stimulated with LPS leads to inhibition of iNOS expression and NO production.

## Conclusions

In summary, we have discovered 1,3,5-trisubstituted and 1,3,4,5-tetrasubstituted pyrazolines as a potent and selective class of allosteric PKC $\zeta$  inhibitors. As suggested by the strongly reduced *in vitro* and cellular activities towards a PIF-pocket mutant of PKC $\zeta$ , the compounds were most likely targeting the PIF-pocket on the kinase catalytic domain. Cellular reporter gene and transfection assays confirmed that PKC $\zeta$  was also targeted in the cells. For the first time we could provide evidence that the putative PIF-pocket-directed compounds triggered a persistent deactivation of the target kinase by cellular regulatory mechanisms.

Our novel PKC $\zeta$  inhibitor scaffold proved to be rich in many modifiable positions, all acting as hot spots for improving binding characteristics and displaying sharp SARs. The phenolic group on the 5-phenyl was essential for the inhibitory activity, with a catechol providing the best activity. The presence of a lipophilic (halogen or alkyl) substituent on the 1-phenyl proved to be essential for the generation of high potency, with the *meta*-position being the most preferable for mono-substitution, and the 3,4-positions for di-substitution. There was a substantial flexibility with respect to the functionality tolerated at the 3-position of the pyrazoline, with the 2,4-dihydroxy phenyl identified as one of the most favorable motifs for

## Results

---

activity. Furthermore, an additional methyl-substitution at the 4-position of the pyrazoline had a profound effect on potency, in addition to its potential role in stabilizing the pyrazoline ring against oxidation.

## EXPERIMENTAL SECTION

### Chemistry

Solvents and reagents were obtained from commercial suppliers and used as received. A Bruker DRX 500 spectrometer was used to obtain  $^1\text{H}$  NMR and  $^{13}\text{C}$  NMR spectra, in very few cases Varian Mercury VX 300 spectrometer was used for recoding the spectra of some enones. The chemical shifts are referenced to the residual protonated solvent signals and occasionally TMS was used as a reference. At least 95% purity in all the tested compounds (Table 1) was could be verified by means of HPLC coupled with mass spectrometry. Mass spectra (HPLC-ESI-MS) were obtained using a TSQ quantum (Thermo Electron Corporation) instrument prepared with a triple quadrupole mass detector (Thermo Finnigan) and an ESI source. All samples were inserted using an autosampler (Surveyor, Thermo Finnigan) by an injection volume of 10  $\mu\text{L}$ . The MS detection was determined using a source CID of 10 V and carried out at a spray voltage of 4.2 kV, a nitrogen sheath gas pressure of  $4.0 \cdot 10^5 \text{ Pa}$ , a capillary temperature of  $400 \text{ }^\circ\text{C}$ , a capillary voltage of 35 V and an auxiliary gas pressure of  $1.0 \cdot 10^5 \text{ Pa}$ . The stationary phase used was an RP C18 NUCLEODUR 100-3 ( $125 \times 3 \text{ mm}$ ) column (Macherey & Nagel). The solvent system consisted of water containing 0.1% TFA (A) and 0.1% TFA in acetonitrile (B). HPLC-Method: flow rate 400  $\mu\text{L}/\text{min}$ . The percentage of B started at an initial of 5%, was increased up to 100% during 16 min, kept at 100% for 2 min, and flushed back to 5% in 2 min. Melting points were determined using a Mettler FP1 melting point apparatus and are uncorrected.

### General synthetic methods and experimental details for some key compounds.

**General procedure for the enone synthesis.** To a an ice-cooled solution of the appropriate ketone (10 mmol) in MeOH (50 mL), 10 % KOH aq. solution (30 ml) was added, followed by gradual addition of the corresponding aryl aldehyde (10 mmol). The mixture was left to attain room temperature and stirred overnight. The solid product was filtered and washed three times with MeOH/ $\text{H}_2\text{O}$  mixture (5:3) and left to dry. In case of oily products the reaction mixture was extracted by  $\text{CH}_2\text{Cl}_2$  ( $4 \times 20 \text{ mL}$ ) and the combined organic layers were washed with water, filtered over anhydrous  $\text{MgSO}_4$ , evaporated under reduced pressure and used without further purification.

**(E)-1-(4-(*tert*-butoxy)phenyl)-4,4-dimethylpent-1-en-3-one (E1).** Synthesized according to the procedure for the enone synthesis using pinacolone and 4-(*tert*-butoxy)benzaldehyde; yellow solid; yield: 2 g (77 %); mp  $110\text{-}111 \text{ }^\circ\text{C}$ ;  $^1\text{H}$  NMR (500 MHz,  $\text{CDCl}_3$ )  $\delta$  7.63 (d,  $J = 15.6 \text{ Hz}$ ,

## Results

---

1H), 7.49 – 7.45 (m, 2H), 7.00 – 6.95 (m, 3H), 1.36 (s, 9H), 1.20 (s, 9H); <sup>13</sup>C NMR (125 MHz, CDCl<sub>3</sub>) δ 204.22, 157.72, 142.55, 129.75, 129.21, 123.75, 119.28, 79.27, 43.16, 28.85, 26.38.

**General procedure for the pyrazoline synthesis.** A mixture of the enone derivative (2 mmol) and the corresponding phenylhydrazine hydrochloride (3 mmol) in 15 mL of anhydrous DMF was heated to 85 °C for 5 h under argon atmosphere. The reaction solution was cooled to room temperature and partitioned between 50 mL of diethyl ether and 20 mL of water. The organic layer was separated and washed with three 20 mL-portions of water. The aqueous layers were combined and extracted with three 20 mL-portions of diethyl ether. The organic layers were combined, dried over anhydrous Na<sub>2</sub>SO<sub>4</sub> and concentrated under reduced pressure. The residue was purified using column chromatography or used in the next step without further purification.

**4-(3-(*tert*-butyl)-1-(4-chlorophenyl)-4,5-dihydro-1H-pyrazol-5-yl)phenol (1a).** The title compound was prepared by reaction of (*E*)-1-(4-(*tert*-butoxy)phenyl)-4,4-dimethylpent-1-en-3-one (**E1**) and 4-chlorophenylhydrazine hydrochloride according to the general procedure for the pyrazoline synthesis. The product was purified by CC (CH<sub>2</sub>Cl<sub>2</sub>/hexane 4:1); beige solid; yield: 0.28 g (44%); mp 111-112 °C; <sup>1</sup>H NMR (500 MHz, DMSO-*d*<sub>6</sub>) δ 9.35 (s, 1H), 7.24 – 7.19 (m, 2H), 7.03 – 6.98 (m, 2H), 6.79 – 6.75 (m, 2H), 6.71 – 6.67 (m, 2H), 5.06 (dd, *J* = 11.6, 6.3 Hz, 1H), 3.48 (dd, *J* = 17.5, 11.6 Hz, 1H), 2.66 (dd, *J* = 17.5, 6.4 Hz, 1H), 1.17 (s, 9H); <sup>13</sup>C NMR (125 MHz, DMSO-*d*<sub>6</sub>) δ 159.87, 156.53, 144.57, 132.56, 131.18, 126.87, 115.58, 114.47, 108.65, 62.71, 42.70, 33.43, 27.88; MS (ESI): *m/z* = 329.18 (M+H)<sup>+</sup>.

**4-(3-(*tert*-butyl)-1-(3,4-difluorophenyl)-4,5-dihydro-1H-pyrazol-5-yl)phenol (1s).** The title compound was prepared by reaction of (*E*)-1-(4-(*tert*-butoxy)phenyl)-4,4-dimethylpent-1-en-3-one (**E1**) and 3,4-difluorophenylphenylhydrazine hydrochloride according to the general procedure for pyrazoline synthesis. The product was purified by CC (CH<sub>2</sub>Cl<sub>2</sub>/hexane 4:1); light brown solid; yield: 0.37 g (57%); mp 95.8 °C; <sup>1</sup>H NMR (500 MHz, DMSO-*d*<sub>6</sub>) δ 9.38 (s, 1H), 7.13 (dt, *J* = 10.6, 9.2 Hz, 1H), 7.07 – 7.00 (m, 2H), 6.80 – 6.73 (m, 1H), 6.73 – 6.68 (m, 2H), 6.55 – 6.50 (m, 1H), 5.04 (dd, *J* = 11.5, 6.7 Hz, 1H), 3.48 (dd, *J* = 17.5, 11.5 Hz, 1H), 2.67 (dd, *J* = 17.5, 6.7 Hz, 1H), 1.17 (s, 9H). <sup>13</sup>C NMR (125 MHz, DMSO-*d*<sub>6</sub>) δ 160.32, 156.61, 149.47 (dd, <sup>1</sup>*J*<sub>C-F</sub> = 241.8, <sup>2</sup>*J*<sub>C-F</sub> = 13.2 Hz), 143.01 (dd, <sup>3</sup>*J*<sub>C-F</sub> = 8.7, <sup>4</sup>*J*<sub>C-F</sub> = 1.2 Hz), 142.15 (dd, <sup>1</sup>*J*<sub>C-F</sub> = 236.1, <sup>2</sup>*J*<sub>C-F</sub> = 11.8 Hz), 132.40, 126.98, 117.28 (d, <sup>2</sup>*J*<sub>C-F</sub> = 17.2 Hz), 115.63, 108.07 (dd, <sup>3</sup>*J*<sub>C-F</sub> = 5.4, <sup>4</sup>*J*<sub>C-F</sub> = 2.7 Hz), 101.16 (d, <sup>2</sup>*J*<sub>C-F</sub> = 21.8 Hz), 63.20, 42.86, 33.42, 27.84; MS (ESI): *m/z* = 330.91 (M+H)<sup>+</sup>.

**General procedure for the ether dealkylation.** A 1 M BBr<sub>3</sub> solution in CH<sub>2</sub>Cl<sub>2</sub> (3-9 equiv) was added dropwise via syringe under nitrogen to a stirred solution of the methyl/ethyl ether derivative (1 mmol, 1 equiv) in CH<sub>2</sub>Cl<sub>2</sub> at -78 °C. Then the reaction was maintained at -78 °C for 1 hour, after that allowed to reach room temperature and stirred for an additional 20 hours. The mixture was cooled to 0 °C and H<sub>2</sub>O was carefully added (15-25 mL). The product was then

## Results

---

repeatedly extracted with EtOAc and the organic layers were dried over anhydrous Na<sub>2</sub>SO<sub>4</sub>. Upon solvent removal the residue was purified by column chromatography.

**4-(3-(*tert*-butyl)-1-(4-chlorophenyl)-4,5-dihydro-1*H*-pyrazol-5-yl)-2-chlorophenol (4e).** The title compound was prepared by demethylation of 3-(*tert*-butyl)-5-(3-chloro-4-methoxyphenyl)-1-(4-chlorophenyl)-4,5-dihydro-1*H*-pyrazole (**3e**) using BBr<sub>3</sub> (3 equiv) according to the general procedure for ether dealkylation. The product was purified by CC (CH<sub>2</sub>Cl<sub>2</sub>/hexane 4:1); off-white solid; yield: 0.18 g (51%); mp 134-136°C; <sup>1</sup>H NMR (500 MHz, DMSO-*d*<sub>6</sub>) δ 10.14 (s, 1H), 7.18 (d, *J* = 2.1 Hz, 1H), 7.15 – 7.11 (m, 2H), 6.96 (dt, *J* = 6.7, 3.4 Hz, 1H), 6.92 – 6.88 (m, 1H), 6.85 – 6.80 (m, 2H), 5.10 (dd, *J* = 11.5, 6.4 Hz, 1H), 3.48 (dd, *J* = 17.6, 11.6 Hz, 1H), 2.69 (dd, *J* = 17.6, 6.4 Hz, 1H), 1.16 (s, 9H); <sup>13</sup>C NMR (125 MHz, DMSO-*d*<sub>6</sub>) δ 159.99, 152.21, 144.12, 134.11, 128.48, 127.17, 125.36, 121.37, 119.74, 117.08, 114.03, 62.25, 42.58, 33.42, 27.85; MS (ESI): *m/z* = 362.65 (M+H)<sup>+</sup>.

**5-(3-(*tert*-butyl)-1-(3-chlorophenyl)-4,5-dihydro-1*H*-pyrazol-5-yl)-2-fluorophenol (4f).** The title compound was prepared by demethylation of 3-(*tert*-butyl)-1-(3-chlorophenyl)-5-(4-fluoro-3-methoxyphenyl)-4,5-dihydro-1*H*-pyrazole (**3f**) using BBr<sub>3</sub> (3 equiv) according to the general procedure for ether dealkylation. The product was purified by CC (CH<sub>2</sub>Cl<sub>2</sub>/hexane 4:1); buff solid; yield: 0.23 g (66%); mp 101-102.5°C; <sup>1</sup>H NMR (500 MHz, DMSO-*d*<sub>6</sub>) δ 9.85 (s, 1H), 7.12 – 7.05 (m, 2H), 6.88 (t, *J* = 2.1 Hz, 1H), 6.78 (dd, *J* = 8.5, 2.1 Hz, 1H), 6.71 – 6.63 (m, 3H), 5.15 (dd, *J* = 11.7, 6.0 Hz, 1H), 3.51 (dd, *J* = 17.6, 11.7 Hz, 1H), 2.69 (dd, *J* = 17.6, 6.0 Hz, 1H), 1.17 (s, 9H); <sup>13</sup>C NMR (125 MHz, DMSO-*d*<sub>6</sub>) δ 160.47, 150.18 (d, <sup>1</sup>*J*<sub>C-F</sub> = 240.5 Hz), 146.33, 145.22 (d, <sup>2</sup>*J*<sub>C-F</sub> = 12.4 Hz), 138.88, 133.38, 130.33, 117.09, 116.59 (d, <sup>3</sup>*J*<sub>C-F</sub> = 6.6 Hz), 116.38 (d, <sup>2</sup>*J*<sub>C-F</sub> = 18.4 Hz), 114.52, 111.81, 110.82, 62.23, 42.53, 33.45, 27.84; MS (ESI): *m/z* = 346.89 (M+H)<sup>+</sup>.

**4-(1-(4-chlorophenyl)-3-(2-hydroxyphenyl)-4,5-dihydro-1*H*-pyrazol-5-yl)benzene-1,2-diol (4g).** The title compound was prepared by demethylation of 1-(4-chlorophenyl)-5-(3,4-dimethoxyphenyl)-3-(2-methoxyphenyl)-4,5-dihydro-1*H*-pyrazole (**3g**) using BBr<sub>3</sub> (9 equiv) according to the general procedure for ether dealkylation. The product was purified by CC (CH<sub>2</sub>Cl<sub>2</sub>/MeOH 99:1); beige solid; yield: 0.31 g (82%); mp 163-164°C; <sup>1</sup>H NMR (500 MHz, DMSO-*d*<sub>6</sub>) δ 10.20 (s, 1H), 8.74 (s, 1H), 8.67 (s, 1H), 7.21 (dd, *J* = 7.8, 1.5 Hz, 1H), 7.05 (dt, *J* = 16.9, 4.9 Hz, 1H), 7.02 – 6.98 (m, 2H), 6.75 (dd, *J* = 8.2, 0.8 Hz, 1H), 6.72 – 6.66 (m, 3H), 6.46 (d, *J* = 8.0 Hz, 1H), 6.42 – 6.33 (m, 2H), 5.04 (dd, *J* = 12.0, 6.3 Hz, 1H), 3.75 (dd, *J* = 17.8, 12.1 Hz, 1H), 3.01 (dd, *J* = 17.8, 6.3 Hz, 1H); <sup>13</sup>C NMR (125 MHz, DMSO-*d*<sub>6</sub>) δ 156.17, 150.59, 145.72, 144.85, 142.48, 132.49, 130.50, 128.76, 128.16, 122.51, 119.56, 116.91, 116.58, 116.09, 115.87, 114.30, 112.69, 61.85, 44.08; MS (ESI): *m/z* = 380.74 (M+H)<sup>+</sup>.

**4-(1-(3-chlorophenyl)-3-(2-hydroxyphenyl)-4,5-dihydro-1*H*-pyrazol-5-yl)-2-fluorophenol (4h).** The title compound was prepared by demethylation of 1-(3-chlorophenyl)-5-(3-fluoro-4-methoxyphenyl)-3-(2-methoxyphenyl)-4,5-dihydro-1*H*-pyrazole (**3h**) using BBr<sub>3</sub> (6 equiv)

## Results

according to the general procedure for the ether dealkylation. The product was purified by CC (CH<sub>2</sub>Cl<sub>2</sub>); beige solid; yield: 0.18 g (49%) ; mp 165-167°C; <sup>1</sup>H NMR (500 MHz, DMSO-*d*<sub>6</sub>) δ 10.32 (s, 1H), 9.89 (s, 1H), 7.48 (dd, *J* = 7.8, 1.6 Hz, 1H), 7.29 (ddd, *J* = 8.3, 7.3, 1.6 Hz, 1H), 7.21 (dd, *J* = 11.0, 5.3 Hz, 1H), 7.12 – 7.07 (m, 1H), 7.00 – 6.89 (m, 5H), 6.85 (ddd, *J* = 8.4, 2.2, 0.8 Hz, 1H), 6.79 (ddd, *J* = 7.9, 2.0, 0.8 Hz, 1H), 5.41 (dd, *J* = 12.0, 6.2 Hz, 1H), 4.01 (dd, *J* = 17.9, 12.0 Hz, 1H), 3.29 (dd, *J* = 17.8, 6.2 Hz, 1H); <sup>13</sup>C NMR (125 MHz, DMSO-*d*<sub>6</sub>) δ 156.21, 151.01 (d, <sup>1</sup>*J*<sub>C-F</sub> = 241.9 Hz), 150.98, 144.79, 144.28 (d, <sup>2</sup>*J*<sub>C-F</sub> = 12.0 Hz), 133.62, 132.86 (d, <sup>3</sup>*J*<sub>C-F</sub> = 5.0 Hz), 130.70 (d, <sup>3</sup>*J*<sub>C-F</sub> = 6.3 Hz), 128.33, 124, 122.05 (d, <sup>4</sup>*J*<sub>C-F</sub> = 3.0 Hz), 119.55, 118.47, 118.30, 116.61, 116.18, 113.83 (d, <sup>2</sup>*J*<sub>C-F</sub> = 18.8 Hz), 112.28, 111.47, 61.12, 44.12; MS (ESI): *m/z* = 382.67 (M+H)<sup>+</sup>.

**4-(1-(3-chlorophenyl)-5-(3-fluoro-4-hydroxyphenyl)-4,5-dihydro-1*H*-pyrazol-3-yl)benzene-1,3-diol (4k).** The title compound was prepared by demethylation of 1-(3-chlorophenyl)-3-(2,4-dimethoxyphenyl)-5-(3-fluoro-4-methoxyphenyl)-4,5-dihydro-1*H*-pyrazole (**3k**) using BBr<sub>3</sub> (9 equiv) according to the general procedure for the ether dealkylation. The product was purified by CC (CH<sub>2</sub>Cl<sub>2</sub>/MeOH 99:1); beige solid; yield: 0.22 g (55%); mp 183-184°C; <sup>1</sup>H NMR (500 MHz, DMSO-*d*<sub>6</sub>) δ 10.41 (s, 1H), 9.89 (d, *J* = 17.4 Hz, 2H), 7.28 – 7.23 (m, 1H), 7.21 – 7.15 (m, 1H), 7.07 (dd, *J* = 9.9, 3.1 Hz, 1H), 6.93 – 6.86 (m, 3H), 6.79 (ddd, *J* = 8.4, 2.2, 0.8 Hz, 1H), 6.75 (ddd, *J* = 7.9, 2.0, 0.8 Hz, 1H), 6.37 (dt, *J* = 8.3, 2.2 Hz, 2H), 5.32 (dd, *J* = 11.8, 6.1 Hz, 1H), 3.94 (dd, *J* = 17.7, 11.8 Hz, 1H), 3.21 (dd, *J* = 17.7, 6.1 Hz, 1H). <sup>13</sup>C NMR (125 MHz, DMSO-*d*<sub>6</sub>) δ 160.14, 158.05, 151.73, 150.99 (d, <sup>1</sup>*J*<sub>C-F</sub> = 241.8 Hz), 145.12, 144.22 (d, <sup>2</sup>*J*<sub>C-F</sub> = 12.1 Hz), 133.59, 132.99 (d, <sup>3</sup>*J*<sub>C-F</sub> = 5.0 Hz), 130.62, 129.58, 122.02 (d, <sup>4</sup>*J*<sub>C-F</sub> = 2.9 Hz), 118.28, 118.02, 113.80 (d, <sup>2</sup>*J*<sub>C-F</sub> = 18.9 Hz), 111.99, 111.22, 108.27, 107.71, 102.55, 60.78, 44.07; MS (ESI): *m/z* = 398.62 (M+H)<sup>+</sup>.

**General reduction procedure.** A suspension of the nitro derivative (1 mmol) and SnCl<sub>2</sub>·2H<sub>2</sub>O (5 mmol, 1.12 g) in MeOH (40 mL) was heated to reflux for 2 h under argon atmosphere. Then MeOH was evaporated under reduced pressure and the residue was dissolved in EtOAc (100 mL) and alkalized with 100 mL aqueous NaHCO<sub>3</sub> solution. The resulting mixture was filtered under vacuum followed by separation of organic and water layers. The aqueous layer was extracted with two 20 mL-portions of EtOAc, the organic fractions were combined, dried over anhydrous Na<sub>2</sub>SO<sub>4</sub> and evaporated under reduced pressure. The residue was purified using column chromatography.

**4-(3-(*tert*-butyl)-1-(4-chlorophenyl)-4,5-dihydro-1*H*-pyrazol-5-yl)aniline (6a).** The title compound was prepared by reduction of 3-(*tert*-butyl)-1-(4-chlorophenyl)-5-(4-nitrophenyl)-4,5-dihydro-1*H*-pyrazole according to the general reduction procedure. The product was purified by CC (CH<sub>2</sub>Cl<sub>2</sub>); buff solid; yield: 0.28 g (87%); mp 131-132°C; <sup>1</sup>H NMR (500 MHz, DMSO-*d*<sub>6</sub>) δ 7.13 – 7.07 (m, 2H), 6.89 – 6.85 (m, 2H), 6.85 – 6.80 (m, 2H), 6.51 – 6.46 (m, 2H), 5.00 (s, 2H), 4.95 (dd, *J* = 11.5, 6.5 Hz, 1H), 3.44 (dd, *J* = 17.5, 11.6 Hz, 1H), 2.64 (dd, *J* = 17.5, 6.6 Hz, 1H),

## Results

1.17 (s, 9H);  $^{13}\text{C}$  NMR (125 MHz, DMSO- $d_6$ )  $\delta$  159.73, 147.86, 144.42, 129.27, 128.28, 126.43, 120.94, 114.14, 113.97, 63.16, 42.73, 33.42, 27.90 ; MS (ESI):  $m/z$ = 327.77 (M+H) $^+$ .

***N*-(4-(3-(*tert*-butyl)-1-(4-chlorophenyl)-4,5-dihydro-1*H*-pyrazol-5-yl)phenyl)acetamide (7a).** Acetylchloride (0.14 mL, 2 mmol) was added gradually to a stirred solution of **6a** (0.33 g, 1 mmol) and  $\text{Na}_2\text{CO}_3$  (0.16 g, 1.5 mmol) in acetone (40 mL) under ice cooling. The mixture was stirred at room temperature under a nitrogen atmosphere for 2h. After pouring to 100 mL of water ice mixture, the solid obtained was separated by filtration followed by CC purification ( $\text{CH}_2\text{Cl}_2/\text{MeOH}$  98:2) to give the title compound as an off-white solid; yield: 0.30 g (81%), mp 119-120°C;  $^1\text{H}$  NMR (500 MHz, DMSO- $d_6$ )  $\delta$  9.91 (s, 1H), 7.53 – 7.49 (m, 2H), 7.17 – 7.07 (m, 4H), 6.83 – 6.79 (m, 2H), 5.11 (dd,  $J$  = 11.6, 6.6 Hz, 1H), 3.51 (dd,  $J$  = 17.5, 11.7 Hz, 1H), 2.68 (dd,  $J$  = 17.5, 6.6 Hz, 1H), 2.01 (s, 3H);  $^{13}\text{C}$  NMR (125 MHz, DMSO- $d_6$ )  $\delta$  168.16, 159.85, 144.25, 138.42, 136.88, 128.41, 126.10, 121.24, 119.50, 113.98, 62.92, 42.64, 33.43, 27.87, 20.73; MS (ESI):  $m/z$ = 369.75 (M+H) $^+$ .

**1-(3-chlorophenyl)-5-(3-fluoro-4-methoxyphenyl)-3-(2-methoxyphenyl)-4-methyl-4,5-dihydro-1*H*-pyrazole (8).** To a three-necked flask containing 20 mL of dry THF 0.6 mL of a lithium diisopropylamide (LDA) solution (2M in THF/*n*-heptane/ethylbenzene) was added under argon atmosphere, followed by a solution of 411 mg (1 mmol) of 1-(3-chlorophenyl)-5-(3-fluoro-4-methoxyphenyl)-3-(2-methoxyphenyl)-4,5-dihydro-1*H*-pyrazole (**3h**) in 10 mL of THF via syringe at -78 °C. The mixture was stirred for 1h. Afterward iodomethane (0.093 mL, 1.5 mmol) was added to the solution, the resulting mixture was stirred at -78 °C for 30 min, then left to attain room temperature and stirred for 20h. The reaction was quenched with 10 mL of brine, the aqueous layer was separated and extracted with two 10 mL- portions of  $\text{CH}_2\text{Cl}_2$ , the combined organic layer was dried over  $\text{MgSO}_4$  and concentrated under reduced pressure. The residue was purified by CC ( $\text{CH}_2\text{Cl}_2/\text{hexane}$ , 1:3) to afford (**8**); off-white solid; yield : 0.26 g (61%); mp 170-171 °C;  $^1\text{H}$  NMR (500 MHz,  $\text{CDCl}_3$ )  $\delta$  7.95 – 7.91 (m, 1H), 7.45 – 7.39 (m, 1H), 7.25 – 7.22 (m, 1H), 7.17 – 7.14 (m, 1H), 7.14 – 7.07 (m, 3H), 7.02 – 6.97 (m, 2H), 6.88 – 6.84 (m, 1H), 6.83 – 6.78 (m, 1H), 4.68 (d,  $J$  = 7.2 Hz, 1H), 3.96 (s, 3H), 3.87 (s, 3H), 3.83 – 3.76 (m, 1H), 1.34 (d,  $J$  = 7.2 Hz, 3H);  $^{13}\text{C}$  NMR (125 MHz,  $\text{CDCl}_3$ )  $\delta$  157.15, 152.98, 152.77 (d,  $^1J_{\text{C-F}}$  = 247.0 Hz), 147.09 (d,  $^2J_{\text{C-F}}$  = 10.8 Hz), 146.06, 134.88 (d,  $^3J_{\text{C-F}}$  = 5.3 Hz), 134.73, 131.74, 130.36, 130.05, 129.79, 126.24, 121.39 (d,  $^4J_{\text{C-F}}$  = 3.5 Hz), 120.97, 118.80, 113.89, 113.61 (d,  $^2J_{\text{C-F}}$  = 18.9 Hz), 113.58, 111.28 (d,  $^3J_{\text{C-F}}$  = 9.8 Hz), 71.81, 56.26, 55.44, 53.58, 18.19;  $m/z$ = 424.81 (M+H) $^+$ .

**3-(*tert*-butyl)-5-(3-chloro-4-methoxyphenyl)-1-(4-chlorophenyl)-1*H*-pyrazole (10).** A mixture of 0.37 g (1 mmol) of 3-(*tert*-butyl)-5-(3-chloro-4-methoxyphenyl)-1-(4-chlorophenyl)-4,5-dihydro-1*H*-pyrazole (**3e**) and 0.34 g (1.5 mmol) of dichlorodicyanoquinone (DDQ) in 10 mL of benzene was heated to reflux for 5h. The mixture was cooled to room temperature and filtered through a plug of silica gel wetted with diethyl ether. The filtrate was concentrated under reduced pressure and the residue was purified by CC ( $\text{CH}_2\text{Cl}_2/\text{hexane}$  1:3) to give the title

## Results

---

compound as a white solid (95%, 0.35 g), mp 182-183 °C; <sup>1</sup>H NMR (500 MHz, CDCl<sub>3</sub>) δ 7.34 – 7.31 (m, 1H), 7.30 – 7.21 (m, 4H), 6.97 (dd, *J* = 8.5, 2.2 Hz, 1H), 6.84 – 6.81 (m, 1H), 6.31 (s, 1H), 3.90 (s, 3H); <sup>13</sup>C NMR (125 MHz, CDCl<sub>3</sub>) δ 162.89, 154.85, 141.56, 138.68, 132.57, 130.38, 129.00, 128.17, 126.19, 124.11, 122.55, 111.77, 104.97, 56.14, 32.23, 30.46; MS (ESI): *m/z* = 374.67 (M+H)<sup>+</sup>.

## BIOLOGICAL ASSAYS

### Fluorescence probing of compound-induced conformational changes

Potential effects of the compounds on the protein conformation were probed using the SYPRO Orange dye, which strongly increases its fluorescence intensity upon binding to solvent exposed hydrophobic areas of proteins.<sup>54</sup> Assays were performed in a final reaction volume of 25 μL, containing 50 mM Tris-HCl, pH 7.4, 140 mM NaCl, 1 mM DTT, 0.8 times concentrated SYPRO Orange (Molecular Probes), 0.5 μM PKCζ, and compounds in the indicated concentrations. Control experiments were set up in the same manner except that PKCζ was omitted. Measurements were done in black 384 well plates (485 nm excitation/585 nm emission) after heating of the samples for 4 min at 37°C in a PolarStar plate reader (BMG Labtech, Germany). To correct for fluorescence emission triggered by direct interaction between the compounds and the dye, the control values obtained in the absence of PKCζ protein were subtracted from the fluorescence units generated in the presence of PKCζ.

### Protein Kinases and Kinase Assays

PKCζ was prepared and purified as described before.<sup>37</sup> The cell-free assay was done basically as previously described except that reaction samples were incubated for 4 min at 37°C before the phosphorylation reactions were started by the addition of γ<sup>32</sup>P-ATP/Mg<sup>2+</sup>.<sup>37,38</sup> Similar conditions were used for the PKCι and mutant PKCζ assays.

### HEK293 cells transfection experiments

To investigate the effect of **4f** on the activity of cellular PKCζ, HEK293 cells were seeded in 6-well plates and, at 80% confluency, transfected using GST-PKCζ wt and GST-PKCζ[V297L] mutant expression plasmids essentially as described.<sup>37</sup> The next day, the medium was exchanged to DMEM containing 0.1% FCS, and the test compounds were added in different concentrations as indicated. After 6h in the incubator, cells were stimulated by the addition of IGF-I (50 ng/ml final concentration) for 30 min at 37°C. The cells were then lysed, and the recombinant PKCζ was isolated and purified using glutathione sepharose beads as previously described.<sup>37</sup> Equal amounts of eluted GST-PKCζ (50 ng per reaction) were assayed for enzymatic activity as described using myelin basic protein as a substrate.<sup>38</sup>

## Results

---

### Reporter Gene Assay

The human histocytic lymphoma cell line U937 was transfected with a NF- $\kappa$ B reporter gene plasmid and the assay performed exactly as previously described.<sup>37</sup>

### Nitrite assay (Griess assay)

RAW 264.7 cells were seeded in 96-well plates ( $8 \cdot 10^4$  cells/200 $\mu$ L DMEM supplemented with 10% FBS and 1% antibiotics), cultured for two days under 5% CO<sub>2</sub> at 37°, and then incubated with or without LPS in the absence or presence of the test compounds or DMSO control for 20h. As a parameter of NO synthesis, nitrite the stable oxidation product was quantified photometrically after its reaction to an azo-dye in the supernatant according to Green et al.<sup>65</sup> Briefly, 100  $\mu$ L of cell culture supernatant were removed and combined with each 90 $\mu$ L of 1 % sulfanilamide in 5% phosphoric acid, and 90 $\mu$ L 0.1 % *N*-(1-naphthyl)ethylenediamine dihydrochloride in water in a 96-well plate. Samples were then measured at 550 nm using a in a PolarStar plate reader (BMG Labtech, Germany). In addition, a background measurement was done at 620 nm and the values obtained were subtracted. Nitrite concentrations in the supernatants were determined by comparison with a sodium nitrite standard curve. Experiments were performed at least four times in triplicates.

To correct for any potential effects on the cell vitality, an MTT assay was performed in parallel each time using the same cell line (cf. Supplementary Table S3).

## SUPPORTING INFORMATION

## 1) Experimental procedures and Analytical data

**4-(3-(*tert*-butyl)-1-(4-fluorophenyl)-4,5-dihydro-1*H*-pyrazol-5-yl)phenol (1b).** The title compound was prepared by reaction of (*E*)-1-(4-(*tert*-butoxy)phenyl)-4,4-dimethylpent-1-en-3-one (**E1**) and 4-fluorophenylhydrazine hydrochloride according to the general procedure for pyrazoline synthesis. The product was purified by CC (CH<sub>2</sub>Cl<sub>2</sub>/hexane 4:1); yellowish white solid; yield: 0.34 g (55%); mp 111-112 °C; <sup>1</sup>H NMR (500 MHz, DMSO-*d*<sub>6</sub>) δ 9.34 (s, 1H), 7.08 – 7.03 (m, 2H), 6.96 – 6.89 (m, 2H), 6.85 – 6.79 (m, 2H), 6.72 – 6.68 (m, 2H), 4.96 (dd, *J* = 11.5, 7.5 Hz, 1H), 3.46 (dd, *J* = 17.4, 11.5 Hz, 1H), 2.64 (dd, *J* = 17.4, 7.6 Hz, 1H), 1.17 (s, 9H); <sup>13</sup>C NMR (125 MHz, DMSO-*d*<sub>6</sub>) δ 159.18, 156.48, 155.41 (d, <sup>1</sup>*J*<sub>C-F</sub> = 233.8 Hz), 142.76, 132.88, 127.02, 115.55, 115.03 (d, <sup>2</sup>*J*<sub>C-F</sub> = 22.1 Hz), 113.86 (d, <sup>3</sup>*J*<sub>C-F</sub> = 7.4 Hz), 63.85, 42.81, 33.37, 27.91; MS (ESI): *m/z* = 311.01 (M-1)<sup>+</sup>.

**4-(1-(4-bromophenyl)-3-(*tert*-butyl)-4,5-dihydro-1*H*-pyrazol-5-yl)phenol (1c).** The title compound was prepared by reaction of (*E*)-1-(4-(*tert*-butoxy)phenyl)-4,4-dimethylpent-1-en-3-one (**E1**) and 4-bromophenylhydrazine hydrochloride according to the general procedure for pyrazoline synthesis. The product was purified by CC (CH<sub>2</sub>Cl<sub>2</sub>/hexane 4:1); off-white solid; yield: 0.45 g (61%); mp 125-126 °C; <sup>1</sup>H NMR (500 MHz, CDCl<sub>3</sub>) δ 7.32 – 7.28 (m, 2H), 7.27 – 7.23 (m, 2H), 7.07 – 7.02 (m, 2H), 6.99 – 6.94 (m, 2H), 5.08 (dd, *J* = 11.6, 7.7 Hz, 1H), 3.61 (dd, *J* = 17.2, 11.7 Hz, 1H), 2.91 (dd, *J* = 17.2, 7.7 Hz, 1H), 1.40 (s, 9H); <sup>13</sup>C NMR (125 MHz, CDCl<sub>3</sub>) δ 159.44, 154.93, 144.82, 134.78, 128.58, 127.18, 123.18, 115.91, 114.40, 64.47, 43.27, 33.82, 28.21; MS (ESI): *m/z* = 372.71 (M+H)<sup>+</sup>.

**4-(3-(*tert*-butyl)-1-(4-(trifluoromethyl)phenyl)-4,5-dihydro-1*H*-pyrazol-5-yl)phenol (1d).** The title compound was prepared by reaction of (*E*)-1-(4-(*tert*-butoxy)phenyl)-4,4-dimethylpent-1-en-3-one (**E1**) and 4-(trifluoromethyl)phenylhydrazine hydrochloride according to the general procedure for pyrazoline synthesis. The product was purified by CC (CH<sub>2</sub>Cl<sub>2</sub>/hexane 4:1); light brown solid; yield: 0.35 g (48%); mp 121-122 °C; <sup>1</sup>H NMR (500 MHz, DMSO-*d*<sub>6</sub>) δ 9.38 (s, 1H), 7.39 (d, *J* = 8.5 Hz, 2H), 7.03 – 6.98 (m, 2H), 6.93 (d, *J* = 8.6 Hz, 2H), 6.75 – 6.65 (m, 2H), 5.21 (dd, *J* = 11.6, 5.4 Hz, 1H), 3.53 (dd, *J* = 17.7, 11.7 Hz, 1H), 2.71 (dd, *J* = 17.7, 5.5 Hz, 1H), 1.18 (s, 9H); <sup>13</sup>C NMR (125 MHz, DMSO-*d*<sub>6</sub>) δ 161.32, 156.62, 147.43, 132.26, 126.76, 125.96, 125.07 (q, <sup>1</sup>*J*<sub>C-F</sub> = 270.2 Hz), 116.96 (q, <sup>2</sup>*J*<sub>C-F</sub> = 31.8 Hz), 115.66, 111.79, 61.97, 42.65, 33.51, 27.83; MS (ESI): *m/z* = 362.74 (M+H)<sup>+</sup>.

**4-(3-(*tert*-butyl)-1-(*p*-tolyl)-4,5-dihydro-1*H*-pyrazol-5-yl)phenol (1e).** The title compound was prepared by reaction of (*E*)-1-(4-(*tert*-butoxy)phenyl)-4,4-dimethylpent-1-en-3-one (**E1**) and *p*-tolylhydrazine hydrochloride according to the general procedure for pyrazoline synthesis. The product was purified by CC (CH<sub>2</sub>Cl<sub>2</sub>/hexane 4: 1); tan solid; yield: 0.24 g (40%); mp 125.9 °C; <sup>1</sup>H NMR (500 MHz, DMSO-*d*<sub>6</sub>) δ 9.31 (s, 1H), 7.06 – 7.00 (m, 2H), 6.88 (d, *J* = 8.2 Hz, 2H),

## Results

---

6.78 – 6.72 (m, 2H), 6.71 – 6.65 (m, 2H), 4.95 (dd,  $J = 11.5, 7.4$  Hz, 1H), 3.43 (dd,  $J = 17.3, 11.6$  Hz, 1H), 2.61 (dd,  $J = 17.3, 7.4$  Hz, 1H), 2.12 (s, 3H), 1.16 (s, 9H);  $^{13}\text{C}$  NMR (125 MHz, DMSO- $d_6$ )  $\delta$  158.34, 156.36, 143.76, 133.24, 128.97, 126.97, 126.25, 115.45, 112.95, 63.55, 42.59, 33.34, 27.96, 20.03; MS (ESI):  $m/z = 308.74$  (M+H) $^+$ .

**4-(3-(*tert*-butyl)-1-(4-(isopropyl)phenyl)-4,5-dihydro-1*H*-pyrazol-5-yl)phenol (1f).** The title compound was prepared by reaction of (*E*)-1-(4-(*tert*-butoxy)phenyl)-4,4-dimethylpent-1-en-3-one (**E1**) and 4-isopropylphenylhydrazine hydrochloride according to the general procedure for pyrazoline synthesis. The product was purified by CC (CH<sub>2</sub>Cl<sub>2</sub>/hexane 3:1); beige solid; yield: 0.19 g (28%); mp 162-163 °C;  $^1\text{H}$  NMR (500 MHz, DMSO- $d_6$ )  $\delta$  9.32 (s, 1H), 7.10 – 7.04 (m, 2H), 6.97 – 6.90 (m, 2H), 6.81 – 6.74 (m, 2H), 6.72 – 6.67 (m, 2H), 4.91 (dt,  $J = 22.8, 11.4$  Hz, 1H), 3.43 (dd,  $J = 17.3, 11.5$  Hz, 1H), 2.70 (hept,  $J = 6.9$  Hz, 1H), 2.60 (dd,  $J = 17.3, 7.9$  Hz, 1H), 1.16 (s, 9H), 1.10 (d,  $J = 6.9$  Hz, 6H);  $^{13}\text{C}$  NMR (125 MHz, DMSO- $d_6$ )  $\delta$  158.39, 156.40, 144.17, 137.77, 133.37, 126.98, 126.26, 115.49, 112.90, 63.75, 42.68, 33.34, 32.46, 27.96, 24.09, 24.06; MS (ESI):  $m/z = 337.08$  (M+H) $^+$ .

**4-(3-(*tert*-butyl)-5-(4-hydroxyphenyl)-4,5-dihydro-1*H*-pyrazol-1-yl)benzoic acid (1g).** The title compound was prepared by reaction of (*E*)-1-(4-(*tert*-butoxy)phenyl)-4,4-dimethylpent-1-en-3-one (**E1**) and 4-hydrazinobenzoic acid hydrochloride according to the general procedure for pyrazoline synthesis. The product was purified by CC (CH<sub>2</sub>Cl<sub>2</sub>/MeOH 98:2); white solid; yield: 0.26 g (39%); mp 259.1-261 °C;  $^1\text{H}$  NMR (500 MHz, DMSO- $d_6$ )  $\delta$  12.14 (s, 1H), 9.37 (s, 1H), 7.66 (d,  $J = 9.1$  Hz, 2H), 7.02 – 6.97 (m, 2H), 6.89 – 6.81 (m, 2H), 6.72 – 6.67 (m, 2H), 5.23 (dd,  $J = 11.6, 5.1$  Hz, 1H), 3.53 (dd,  $J = 17.7, 11.7$  Hz, 1H), 2.70 (dd,  $J = 17.7, 5.1$  Hz, 1H), 1.18 (s, 9H);  $^{13}\text{C}$  NMR (125 MHz, DMSO- $d_6$ )  $\delta$  167.28, 161.45, 156.59, 147.88, 132.43, 130.67, 126.74, 118.72, 115.63, 111.30, 61.80, 42.58, 33.53, 27.84; MS (ESI):  $m/z = 338.87$  (M+H) $^+$ .

**4-(3-(*tert*-butyl)-1-(3-chlorophenyl)-4,5-dihydro-1*H*-pyrazol-5-yl)phenol (1h).** The title compound was prepared by reaction of (*E*)-1-(4-(*tert*-butoxy)phenyl)-4,4-dimethylpent-1-en-3-one (**E1**) and 3-chlorophenylhydrazine hydrochloride according to the general procedure for pyrazoline synthesis. The product was purified by CC (CH<sub>2</sub>Cl<sub>2</sub>/hexane 4:1); yellowish white solid; yield: 0.2 g (31%); mp 143.3-145.2 °C;  $^1\text{H}$  NMR (500 MHz, DMSO- $d_6$ )  $\delta$  9.37 (s, 1H), 7.09 – 7.04 (m, 1H), 7.04 – 7.00 (m, 2H), 6.88 (t,  $J = 2.1$  Hz, 1H), 6.73 – 6.68 (m, 3H), 6.63 (ddd,  $J = 7.9, 2.1, 0.9$  Hz, 1H), 5.10 (dd,  $J = 11.6, 6.1$  Hz, 1H), 3.49 (dd,  $J = 17.6, 11.6$  Hz, 1H), 2.67 (dd,  $J = 17.6, 6.2$  Hz, 1H), 1.17 (s, 9H);  $^{13}\text{C}$  NMR (125 MHz, DMSO- $d_6$ )  $\delta$  160.34, 156.57, 146.53, 133.29, 132.54, 130.20, 126.85, 116.88, 115.64, 111.85, 110.91, 62.55, 42.67, 33.46, 27.86; MS (ESI):  $m/z = 328.86$  (M+H) $^+$ .

**4-(3-(*tert*-butyl)-1-(3-fluorophenyl)-4,5-dihydro-1*H*-pyrazol-5-yl)phenol (1i).** The title compound was prepared by reaction of (*E*)-1-(4-(*tert*-butoxy)phenyl)-4,4-dimethylpent-1-en-3-one (**E1**) and 3-fluorophenylhydrazine hydrochloride according to the general procedure for pyrazoline synthesis. The product was purified by CC (CH<sub>2</sub>Cl<sub>2</sub>/hexane 4:1); light brown solid;

## Results

yield: 0.21 g (35%) ; mp 140.4 °C;  $^1\text{H}$  NMR (500 MHz, DMSO- $d_6$ )  $\delta$  9.36 (s, 1H), 7.12 – 6.96 (m, 3H), 6.74 – 6.66 (m, 2H), 6.62 – 6.55 (m, 2H), 6.44 – 6.34 (m, 1H), 5.08 (dd,  $J$  = 11.6, 6.3 Hz, 1H), 3.49 (dd,  $J$  = 17.6, 11.7 Hz, 1H), 2.67 (dd,  $J$  = 17.6, 6.3 Hz, 1H), 1.17 (s, 9H);  $^{13}\text{C}$  NMR (125 MHz, DMSO- $d_6$ )  $\delta$  162.81 (d,  $^1J_{\text{C-F}}$  = 239.7 Hz), 160.10, 156.56, 147.11 (d,  $^3J_{\text{C-F}}$  = 11.1 Hz), 132.69, 130.14 (d,  $^3J_{\text{C-F}}$  = 10.1 Hz), 126.86, 115.61, 108.43, 103.61 (d,  $^2J_{\text{C-F}}$  = 21.3 Hz), 99.14 (d,  $^2J_{\text{C-F}}$  = 26.5 Hz), 62.72, 42.69, 33.43, 27.86; MS (ESI):  $m/z$  = 312.10 ( $\text{M}^+$ ).

**4-(3-(*tert*-butyl)-1-(3-(trifluoromethyl)phenyl)-4,5-dihydro-1H-pyrazol-5-yl)phenol (1j).** The title compound was prepared by reaction of (*E*)-1-(4-(*tert*-butoxy)phenyl)-4,4-dimethylpent-1-en-3-one (**E1**) and 3-(trifluoromethyl)phenylhydrazine hydrochloride according to the general procedure for pyrazoline synthesis. The product was purified by CC ( $\text{CH}_2\text{Cl}_2$ /hexane 4:1); yellow solid; yield: 0.35 g (49%); mp 130.5 °C;  $^1\text{H}$  NMR (500 MHz, DMSO- $d_6$ )  $\delta$  9.37 (s, 1H), 7.27 (t,  $J$  = 7.9 Hz, 1H), 7.16 (s, 1H), 7.06 – 7.02 (m, 2H), 6.98 (dd,  $J$  = 8.3, 2.1 Hz, 1H), 6.93 – 6.89 (m, 1H), 6.73 – 6.68 (m, 2H), 5.16 (dd,  $J$  = 11.6, 6.2 Hz, 1H), 3.52 (dd,  $J$  = 17.6, 11.6 Hz, 1H), 2.71 (dd,  $J$  = 17.6, 6.2 Hz, 1H), 1.19 (s, 9H);  $^{13}\text{C}$  NMR (125 MHz, DMSO- $d_6$ )  $\delta$  160.70, 156.60, 145.54, 132.33, 129.89, 129.49 (q,  $^2J_{\text{C-F}}$  = 31.2 Hz), 126.91, 124.33 (q,  $^1J_{\text{C-F}}$  = 272.3 Hz), 115.66, 115.45, 113.37, 108.38, 62.53, 42.69, 33.48, 27.84; MS (ESI):  $m/z$  = 362.84 ( $\text{M}+\text{H}^+$ ).

**4-(3-(*tert*-butyl)-1-(*m*-tolyl)-4,5-dihydro-1H-pyrazol-5-yl)phenol (1k).** The title compound was prepared by reaction of (*E*)-1-(4-(*tert*-butoxy)phenyl)-4,4-dimethylpent-1-en-3-one (**E1**) and *m*-tolylhydrazine hydrochloride according to the general procedure for pyrazoline synthesis. The product was purified by CC ( $\text{CH}_2\text{Cl}_2$ /hexane 4:1); yellowish white solid; yield: 0.25 g (41%); mp 119.3-121.2 °C;  $^1\text{H}$  NMR (500 MHz, DMSO- $d_6$ )  $\delta$  9.31 (s, 1H), 7.06 – 7.00 (m, 2H), 6.95 – 6.89 (m, 1H), 6.75 (s, 1H), 6.71 – 6.67 (m, 2H), 6.56 (dd,  $J$  = 8.2, 2.1 Hz, 1H), 6.46 – 6.42 (m, 1H), 5.00 (dd,  $J$  = 11.6, 6.8 Hz, 1H), 3.45 (dd,  $J$  = 17.4, 11.7 Hz, 1H), 2.62 (dd,  $J$  = 17.4, 6.8 Hz, 1H), 2.15 (s, 3H), 1.17 (s, 9H);  $^{13}\text{C}$  NMR (125 MHz, DMSO- $d_6$ )  $\delta$  158.59, 156.36, 145.66, 137.50, 133.34, 128.39, 126.87, 118.52, 115.49, 113.36, 109.84, 63.01, 42.56, 33.36, 27.96, 21.42; MS (ESI):  $m/z$  = 308.94 ( $\text{M}+\text{H}^+$ ).

**4-(3-(*tert*-butyl)-1-(2-chlorophenyl)-4,5-dihydro-1H-pyrazol-5-yl)phenol (1l).** The title compound was prepared by reaction of (*E*)-1-(4-(*tert*-butoxy)phenyl)-4,4-dimethylpent-1-en-3-one (**E1**) and 2-chlorophenylhydrazine hydrochloride according to the general procedure for pyrazoline synthesis. The product was purified by CC ( $\text{CH}_2\text{Cl}_2$ /hexane 4:1); light brown solid; yield: 0.33 g (51%); mp 162-163 °C;  $^1\text{H}$  NMR (500 MHz, DMSO- $d_6$ )  $\delta$  9.25 (s, 1H), 7.28 (dd,  $J$  = 8.1, 1.5 Hz, 1H), 7.19 (dd,  $J$  = 7.9, 1.4 Hz, 1H), 7.11 – 7.05 (m, 1H), 6.90 (d,  $J$  = 8.5 Hz, 2H), 6.83 (td,  $J$  = 7.8, 1.5 Hz, 1H), 6.53 (d,  $J$  = 8.5 Hz, 2H), 5.46 (dd,  $J$  = 10.9, 4.7 Hz, 1H), 3.43 – 3.35 (m, 1H), 2.88 (dd,  $J$  = 17.2, 4.7 Hz, 1H), 1.22 (s, 9H);  $^{13}\text{C}$  NMR (125 MHz, DMSO- $d_6$ )  $\delta$  161.25, 156.47, 143.68, 131.40, 129.72, 127.51, 126.94, 123.63, 123.28, 122.66, 114.94, 65.06, 41.50, 33.60, 27.93; MS (ESI):  $m/z$  = 328.86 ( $\text{M}+\text{H}^+$ ).

## Results

---

**4-(3-(*tert*-butyl)-1-(2-fluorophenyl)-4,5-dihydro-1*H*-pyrazol-5-yl)phenol (1m).** The title compound was prepared by reaction of (*E*)-1-(4-(*tert*-butoxy)phenyl)-4,4-dimethylpent-1-en-3-one (**E1**) and 2-fluorophenylhydrazine hydrochloride according to the general procedure for pyrazoline synthesis. The product was purified by CC (CH<sub>2</sub>Cl<sub>2</sub>/hexane 4:1); light brown solid; yield: 0.25 g (41%); mp 147.3 °C; <sup>1</sup>H NMR (500 MHz, DMSO-*d*<sub>6</sub>) δ 9.26 (s, 1H), 7.34 (td, *J* = 8.3, 1.7 Hz, 1H), 6.98 – 6.88 (m, 4H), 6.73 (dddd, *J* = 8.1, 7.3, 4.6, 1.7 Hz, 1H), 6.59 – 6.54 (m, 2H), 5.25 (dt, *J* = 11.0, 3.9 Hz, 1H), 3.40 (dd, *J* = 17.1, 11.0 Hz, 1H), 2.79 (dd, *J* = 17.2, 4.3 Hz, 1H), 1.20 (s, 9H); <sup>13</sup>C NMR (125 MHz, DMSO-*d*<sub>6</sub>) δ 160.50, 156.45, 150.79 (d, <sup>1</sup>*J*<sub>C-F</sub> = 242.7 Hz), 134.19 (d, <sup>2</sup>*J*<sub>C-F</sub> = 9.3 Hz), 132.21, 127.12, 124.21, 120.73, 119.22, 115.60 (d, <sup>2</sup>*J*<sub>C-F</sub> = 20.0 Hz), 115.06, 65.18, 41.91, 33.51, 27.86; MS (ESI): *m/z* = 312.93 (M+H)<sup>+</sup>.

**4-(3-(*tert*-butyl)-1-(2,4-dichlorophenyl)-4,5-dihydro-1*H*-pyrazol-5-yl)phenol (1n).** The title compound was prepared by reaction of (*E*)-1-(4-(*tert*-butoxy)phenyl)-4,4-dimethylpent-1-en-3-one (**E1**) and 2,4-dichlorophenylhydrazine hydrochloride according to the general procedure for pyrazoline synthesis. The product was purified by CC (CH<sub>2</sub>Cl<sub>2</sub>/hexane 3:1); off-white solid; yield: 0.38 g (52%); mp 137.1-138.5 °C; <sup>1</sup>H NMR (500 MHz, DMSO-*d*<sub>6</sub>) δ 9.29 (s, 1H), 7.32 – 7.27 (m, 2H), 7.15 (dt, *J* = 4.1, 2.1 Hz, 1H), 6.91 – 6.84 (m, 2H), 6.56 – 6.52 (m, 2H), 5.49 (dd, *J* = 10.9, 4.2 Hz, 1H), 3.41 (dd, *J* = 17.3, 10.9 Hz, 1H), 2.90 (dd, *J* = 17.3, 4.2 Hz, 1H), 1.22 (s, 9H); <sup>13</sup>C NMR (125 MHz, DMSO-*d*<sub>6</sub>) δ 162.08, 156.59, 142.94, 131.18, 128.96, 127.46, 127.03, 125.92, 123.86, 123.59, 115.04, 64.93, 41.59, 33.64, 27.88; MS (ESI): *m/z* = 362.82 (M+H)<sup>+</sup>.

**4-(3-(*tert*-butyl)-1-(2,4-difluorophenyl)-4,5-dihydro-1*H*-pyrazol-5-yl)phenol (1o),** The title compound was prepared by reaction of (*E*)-1-(4-(*tert*-butoxy)phenyl)-4,4-dimethylpent-1-en-3-one (**E1**) and 2,4-difluorophenylhydrazine hydrochloride according to the general procedure for pyrazoline synthesis. The product was purified by CC (CH<sub>2</sub>Cl<sub>2</sub>/hexane 4:1); yellowish white solid; yield: 0.22 g (33%); mp 163-164 °C; <sup>1</sup>H NMR (500 MHz, DMSO-*d*<sub>6</sub>) δ 9.29 (s, 1H), 7.29 (td, *J* = 9.3, 6.1 Hz, 1H), 6.99 (ddd, *J* = 12.0, 9.0, 2.9 Hz, 1H), 6.93 – 6.88 (m, 2H), 6.88 – 6.82 (m, 1H), 6.59 – 6.54 (m, 2H), 5.15 (ddd, *J* = 10.8, 4.7, 3.4 Hz, 1H), 3.38 (dd, *J* = 17.1, 10.9 Hz, 1H), 2.81 (dd, *J* = 17.1, 4.9 Hz, 1H), 1.19 (s, 9H); <sup>13</sup>C NMR (125 MHz, DMSO-*d*<sub>6</sub>) δ 161.06, 156.55, 156.21 (dd, <sup>1</sup>*J*<sub>C-F</sub> = 239.3, <sup>3</sup>*J*<sub>C-F</sub> = 11.2 Hz), 150.95 (dd, <sup>1</sup>*J*<sub>C-F</sub> = 246.7, <sup>3</sup>*J*<sub>C-F</sub> = 12.2 Hz), 131.65, 131.32 (dd, <sup>2</sup>*J*<sub>C-F</sub> = 9.7, <sup>4</sup>*J*<sub>C-F</sub> = 3.1 Hz), 127.34, 120.21 (dd, <sup>3</sup>*J*<sub>C-F</sub> = 9.0, 4.9 Hz), 115.07, 110.71 (dd, <sup>2</sup>*J*<sub>C-F</sub> = 21.5, <sup>4</sup>*J*<sub>C-F</sub> = 3.3 Hz), 104.02 (dd, <sup>2</sup>*J*<sub>C-F</sub> = 26.4, 24.4 Hz), 65.70, 41.80, 33.53, 27.85; MS (ESI): *m/z* = 330.80 (M+H)<sup>+</sup>.

**4-(3-(*tert*-butyl)-1-(2,4-dimethylphenyl)-4,5-dihydro-1*H*-pyrazol-5-yl)phenol (1p).** The title compound was prepared by reaction of (*E*)-1-(4-(*tert*-butoxy)phenyl)-4,4-dimethylpent-1-en-3-one (**E1**) and 2,4-dimethylphenylhydrazine hydrochloride according to the general procedure for pyrazoline synthesis. The product was purified by CC (CH<sub>2</sub>Cl<sub>2</sub>/hexane 4:1); light brown solid; yield: 0.26 g (41%); mp 77-79 °C; <sup>1</sup>H NMR (500 MHz, DMSO-*d*<sub>6</sub>) δ 9.26 (s, 1H), 7.10 – 7.06 (m, 2H), 6.86 – 6.83 (m, 1H), 6.78 – 6.76 (m, 2H), 6.63 – 6.59 (m, 2H), 4.87 (t, *J* = 10.6 Hz, 1H), 3.24 (dd, *J* = 16.5, 10.1 Hz, 1H), 2.65 (dd, *J* = 16.5, 11.1 Hz, 1H), 2.18 (s, 3H), 2.13 (s, 3H),

## Results

---

1.16 (s, 9H);  $^{13}\text{C}$  NMR (125 MHz, DMSO- $d_6$ )  $\delta$  159.41, 156.44, 142.97, 131.32, 131.18, 130.79, 128.84, 127.91, 126.04, 118.81, 115.02, 66.78, 41.49, 33.46, 27.97, 20.20, 19.56; MS (ESI):  $m/z$  = 323.02 (M+H) $^+$ .

**4-(3-(*tert*-butyl)-1-(2,6-dichlorophenyl)-4,5-dihydro-1H-pyrazol-5-yl)phenol (1q).** The title compound was prepared by reaction of (*E*)-1-(4-(*tert*-butoxy)phenyl)-4,4-dimethylpent-1-en-3-one (**E1**) and 2,6-dichlorophenylhydrazine hydrochloride according to the general procedure for pyrazoline synthesis. The product was purified by CC ( $\text{CH}_2\text{Cl}_2$ /hexane 3:1); off-white solid; yield: 0.24 g (33%) ; mp 172-173 °C;  $^1\text{H}$  NMR (500 MHz, DMSO- $d_6$ )  $\delta$  9.30 (s, 1H), 7.33 – 7.29 (m, 2H), 7.15 – 7.10 (m, 1H), 7.09 – 7.04 (m, 2H), 6.62 – 6.57 (m, 2H), 5.15 (t,  $J$  = 10.6 Hz, 1H), 3.35 (dd,  $J$  = 17.2, 11.1 Hz, 1H), 2.93 (dd,  $J$  = 17.2, 10.1 Hz, 1H), 1.20 (s, 9H);  $^{13}\text{C}$  NMR (125 MHz, DMSO- $d_6$ )  $\delta$  159.02, 156.83, 139.82, 134.06, 130.41, 129.34, 128.87, 127.86, 114.77, 67.20, 40.73, 33.43, 27.87; MS (ESI):  $m/z$  = 362.79 (M+H) $^+$ .

**4-(3-(*tert*-butyl)-1-(3-chloro-4-fluorophenyl)-4,5-dihydro-1H-pyrazol-5-yl)phenol (1r).** The title compound was prepared by reaction of (*E*)-1-(4-(*tert*-butoxy)phenyl)-4,4-dimethylpent-1-en-3-one (**E1**) and 3-chloro-4-fluorophenylhydrazine hydrochloride according to the general procedure for pyrazoline synthesis. The product was purified by CC ( $\text{CH}_2\text{Cl}_2$ /hexane 4:1); brown solid; yield: 0.23 g (34%) ; mp 94.2 °C;  $^1\text{H}$  NMR (500 MHz, DMSO)  $\delta$  9.38 (s, 1H), 7.12 (t,  $J$  = 9.2 Hz, 1H), 7.05 – 7.01 (m, 2H), 6.93 (dd,  $J$  = 6.5, 2.8 Hz, 1H), 6.73 – 6.67 (m, 3H), 5.06 (dd,  $J$  = 11.5, 6.6 Hz, 1H), 3.48 (dd,  $J$  = 17.5, 11.5 Hz, 1H), 2.68 (dd,  $J$  = 17.5, 6.7 Hz, 1H), 1.17 (s, 9H);  $^{13}\text{C}$  NMR (125 MHz, DMSO- $d_6$ )  $\delta$  160.44, 156.61, 150.08 (d,  $^1J_{\text{C-F}}$  = 236.4 Hz), 142.99 (d,  $^4J_{\text{C-F}}$  = 1.8 Hz), 132.31, 126.98, 119.21 (d,  $^2J_{\text{C-F}}$  = 18.3 Hz), 116.75 (d,  $^2J_{\text{C-F}}$  = 21.6 Hz), 115.65, 113.30, 112.21 (d,  $^3J_{\text{C-F}}$  = 6.3 Hz), 63.13, 42.84, 33.44, 27.85; MS (ESI):  $m/z$  = 346.91 (M+H) $^+$ .

**4-(3-(*tert*-butyl)-1-(2,3,4-trifluorophenyl)-4,5-dihydro-1H-pyrazol-5-yl)phenol (1t).** The title compound was prepared by reaction of (*E*)-1-(4-(*tert*-butoxy)phenyl)-4,4-dimethylpent-1-en-3-one (**E1**) and 2,3,4-trifluorophenylhydrazine hydrochloride according to the general procedure for pyrazoline synthesis. The product was purified by CC ( $\text{CH}_2\text{Cl}_2$ /hexane 3:1); yellow solid; yield: 0.22 g (32%); mp 159-161 °C;  $^1\text{H}$  NMR (500 MHz, DMSO- $d_6$ )  $\delta$  9.34 (s, 1H), 7.11 – 7.02 (m, 2H), 6.94 – 6.89 (m, 2H), 6.63 – 6.58 (m, 2H), 5.24 – 5.18 (m, 1H), 3.42 (dd,  $J$  = 17.3, 11.0 Hz, 1H), 2.82 (dd,  $J$  = 17.3, 4.8 Hz, 1H), 1.19 (s, 9H); MS (ESI):  $m/z$  = 348.99 (M+H) $^+$ .

**4-(3-(*tert*-butyl)-1-phenyl-4,5-dihydro-1H-pyrazol-5-yl)phenol (1u).** The title compound was prepared by reaction of (*E*)-1-(4-(*tert*-butoxy)phenyl)-4,4-dimethylpent-1-en-3-one (**E1**) and phenylhydrazine hydrochloride according to the general procedure for pyrazoline synthesis. The product was purified by CC ( $\text{CH}_2\text{Cl}_2$ /hexane 4:1); yellowish white solid; yield: 0.23 g (39%) ; mp 175-176 °C;  $^1\text{H}$  NMR (500 MHz, DMSO- $d_6$ )  $\delta$  9.33 (s, 1H), 7.11 – 6.99 (m, 4H), 6.87 – 6.80 (m, 2H), 6.73 – 6.66 (m, 2H), 6.62 (tt,  $J$  = 7.3, 1.1 Hz, 1H), 5.01 (dd,  $J$  = 11.6, 7.0 Hz, 1H), 3.46 (dd,  $J$  = 17.4, 11.6 Hz, 1H), 2.63 (dd,  $J$  = 17.4, 7.0 Hz, 1H), 1.17 (s, 9H);  $^{13}\text{C}$  NMR (125 MHz,

## Results

---

DMSO- $d_6$ )  $\delta$  158.83, 156.42, 145.70, 133.21, 128.55, 126.91, 117.64, 115.52, 112.66, 63.13, 42.63, 33.38, 27.94; MS (ESI):  $m/z$  = 294.91 (M+H)<sup>+</sup>.

**4-(1-(4-chlorophenyl)-3-phenyl-4,5-dihydro-1H-pyrazol-5-yl)phenol (2a).** The title compound was prepared by reaction of (*E*)-3-(4-(*tert*-butoxy)phenyl)-1-phenylprop-2-en-1-one (**E2**) and 4-chlorophenylhydrazine hydrochloride according to the general procedure for pyrazoline synthesis. The product was purified by CC (CH<sub>2</sub>Cl<sub>2</sub>/hexane 4:1); yellow solid; yield: 0.19 g (28%); mp 164-165 °C; <sup>1</sup>H NMR (500 MHz, DMSO- $d_6$ )  $\delta$  9.40 (s, 1H), 7.74 (dt,  $J$  = 8.3, 1.8 Hz, 2H), 7.47 – 7.31 (m, 3H), 7.21 – 7.14 (m, 2H), 7.09 – 7.03 (m, 2H), 7.02 – 6.95 (m, 2H), 6.75 – 6.67 (m, 2H), 5.36 (dd,  $J$  = 12.1, 6.1 Hz, 1H), 3.87 (dd,  $J$  = 17.5, 12.1 Hz, 1H), 3.08 (dd,  $J$  = 17.5, 6.2 Hz, 1H); <sup>13</sup>C NMR (125 MHz, DMSO- $d_6$ )  $\delta$  156.70, 147.99, 143.07, 132.19, 132.15, 128.81, 128.63, 128.55, 127.03, 125.74, 121.98, 115.69, 114.37, 62.73, 43.12; MS (ESI):  $m/z$  = 348.71 (M+H)<sup>+</sup>.

**4-(1-(3-chlorophenyl)-3-phenyl-4,5-dihydro-1H-pyrazol-5-yl)phenol (2b).** The title compound was prepared by reaction of (*E*)-3-(4-(*tert*-butoxy)phenyl)-1-phenylprop-2-en-1-one (**E2**) and 3-chlorophenylhydrazine hydrochloride according to the general procedure for pyrazoline synthesis. The product was purified by CC (CH<sub>2</sub>Cl<sub>2</sub>/hexane 4:1); yield: light brown solid; 0.23 g (33%); mp 161.2-163.3 °C; <sup>1</sup>H NMR (500 MHz, DMSO- $d_6$ )  $\delta$  9.41 (s, 1H), 7.78 – 7.74 (m, 2H), 7.46 – 7.36 (m, 3H), 7.16 – 7.12 (m, 1H), 7.11 – 7.05 (m, 3H), 6.87 (ddd,  $J$  = 8.4, 2.2, 0.9 Hz, 1H), 6.75 – 6.66 (m, 3H), 5.40 (dd,  $J$  = 12.1, 5.9 Hz, 1H), 3.88 (dd,  $J$  = 17.5, 12.1 Hz, 1H), 3.10 (dd,  $J$  = 17.5, 6.0 Hz, 1H); <sup>13</sup>C NMR (125 MHz, DMSO- $d_6$ )  $\delta$  156.73, 148.56, 145.39, 133.48, 132.12, 132.01, 130.37, 128.98, 128.65, 127.01, 125.88, 117.75, 115.73, 112.32, 111.35, 62.51, 43.10; MS (ESI):  $m/z$  = 348.74 (M+H)<sup>+</sup>.

**2-(1-(4-chlorophenyl)-5-(4-hydroxyphenyl)-4,5-dihydro-1H-pyrazol-3-yl)phenol (2c)** . The title compound was prepared by reaction of (*E*)-3-(4-(*tert*-butoxy)phenyl)-1-(2-hydroxyphenyl)prop-2-en-1-one (**E3**) and 4-chlorophenylhydrazine hydrochloride according to the general procedure for pyrazoline synthesis. The product was purified by CC (CH<sub>2</sub>Cl<sub>2</sub>/MeOH 99:1); beige solid; yield: 0.27 g (38%); mp 214.2 °C; <sup>1</sup>H NMR (500 MHz, DMSO- $d_6$ )  $\delta$  10.41 (s, 1H), 9.42 (s, 1H), 7.44 (dd,  $J$  = 7.8, 1.5 Hz, 1H), 7.31 – 7.25 (m, 1H), 7.25 – 7.19 (m, 2H), 7.12 – 7.08 (m, 2H), 6.97 (ddd,  $J$  = 7.8, 6.9, 1.0 Hz, 1H), 6.95 – 6.88 (m, 3H), 6.74 – 6.69 (m, 2H), 5.35 (dd,  $J$  = 12.0, 6.4 Hz, 1H), 4.00 (dd,  $J$  = 17.7, 12.0 Hz, 1H), 3.24 (dd,  $J$  = 17.8, 6.5 Hz, 1H); <sup>13</sup>C NMR (125 MHz, DMSO- $d_6$ )  $\delta$  156.80, 156.19, 150.61, 142.51, 131.77, 130.51, 128.77, 128.17, 127.15, 122.59, 119.54, 116.59, 116.10, 115.73, 114.41, 61.79, 44.11; MS (ESI):  $m/z$  = 364.34 (M)<sup>+</sup>.

**4-(1-(4-chlorophenyl)-3-(2-methoxyphenyl)-4,5-dihydro-1H-pyrazol-5-yl)phenol (2d).** The title compound was prepared by reaction of (*E*)-3-(4-(*tert*-butoxy)phenyl)-1-(2-methoxyphenyl)prop-2-en-1-one (**E4**) and 4-chlorophenylhydrazine hydrochloride according to the general procedure for pyrazoline synthesis. The product was purified by CC (CH<sub>2</sub>Cl<sub>2</sub>); tan

## Results

solid; yield: 0.31 g (41%) ; mp 205-206 °C; <sup>1</sup>H NMR (500 MHz, DMSO-*d*<sub>6</sub>) δ 9.37 (s, 1H), 7.87 (dd, *J* = 7.8, 1.7 Hz, 1H), 7.39 – 7.34 (m, 1H), 7.19 – 7.14 (m, 2H), 7.10 – 7.03 (m, 3H), 7.00 (td, *J* = 7.7, 1.0 Hz, 1H), 6.98 – 6.93 (m, 2H), 6.72 – 6.68 (m, 2H), 5.28 (dd, *J* = 12.0, 6.2 Hz, 1H), 3.92 (dd, *J* = 18.1, 12.0 Hz, 1H), 3.79 (s, 3H), 3.15 (dd, *J* = 18.1, 6.3 Hz, 1H); <sup>13</sup>C NMR (125 MHz, DMSO-*d*<sub>6</sub>) δ 157.29, 156.62, 147.28, 143.26, 132.39, 130.37, 128.51, 128.14, 126.95, 121.76, 121.08, 120.64, 115.65, 114.31, 112.31, 62.69, 55.61, 46.50; MS (ESI): *m/z* = 378.82 (M+H)<sup>+</sup>.

**4-(1-(4-chlorophenyl)-3-(2-ethoxyphenyl)-4,5-dihydro-1H-pyrazol-5-yl)phenol (2e).** The title compound was prepared by reaction of (*E*)-3-(4-(*tert*-butoxy)phenyl)-1-(2-ethoxyphenyl)prop-2-en-1-one (**E5**) and 4-chlorophenylhydrazine hydrochloride according to the general procedure for pyrazoline synthesis. The product was purified by CC (CH<sub>2</sub>Cl<sub>2</sub>/hexane 4:1); yellowish white solid; yield: 0.19 g (25%) ; mp 194-196 °C; <sup>1</sup>H NMR (500 MHz, CDCl<sub>3</sub>) δ 8.21 (d, *J* = 7.6 Hz, 1H), 7.60 – 7.51 (m, 2H), 7.45 – 7.30 (m, 4H), 7.25 (dd, *J* = 14.2, 7.7 Hz, 2H), 7.14 (d, *J* = 8.3 Hz, 1H), 7.10 – 6.98 (m, 2H), 5.37 (dd, *J* = 12.0, 7.0 Hz, 1H), 4.43 (q, *J* = 6.8 Hz, 2H), 4.29 (dd, *J* = 17.8, 12.1 Hz, 1H), 3.55 (dd, *J* = 17.9, 7.0 Hz, 1H), 1.64 (t, *J* = 6.9 Hz, 3H); <sup>13</sup>C NMR (125 MHz, CDCl<sub>3</sub>) δ 156.41, 156.21, 155.02, 143.69, 130.81, 129.06, 128.65, 126.60, 125.80, 122.47, 120.73, 115.90, 114.47, 112.32, 109.15, 66.11, 63.89, 46.97, 14.94; MS (ESI): *m/z* = 393.11 (M+H)<sup>+</sup>.

**4-(1-(4-chlorophenyl)-3-(2-chlorophenyl)-4,5-dihydro-1H-pyrazol-5-yl)phenol (2f)** . The title compound was prepared by reaction of (*E*)-3-(4-(*tert*-butoxy)phenyl)-1-(2-chlorophenyl)prop-2-en-1-one (**E6**) and 4-chlorophenylhydrazine hydrochloride according to the general procedure for pyrazoline synthesis. The product was purified by CC (CH<sub>2</sub>Cl<sub>2</sub>/hexane 4:1); off-white solid; yield: 0.35 g (46%) ; mp 124-125 °C; <sup>1</sup>H NMR (500 MHz, DMSO-*d*<sub>6</sub>) δ 9.42 (s, 1H), 7.78 – 7.72 (m, 1H), 7.55 – 7.47 (m, 1H), 7.44 – 7.32 (m, 2H), 7.23 – 7.15 (m, 2H), 7.11 – 7.04 (m, 2H), 7.03 – 6.94 (m, 2H), 6.75 – 6.66 (m, 2H), 5.39 (dd, *J* = 12.1, 6.1 Hz, 1H), 4.00 (dd, *J* = 17.5, 12.1 Hz, 1H), 3.20 (dd, *J* = 17.5, 6.1 Hz, 1H); <sup>13</sup>C NMR (125 MHz, DMSO-*d*<sub>6</sub>) δ 156.77, 146.30, 142.89, 131.86, 130.99, 130.86, 130.74, 130.16, 129.90, 128.60, 127.30, 127.07, 122.44, 115.70, 114.61, 62.78, 45.59; MS (ESI): *m/z* = 382.59 (M+H)<sup>+</sup>.

**4-(1-(4-chlorophenyl)-3-(thiophen-2-yl)-4,5-dihydro-1H-pyrazol-5-yl)phenol (2g).** The title compound was prepared by reaction of (*E*)-3-(4-(*tert*-butoxy)phenyl)-1-(thiophen-2-yl)prop-2-en-1-one (**E7**) and 4-chlorophenylhydrazine hydrochloride according to the general procedure for pyrazoline synthesis. The product was purified by CC (CH<sub>2</sub>Cl<sub>2</sub>/hexane 3:1); greenish yellow solid; yield: 0.14 g (20%); mp 169.9 °C; <sup>1</sup>H NMR (500 MHz, DMSO-*d*<sub>6</sub>) δ 9.41 (s, 1H), 7.61 (dd, *J* = 5.1, 1.1 Hz, 1H), 7.26 (dd, *J* = 3.6, 1.1 Hz, 1H), 7.20 – 7.14 (m, 2H), 7.10 (dd, *J* = 5.1, 3.6 Hz, 1H), 7.08 – 7.04 (m, 2H), 6.95 – 6.89 (m, 2H), 6.74 – 6.68 (m, 2H), 5.37 (dd, *J* = 12.0, 6.1 Hz, 1H), 3.87 (dd, *J* = 17.3, 12.0 Hz, 1H), 3.09 (dd, *J* = 17.3, 6.1 Hz, 1H); <sup>13</sup>C NMR (125 MHz, DMSO-*d*<sub>6</sub>) δ 156.74, 144.42, 142.85, 135.51, 131.91, 128.58, 127.82, 127.70, 127.61, 127.01, 122.00, 115.71, 114.33, 62.81, 43.88; MS (ESI): *m/z* = 354.47 (M<sup>+</sup>).

## Results

**4-(1-(4-bromophenyl)-3-(thiophen-2-yl)-4,5-dihydro-1H-pyrazol-5-yl)phenol (2h).** The title compound was prepared by reaction of (*E*)-3-(4-(*tert*-butoxy)phenyl)-1-(thiophen-2-yl)prop-2-en-1-one (**E7**) and 4-bromophenylhydrazine hydrochloride according to the general procedure for pyrazoline synthesis. The product was purified by CC (CH<sub>2</sub>Cl<sub>2</sub>/hexane 3:1); greenish yellow solid; yield: 0.15 g (19%); mp 162-164 °C; <sup>1</sup>H NMR (500 MHz, DMSO-*d*<sub>6</sub>) δ 9.40 (s, 1H), 7.62 – 7.59 (m, 1H), 7.31 – 7.25 (m, 3H), 7.11 – 7.08 (m, 1H), 7.07 – 7.03 (m, 2H), 6.89 – 6.85 (m, 2H), 6.74 – 6.69 (m, 2H), 5.37 (dd, *J* = 12.0, 6.0 Hz, 1H), 3.87 (dd, *J* = 17.3, 12.0 Hz, 1H), 3.09 (dd, *J* = 17.3, 6.0 Hz, 1H). <sup>13</sup>C NMR (125 MHz, DMSO-*d*<sub>6</sub>) δ 156.74, 144.50, 143.15, 135.49, 131.86, 131.41, 127.83, 127.75, 127.65, 126.99, 115.71, 114.82, 109.62, 62.70, 43.87; MS (ESI): *m/z* = 398.70 (M+H)<sup>+</sup>.

**4-(3-(thiophen-2-yl)-1-(4-(trifluoromethyl)phenyl)-4,5-dihydro-1H-pyrazol-5-yl)phenol (2i).** The title compound was prepared by reaction of (*E*)-3-(4-(*tert*-butoxy)phenyl)-1-(thiophen-2-yl)prop-2-en-1-one (**E7**) and 4-(trifluoromethyl)phenylhydrazine hydrochloride according to the general procedure for pyrazoline synthesis. The product was purified by CC (CH<sub>2</sub>Cl<sub>2</sub>/hexane 3:1); yellowish white solid; yield: 0.25 g (33%); mp 162-163.6 °C; <sup>1</sup>H NMR (500 MHz, DMSO-*d*<sub>6</sub>) δ 9.43 (s, 1H), 7.65 (dd, *J* = 5.1, 1.1 Hz, 1H), 7.46 (dd, *J* = 9.0, 0.5 Hz, 2H), 7.32 (dd, *J* = 3.6, 1.1 Hz, 1H), 7.12 (dt, *J* = 7.7, 3.8 Hz, 1H), 7.09 – 7.01 (m, 4H), 6.76 – 6.66 (m, 2H), 5.49 (dd, *J* = 11.9, 5.3 Hz, 1H), 3.92 (dd, *J* = 17.4, 12.0 Hz, 1H), 3.15 (dd, *J* = 17.4, 5.4 Hz, 1H); <sup>13</sup>C NMR (125 MHz, DMSO-*d*<sub>6</sub>) δ 156.82, 146.28, 145.86, 135.16, 131.60, 128.39, 128.16, 127.90, 126.91, 126.14, 124.96 (q, <sup>1</sup>*J*<sub>C-F</sub> = 270.3 Hz), 117.90 (q, <sup>2</sup>*J*<sub>C-F</sub> = 31.9 Hz), 115.78, 112.34, 62.19, 43.86; MS (ESI): *m/z* = 388.81 (M+1)<sup>+</sup>.

**4-(1-(3-chlorophenyl)-3-(pyridin-2-yl)-4,5-dihydro-1H-pyrazol-5-yl)phenol (2j).** The title compound was prepared by reaction of (*E*)-3-(4-(*tert*-butoxy)phenyl)-1-(pyridin-2-yl)prop-2-en-1-one (**E8**) and 3-chlorophenylhydrazine hydrochloride according to the general procedure for pyrazoline synthesis. The product was purified by CC (CH<sub>2</sub>Cl<sub>2</sub>/MeOH 98:2); dark yellow solid; yield: 0.25 g (36%); mp 245.9-247 °C; <sup>1</sup>H NMR (500 MHz, DMSO-*d*<sub>6</sub>) δ 9.42 (s, 1H), 8.56 (ddd, *J* = 4.9, 1.8, 1.0 Hz, 1H), 8.11 (dt, *J* = 8.0, 1.1 Hz, 1H), 7.84 (ddd, *J* = 8.0, 7.5, 1.8 Hz, 1H), 7.35 (ddd, *J* = 7.5, 4.9, 1.2 Hz, 1H), 7.19 – 7.14 (m, 1H), 7.12 (t, *J* = 2.1 Hz, 1H), 7.10 – 7.05 (m, 2H), 6.91 (ddd, *J* = 8.4, 2.2, 0.8 Hz, 1H), 6.76 (ddd, *J* = 7.9, 2.0, 0.8 Hz, 1H), 6.74 – 6.69 (m, 2H), 5.47 (dd, *J* = 12.2, 5.8 Hz, 1H), 3.91 (dd, *J* = 18.1, 12.3 Hz, 1H), 3.14 (dd, *J* = 18.1, 5.8 Hz, 1H); <sup>13</sup>C NMR (125 MHz, DMSO-*d*<sub>6</sub>) δ 156.75, 151.05, 149.54, 149.25, 144.92, 136.45, 133.54, 131.92, 130.44, 126.97, 123.39, 120.40, 118.34, 115.76, 112.63, 111.63, 62.65, 42.91; MS (ESI): *m/z* = 349.78 (M+H)<sup>+</sup>.

**4-(1-(3-chlorophenyl)-3-(1H-pyrrol-2-yl)-4,5-dihydro-1H-pyrazol-5-yl)phenol (2k).** The title compound was prepared by reaction of (*E*)-3-(4-(*tert*-butoxy)phenyl)-1-(1H-pyrrol-2-yl)prop-2-en-1-one (**E9**) and 3-chlorophenylhydrazine hydrochloride according to the general procedure for pyrazoline synthesis. The product was purified by CC (CH<sub>2</sub>Cl<sub>2</sub>); grey solid; yield: 0.094 g (14%); mp 174.6-176.4 °C; <sup>1</sup>H NMR (500 MHz, DMSO-*d*<sub>6</sub>) 10.12 (s, 1H), 9.39 (s, 1H), δ 7.78-

## Results

---

7.71 (m, 1H), 7.15 – 7.09 (m, 1H), 6.99 (t,  $J = 2.1$  Hz, 1H), 6.98 – 6.92 (m, 2H), 6.84 (ddd,  $J = 8.4, 2.2, 0.9$  Hz, 1H), 6.81 (dd,  $J = 3.4, 0.7$  Hz, 1H), 6.72 (ddd,  $J = 7.9, 2.1, 0.9$  Hz, 1H), 6.68–6.60 (m, 1H), 6.57 – 6.49 (m, 2H), 5.09 (dd,  $J = 11.5, 5.6$  Hz, 1H), 3.69 (dd,  $J = 17.4, 11.6$  Hz, 1H), 2.89 (dd,  $J = 17.4, 5.6$  Hz, 1H);  $^{13}\text{C}$  NMR (125 MHz, DMSO- $d_6$ )  $\delta$  151.28, 148.15, 146.21, 142.65, 140.47, 134.40, 130.75, 128.46, 126.87, 117.75, 114.22, 113.60, 113.00, 112.93, 112.51, 61.99, 42.03; MS (ESI):  $m/z = 337.76$  (M+H) $^+$ .

**4-(3-(4-aminophenyl)-1-(4-chlorophenyl)-4,5-dihydro-1H-pyrazol-5-yl)phenol (2l).** The title compound was prepared by reaction of (*E*)-1-(4-aminophenyl)-3-(4-(*tert*-butoxy)phenyl)prop-2-en-1-one (**E10**) and 4-chlorophenylhydrazine hydrochloride according to the general procedure for pyrazoline synthesis. The product was purified by CC (CH<sub>2</sub>Cl<sub>2</sub>/MeOH 98:2); yellow solid; yield: 0.33g (46%); mp 181.5 °C;  $^1\text{H}$  NMR (500 MHz, DMSO- $d_6$ )  $\delta$  9.36 (s, 1H), 7.42 (d,  $J = 8.6$  Hz, 2H), 7.18 – 7.09 (m, 2H), 7.04 (d,  $J = 8.6$  Hz, 2H), 6.95 – 6.87 (m, 2H), 6.74 – 6.66 (m, 2H), 6.59 (t,  $J = 11.8$  Hz, 2H), 5.49 (s, 2H), 5.21 (dd,  $J = 11.8, 6.0$  Hz, 1H), 3.76 (dd,  $J = 17.2, 11.8$  Hz, 1H), 2.96 (dd,  $J = 17.2, 6.0$  Hz, 1H);  $^{13}\text{C}$  NMR (125 MHz, DMSO- $d_6$ )  $\delta$  156.55, 149.91, 149.04, 143.69, 132.56, 128.41, 127.19, 126.98, 120.94, 119.43, 115.61, 113.90, 113.47, 62.30, 43.52; MS (ESI):  $m/z = 363.85$  (M+H) $^+$ .

**3-(*tert*-butyl)-1-(4-chlorophenyl)-5-(3-methoxyphenyl)-4,5-dihydro-1H-pyrazole (3a).** The title compound was prepared by reaction of (*E*)-1-(3-methoxyphenyl)-4,4-dimethylpent-1-en-3-one (**E11**) and 4-chlorophenylhydrazine hydrochloride according to the general procedure for pyrazoline synthesis. The residue obtained after solvent removal was used for the next step without further purification; yellow solid; yield: 0.45 g (66%); MS (ESI):  $m/z = 342.77$  (M+H) $^+$ .

**3-(*tert*-butyl)-1,5-bis(4-methoxyphenyl)-4,5-dihydro-1H-pyrazole (3b).** The title compound was prepared by reaction of 1-(4-methoxyphenyl)-4,4-dimethylpent-1-en-3-one (**E12**) and 4-methoxyphenylhydrazine hydrochloride according to the general procedure for pyrazoline synthesis. The residue obtained after solvent removal was used for the next step without further purification; grey solid; yield: 0.40 g (59%); MS (ESI):  $m/z = 338.82$  (M+H) $^+$ .

**3-(*tert*-butyl)-5-(4-chlorophenyl)-1-(4-methoxyphenyl)-4,5-dihydro-1H-pyrazole (3c).** The title compound was prepared by reaction of 1-(4-chlorophenyl)-4,4-dimethylpent-1-en-3-one (**E13**) and 4-methoxyphenylhydrazine hydrochloride according to the general procedure for pyrazoline synthesis. The residue obtained after solvent removal was used for the next step without further purification; brown solid; yield: 0.48 g (71 %); MS (ESI):  $m/z = 342.68$  (M+H) $^+$ .

**3-(*tert*-butyl)-1-(4-chlorophenyl)-5-(3-fluoro-4-methoxyphenyl)-4,5-dihydro-1H-pyrazole (3d).** The title compound was prepared by reaction of (*E*)-1-(3-fluoro-4-methoxyphenyl)-4,4-dimethylpent-1-en-3-one (**E14**) and 4-chlorophenylhydrazine hydrochloride according to the general procedure for pyrazoline synthesis. The product was purified by CC (CH<sub>2</sub>Cl<sub>2</sub>/hexane 1:3); colorless oil; yield: 0.5 g (70%);  $^1\text{H}$  NMR (500 MHz, DMSO- $d_6$ )  $\delta$  7.48 – 7.42 (m, 2H), 6.90 – 6.86 (m, 1H), 6.79 (dd,  $J = 12.2, 2.1$  Hz, 1H), 6.74 – 6.70 (m, 1H), 6.66 – 6.59 (m, 2H),

## Results

---

5.10 (dd,  $J = 11.6, 5.0$  Hz, 1H), 3.56 (s, 3H), 3.32 (dd,  $J = 17.7, 11.7$  Hz, 1H), 2.52 (dd,  $J = 17.8, 5.1$  Hz, 1H), 1.12 (s, 9H); MS (ESI):  $m/z = 360.71$  (M+H)<sup>+</sup>.

**3-(*tert*-butyl)-5-(3-chloro-4-methoxyphenyl)-1-(4-chlorophenyl)-4,5-dihydro-1*H*-pyrazole (3e).** The title compound was prepared by reaction of (*E*)-1-(3-chloro-4-methoxyphenyl)-4,4-dimethylpent-1-en-3-one (**E15**) and 4-chlorophenylhydrazine hydrochloride according to the general procedure for pyrazoline synthesis. The product was purified by CC (CH<sub>2</sub>Cl<sub>2</sub>/hexane 1:4); yellowish white solid; yield: 0.43 g (58%); mp 150-152 °C; <sup>1</sup>H NMR (500 MHz, DMSO)  $\delta$  7.18 (d,  $J = 2.1$  Hz, 1H), 7.15 – 7.11 (m, 2H), 6.96 (dt,  $J = 6.7, 3.4$  Hz, 1H), 6.90 – 6.85 (m, 1H), 6.81 – 6.78 (m, 2H), 5.14 (dd,  $J = 11.7, 6.5$  Hz, 1H), 3.82 (s, 3H), 3.48 (dd,  $J = 17.6, 11.6$  Hz, 1H), 2.76 (dt,  $J = 21.7, 10.9$  Hz, 1H), 1.13 (s, 9H). MS (ESI):  $m/z = 376.78$  (M+H)<sup>+</sup>.

**3-(*tert*-butyl)-1-(3-chlorophenyl)-5-(4-fluoro-3-methoxyphenyl)-4,5-dihydro-1*H*-pyrazole (3f).** The title compound was prepared by reaction of (*E*)-1-(4-fluoro-3-methoxy phenyl)-4,4-dimethylpent-1-en-3-one (**E16**) and 3-chlorophenylhydrazine hydrochloride according to the general procedure for pyrazoline synthesis. The residue obtained after solvent removal was used for the next step without further purification; yellow oil; yield: 56% (0.4 g); MS (ESI):  $m/z = 360.74$  (M+H)<sup>+</sup>.

**1-(4-chlorophenyl)-5-(3,4-dimethoxyphenyl)-3-(2-methoxyphenyl)-4,5-dihydro-1*H*-pyrazole (3g).** The title compound was prepared by reaction of 3-(3,4-dimethoxyphenyl)-1-(2-methoxyphenyl)prop-2-en-1-one (**E17**) and 4-chlorophenylhydrazine hydrochloride according to the general procedure for pyrazoline synthesis. The residue obtained after solvent removal was used for the next step without further purification; brown solid; yield: 0.54 g (64%); MS (ESI):  $m/z = 422.81$  (M+H)<sup>+</sup>.

**1-(3-chlorophenyl)-5-(3-fluoro-4-methoxyphenyl)-3-(2-methoxyphenyl)-4,5-dihydro-1*H*-pyrazole (3h).** The title compound was prepared by reaction of (*E*)-3-(3-fluoro-4-methoxyphenyl)-1-(2-methoxyphenyl)prop-2-en-1-one (**E18**) and 3-chlorophenylhydrazine hydrochloride according to the general procedure for pyrazoline synthesis. The product was purified by CC (CH<sub>2</sub>Cl<sub>2</sub>/hexane 1:3); buff solid; yield: 0.43 g (53%); mp 182-184 °C; <sup>1</sup>H NMR (500 MHz, CDCl<sub>3</sub>)  $\delta$  8.21 (dd,  $J = 16.5, 7.8$  Hz, 1H), 7.57 – 7.47 (m, 2H), 7.39 (s, 1H), 7.31 – 7.21 (m, 3H), 7.14 (t,  $J = 7.0$  Hz, 2H), 6.98 (dd,  $J = 25.1, 8.0$  Hz, 2H), 5.33 (dd,  $J = 12.2, 6.9$  Hz, 1H), 4.21 (dd,  $J = 20.3, 7.7$  Hz, 1H), 4.08 (s, 3H), 4.03 (s, 3H), 3.50 (dd,  $J = 17.9, 6.8$  Hz, 1H); MS (ESI):  $m/z = 410.76$  (M+H)<sup>+</sup>.

**1-(3-chlorophenyl)-5-(4-ethoxy-3,5-difluorophenyl)-3-(2-methoxyphenyl)-4,5-dihydro-1*H*-pyrazole (3i).** The title compound was prepared by reaction of (*E*)-3-(4-ethoxy-3,5-difluorophenyl)-1-(2-methoxyphenyl)prop-2-en-1-one (**E19**) and 3-chlorophenylhydrazine hydrochloride according to the general procedure for pyrazoline synthesis. The product was purified by CC (CH<sub>2</sub>Cl<sub>2</sub>/hexane 1:4); buff solid; yield: 0.55 g (63%); mp 166-167 °C; <sup>1</sup>H NMR (500 MHz, CDCl<sub>3</sub>)  $\delta$  8.00 (dd,  $J = 7.8, 1.8$  Hz, 1H), 7.35 – 7.30 (m, 2H), 7.15 (t,  $J = 2.1$  Hz, 1H),

## Results

7.04 – 6.99 (m, 2H), 6.92 – 6.89 (m, 1H), 6.84 (ddd,  $J = 6.0, 3.4, 2.7$  Hz, 2H), 6.77 – 6.73 (m, 1H), 5.07 (dd,  $J = 12.2, 6.7$  Hz, 1H), 4.18 (q,  $J = 7.1$  Hz, 2H), 4.00 (dd,  $J = 20.1, 7.9$  Hz, 1H), 3.81 (s, 3H), 3.30 – 3.22 (m, 1H), 1.41 (t,  $J = 7.1$  Hz, 3H) ; MS (ESI):  $m/z = 442.71$  (M+H)<sup>+</sup>.

**1-(3-chlorophenyl)-5-(2,3-difluoro-4-methoxyphenyl)-3-(2-methoxyphenyl)-4,5-dihydro-1H-pyrazole (3j).** The title compound was prepared by reaction of (*E*)-3-(2,3-difluoro-4-methoxyphenyl)-1-(2-methoxyphenyl)prop-2-en-1-one (**E20**) and 3-chlorophenylhydrazine hydrochloride according to the general procedure for pyrazoline synthesis. The product was purified by CC (CH<sub>2</sub>Cl<sub>2</sub>/hexane 1:4); yellowish white solid; yield: 0.62 g (73%); mp 209-210 °C; <sup>1</sup>H NMR (500 MHz, CDCl<sub>3</sub>) δ 8.16 (ddd,  $J = 7.7, 3.6, 1.8$  Hz, 1H), 7.52 – 7.47 (m, 1H), 7.27 – 7.25 (m, 1H), 7.24 – 7.22 (m, 1H), 7.19 – 7.16 (m, 1H), 7.09 – 7.05 (m, 1H), 6.99 (tt,  $J = 7.1, 3.5$  Hz, 1H), 6.91 (dddd,  $J = 8.3, 4.2, 2.1, 0.9$  Hz, 2H), 6.79 (ddd,  $J = 13.3, 7.6, 3.9$  Hz, 1H), 5.60 (dd,  $J = 12.2, 6.1$  Hz, 1H), 4.18 (dt,  $J = 16.5, 7.7$  Hz, 1H), 4.02 (s, 3H), 3.99 (s, 3H), 3.45 (dd,  $J = 17.8, 6.1$  Hz, 1H) ; MS (ESI):  $m/z = 429.26$  (M+H)<sup>+</sup>.

**1-(3-chlorophenyl)-3-(2,4-dimethoxyphenyl)-5-(3-fluoro-4-methoxyphenyl)-4,5-dihydro-1H-pyrazole (3k).** The title compound was prepared by reaction of (*E*)-3-(3-fluoro-4-methoxyphenyl)-1-(2,4-dimethoxyphenyl)prop-2-en-1-one (**E21**) and 3-chlorophenylhydrazine hydrochloride according to the general procedure for pyrazoline synthesis. The residue obtained after solvent removal was used for the next step without further purification; yellowish white solid; 0.51g (58%); MS (ESI):  $m/z = 440.69$  (M+H)<sup>+</sup>.

**3-(tert-butyl)-1-(4-chlorophenyl)-5-(4-fluorophenyl)-4,5-dihydro-1H-pyrazole (3l).** The title compound was prepared by reaction of 1-(4-fluorophenyl)-4,4-dimethylpent-1-en-3-one (**E22**) and 4-chlorophenylhydrazine hydrochloride according to the general procedure for pyrazoline synthesis. The product was purified by CC (CH<sub>2</sub>Cl<sub>2</sub>/hexane 1:3); yellow solid; yield: 0.18 g (28%); mp 71.2 °C; <sup>1</sup>H NMR (500 MHz, CDCl<sub>3</sub>) δ 7.42 – 7.39 (m, 2H), 7.27 – 7.22 (m, 2H), 7.22 – 7.16 (m, 2H), 7.03 – 6.99 (m, 2H), 5.13 (dd,  $J = 11.7, 7.6$  Hz, 1H), 3.63 (dd,  $J = 17.2, 11.7$  Hz, 1H), 2.89 (dd,  $J = 17.2, 7.6$  Hz, 1H), 1.39 (s, 9H). <sup>13</sup>C NMR (125 MHz, CDCl<sub>3</sub>) δ 162.09 (d, <sup>1</sup> $J_{C-F} = 246.0$  Hz), 159.25, 144.62, 138.29 (d, <sup>4</sup> $J_{C-F} = 3.1$  Hz), 128.65, 127.44 (d, <sup>3</sup> $J_{C-F} = 8.1$  Hz), 123.41, 115.99 (d, <sup>2</sup> $J_{C-F} = 21.5$  Hz), 114.35, 64.26, 43.24, 33.82, 28.20; MS (ESI):  $m/z = 331.18$  (M+1)<sup>+</sup>.

**3-(tert-butyl)-1,5-bis(4-chlorophenyl)-4,5-dihydro-1H-pyrazole (3m).** The title compound was prepared by reaction of 1-(4-chlorophenyl)-4,4-dimethylpent-1-en-3-one (**E13**) and 4-chlorophenylhydrazine hydrochloride according to the general procedure for pyrazoline synthesis. The product was purified by CC (CH<sub>2</sub>Cl<sub>2</sub>/hexane 1:5); white solid; yield: 0.34 g (49.5%); mp 85.3-87 °C; <sup>1</sup>H NMR (500 MHz, CDCl<sub>3</sub>) δ 7.33 – 7.28 (m, 2H), 7.21 – 7.17 (m, 2H), 7.10 – 7.05 (m, 2H), 6.85 – 6.80 (m, 2H), 4.94 (dd,  $J = 11.7, 7.6$  Hz, 1H), 3.46 (dd,  $J = 17.2, 11.7$  Hz, 1H), 2.71 (dd,  $J = 17.2, 7.6$  Hz, 1H), 1.21 (s, 9H); <sup>13</sup>C NMR (125 MHz, CDCl<sub>3</sub>) δ

## Results

---

159.25, 144.53, 141.07, 133.26, 129.29, 128.68, 127.24, 123.48, 114.33, 64.28, 43.14, 33.82, 28.20; MS (ESI):  $m/z = 347.16$  (M+H)<sup>+</sup>.

**5-(4-bromophenyl)-3-(tert-butyl)-1-(4-chlorophenyl)-4,5-dihydro-1H-pyrazole (3n).** The title compound was prepared by reaction of 1-(4-bromophenyl)-4,4-dimethylpent-1-en-3-one (**E23**) and 4-chlorophenylhydrazine hydrochloride according to the general procedure for pyrazoline synthesis. The product was purified by CC (CH<sub>2</sub>Cl<sub>2</sub>/hexane 1:5); off-white solid; yield: 0.4 g (52%); mp 108.8 °C; <sup>1</sup>H NMR (500 MHz, CDCl<sub>3</sub>) δ 7.47 – 7.43 (m, 2H), 7.15 – 7.11 (m, 2H), 7.10 – 7.05 (m, 2H), 6.85 – 6.79 (m, 2H), 4.92 (dd,  $J = 11.7, 7.6$  Hz, 1H), 3.46 (dt,  $J = 17.2, 7.5$  Hz, 1H), 2.71 (dd,  $J = 17.2, 7.6$  Hz, 1H), 1.21 (s, 9H); <sup>13</sup>C NMR (125 MHz, CDCl<sub>3</sub>) δ 159.50, 144.76, 141.85, 132.49, 128.94, 127.84, 123.75, 121.57, 114.58, 64.57, 43.34, 34.07, 28.45; MS (ESI):  $m/z = 392.71$  (M+H)<sup>+</sup>.

**4-(3-(tert-butyl)-1-(4-chlorophenyl)-4,5-dihydro-1H-pyrazol-5-yl)benzotrile (3o).** The title compound was prepared by reaction of 4-(4,4-dimethyl-3-oxopent-1-en-1-yl)benzotrile (**E24**) and 4-chlorophenylhydrazine hydrochloride according to the general procedure for pyrazoline synthesis. The product was purified by CC (CH<sub>2</sub>Cl<sub>2</sub>/hexane 1:1); buff solid; yield: 0.44 g (66%); mp 109.5 °C; <sup>1</sup>H NMR (500 MHz, DMSO-*d*<sub>6</sub>) δ 7.83 – 7.78 (m, 2H), 7.42 – 7.38 (m, 2H), 7.16 – 7.10 (m, 2H), 6.83 – 6.77 (m, 2H), 5.33 (dd,  $J = 11.8, 6.3$  Hz, 1H), 3.58 (dd,  $J = 17.6, 11.8$  Hz, 1H), 2.73 (dd,  $J = 17.6, 6.3$  Hz, 1H), 1.16 (s, 9H); <sup>13</sup>C NMR (125 MHz, DMSO-*d*<sub>6</sub>) δ 160.05, 147.90, 143.86, 132.95, 128.61, 126.91, 121.68, 118.58, 113.97, 110.21, 62.66, 42.33, 33.45, 27.83; MS (ESI):  $m/z = 337.03$  (M<sup>+</sup>).

**1-(4-chlorophenyl)-5-(4-methoxyphenyl)-3-phenyl-4,5-dihydro-1H-pyrazole (3p).** The title compound was prepared by reaction of 3-(4-methoxyphenyl)-1-phenylprop-2-en-1-one (**E25**) and 4-chlorophenylhydrazine hydrochloride according to the general procedure for pyrazoline synthesis. The product was purified by CC (CH<sub>2</sub>Cl<sub>2</sub>/hexane 1:3); yellow solid; yield: 0.43 g (59%); mp 173-175 °C; <sup>1</sup>H NMR (500 MHz, CDCl<sub>3</sub>) δ 7.62 (ddd,  $J = 4.2, 3.5, 1.8$  Hz, 2H), 7.38 – 7.33 (m, 1H), 7.32 – 7.28 (m, 2H), 7.14 – 7.07 (m, 3H), 7.05 – 7.00 (m, 2H), 6.92 – 6.88 (m, 1H), 6.79 – 6.74 (m, 2H), 5.10 (dd,  $J = 12.2, 7.1$  Hz, 1H), 3.75 – 3.70 (m, 1H), 3.68 (s, 3H), 3.03 (dd,  $J = 17.1, 7.1$  Hz, 1H). <sup>13</sup>C NMR (125 MHz, CDCl<sub>3</sub>) δ 159.08, 147.33, 143.37, 134.05, 130.07, 129.09, 128.76, 127.00, 126.50, 125.75, 123.76, 114.54, 105.03, 63.97, 55.29, 43.6 9; MS (ESI):  $m/z = 362.33$  (M<sup>+</sup>).

**4-(1-(4-chlorophenyl)-3-methyl-4,5-dihydro-1H-pyrazol-5-yl)phenol (3q).** The title compound was prepared by reaction of the commercially available 4-hydroxybenzylideneacetone and 4-chlorophenylhydrazine hydrochloride according to the general procedure for pyrazoline synthesis. The product was purified by CC (CH<sub>2</sub>Cl<sub>2</sub>); white solid; yield: 0.20 g (35%); mp 184-186 °C; <sup>1</sup>H NMR (500 MHz, DMSO-*d*<sub>6</sub>) δ 9.35 (s, 1H), 7.12 – 7.07 (m, 2H), 7.05 – 7.01 (m, 2H), 6.82 – 6.77 (m, 2H), 6.72 – 6.68 (m, 2H), 5.02 (dd,  $J = 11.7, 6.9$  Hz, 1H), 3.44 (ddd,  $J = 17.7, 11.7, 1.1$  Hz, 1H), 2.61 (ddd,  $J = 17.8, 6.9, 1.0$  Hz, 1H), 2.00 (s, 3H); <sup>13</sup>C NMR (125 MHz,

## Results

---

DMSO- $d_6$ )  $\delta$  156.52, 150.03, 144.28, 132.66, 128.37, 126.96, 121.06, 115.58, 113.84, 62.71, 47.40, 15.54; MS (ESI):  $m/z$  = 286.89 (M+H)<sup>+</sup>.

**3-(3-(*tert*-butyl)-1-(4-chlorophenyl)-4,5-dihydro-1H-pyrazol-5-yl)phenol (4a).** The title compound was prepared by demethylation of 3-(*tert*-butyl)-1-(4-chlorophenyl)-5-(3-methoxyphenyl)-4,5-dihydro-1H-pyrazole (**3a**) using BBr<sub>3</sub> (3 equiv) according to the general procedure for ether dealkylation. The product was purified by CC (CH<sub>2</sub>Cl<sub>2</sub>/hexane 4:1); beige solid; yield: 0.21 g (64%); mp 131-133 °C; <sup>1</sup>H NMR (500 MHz, DMSO- $d_6$ )  $\delta$  9.39 (s, 1H), 7.15 – 7.09 (m, 3H), 6.83 – 6.79 (m, 2H), 6.66 (ddd,  $J$  = 6.5, 3.8, 1.4 Hz, 1H), 6.64 – 6.59 (m, 2H), 5.06 (dd,  $J$  = 11.7, 6.6 Hz, 1H), 3.52 (dd,  $J$  = 17.6, 11.8 Hz, 1H), 2.68 (dd,  $J$  = 17.6, 6.6 Hz, 1H), 1.17 (s, 9H); <sup>13</sup>C NMR (125 MHz, DMSO- $d_6$ )  $\delta$  159.84, 157.81, 144.23, 144.05, 129.96, 128.43, 121.18, 116.28, 114.34, 113.83, 112.10, 63.14, 42.65, 33.42, 27.89. MS (ESI):  $m/z$  = 328.91 (M+H)<sup>+</sup>.

**4,4'-(3-(*tert*-butyl)-4,5-dihydro-1H-pyrazole-1,5-diyl)diphenol (4b).** The title compound was prepared by demethylation of 3-(*tert*-butyl)-1,5-bis(4-methoxyphenyl)-4,5-dihydro-1H-pyrazole (**3b**) using BBr<sub>3</sub> (6 equiv) according to the general procedure for ether dealkylation. The product was purified by CC (CH<sub>2</sub>Cl<sub>2</sub>/MeOH 98:2); grey solid; yield: 0.22 g (73%); mp 104-106 °C; <sup>1</sup>H NMR (500 MHz, DMSO- $d_6$ )  $\delta$  9.63 (s, 1H), 9.32 (s, 1H), 7.08 (d,  $J$  = 8.5 Hz, 2H), 7.04 – 6.98 (m, 2H), 6.69 (ddd,  $J$  = 11.4, 7.7, 3.3 Hz, 2H), 6.55 – 6.50 (m, 2H), 4.77 (dd,  $J$  = 11.0, 9.2 Hz, 1H), 3.52 (dd,  $J$  = 17.1, 11.1 Hz, 1H), 2.57 (dd,  $J$  = 17.1, 9.1 Hz, 1H), 1.15 (s, 9H); <sup>13</sup>C NMR (125 MHz, DMSO- $d_6$ )  $\delta$  160.58, 157.95, 157, 139.68, 133.36, 132.05, 121.27, 115.14, 114.93, 65.25, 42.73, 31.77, 27.99; MS (ESI):  $m/z$  = 311.10 (M+H)<sup>+</sup>.

**4-(3-(*tert*-butyl)-5-(4-chlorophenyl)-4,5-dihydro-1H-pyrazol-1-yl)phenol (4c).** The title compound was prepared by demethylation of 3-(*tert*-butyl)-5-(4-chlorophenyl)-1-(4-methoxyphenyl)-4,5-dihydro-1H-pyrazole (**3c**) using BBr<sub>3</sub> (3 equiv) according to the general procedure for ether dealkylation. The product was purified by CC (CH<sub>2</sub>Cl<sub>2</sub>/hexane 4:1); grey solid; yield: 0.14 g (44%); mp 142-143 °C; <sup>1</sup>H NMR (500 MHz, DMSO- $d_6$ )  $\delta$  8.68 (s, 1H), 7.41 – 7.32 (m, 2H), 7.33 – 7.26 (m, 2H), 6.71 – 6.63 (m, 2H), 6.59 – 6.50 (m, 2H), 4.95 (dd,  $J$  = 11.3, 8.7 Hz, 1H), 3.45 (dd,  $J$  = 17.2, 11.4 Hz, 1H), 2.61 (dd,  $J$  = 17.2, 8.7 Hz, 1H), 1.15 (s, 9H); <sup>13</sup>C NMR (125 MHz, DMSO- $d_6$ )  $\delta$  158.11, 150.35, 142.17, 139.24, 131.54, 128.69, 128.05, 115.29, 114.87, 64.66, 42.51, 33.32, 27.96; MS (ESI):  $m/z$  = 328.71 (M+H)<sup>+</sup>.

**4-(3-(*tert*-butyl)-1-(4-chlorophenyl)-4,5-dihydro-1H-pyrazol-5-yl)-2-fluorophenol (4d).** The title compound was prepared by demethylation of 3-(*tert*-butyl)-1-(4-chlorophenyl)-5-(3-fluoro-4-methoxyphenyl)-4,5-dihydro-1H-pyrazole (**3d**) using BBr<sub>3</sub> (3 equiv) according to the general procedure for ether dealkylation. The product was purified by CC (CH<sub>2</sub>Cl<sub>2</sub>/hexane 4:1); off-white solid; yield: 0.15 g (44%); mp 130-132 °C; <sup>1</sup>H NMR (500 MHz, DMSO- $d_6$ )  $\delta$  9.80 (s, 1H), 7.15 – 7.10 (m, 2H), 6.95 (dd,  $J$  = 12.1, 2.0 Hz, 1H), 6.92 – 6.86 (m, 1H), 6.86 – 6.81 (m, 3H), 5.09 (dd,  $J$  = 11.5, 6.4 Hz, 1H), 3.48 (dd,  $J$  = 17.5, 11.6 Hz, 1H), 2.69 (dd,  $J$  = 17.5, 6.4 Hz, 1H),

## Results

1.16 (s, 9H);  $^{13}\text{C}$  NMR (125 MHz, DMSO- $d_6$ )  $\delta$  159.94, 150.94 (d,  $^1J_{\text{C-F}} = 241.5$  Hz), 144.17, 143.96 (d,  $^2J_{\text{C-F}} = 12.1$  Hz), 133.71 (d,  $^3J_{\text{C-F}} = 5.0$  Hz), 128.45, 121.84 (d,  $^4J_{\text{C-F}} = 3.0$  Hz), 121.35, 118.17, 114.03, 113.52 (d,  $^2J_{\text{C-F}} = 18.7$  Hz), 62.40, 42.56, 33.42, 27.85.; MS (ESI):  $m/z = 347.37$  (M+H) $^+$ .

### **4-(1-(3-chlorophenyl)-3-(2-hydroxyphenyl)-4,5-dihydro-1H-pyrazol-5-yl)-2,6-**

**difluorophenol (4i).** The title compound was prepared by deprotection of 1-(3-chlorophenyl)-5-(4-ethoxy-3,5-difluorophenyl)-3-(2-methoxyphenyl)-4,5-dihydro-1H-pyrazole (**3i**) using BBr<sub>3</sub> (6 equiv) according to the general procedure for ether dealkylation. The product was purified by CC (CH<sub>2</sub>Cl<sub>2</sub>); off-white solid; yield: 0.30 g (77%); mp 179-181 °C;  $^1\text{H}$  NMR (500 MHz, DMSO- $d_6$ )  $\delta$  10.28 (s, 1H), 10.24 (s, 1H), 7.48 (dd,  $J = 7.8, 1.6$  Hz, 1H), 7.29 (ddt,  $J = 11.1, 5.4, 2.7$  Hz, 1H), 7.24 – 7.19 (m, 1H), 7.00 – 6.96 (m, 4H), 6.92 (ddd,  $J = 7.8, 7.3, 1.2$  Hz, 1H), 6.82 (dddd,  $J = 15.3, 7.9, 2.1, 0.8$  Hz, 2H), 5.42 (dd,  $J = 12.0, 6.2$  Hz, 1H), 4.02 (dd,  $J = 17.9, 12.0$  Hz, 1H), 3.31 (dd,  $J = 17.9, 6.2$  Hz, 1H);  $^{13}\text{C}$  NMR (125 MHz, DMSO- $d_6$ )  $\delta$  156.21, 152.40 (dd,  $^1J_{\text{C-F}} = 243.0, ^3J_{\text{C-F}} = 7.1$  Hz), 150.99, 144.73, 133.68, 132.99 (t,  $^2J_{\text{C-F}} = 16.1$  Hz), 132.31 (t,  $^3J_{\text{C-F}} = 6.9$  Hz), 130.78, 130.74, 128.37, 119.53, 118.65, 116.60, 116.21, 112.36, 111.46, 109.47 (dd,  $^2J_{\text{C-F}} = 16.1, ^4J_{\text{C-F}} = 6.4$  Hz), 60.89, 44.03; MS (ESI):  $m/z = 400.74$  (M+H) $^+$ .

### **4-(1-(3-chlorophenyl)-3-(2-hydroxyphenyl)-4,5-dihydro-1H-pyrazol-5-yl)-2,3-**

**difluorophenol (4j).** The title compound was prepared by demethylation of 1-(3-chlorophenyl)-5-(2,3-difluoro-4-methoxyphenyl)-3-(2-methoxyphenyl)-4,5-dihydro-1H-pyrazole (**3j**) using BBr<sub>3</sub> (6 equiv) according to the general procedure for ether dealkylation. The product was purified by CC (CH<sub>2</sub>Cl<sub>2</sub>); off-white solid; yield: 0.27 g (69%); mp 196-197 °C;  $^1\text{H}$  NMR (500 MHz, DMSO- $d_6$ )  $\delta$  10.48 (s, 1H), 10.30 (s, 1H), 7.50 (d,  $J = 7.7$  Hz, 1H), 7.29 (dd,  $J = 11.4, 4.0$  Hz, 1H), 7.25 – 7.18 (m, 1H), 7.01 – 6.94 (m, 2H), 6.94 – 6.89 (m, 1H), 6.87 – 6.78 (m, 3H), 6.73 (t,  $J = 8.2$  Hz, 1H), 5.61 (dd,  $J = 12.2, 5.5$  Hz, 1H), 4.05 (dd,  $J = 17.8, 12.5$  Hz, 1H), 3.40 (dd,  $J = 18.0, 5.5$  Hz, 1H);  $^{13}\text{C}$  NMR (125 MHz, DMSO- $d_6$ )  $\delta$  156.17, 151.20, 148.50 (dd,  $^1J_{\text{C-F}} = 245.8, ^2J_{\text{C-F}} = 10.8$  Hz), 146.24, 144.51, 139.84 (dd,  $^1J_{\text{C-F}} = 243.7, ^2J_{\text{C-F}} = 13.6$  Hz), 133.72, 130.78, 128.35, 121.67, 119.55, 119.46, 119.38, 118.56, 116.51, 116.19, 113.11, 112.13, 111.22, 56.11, 42.83.; MS (ESI):  $m/z = 400.81$  (M+H) $^+$ .

**3-(tert-butyl)-1-(4-chlorophenyl)-5-(4-nitrophenyl)-4,5-dihydro-1H-pyrazole (5a).** The title compound was prepared by reaction of 4,4-dimethyl-1-(4-nitrophenyl)pent-1-en-3-one (**E26**) and 4-chlorophenylhydrazine hydrochloride according to the general procedure for pyrazoline synthesis. The product was purified by CC (CH<sub>2</sub>Cl<sub>2</sub>/hexane 1:2); orange solid; yield: 0.50 g (71%); mp 146-147 °C;  $^1\text{H}$  NMR (500 MHz, CDCl<sub>3</sub>)  $\delta$  8.23 – 8.18 (m, 2H), 7.45 – 7.41 (m, 2H), 7.11 – 7.04 (m, 2H), 6.81 – 6.77 (m, 2H), 5.07 (dd,  $J = 11.9, 7.6$  Hz, 1H), 3.53 (dd,  $J = 17.3, 11.9$  Hz, 1H), 2.73 (dd,  $J = 17.3, 7.6$  Hz, 1H), 1.22 (s, 9H).  $^{13}\text{C}$  NMR (125 MHz, CDCl<sub>3</sub>)  $\delta$  159.23, 149.82, 147.43, 144.18, 128.82, 126.79, 124.50, 123.93, 114.32, 64.23, 42.96, 33.87, 28.17; MS (ESI):  $m/z = 357.75$  (M $^+$ ).

## Results

---

**3-(tert-butyl)-1-(2,4-difluorophenyl)-5-(4-nitrophenyl)-4,5-dihydro-1H-pyrazole (5b).** The title compound was prepared by reaction of 4,4-dimethyl-1-(4-nitrophenyl)pent-1-en-3-one (**E26**) and 2,4-difluorophenylhydrazine hydrochloride according to the general procedure for pyrazoline synthesis. The product was purified by CC (CH<sub>2</sub>Cl<sub>2</sub>/hexane 1:2); orange oil; yield: 0.34 g (48%); <sup>1</sup>H NMR (500 MHz, CDCl<sub>3</sub>) δ 8.03 – 7.98 (m, 2H), 7.32 (tt, *J* = 8.9, 4.4 Hz, 1H), 7.26 – 7.20 (m, 2H), 6.64 (dddd, *J* = 9.1, 7.9, 2.8, 1.4 Hz, 1H), 6.56 – 6.49 (m, 1H), 5.26 (ddd, *J* = 11.3, 5.0, 3.3 Hz, 1H), 3.40 (dd, *J* = 17.1, 11.3 Hz, 1H), 2.76 (dd, *J* = 17.1, 5.0 Hz, 1H), 1.16 (s, 9H); <sup>13</sup>C NMR (125 MHz, CDCl<sub>3</sub>) δ 160.77, 157.40 (dd, <sup>1</sup>*J*<sub>C-F</sub> = 242.7, <sup>3</sup>*J*<sub>C-F</sub> = 11.1 Hz), 151.26 (dd, <sup>1</sup>*J*<sub>C-F</sub> = 246.9, <sup>3</sup>*J*<sub>C-F</sub> = 11.7 Hz), 149.24, 147.29, 130.66 (dd, <sup>2</sup>*J*<sub>C-F</sub> = 9.7, <sup>4</sup>*J*<sub>C-F</sub> = 3.4 Hz), 127.07, 123.92, 120.47 (dd, <sup>3</sup>*J*<sub>C-F</sub> = 8.9, 4.6 Hz), 111.09 (dd, <sup>2</sup>*J*<sub>C-F</sub> = 21.6, <sup>4</sup>*J*<sub>C-F</sub> = 3.4 Hz), 104.27 (dd, <sup>2</sup>*J*<sub>C-F</sub> = 26.3, 24.2 Hz), 66.25, 42.48, 33.93, 28.13; MS (ESI): *m/z* = 359.83 (M+H)<sup>+</sup>.

**3-(tert-butyl)-1-(3-chlorophenyl)-5-(4-nitrophenyl)-4,5-dihydro-1H-pyrazole (5c).** The title compound was prepared by reaction of 4,4-dimethyl-1-(4-nitrophenyl)pent-1-en-3-one (**E26**) and 3-chlorophenylhydrazine hydrochloride according to the general procedure for pyrazoline synthesis. The residue obtained after solvent removal was used for the next step without further purification; orange solid; yield: 0.44 g (62%); MS (ESI): *m/z* = 357.92 (M+H)<sup>+</sup>.

**3-(tert-butyl)-1-(4-chlorophenyl)-5-(3-nitrophenyl)-4,5-dihydro-1H-pyrazole (5d).** The title compound was prepared by reaction of 4,4-dimethyl-1-(3-nitrophenyl)pent-1-en-3-one (**E27**) and 4-chlorophenylhydrazine hydrochloride according to the general procedure for pyrazoline synthesis. The product was purified by CC (CH<sub>2</sub>Cl<sub>2</sub>/hexane 1:2); orange solid; yield: 0.40 g (57%); mp 115-116 °C; <sup>1</sup>H NMR (500 MHz, CDCl<sub>3</sub>) δ 8.17 – 8.15 (m, 1H), 8.13 (ddd, *J* = 8.0, 2.3, 1.2 Hz, 1H), 7.58 (dt, *J* = 7.7, 1.3 Hz, 1H), 7.53 – 7.49 (m, 1H), 7.10 – 7.06 (m, 2H), 6.84 – 6.79 (m, 2H), 5.08 (dd, *J* = 11.8, 7.6 Hz, 1H), 3.54 (dd, *J* = 17.3, 11.8 Hz, 1H), 2.75 (dd, *J* = 17.3, 7.6 Hz, 1H), 1.23 (s, 9H); <sup>13</sup>C NMR (125 MHz, CDCl<sub>3</sub>) δ 159.28, 148.80, 144.76, 144.21, 131.92, 130.25, 128.80, 123.90, 122.70, 121.04, 114.37, 64.16, 43.07, 33.85, 28.16; MS (ESI): *m/z* = 357.80 (M+H)<sup>+</sup>.

**1-(3-chlorophenyl)-3-cyclopropyl-5-(4-nitrophenyl)-4,5-dihydro-1H-pyrazole (5e).** The title compound was prepared by reaction of 1-cyclopropyl-3-(4-nitrophenyl)prop-2-en-1-one (**E28**) and 3-chlorophenylhydrazine hydrochloride according to the general procedure for pyrazoline synthesis. The residue obtained after solvent removal was used for the next step without further purification; orange solid; yield: 0.35g (51%); MS (ESI): *m/z* = 341.63 (M+H)<sup>+</sup>.

**1-(3-chlorophenyl)-3-(1-methylcyclopropyl)-5-(4-nitrophenyl)-4,5-dihydro-1H-pyrazole (5f).** The title compound was prepared by reaction of (*E*)-1-(1-methylcyclopropyl)-3-(4-nitrophenyl)prop-2-en-1-one (**E29**) and 3-chlorophenylhydrazine hydrochloride according to the general procedure for pyrazoline synthesis. The residue obtained after solvent removal was used for the next step without further purification; orange solid; yield: 0.57 g (81%); MS (ESI): *m/z* = 355.75 (M+H)<sup>+</sup>.

## Results

---

**1-(4-chlorophenyl)-3-cyclohexyl-5-(4-nitrophenyl)-4,5-dihydro-1H-pyrazole (5g).** The title compound was prepared by reaction of (*E*)-1-cyclohexyl-3-(4-nitrophenyl)prop-2-en-1-one (**E30**) and 4-chlorophenylhydrazine hydrochloride according to the general procedure for pyrazoline synthesis. The product was purified by CC (CH<sub>2</sub>Cl<sub>2</sub>/hexane 1:2); orange solid; yield: 0.49 g (64%); mp 112-113 °C; <sup>1</sup>H NMR (500 MHz, CDCl<sub>3</sub>) δ 8.22 – 8.16 (m, 2H), 7.45 – 7.39 (m, 2H), 7.10 – 7.05 (m, 2H), 6.80 – 6.74 (m, 2H), 5.05 (dd, *J* = 11.9, 7.5 Hz, 1H), 3.48 (ddd, *J* = 17.4, 12.0, 0.8 Hz, 1H), 2.69 (ddd, *J* = 17.4, 7.5, 0.8 Hz, 1H), 2.45 – 2.37 (m, 1H), 1.93 – 1.87 (m, 2H), 1.80 (dd, *J* = 9.0, 3.8 Hz, 2H), 1.73 – 1.67 (m, 1H), 1.41 – 1.28 (m, 4H), 1.28 – 1.17 (m, 1H); <sup>13</sup>C NMR (125 MHz, CDCl<sub>3</sub>) δ 156.25, 149.81, 147.38, 144.06, 128.82, 126.79, 124.48, 123.85, 114.22, 63.55, 44.17, 39.04, 30.57, 30.54, 25.91, 25.74; MS (ESI): *m/z* = 383.83 (M+H)<sup>+</sup>.

**1-(3-chlorophenyl)-5-(4-nitrophenyl)-3-(thiophen-2-yl)-4,5-dihydro-1H-pyrazole (5h).** The title compound was prepared by reaction of 3-(4-nitrophenyl)-1-(thiophen-2-yl)prop-2-en-1-one (**E31**) and 3-chlorophenylhydrazine hydrochloride according to the general procedure for pyrazoline synthesis. The residue obtained after solvent removal was used for the next step without further purification; orange solid; yield: 0.44 g (58%); MS (ESI): *m/z* = 383.71 (M+H)<sup>+</sup>.

**1-(3-chlorophenyl)-3-(furan-2-yl)-5-(4-nitrophenyl)-4,5-dihydro-1H-pyrazole (5i).** The title compound was prepared by reaction of 1-(furan-2-yl)-3-(4-nitrophenyl)prop-2-en-1-one (**E32**) and 3-chlorophenylhydrazine hydrochloride according to the general procedure for pyrazoline synthesis. The residue obtained after solvent removal was used for the next step without further purification; orange solid; yield: 0.44 g (61%); MS (ESI): *m/z* = 367.66 (M+H)<sup>+</sup>.

**3-(2-chlorophenyl)-1-(3-chlorophenyl)-5-(4-nitrophenyl)-4,5-dihydro-1H-pyrazole (5j).** The title compound was prepared by reaction of 1-(2-chlorophenyl)-3-(4-nitrophenyl)prop-2-en-1-one (**E33**) and 3-chlorophenylhydrazine hydrochloride according to the general procedure for pyrazoline synthesis. The residue obtained after solvent removal was used for the next step without further purification; orange solid; yield: 0.42 g (51%); MS (ESI): *m/z* = 411.73 (M+H)<sup>+</sup>.

**1-(3-chlorophenyl)-5-(4-nitrophenyl)-3-(2-(trifluoromethyl)phenyl)-4,5-dihydro-1H-pyrazole (5k).** The title compound was prepared by reaction of (*E*)-3-(4-nitrophenyl)-1-(2-(trifluoromethyl)phenyl)prop-2-en-1-one (**E34**) and 3-chlorophenylhydrazine hydrochloride according to the general procedure for pyrazoline synthesis. The residue obtained after solvent removal was used for the next step without further purification; orange solid; yield: 0.47 g (53%); MS (ESI): *m/z* = 445.67 (M+H)<sup>+</sup>.

**1-(3-chlorophenyl)-5-(4-nitrophenyl)-3-(*o*-tolyl)-4,5-dihydro-1H-pyrazole (5l).** The title compound was prepared by reaction of (*E*)-3-(4-nitrophenyl)-1-(*o*-tolyl)prop-2-en-1-one (**E35**) and 3-chlorophenylhydrazine hydrochloride according to the general procedure for pyrazoline synthesis. The residue obtained after solvent removal was used for the next step without further purification; orange solid; yield: 0.37 g (47.5%); MS (ESI): *m/z* = 391.87 (M+H)<sup>+</sup>.

## Results

### **1-(3-chlorophenyl)-3-(2-methoxyphenyl)-5-(4-nitrophenyl)-4,5-dihydro-1H-pyrazole (5m).**

The title compound was prepared by reaction of 1-(2-methoxyphenyl)-3-(4-nitrophenyl)prop-2-en-1-one (**E36**) and 3-chlorophenylhydrazine hydrochloride according to the general procedure for pyrazoline synthesis. The residue obtained after solvent removal was used for the next step without further purification; orange solid; yield: 0.34 g (42%); MS (ESI):  $m/z = 408.02$  (M+H).<sup>+</sup>

### **3-(benzo[d][1,3]dioxol-5-yl)-1-(3-chlorophenyl)-5-(4-nitrophenyl)-4,5-dihydro-1H-pyrazole (5n).**

The title compound was prepared by reaction of 1-(benzo[d][1,3]dioxol-5-yl)-3-(4-nitrophenyl)prop-2-en-1-one (**E37**) and 3-chlorophenylhydrazine hydrochloride according to the general procedure for pyrazoline synthesis. The residue obtained after solvent removal was used for the next step without further purification; yield: orange solid; 0.51 g (61%); MS (ESI):  $m/z = 421.71$  (M+H).<sup>+</sup>

### **4-(3-(tert-butyl)-1-(2,4-difluorophenyl)-4,5-dihydro-1H-pyrazol-5-yl)aniline (6b).**

The title compound was prepared by reduction of 3-(tert-butyl)-1-(2,4-difluorophenyl)-5-(4-nitrophenyl)-4,5-dihydro-1H-pyrazole (**5b**) according to the general reduction procedure. The product was purified by CC (CH<sub>2</sub>Cl<sub>2</sub>); buff solid; yield: 0.24 g (75%); mp 139-140 °C; <sup>1</sup>H NMR (500 MHz, DMSO-*d*<sub>6</sub>) δ 7.28 (td,  $J = 9.3, 6.2$  Hz, 1H), 6.98 (ddd,  $J = 12.1, 9.0, 2.9$  Hz, 1H), 6.84 (tdd,  $J = 9.2, 2.9, 1.2$  Hz, 1H), 6.78 – 6.73 (m, 2H), 6.38 – 6.33 (m, 2H), 5.10 – 5.04 (m, 1H), 4.93 (s, 2H), 3.37 – 3.30 (m, 1H), 2.79 (dd,  $J = 17.1, 4.7$  Hz, 1H), 1.20 (s, 9H); <sup>13</sup>C NMR (125 MHz, DMSO-*d*<sub>6</sub>) δ 160.98, 156.17 (dd,  $^1J_{C-F} = 239.0, ^3J_{C-F} = 11.2$  Hz), 150.99 (dd,  $^1J_{C-F} = 246.7, ^3J_{C-F} = 12.0$  Hz), 147.88, 131.45 (dd,  $^2J_{C-F} = 9.8, ^4J_{C-F} = 3.1$  Hz), 128.28, 126.90, 120.26 (dd,  $^3J_{C-F} = 9.1, 5.0$  Hz), 113.60, 110.62 (dd,  $^2J_{C-F} = 21.4, ^4J_{C-F} = 3.2$  Hz), 103.94 (dd,  $^2J_{C-F} = 26.4, 24.5$  Hz), 65.95, 41.67, 33.53, 27.87.; MS (ESI):  $m/z = 329.89$  (M+H).<sup>+</sup>

### **4-(3-(tert-butyl)-1-(3-chlorophenyl)-4,5-dihydro-1H-pyrazol-5-yl)aniline (6c).**

The title compound was prepared by reduction of 3-(tert-butyl)-1-(3-chlorophenyl)-5-(4-nitrophenyl)-4,5-dihydro-1H-pyrazole according to the general reduction procedure (**5c**). The product was purified by CC (CH<sub>2</sub>Cl<sub>2</sub>); tan solid; yield: 0.20g (62%); mp 136.4 °C; <sup>1</sup>H NMR (500 MHz, DMSO-*d*<sub>6</sub>) δ 7.09 – 7.03 (m, 1H), 6.89 – 6.85 (m, 3H), 6.72 (ddd,  $J = 8.4, 2.2, 0.9$  Hz, 1H), 6.61 (ddd,  $J = 7.9, 2.1, 0.9$  Hz, 1H), 6.52 – 6.47 (m, 2H), 5.02 – 4.97 (m, 3H), 3.45 (dd,  $J = 17.6, 11.6$  Hz, 1H), 2.65 (dd,  $J = 17.6, 6.2$  Hz, 1H), 1.18 (s, 9H); <sup>13</sup>C NMR (125 MHz, DMSO-*d*<sub>6</sub>) δ 160.30, 147.90, 146.64, 133.22, 130.12, 129.18, 126.40, 116.71, 114.17, 111.81, 110.94, 62.85, 42.68, , 33.46, 27.88.; MS (ESI):  $m/z = 328.06$  (M+H).<sup>+</sup>

### **3-(3-(tert-butyl)-1-(4-chlorophenyl)-4,5-dihydro-1H-pyrazol-5-yl)aniline (6d).**

The title compound was prepared by reduction of 3-(tert-butyl)-1-(4-chlorophenyl)-5-(3-nitrophenyl)-4,5-dihydro-1H-pyrazole (**5d**) according to the general reduction procedure. The product was purified by CC (CH<sub>2</sub>Cl<sub>2</sub>); yellow solid; yield: 0.24 g (74%); mp 104-106 °C; <sup>1</sup>H NMR (500 MHz, DMSO-*d*<sub>6</sub>) δ 7.15 – 7.09 (m, 2H), 6.99 – 6.92 (m, 1H), 6.84 – 6.78 (m, 2H), 6.44 – 6.36 (m, 3H), 5.08 (s, 2H), 4.92 (dd,  $J = 11.8, 7.2$  Hz, 1H), 3.50 (dd,  $J = 17.6, 11.8$  Hz, 1H), 2.66 (dd,  $J = 17.6,$

## Results

---

7.2 Hz, 1H), 1.17 (s, 9H);  $^{13}\text{C}$  NMR (125 MHz, DMSO- $d_6$ )  $\delta$  159.79, 149.26, 144.49, 143.42, 128.38, 125.11, 121.11, 115.82, 113.82, 112.99, 110.33, 63.71, 42.78, 33.42, 27.93; MS (ESI):  $m/z = 327.87$  (M+H) $^+$ .

**4-(1-(3-chlorophenyl)-3-cyclopropyl-4,5-dihydro-1H-pyrazol-5-yl)aniline (6e).** The title compound was prepared by reduction of 1-(3-chlorophenyl)-3-cyclopropyl-5-(4-nitrophenyl)-4,5-dihydro-1H-pyrazole (**5e**) according to the general reduction procedure. The product was purified by CC ( $\text{CH}_2\text{Cl}_2$ ); beige solid; yield: 0.24 g (77%); mp 90.5-92.5 °C;  $^1\text{H}$  NMR (500 MHz, DMSO- $d_6$ )  $\delta$  7.08 – 7.02 (m, 1H), 6.89 – 6.83 (m, 3H), 6.69 (ddd,  $J = 8.4, 2.2, 0.9$  Hz, 1H), 6.61 (ddd,  $J = 7.9, 2.1, 0.9$  Hz, 1H), 6.52 – 6.47 (m, 2H), 5.02 (s, 2H), 4.95 (dd,  $J = 11.6, 6.5$  Hz, 1H), 3.27 (dd,  $J = 17.6, 11.6$  Hz, 1H), 2.43 (dd,  $J = 17.5, 6.5$  Hz, 1H), 1.84 (tt,  $J = 8.3, 5.0$  Hz, 1H), 0.87 – 0.81 (m, 2H), 0.81 – 0.69 (m, 2H).  $^{13}\text{C}$  NMR (125 MHz, DMSO- $d_6$ )  $\delta$  155.22, 147.92, 146.49, 133.24, 130.12, 129.01, 126.45, 116.60, 114.16, 111.72, 110.80, 62.36, 43.16, 11.28, 5.84, 5.53; MS (ESI):  $m/z = 311.91$  (M+H) $^+$ .

**4-(1-(3-chlorophenyl)-3-(1-methylcyclopropyl)-4,5-dihydro-1H-pyrazol-5-yl)aniline (6f).** The title compound was prepared by reduction of 1-(3-chlorophenyl)-3-(1-methylcyclopropyl)-5-(4-nitrophenyl)-4,5-dihydro-1H-pyrazole (**5f**) according to the general reduction procedure. The product was purified by CC ( $\text{CH}_2\text{Cl}_2$ ); beige solid; yield: 0.27g (83%); mp 106.2 °C;  $^1\text{H}$  NMR (500 MHz, DMSO- $d_6$ )  $\delta$  7.09 – 7.03 (m, 1H), 6.89 – 6.84 (m, 3H), 6.71 (ddd,  $J = 8.4, 2.2, 0.9$  Hz, 1H), 6.61 (ddd,  $J = 7.9, 2.1, 0.9$  Hz, 1H), 6.52 – 6.46 (m, 2H), 5.02 (s, 2H), 4.96 (dd,  $J = 11.5, 6.6$  Hz, 1H), 3.27 (dd,  $J = 17.4, 11.5$  Hz, 1H), 2.43 (dd,  $J = 17.4, 6.7$  Hz, 1H), 1.35 (s, 3H), 0.98 – 0.88 (m, 2H), 0.71 – 0.64 (m, 2H);  $^{13}\text{C}$  NMR (125 MHz, DMSO- $d_6$ )  $\delta$  157.32, 147.93, 146.63, 133.22, 130.11, 129.05, 126.44, 116.64, 114.17, 111.76, 110.87, 63.03, 42.94, 21.18, 16.90, 13.71, 13.48; MS (ESI):  $m/z = 325.91$  (M+H) $^+$ .

**4-(1-(4-chlorophenyl)-3-cyclohexyl-4,5-dihydro-1H-pyrazol-5-yl)aniline (6g).** The title compound was prepared by reduction of 1-(4-chlorophenyl)-3-cyclohexyl-5-(4-nitrophenyl)-4,5-dihydro-1H-pyrazole (**5g**) according to the general reduction procedure. The product was purified by CC ( $\text{CH}_2\text{Cl}_2$ ); tan solid; yield: 0.31 g (88%); mp 145-146 °C;  $^1\text{H}$  NMR (500 MHz, DMSO- $d_6$ )  $\delta$  7.12 – 7.06 (m, 2H), 6.89 – 6.84 (m, 2H), 6.84 – 6.78 (m, 2H), 6.51 – 6.46 (m, 2H), 5.00 (s, 2H), 4.92 (dd,  $J = 11.6, 6.6$  Hz, 1H), 3.44 – 3.34 (m, 1H), 2.59 (dd,  $J = 17.8, 6.4$  Hz, 1H), 2.39 – 2.31 (m, 1H), 1.82 (dd,  $J = 16.1, 8.5$  Hz, 2H), 1.73 (dt,  $J = 7.0, 4.8$  Hz, 2H), 1.63 (d,  $J = 12.4$  Hz, 1H), 1.40 – 1.13 (m, 5H); MS (ESI):  $m/z = 353.80$  (M+H) $^+$ .

**4-(1-(3-chlorophenyl)-3-(thiophen-2-yl)-4,5-dihydro-1H-pyrazol-5-yl)aniline (6h).** The title compound was prepared by reduction of 1-(3-chlorophenyl)-5-(4-nitrophenyl)-3-(thiophen-2-yl)-4,5-dihydro-1H-pyrazole (**5h**) according to the general reduction procedure. The product was purified by CC ( $\text{CH}_2\text{Cl}_2$ ); greenish yellow solid; yield: 0.19 g (53%); mp 154.4 °C;  $^1\text{H}$  NMR (500 MHz, DMSO- $d_6$ )  $\delta$  7.62 (dt,  $J = 5.1, 2.3$  Hz, 1H), 7.28 (dd,  $J = 3.6, 1.1$  Hz, 1H), 7.28 (dd,  $J = 3.6, 1.1$  Hz, 1H), 7.11 (dd,  $J = 5.0, 3.6$  Hz, 1H), 6.96 (t,  $J = 2.1$  Hz, 1H), 6.94 – 6.90 (m, 2H),

## Results

6.84 (ddd,  $J = 8.4, 2.2, 0.9$  Hz, 1H), 6.72 – 6.68 (m, 1H), 6.53 – 6.48 (m, 2H), 5.29 (dd,  $J = 11.9, 6.0$  Hz, 1H), 5.06 (s, 2H), 3.85 (dd,  $J = 17.3, 12.0$  Hz, 1H), 3.08 (dd,  $J = 17.3, 6.0$  Hz, 1H);  $^{13}\text{C}$  NMR (125 MHz, DMSO- $d_6$ )  $\delta$  148.15, 145.27, 144.91, 135.48, 133.38, 130.34, 130.03, 128.41, 127.84, 127.72, 126.53, 117.65, 114.19, 112.20, 111.41, 62.93, 43.88; MS (ESI):  $m/z = 353.74$  (M+H) $^+$ .

**4-(1-(3-chlorophenyl)-3-(furan-2-yl)-4,5-dihydro-1H-pyrazol-5-yl)aniline (6i).** The title compound was prepared by reduction of 1-(3-chlorophenyl)-3-(furan-2-yl)-5-(4-nitrophenyl)-4,5-dihydro-1H-pyrazole (**5i**) according to the general reduction procedure. The product was purified by CC ( $\text{CH}_2\text{Cl}_2$ ); tan solid; yield: 0.22g (64%) ; mp 115.2-116.9 °C;  $^1\text{H}$  NMR (500 MHz, DMSO- $d_6$ )  $\delta$  7.82 (dd,  $J = 1.8, 0.7$  Hz, 1H), 7.15 – 7.09 (m, 1H), 6.99 (t,  $J = 2.1$  Hz, 1H), 6.92 – 6.88 (m, 2H), 6.84 (ddd,  $J = 8.4, 2.2, 0.9$  Hz, 1H), 6.81 (dd,  $J = 3.4, 0.7$  Hz, 1H), 6.70 (ddd,  $J = 7.9, 2.1, 0.9$  Hz, 1H), 6.61 (ddd,  $J = 7.5, 3.4, 1.8$  Hz, 1H), 6.52 – 6.47 (m, 2H), 5.27 (dd,  $J = 11.9, 5.8$  Hz, 1H), 5.06 (s, 2H), 3.77 (dd,  $J = 17.3, 12.0$  Hz, 1H), 2.98 (dd,  $J = 17.3, 5.8$  Hz, 1H);  $^{13}\text{C}$  NMR (125 MHz, DMSO- $d_6$ )  $\delta$  148.14, 147.30, 145.35, 144.41, 140.46, 133.39, 130.32, 128.27, 126.51, 117.66, 114.18, 112.30, 112.00, 111.41, 111.21, 62.26, 43.03; MS (ESI):  $m/z = 337.85$  (M+H) $^+$ .

**4-(3-(2-chlorophenyl)-1-(3-chlorophenyl)-4,5-dihydro-1H-pyrazol-5-yl)aniline (6j).** The title compound was prepared by reduction of 3-(2-chlorophenyl)-1-(3-chlorophenyl)-5-(4-nitrophenyl)-4,5-dihydro-1H-pyrazole (**5j**) according to the general reduction procedure. The product was purified by CC ( $\text{CH}_2\text{Cl}_2$ /hexane 4:1); yellow solid; yield: 0.20 g (52%); mp. 170-171 °C;  $^1\text{H}$  NMR (500 MHz, DMSO- $d_6$ )  $\delta$  7.77 – 7.74 (m, 1H), 7.39 (ddd,  $J = 5.4, 2.9, 1.7$  Hz, 2H), 7.22 – 7.19 (m, 1H), 7.17 – 7.12 (m, 2H), 7.03 (t,  $J = 2.1$  Hz, 1H), 6.88 (ddd,  $J = 8.4, 2.2, 0.8$  Hz, 1H), 6.73 (ddd,  $J = 7.9, 2.0, 0.9$  Hz, 1H), 6.56 – 6.50 (m, 2H), 6.29 (t,  $J = 5.9$  Hz, 1H), 5.33 (dd,  $J = 12.0, 5.9$  Hz, 1H), 4.21 (s, Hz, 2H), 3.96 (dd,  $J = 17.6, 12.0$  Hz, 1H), 3.18 (dd,  $J = 17.5, 5.9$  Hz, 1H).  $^{13}\text{C}$  NMR (125 MHz, DMSO- $d_6$ )  $\delta$  148.16, 146.86, 145.30, 140.11, 133.41, 131.00, 130.84, 130.72, 130.25, 130.00, 128.24, 127.33, 127.19, 126.61, 118.08, 112.51, 111.60, 62.76, 46.44; MS (ESI):  $m/z = 381.72$  (M+H) $^+$ .

**4-(1-(3-chlorophenyl)-3-(2-(trifluoromethyl)phenyl)-4,5-dihydro-1H-pyrazol-5-yl)aniline (6k).** The title compound was prepared by reduction of 1-(3-chlorophenyl)-5-(4-nitrophenyl)-3-(2-(trifluoromethyl)phenyl)-4,5-dihydro-1H-pyrazole (**5k**) according to the general reduction procedure. The product was purified by CC ( $\text{CH}_2\text{Cl}_2$ /hexane 4:1); tan solid; yield: 0.083 (20%); mp 159-160 °C;  $^1\text{H}$  NMR (500 MHz, DMSO- $d_6$ )  $\delta$  7.87 (d,  $J = 7.8$  Hz, 1H), 7.74 – 7.69 (m, 2H), 7.63 – 7.57 (m, 1H), 7.15 (dd,  $J = 10.6, 5.7$  Hz, 1H), 7.02 – 6.99 (m, 1H), 6.97 – 6.92 (m, 2H), 6.86 (ddd,  $J = 8.4, 2.2, 0.8$  Hz, 1H), 6.73 (ddd,  $J = 7.9, 2.0, 0.8$  Hz, 1H), 6.54 – 6.49 (m, 2H), 5.34 (dd,  $J = 12.1, 6.0$  Hz, 1H), 5.09 (s, 2H), 3.93 (dd,  $J = 17.5, 12.1$  Hz, 1H), 3.08 (dd,  $J = 17.5, 6.0$  Hz, 1H);  $^{13}\text{C}$  NMR (125 MHz, DMSO- $d_6$ )  $\delta$  148.18, 146.15, 145.35, 133.39, 132.56, 131.31, 130.37, 128.97, 128.33, 127.04, 126.57, 126.53, 125.97 (q,  $^2J_{\text{C-F}} = 30.8$  Hz), 124.10 (q,  $^1J_{\text{C-F}} = 273.3$  Hz), 118.10, 114.19, 112.48, 111.47, 62.81, 45.70; MS (ESI):  $m/z = 415.78$  (M+H) $^+$ .

## Results

**4-(1-(3-chlorophenyl)-3-(*o*-tolyl)-4,5-dihydro-1*H*-pyrazol-5-yl)aniline (6l).** The title compound was prepared by reduction of 1-(3-chlorophenyl)-5-(4-nitrophenyl)-3-(*o*-tolyl)-4,5-dihydro-1*H*-pyrazole (**5l**) according to the general reduction procedure. The product was purified by CC (CH<sub>2</sub>Cl<sub>2</sub>); brown solid; yield: 0.21 g (59%); mp 122.2 °C; <sup>1</sup>H NMR (500 MHz, DMSO-*d*<sub>6</sub>) δ 7.45 – 7.41 (m, 1H), 7.34 – 7.31 (m, 1H), 7.30 – 7.23 (m, 2H), 7.18 – 7.13 (m, 1H), 6.98 (t, *J* = 2.1 Hz, 1H), 6.96 – 6.92 (m, 2H), 6.89 (ddd, *J* = 8.4, 2.2, 0.9 Hz, 1H), 6.74 – 6.68 (m, 1H), 6.54 – 6.48 (m, 2H), 5.24 (dd, *J* = 11.9, 5.9 Hz, 1H), 5.06 (s, 2H), 3.92 (dd, *J* = 17.3, 12.0 Hz, 1H), 3.13 (dd, *J* = 17.3, 6.0 Hz, 1H), 2.68 (s, 3H); <sup>13</sup>C NMR (125 MHz, DMSO-*d*<sub>6</sub>) δ 149.35, 148.07, 145.62, 136.48, 133.39, 131.45, 130.66, 130.35, 128.75, 128.51, 128.18, 126.59, 126.00, 117.56, 114.21, 112.20, 111.42, 61.87, 45.24, 23.42; MS (ESI): *m/z* = 361.77 (M+H)<sup>+</sup>.

**4-(1-(3-chlorophenyl)-3-(2-methoxyphenyl)-4,5-dihydro-1*H*-pyrazol-5-yl)aniline (6m).** The title compound was prepared by reduction of 1-(3-chlorophenyl)-3-(2-methoxyphenyl)-5-(4-nitrophenyl)-4,5-dihydro-1*H*-pyrazole (**5m**) according to the general reduction procedure. The product was purified by CC (CH<sub>2</sub>Cl<sub>2</sub>); tan solid; yield: 0.25 g (66%); mp 122.9 °C; <sup>1</sup>H NMR (500 MHz, DMSO-*d*<sub>6</sub>) δ 7.89 (dd, *J* = 7.8, 1.7 Hz, 1H), 7.37 (ddd, *J* = 8.4, 7.3, 1.8 Hz, 1H), 7.14 – 7.10 (m, 1H), 7.08 (dd, *J* = 8.4, 1.0 Hz, 1H), 7.03 – 6.99 (m, 2H), 6.95 – 6.90 (m, 2H), 6.86 (ddd, *J* = 8.4, 2.2, 0.9 Hz, 1H), 6.71 – 6.67 (m, 1H), 6.53 – 6.48 (m, 2H), 5.21 (dd, *J* = 12.0, 6.1 Hz, 1H), 5.04 (s, 2H), 3.94 – 3.86 (m, 1H), 3.79 (s, 3H), 3.15 (dd, *J* = 18.1, 6.2 Hz, 1H); <sup>13</sup>C NMR (125 MHz, DMSO-*d*<sub>6</sub>) δ 157.35, 148.02, 147.82, 145.68, 133.37, 130.44, 130.26, 128.95, 128.22, 126.48, 121.06, 120.67, 117.41, 114.20, 112.30, 112.24, 111.33, 62.78, 55.60, 46.52; MS (ESI): *m/z* = 377.72 (M+H)<sup>+</sup>.

**4-(3-(benzo[d][1,3]dioxol-5-yl)-1-(3-chlorophenyl)-4,5-dihydro-1*H*-pyrazol-5-yl)aniline (6n).** The title compound was prepared by reduction of 3-(benzo[d][1,3]dioxol-5-yl)-1-(3-chlorophenyl)-5-(4-nitrophenyl)-4,5-dihydro-1*H*-pyrazole (**5n**) according to the general reduction procedure. The product was purified by CC (CH<sub>2</sub>Cl<sub>2</sub>); brown solid; yield: 0.34 g (87%); mp 140.4 °C; <sup>1</sup>H NMR (500 MHz, DMSO-*d*<sub>6</sub>) δ 7.40 – 7.38 (m, 1H), 7.17 (dd, *J* = 8.1, 1.7 Hz, 1H), 7.13 – 7.09 (m, 1H), 7.03 (t, *J* = 2.1 Hz, 1H), 6.97 – 6.94 (m, 1H), 6.93 – 6.89 (m, 2H), 6.87 (ddd, *J* = 8.4, 2.2, 0.9 Hz, 1H), 6.68 (ddd, *J* = 7.9, 2.1, 0.9 Hz, 1H), 6.53 – 6.47 (m, 2H), 6.07 (s, 2H), 5.24 (dd, *J* = 12.0, 6.1 Hz, 1H), 5.04 (s, 2H), 3.78 (dd, *J* = 17.5, 12.0 Hz, 1H), 3.02 (dd, *J* = 17.5, 6.1 Hz, 1H); <sup>13</sup>C NMR (125 MHz, DMSO-*d*<sub>6</sub>) δ 148.41, 148.09, 148.07, 147.71, 145.61, 133.38, 130.23, 128.77, 126.54, 126.43, 120.62, 117.37, 114.18, 112.19, 111.30, 108.31, 105.42, 101.32, 62.85, 43.36; MS (ESI): *m/z* = 391.68 (M+H)<sup>+</sup>.

**4-(1-(3-chlorophenyl)-3-(2-hydroxyphenyl)-4-methyl-4,5-dihydro-1*H*-pyrazol-5-yl)-2-fluorophenol (9).** The title compound was prepared by demethylation of 1-(3-chlorophenyl)-5-(3-fluoro-4-methoxyphenyl)-3-(2-methoxyphenyl)-4-methyl-4,5-dihydro-1*H*-pyrazole (**8**) using BBr<sub>3</sub> (6 equiv) according to the general procedure for ether dealkylation. The product was purified by CC (CH<sub>2</sub>Cl<sub>2</sub>); beige solid; yield: 0.27 g (69%); mp 160.1-161.4 °C; <sup>1</sup>H NMR (500 MHz, DMSO-*d*<sub>6</sub>) δ 10.30 (s, 1H), 9.87 (s, 1H), 7.56 (ddd, *J* = 6.1, 4.5, 1.6 Hz, 1H), 7.31 – 7.24

## Results

(m, 1H), 7.20 (dd,  $J = 12.7, 4.6$  Hz, 1H), 7.04 (dd,  $J = 12.0, 2.1$  Hz, 1H), 6.99 – 6.96 (m, 2H), 6.93 – 6.90 (m, 1H), 6.90 – 6.85 (m, 2H), 6.84 – 6.80 (m, 1H), 6.78 (ddd,  $J = 7.9, 2.0, 0.8$  Hz, 1H), 5.11 (d,  $J = 3.5$  Hz, 1H), 3.71 (qd,  $J = 7.1, 3.5$  Hz, 1H), 1.35 (d,  $J = 7.2$  Hz, 3H);  $^{13}\text{C}$  NMR (125 MHz, DMSO- $d_6$ )  $\delta$  156.26, 154.88, 150.94 (d,  $^1J_{\text{C-F}} = 241.8$  Hz), 144.47, 144.30 (d,  $^2J_{\text{C-F}} = 12.1$  Hz), 133.70, 131.68 (d,  $^3J_{\text{C-F}} = 5.0$  Hz), 130.71, 130, 128.40, 121.68 (d,  $^4J_{\text{C-F}} = 2.9$  Hz), 119.59, 118.31, 118.27, 116.47, 115.96, 113.63 (d,  $^2J_{\text{C-F}} = 18.8$  Hz), 112.15, 111.35, 68.33, 50.92, 18.63 ; MS (ESI):  $m/z = 396.74$  (M+H) $^+$ .

**4-(3-(*tert*-butyl)-1-(4-chlorophenyl)-1*H*-pyrazol-5-yl)-2-chlorophenol (11).** The title compound was prepared by demethylation of 3-(*tert*-butyl)-5-(3-chloro-4-methoxyphenyl)-1-(4-chlorophenyl)-1*H*-pyrazole (**10**) using BBr<sub>3</sub> (3 equiv) according to the general procedure for ether dealkylation. The product was purified by CC (CH<sub>2</sub>Cl<sub>2</sub>); off-white solid; yield: 0.18 g (50%); mp 176.5-177.5 °C;  $^1\text{H}$  NMR (500 MHz, DMSO- $d_6$ )  $\delta$  10.49 (s, 1H), 7.47 – 7.43 (m, 2H), 7.28 – 7.24 (m, 3H), 6.94 – 6.89 (m, 2H), 6.53 (s, 1H), 1.31 (s, 9H);  $^{13}\text{C}$  NMR (125 MHz, DMSO- $d_6$ )  $\delta$  161.85, 153.16, 141.69, 138.68, 131.28, 129.72, 128.90, 128.29, 126.36, 122.04, 119.75, 116.60, 104.90, 31.89, 30.23. ; MS (ESI):  $m/z = 360.77$  (M+H) $^+$ .

**(*E*)-3-(4-(*tert*-butoxy)phenyl)-1-phenylprop-2-en-1-one (E2).** Synthesized according to the general procedure for enone synthesis using acetophenone and 4-(*tert*-butoxy)benzaldehyde; yellow solid; yield: 2.46 g (88 %); mp 117.5-119 °C;  $^1\text{H}$  NMR (500 MHz, DMSO- $d_6$ )  $\delta$  8.18 – 8.08 (m, 2H), 7.85 – 7.79 (m, 3H), 7.72 (d,  $J = 15.6$  Hz, 1H), 7.69 – 7.63 (m, 1H), 7.60 – 7.54 (m, 2H), 7.08 – 7.02 (m, 2H), 1.35 (s, 9H);  $^{13}\text{C}$  NMR (125 MHz, DMSO- $d_6$ )  $\delta$  189.07, 157.72, 143.77, 137.73, 132.96, 130.11, 129.16, 128.73, 128.41, 123.02, 120.45, 78.89, 28.53.

**(*E*)-3-(4-(*tert*-butoxy)phenyl)-1-(2-hydroxyphenyl)prop-2-en-1-one (E3).** Synthesized according to the general procedure for enone synthesis using 1-(2-hydroxyphenyl)ethanone and 4-(*tert*-butoxy)benzaldehyde, the product was precipitated after neutralization with 2M HCl; yellow solid; yield: 2.57 g (87 %); mp 137-138 °C;  $^1\text{H}$  NMR (500 MHz, DMSO- $d_6$ )  $\delta$  9.35 (s, 1H), 7.89 – 7.84 (m, 1H), 7.76 (d,  $J = 15.9$  Hz, 1H), 7.73 – 7.69 (m, 2H), 7.68 (d,  $J = 11.3$  Hz, 1H), 7.66 – 7.61 (m, 3H), 6.92 (td,  $J = 7.5, 0.8$  Hz, 1H), 6.86 (t,  $J = 7.4$  Hz, 1H), 1.39 (s, 9H).

**(*E*)-3-(4-(*tert*-butoxy)phenyl)-1-(2-methoxyphenyl)prop-2-en-1-one (E4).** Synthesized according to the general procedure for enone synthesis using 1-(2-methoxyphenyl)ethanone and 4-(*tert*-butoxy)benzaldehyde; yellow oil; yield: 2.51g (81 %);  $^1\text{H}$  NMR (300 MHz, CDCl<sub>3</sub>)  $\delta$  7.59 (dd,  $J = 8.7, 7.0$  Hz, 2H), 7.54 – 7.45 (m, 3H), 7.31 – 7.23 (m, 1H), 7.08 – 6.96 (m, 4H), 3.90 (s, 3H), 1.40 (s, 9H).

**(*E*)-3-(4-(*tert*-butoxy)phenyl)-1-(2-ethoxyphenyl)prop-2-en-1-one (E5).** Synthesized according to the general procedure for enone synthesis using 1-(2-ethoxyphenyl)ethanone and 4-(*tert*-butoxy)benzaldehyde; yellow oil; yield: 2.65 g (82%);  $^1\text{H}$  NMR (500 MHz, CDCl<sub>3</sub>)  $\delta$  7.64 (dd,  $J = 7.6, 1.8$  Hz, 1H), 7.60 (d,  $J = 15.9$  Hz, 1H), 7.51 – 7.47 (m, 2H), 7.44 – 7.40 (m, 1H),

## Results

---

7.38 (d,  $J = 15.9$  Hz, 1H), 7.02 – 6.98 (m, 3H), 6.97 – 6.93 (m, 1H), 4.11 (q,  $J = 7.0$  Hz, 2H), 1.41 (t,  $J = 7.0$  Hz, 3H), 1.38 (s, 9H);  $^{13}\text{C}$  NMR (125 MHz,  $\text{CDCl}_3$ )  $\delta$  192.66, 157.66, 157.48, 142.37, 132.66, 130.32, 129.87, 129.46, 129.12, 125.79, 123.58, 120.55, 112.56, 79.13, 64.14, 28.80, 14.74

**(E)-3-(4-(*tert*-butoxy)phenyl)-1-(2-chlorophenyl)prop-2-en-1-one (E6).** Synthesized according to the general procedure for enone synthesis using 1-(2-chlorophenyl)ethanone and 4-(*tert*-butoxy)benzaldehyde; yellow oil; yield: 2.85 g (91 %);  $^1\text{H}$  NMR (500 MHz,  $\text{CDCl}_3$ )  $\delta$  7.68 (dd,  $J = 7.6, 1.8$  Hz, 1H), 7.58 (d,  $J = 15.9$  Hz, 1H), 7.53 – 7.49 (m, 2H), 7.49 – 7.47 (m, 1H), 7.47 – 7.44 (m, 1H), 7.39 – 7.35 (m, 2H), 7.03 (td,  $J = 7.5, 0.9$  Hz, 1H), 6.98 (d,  $J = 7.9$  Hz, 1H), 1.36 (s, 9H).

**(E)-3-(4-(*tert*-butoxy)phenyl)-1-(thiophen-2-yl)prop-2-en-1-one (E7).** Synthesized according to the general procedure for enone synthesis using 1-(thiophen-2-yl)ethanone and 4-(*tert*-butoxy)benzaldehyde; yellowish white solid; yield: 2.57 g (90 %); mp 128.1 °C;  $^1\text{H}$  NMR (500 MHz,  $\text{DMSO-}d_6$ )  $\delta$  8.30 (dd,  $J = 3.8, 1.1$  Hz, 1H), 8.04 (dd,  $J = 4.9, 1.1$  Hz, 1H), 7.83 – 7.79 (m, 2H), 7.77 (d,  $J = 15.6$  Hz, 1H), 7.70 (d,  $J = 15.6$  Hz, 1H), 7.31 (dt,  $J = 10.0, 5.0$  Hz, 1H), 7.08 – 7.02 (m, 2H), 1.35 (s, 9H);  $^{13}\text{C}$  NMR (125 MHz,  $\text{DMSO-}d_6$ )  $\delta$  181.53, 157.75, 145.66, 142.86, 135.27, 133.36, 130.12, 128.99, 128.85, 122.99, 120.28, 78.91, 28.53.

**(E)-3-(4-(*tert*-butoxy)phenyl)-1-(pyridin-2-yl)prop-2-en-1-one (E8).** Synthesized according to the general procedure for enone synthesis using 1-(pyridin-2-yl)ethanone and 4-(*tert*-butoxy)benzaldehyde; greenish yellow solid; yield: 2.56 g (91 %); mp 117.1-118.5 °C;  $^1\text{H}$  NMR (500 MHz,  $\text{DMSO-}d_6$ )  $\delta$  8.79 (ddd,  $J = 4.7, 1.7, 0.9$  Hz, 1H), 8.17 (d,  $J = 16.1$  Hz, 1H), 8.11 – 8.09 (m, 1H), 8.07 – 8.03 (m, 1H), 7.85 – 7.81 (m, 1H), 7.76 – 7.73 (m, 2H), 7.69 (ddd,  $J = 7.5, 4.7, 1.4$  Hz, 1H), 7.08 – 7.03 (m, 2H), 1.35 (s, 9H);  $^{13}\text{C}$  NMR (125 MHz,  $\text{DMSO-}d_6$ )  $\delta$  188.52, 157.95, 153.55, 149.13, 143.79, 137.69, 129.98, 129.01, 127.50, 123.04, 122.38, 119.12, 78.95, 28.52.

**(E)-3-(4-(*tert*-butoxy)phenyl)-1-(1*H*-pyrrol-2-yl)prop-2-en-1-one (E9).** Synthesized according to the general procedure for enone synthesis using 1-(1*H*-pyrrol-2-yl)ethanone and 4-(*tert*-butoxy)benzaldehyde; yellowish white solid; yield: 2.26 g (84 %); mp 116.5-118.5 °C;  $^1\text{H}$  NMR (500 MHz,  $\text{CDCl}_3$ )  $\delta$  9.92 (s, 1H), 7.81 (d,  $J = 15.6$  Hz, 1H), 7.58 – 7.54 (m, 2H), 7.27 (d,  $J = 15.7$  Hz, 1H), 7.11 (td,  $J = 2.7, 1.3$  Hz, 1H), 7.07 (ddd,  $J = 3.7, 2.3, 1.3$  Hz, 1H), 7.05 – 7.00 (m, 2H), 6.35 (dt,  $J = 3.8, 2.5$  Hz, 1H), 1.40 (s, 9H);  $^{13}\text{C}$  NMR (125 MHz,  $\text{CDCl}_3$ )  $\delta$  178.97, 157.75, 141.95, 133.24, 129.81, 129.25, 125.14, 123.76, 120.49, 116.03, 110.88, 79.31, 28.89.

**(E)-1-(4-aminophenyl)-3-(4-(*tert*-butoxy)phenyl)prop-2-en-1-one (E10).** Synthesized according to the general procedure for enone synthesis using 1-(4-aminophenyl)ethanone and 4-(*tert*-butoxy)benzaldehyde; yellow solid; yield: 2.30 g (78 %); mp 113.7-115.5 °C;  $^1\text{H}$  NMR (300 MHz,  $\text{DMSO-}d_6$ )  $\delta$  7.90 (d,  $J = 8.6$  Hz, 2H), 7.77 – 7.69 (m, 3H), 7.57 (d,  $J = 15.5$  Hz, 1H), 7.02 (d,  $J = 8.6$  Hz, 2H), 6.61 (d,  $J = 8.2$  Hz, 2H), 6.09 (s, 2H), 1.35 (s, 9H).

## Results

---

**(E)-1-(3-methoxyphenyl)-4,4-dimethylpent-1-en-3-one (E11).** Synthesized according to the general procedure for enone synthesis using pinacolone and 3-methoxybenzaldehyde; yellow oil; yield: 1.87 g (86 %);  $^1\text{H NMR}$  (300 MHz,  $\text{CDCl}_3$ )  $\delta$  7.64 (d,  $J = 15.6$  Hz, 1H), 7.33 – 7.24 (m, 1H), 7.19 – 7.14 (m, 1H), 7.08 (dd,  $J = 5.3, 2.6$  Hz, 2H), 6.92 (dt,  $J = 7.2, 3.6$  Hz, 1H), 3.83 (s, 3H), 1.23 (s, 9H).

**1-(4-methoxyphenyl)-4,4-dimethylpent-1-en-3-one (E12).** Synthesized according to general procedure for enone synthesis using pinacolone and 4-methoxybenzaldehyde; yellow oil; yield: 1.97 g (90.5 %).<sup>1</sup>

**1-(4-chlorophenyl)-4,4-dimethylpent-1-en-3-one (E13).** Synthesized according to the general procedure for enone synthesis pinacolone and 4-chlorobenzaldehyde; white solid; yield: 2.11 g (95 %); mp 85-87 °C.<sup>2</sup>

**(E)-1-(3-fluoro-4-methoxyphenyl)-4,4-dimethylpent-1-en-3-one (E14).** Synthesized according to the general procedure for enone synthesis using pinacolone and 3-fluoro-4-methoxybenzaldehyde; yellowish white solid; yield: 2.22 g (94 %); mp 84.6 °C;  $^1\text{H NMR}$  (500 MHz,  $\text{DMSO}-d_6$ )  $\delta$  7.80 (dd,  $J = 12.9, 2.1$  Hz, 1H), 7.52 (dd,  $J = 5.5, 4.3$  Hz, 1H), 7.48 (d,  $J = 15.6$  Hz, 1H), 7.35 (d,  $J = 15.6$  Hz, 1H), 7.21 – 7.16 (m, 1H), 3.88 (s, 3H), 1.15 (s, 9H);  $^{13}\text{C NMR}$  (125 MHz,  $\text{DMSO}-d_6$ )  $\delta$  203.24, 151.53 (d,  $^1J_{\text{C-F}} = 244.2$  Hz), 148.83 (d,  $^2J_{\text{C-F}} = 10.9$  Hz), 140.80, 127.86 (d,  $^3J_{\text{C-F}} = 6.8$  Hz), 126.67 (d,  $^4J_{\text{C-F}} = 2.9$  Hz), 120.49, 114.79 (d,  $^2J_{\text{C-F}} = 18.4$  Hz), 113.66, 56.09, 42.76, 25.76.

**(E)-1-(3-chloro-4-methoxyphenyl)-4,4-dimethylpent-1-en-3-one (E15).** Synthesized according to the general procedure for enone synthesis using pinacolone and 3-chloro-4-methoxybenzaldehyde; white solid; yield: 2.24 g (89 %); mp 75.2-77.1 °C;  $^1\text{H NMR}$  (500 MHz,  $\text{DMSO}-d_6$ )  $\delta$  8.00 (d,  $J = 2.1$  Hz, 1H), 7.70 (dd,  $J = 8.7, 2.1$  Hz, 1H), 7.47 (d,  $J = 15.6$  Hz, 1H), 7.38 (d,  $J = 15.6$  Hz, 1H), 7.19 – 7.15 (m, 1H), 3.90 (s, 3H), 1.16 (s, 9H);  $^{13}\text{C NMR}$  (125 MHz,  $\text{DMSO}-d_6$ )  $\delta$  203.27, 155.89, 140.44, 129.73, 129.26, 128.27, 121.69, 120.52, 112.77, 56.30, 42.77, 25.76.

**(E)-1-(4-fluoro-3-methoxyphenyl)-4,4-dimethylpent-1-en-3-one (E16).** Synthesized according to the general procedure for enone synthesis using pinacolone and 4-fluoro-3-methoxybenzaldehyde; yellow oil; yield: 1.96 g (83 %);  $^1\text{H NMR}$  (300 MHz,  $\text{DMSO}$ )  $\delta$  7.91 – 7.83 (m, 1H), 7.73 (d,  $J = 8.4$  Hz, 1H), 7.51 (d,  $J = 15.6$  Hz, 1H), 7.27 (dd,  $J = 15.6, 1.0$  Hz, 1H), 6.98-6.93 (m, 1H), 3.80 (s, 3H), 1.16 (s, 9H).

**3-(3,4-dimethoxyphenyl)-1-(2-methoxyphenyl)prop-2-en-1-one (E17).** Synthesized according to the general procedure for enone synthesis using 1-(2-methoxyphenyl)ethanone and 3,4-dimethoxybenzaldehyde; yellow oil; yield: 2.38 g (80 %).<sup>3</sup>

**(E)-3-(3-fluoro-4-methoxyphenyl)-1-(2-methoxyphenyl)prop-2-en-1-one (E18).** Synthesized according to the general procedure for enone synthesis using 1-(2-methoxyphenyl)ethanone and

## Results

3-fluoro-4-methoxybenzaldehyde; yellow solid; yield: 2.66 g (93 %); mp 97.5 °C; <sup>1</sup>H NMR (500 MHz, DMSO-*d*<sub>6</sub>) δ 7.70 (dd, *J* = 12.7, 2.1 Hz, 1H), 7.55 – 7.50 (m, 2H), 7.47 (dd, *J* = 7.6, 1.6 Hz, 1H), 7.43 (d, *J* = 15.9 Hz, 1H), 7.31 (d, *J* = 15.9 Hz, 1H), 7.23 – 7.16 (m, 2H), 7.07 – 7.02 (m, 1H), 3.88 (s, 3H), 3.85 (s, 3H). <sup>13</sup>C NMR (125 MHz, DMSO-*d*<sub>6</sub>) δ 192.14, 157.59, 151.53 (d, <sup>1</sup>*J*<sub>C-F</sub> = 244.5 Hz), 149.04 (d, <sup>2</sup>*J*<sub>C-F</sub> = 10.9 Hz), 141.58 (d, <sup>4</sup>*J*<sub>C-F</sub> = 2.2 Hz), 132.82, 129.37, 128.98, 127.77 (d, <sup>3</sup>*J*<sub>C-F</sub> = 6.8 Hz), 126.40 (d, <sup>4</sup>*J*<sub>C-F</sub> = 2.9 Hz), 126.02, 120.48, 114.99 (d, <sup>2</sup>*J*<sub>C-F</sub> = 18.4 Hz), 113.85, 112.28, 56.12, 55.78.

### **(*E*)-3-(4-ethoxy-3,5-difluorophenyl)-1-(2-methoxyphenyl)prop-2-en-1-one (E19).**

Synthesized according to the general procedure for enone synthesis using 1-(2-methoxyphenyl)ethanone and 4-ethoxy-3,5-difluorobenzaldehyde; yellow solid; yield: 2.92 g (92 %); mp 85.6 °C; <sup>1</sup>H NMR (500 MHz, DMSO-*d*<sub>6</sub>) δ 7.64 – 7.58 (m, 2H), 7.55 (ddd, *J* = 8.4, 7.3, 1.8 Hz, 1H), 7.48 (dt, *J* = 6.6, 2.4 Hz, 1H), 7.42-7.39 (m, 1H), 7.19 (d, *J* = 15.9 Hz, 1H), 7.06 (td, *J* = 7.4, 0.9 Hz, 1H), 6.95 – 6.89 (m, 1H), 4.22 (q, *J* = 7.0 Hz, 2H), 3.86 (s, 3H), 1.30 (t, *J* = 7.0 Hz, 3H); <sup>13</sup>C NMR (125 MHz, DMSO-*d*<sub>6</sub>) δ 191.97, 157.78, 155.28 (dd, <sup>1</sup>*J*<sub>C-F</sub> = 246.3, <sup>3</sup>*J*<sub>C-F</sub> 6.5 Hz), 139.87, 135.95 (t, <sup>2</sup>*J*<sub>C-F</sub> = 14.7 Hz), 133.87, 130.26 (t, <sup>3</sup>*J*<sub>C-F</sub> = 9.3 Hz), 129.49, 128.68, 128.17, 120.49, 112.54 (dd, <sup>2</sup>*J*<sub>C-F</sub> = 17.6, <sup>4</sup>*J*<sub>C-F</sub> = 5.7 Hz), 112.31, 70.11, 55.82, 15.23.

### **(*E*)-3-(2,3-difluoro-4-methoxyphenyl)-1-(2-methoxyphenyl)prop-2-en-1-one (E20).**

Synthesized according to the general procedure for enone synthesis using 1-(2-methoxyphenyl)ethanone and 2,3-difluoro-4-methoxybenzaldehyde; yellow solid; yield: 2.91 g (96 %); mp 128-130 °C; <sup>1</sup>H NMR (500 MHz, DMSO-*d*<sub>6</sub>) δ 7.66 (td, *J* = 8.8, 2.2 Hz, 1H), 7.58 – 7.53 (m, 1H), 7.53 – 7.50 (m, 1H), 7.45 (dd, *J* = 15.6, 13.2 Hz, 2H), 7.20 (dd, *J* = 8.5, 0.7 Hz, 1H), 7.13 – 7.08 (m, 1H), 7.08 – 7.04 (m, 1H), 3.93 (s, 3H), 3.87 (s, 3H); <sup>13</sup>C NMR (125 MHz, DMSO-*d*<sub>6</sub>) δ 191.57, 157.83, 150.14, 149.45 (dd, <sup>1</sup>*J*<sub>C-F</sub> = 251.6, <sup>2</sup>*J*<sub>C-F</sub> = 10.6 Hz), 140.16 (dd, <sup>1</sup>*J*<sub>C-F</sub> = 245.6, <sup>2</sup>*J*<sub>C-F</sub> 14.3 Hz), 133.60, 133.30, 129.63, 128.48, 127.99, 124.37, 120.60, 116.20, 112.39, 109.51, 56.79, 55.79.

### **(*E*)-1-(2,4-dimethoxyphenyl)-3-(3-fluoro-4-methoxyphenyl)prop-2-en-1-one (E21).**

Synthesized according to the general procedure for enone synthesis using 1-(2,4-dimethoxyphenyl)ethanone and 3-fluoro-4-methoxybenzaldehyde; yellow solid; yield: 2.71 g (86 %); mp 85-86 °C; <sup>1</sup>H NMR (500 MHz, DMSO-*d*<sub>6</sub>) δ 7.65 (dt, *J* = 14.9, 3.5 Hz, 1H), 7.59 (d, *J* = 8.6 Hz, 1H), 7.53 – 7.45 (m, 2H), 7.43 (d, *J* = 15.8 Hz, 1H), 7.21 (dd, *J* = 11.0, 6.5 Hz, 1H), 6.68 (d, *J* = 2.3 Hz, 1H), 6.63 (dd, *J* = 8.6, 2.3 Hz, 1H), 3.89 (d, *J* = 2.3 Hz, 6H), 3.85 (s, 3H); <sup>13</sup>C NMR (125 MHz, DMSO-*d*<sub>6</sub>) δ 189.30, 163.83, 160.12, 151.53 (d, <sup>1</sup>*J*<sub>C-F</sub> = 244.4 Hz), 148.80 (d, <sup>2</sup>*J*<sub>C-F</sub> = 10.8 Hz), 140.19, 131.91, 128.09 (d, <sup>3</sup>*J*<sub>C-F</sub> = 6.8 Hz), 126.11, 126.06 (d, <sup>4</sup>*J*<sub>C-F</sub> = 2.9 Hz), 121.50, 114.84 (d, <sup>2</sup>*J*<sub>C-F</sub> = 18.3 Hz), 113.87, 105.88, 98.60, 56.10, 55.91, 55.56.

**1-(4-fluorophenyl)-4,4-dimethylpent-1-en-3-one (E22).** Synthesized according to the general procedure for enone synthesis using pinacolone and 4-fluorobenzaldehyde; yellow solid; yield: 1.73 g (84 %); mp 42.5-44.1 °C.<sup>4</sup>

## Results

---

**1-(4-bromophenyl)-4,4-dimethylpent-1-en-3-one (E23).** Synthesized according to the general procedure for enone synthesis using pinacolone and 4-bromobenzaldehyde; white solid; yield: 2.48 g (93 %); mp 102-103 °C.<sup>5,6</sup>

**4-(4,4-dimethyl-3-oxopent-1-en-1-yl)benzotrile (E24).** Synthesized according to the general procedure for enone synthesis using pinacolone and 4-formylbenzotrile; white solid; yield: 1.95 g (92 %); mp 131-133 °C.<sup>7,8</sup>

**3-(4-methoxyphenyl)-1-phenylprop-2-en-1-one (E25).** Synthesized according to the general procedure for enone synthesis using acetophenone and 4-methoxybenzaldehyde; yellow solid; yield: 1.88 g (79 %); mp 73-74 °C.<sup>9</sup>

**4,4-dimethyl-1-(4-nitrophenyl)pent-1-en-3-one (E26).** Synthesized according to the the general procedure for enone synthesis using pinacolone and 4-nitrobenzaldehyde; beige solid; yield: 2.23 g (96 %); mp 107-109 °C.<sup>10</sup>

**4,4-dimethyl-1-(3-nitrophenyl)pent-1-en-3-one (E27).** Synthesized according to the general procedure for enone synthesis using pinacolone and 3-nitrobenzaldehyde; yellow solid; yield: 2.16 g (93 %); mp 92-94 °C.<sup>11</sup>

**1-cyclopropyl-3-(4-nitrophenyl)prop-2-en-1-one (E28).** Synthesized according to the general procedure for enone synthesis using 1-cyclopropylethanone and 4-nitrobenzaldehyde; yellowish white solid; yield: 1.82 g (84 %); mp 118.9-120 °C.<sup>12</sup>

**(E)-1-(1-methylcyclopropyl)-3-(4-nitrophenyl)prop-2-en-1-one (E29).** Synthesized according to the general procedure for enone synthesis using 1-(1-methylcyclopropyl)ethanone and 4-nitrobenzaldehyde; yellowish white solid; yield: 1.96 g (85 %); mp 133.1 °C; <sup>1</sup>H NMR (500 MHz, CDCl<sub>3</sub>) δ 8.29 – 8.22 (m, 2H), 7.74 – 7.69 (m, 2H), 7.62 (d, *J* = 16.1 Hz, 1H), 6.98 (d, *J* = 16.1 Hz, 1H), 2.26 (s, 3H), 1.24 – 1.18 (m, 2H), 1.07 – 1.01 (m, 2H), <sup>13</sup>C NMR (125 MHz, CDCl<sub>3</sub>) δ 199.41, 148.46, 140.97, 138.72, 129.77, 128.77, 124.15, 23.12, 20.26, 11.90.

**(E)-1-cyclohexyl-3-(4-nitrophenyl)prop-2-en-1-one (E30).** Synthesized according to the general procedure for enone synthesis using 1-cyclohexylethanone and 4-nitrobenzaldehyde; beige solid; yield: 2.53 g (98 %); mp 132-134 °C; <sup>1</sup>H NMR (300 MHz, CDCl<sub>3</sub>) δ 8.25 (d, *J* = 8.3 Hz, 2H), 7.71 (d, *J* = 8.5 Hz, 2H), 7.61 (d, *J* = 16.0 Hz, 1H), 6.93 (d, *J* = 15.9 Hz, 1H), 2.76 – 2.56 (m, 1H), 1.90 (dd, *J* = 22.1, 11.2 Hz, 4H), 1.54 – 1.18 (m, 6H).

**3-(4-nitrophenyl)-1-(thiophen-2-yl)prop-2-en-1-one (E31).** Synthesized according to the general procedure for enone synthesis using 1-(thiophen-2-yl)ethanone and 4-nitrobenzaldehyde; yellow solid; yield: 2.14 g (83 %); mp 207-209 °C.<sup>13</sup>

**1-(furan-2-yl)-3-(4-nitrophenyl)prop-2-en-1-one (E32).** Synthesized according to the general procedure for enone synthesis using 1-(furan-2-yl)ethanone and 4-nitrobenzaldehyde; yellow solid; yield: 2.13 g (88 %); mp 224.4 °C.<sup>14</sup>

## Results

**1-(2-chlorophenyl)-3-(4-nitrophenyl)prop-2-en-1-one (E33).** Synthesized according to the general procedure for enone synthesis using 1-(2-chlorophenyl)ethanone and 4-nitrobenzaldehyde; yellow solid; yield: 2.21 g (77 %); mp 162-163 °C.<sup>15</sup>

**(E)-3-(4-nitrophenyl)-1-(2-(trifluoromethyl)phenyl)prop-2-en-1-one (E34).** Synthesized according to the general procedure for enone synthesis using 1-(2-(trifluoromethyl)phenyl)ethanone and 4-nitrobenzaldehyde; yellow solid; yield: 2.85 g (89 %); mp 142-144 °C; <sup>1</sup>H NMR (500 MHz, CDCl<sub>3</sub>) δ 8.23 – 8.18 (m, 2H), 7.70 – 7.64 (m, 2H), 7.51 – 7.46 (m, 2H), 7.41 (ddd, *J* = 8.0, 4.4, 1.2 Hz, 2H), 7.34 (ddd, *J* = 7.5, 6.5, 2.1 Hz, 1H), 7.22 (d, *J* = 16.1 Hz, 1H).

**(E)-3-(4-nitrophenyl)-1-(*o*-tolyl)prop-2-en-1-one (E35).** Synthesized according to the general procedure for enone synthesis using 1-(*o*-tolyl)ethanone and 4-nitrobenzaldehyde; yellowish white solid; yield: 2.16 g (81 %); mp 128-129 °C; <sup>1</sup>H NMR (500 MHz, CDCl<sub>3</sub>) δ 8.27 – 8.20 (m, 2H), 8.07 – 7.97 (m, 1H), 7.73 – 7.66 (m, 2H), 7.55 – 7.48 (m, 2H), 7.41 (ddd, *J* = 8.9, 6.2, 2.4 Hz, 1H), 7.30 – 7.28 (m, 1H), 7.26 (d, *J* = 16.0 Hz, 1H), 2.46 (s, 3H); <sup>13</sup>C NMR (125 MHz, CDCl<sub>3</sub>) δ 194.98, 148.58, 142.02, 140.84, 138.17, 137.58, 131.64, 129.97, 128.88, 128.59, 128.33, 125.63, 123.74, 20.40.

**1-(2-methoxyphenyl)-3-(4-nitrophenyl)prop-2-en-1-one (E36).** Synthesized according to the general procedure for enone synthesis using 1-(2-methoxyphenyl)ethanone and 4-nitrobenzaldehyde; yellowish white solid; yield: 2.43 g (86 %); mp 116.5-118 °C.<sup>16</sup>

**1-(benzo[d][1,3]dioxol-5-yl)-3-(4-nitrophenyl)prop-2-en-1-one (E37).** Synthesized according to the general procedure for enone synthesis using 1-(benzo[d][1,3]dioxol-5-yl)ethanone and 4-nitrobenzaldehyde; dark yellow solid; yield: 2.34 g (79 %); mp 182.4 °C.<sup>17</sup>

**2) Supplementary Table S1.** Hit compound **1a** does not inhibit other potential target kinases in the NF-κB pathway nor PKCβII

Kinase (human)	% inhibition at 10 μM of <b>1a</b>
IKKβ	n.i.
PKCι	n.i.
RIPK2	n.i.
p38α MAPK	10%
TAK1	n.i.
TBK1	n.i.
PKCβII	n.i.

n.i.: no inhibition. Each value is representative of at least two independent assays which essentially gave the same results.

## Results

### 3) Table S2. Wilcoxon's signed rank test

Group 1: low potency (less than 75% inhibition at 62.5 $\mu$ M in the cell free assay)					
compound #	% inhibition at 5 $\mu$ M (U937 cells)	compound #	% inhibition at 5 $\mu$ M (U937 cells)	compound #	% inhibition at 5 $\mu$ M (U937 cells)
<b>1g</b>	40.7	<b>3n</b>	9.3	<b>6e</b>	24.5
<b>1l</b>	23.5	<b>3o</b>	20.1	<b>6f</b>	47.7
<b>1m</b>	48.7	<b>3p</b>	2.9	<b>6g</b>	30.9
<b>1n</b>	50.2	<b>3q</b>	50.8	<b>6h</b>	44.9
<b>1o</b>	51.8	<b>4b</b>	35	<b>6i</b>	26.1
<b>1p</b>	41.5	<b>4c</b>	37.3	<b>6j</b>	24.4
<b>1q</b>	12.3	<b>5a</b>	5.9	<b>6K</b>	50.8
<b>2d</b>	26.5	<b>6a</b>	22.7	<b>6l</b>	31.3
<b>2e</b>	48.2	<b>6b</b>	23.5	<b>6m</b>	28.2
<b>2f</b>	38.7	<b>6C</b>	42.3	<b>6n</b>	22.2
<b>3l</b>	3.7	<b>6d</b>	21.9	<b>7a</b>	25.5
<b>3m</b>	5.5				
Group 2: moderate potency ( $IC_{50}$ = 5-15 $\mu$ M in the cell free assay)					
compound #	% inhibition at 5 $\mu$ M (U937 cells)	compound #	% inhibition at 5 $\mu$ M (U937 cells)	compound #	% inhibition at 5 $\mu$ M (U937 cells)
<b>1a</b>	75.1	<b>1h</b>	64.6	<b>4a</b>	89.9
<b>1b</b>	63.8	<b>2j</b>	70.2	<b>4i</b>	75.1
<b>1c</b>	58.4	<b>2l</b>	42.3	<b>4j</b>	81.7
<b>1e</b>	62.9				
Group 3: high potency ( $IC_{50}$ <5 $\mu$ M in the cell free assay)					
compound #	% inhibition at 5 $\mu$ M (U937 cells)	compound #	% inhibition at 5 $\mu$ M (U937 cells)	compound #	% inhibition at 5 $\mu$ M (U937 cells)
<b>1i</b>	73.5	<b>1t</b>	84.2	<b>4f</b>	92.8
<b>1j</b>	89.7	<b>2c</b>	68.2	<b>4g</b>	62
<b>1k</b>	73.7	<b>4d</b>	95	<b>4h</b>	71.7
<b>1r</b>	92	<b>4e</b>	85	<b>4k</b>	87.4
<b>1s</b>	90.1				

Group 1 vs. group 2, exact P value is 0.002; group 1 vs. group 3, exact P value is 0.0017; group 2 vs. group 3, exact P value is 0.0273.

## Results

---

4) Table S3. MTT toxicity assay using RAW 264.7 cells\*

Compound (7.5 $\mu$ M)	% living cells compared to DMSO control*	Compound (7.5 $\mu$ M)	% living cells compared to DMSO control*
1a	97	2e	92
1b	78	2f	95
1c	100	2g	94
1d	9	2h	90
1e	95	2i	94
1f	49	2j	89
1g	99	2k	100
1h	92	2l	92
1i	100	3o	88
1j	88	4a	92
1k	86	4b	63
1l	98	4d	100
1m	83	4e	99
1n	90	4f	98
1o	95	4g	99
1p	94	4h	100
1q	100	4i	92
1r	100	4j	84
1s	96	4k	100
1t	100	6a	91
1u	100	6c	85
2a	83	6h	84
2b	84	9	100
2c	94	11	100
2d	93		

\* Average of at least two independent experiments.

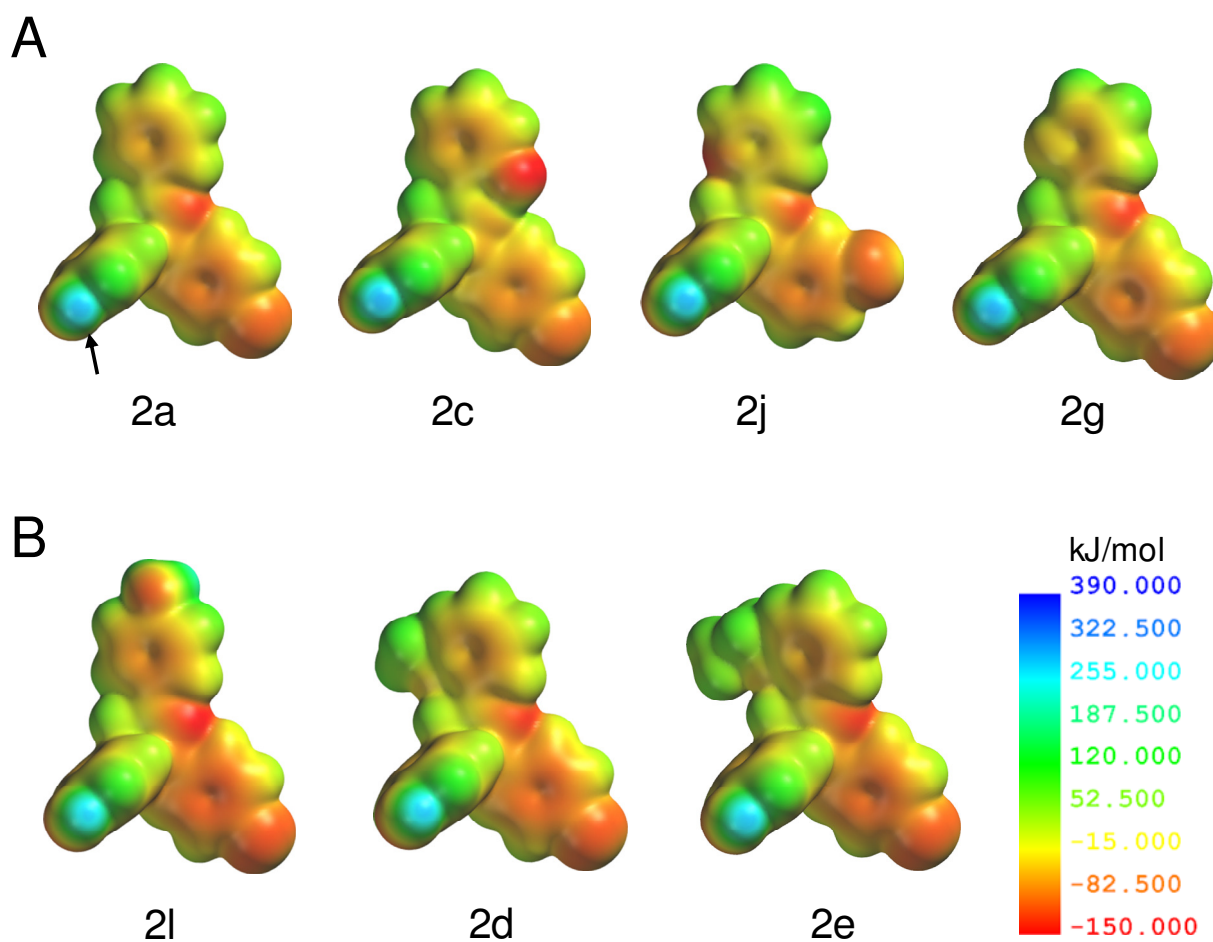
## Results

---

### 5) Supplementary Table S4. Selectivity profile of 4f vs. PKC family and some AGC kinases,

Kinase (human)	% inhibition at 10 $\mu$ M of 4f
PKC $\alpha$	4
PKC $\beta$ I	n.i.
PKC $\beta$ II	12
PKC $\gamma$	6
PKC $\delta$	n.i.
PKC $\epsilon$	n.i.
PKC $\eta$	n.i.
PKC $\theta$	n.i.
PKC $\iota$	n.i.
PDK1	8
PKA	n.i.
RSK1	3
MSK1	11
p70S6K	n.i.
SGK1	18

n.i.: no inhibition. Each value is representative of at least two independent assays which essentially gave the same results.



**6) Supplementary Figure S1.** Molecular electrostatic potentials (MEP) mapped on the isoelectronic density surfaces of  $0.002 e/a_0^3$ . The *ab initio* calculations of the lowest energy conformers and the electrostatic potentials were carried out at the B3LYP density functional scheme with the 6-31G\*\* basis set in water, as implemented in the Gaussian 03 suite of programs.<sup>18</sup> The color codes were uniformly adjusted to range from -150 to +390 kJ/mol. The arrow points to the hydrogen of the phenolic hydroxyl, which shows a higher positive potential in compounds from panel (A) than in those from (B). Hence the OH hydrogen in compounds from (A) is expected to exhibit a higher donor strength.

### 6) References of the supporting information

1. Garcia-Raso, A.; Sinisterra, J. V.; Marinas, J. M., Activated barium hydroxide as a catalyst in organic synthesis. *Pol. J. Chem.* **1982**, 56, (10-12), 1435-45.
2. Reiser, W.; Schnalke, K. E.; Baumert, J. Preparation of 1-(4-chlorophenyl)-4,4-dimethyl-pent-1-en-3-one as an agrochemical intermediate. DE3921167C1, **1990**.
3. Savkar, G. S.; Bokil, K. V.; Nargund, K. S., Condensation of o-anisylsuccinic anhydride with phenyl methyl ethers. *J. Univ. Bombay, Sci.* **1940**, 9, (Pt. 3), 150-5.
4. Esen, I.; Yolacan, C.; Aydogan, F., Long chain dicationic phase transfer catalysts in the condensation reactions of aromatic aldehydes in water under ultrasonic effect. *Bulletin of the Korean Chemical Society* **2010**, 31, 2289-2292.
5. Boyer, J.; Corriu, R. J. P.; Perz, R.; Reye, C., Heterogeneous catalysis by salts and without solvent. III. Synthesis of  $\alpha,\beta$ -unsaturated carbonyl compounds from silyl enol ethers. *J. Organomet. Chem.* **1980**, 184, (2), 157-66.
6. Unterhalt, B.; Reinhold, H. J., Unsaturated oximes. XXV. Reactions of 1-aryl-4,4-dimethyl-1-penten-3-ones with hydroxylamine. *Arch. Pharm. (Weinheim, Ger.)* **1983**, 316, (1), 68-75.
7. Unterhalt, B.; Koehler, H.; Reinhold, H. J., Unsaturated oximes, part 19. Uniform styrylalkyl oximes. *Arch. Pharm. (Weinheim, Ger.)* **1978**, 311, (7), 604-8.
8. Chen, K.-W.; Syu, S.-e.; Jang, Y.-J.; Lin, W., A facile approach to highly functional trisubstituted furans via intramolecular Wittig reactions. *Organic & biomolecular chemistry* **2011**, 9, 2098-106.
9. Irie, K.; Watanabe, K., Aldol condensations with metal(II) complex catalysts. *Bull. Chem. Soc. Jpn.* **1980**, 53, (5), 1366-71.
10. Sinisterra, J. V.; Garcia-Raso, A.; Cabello, J. A.; Marinas, J. M., An improved procedure for the Claisen-Schmidt reaction. *Synthesis* **1984**, (6), 502-4.
11. Yang, G.-C.; Huang, J.-X.; Zhong, J.-H.; Chen, J.-W., Catalytic synthesis of  $\alpha,\beta$ -unsaturated carbonyl compounds by tellurium(IV) chloride. *Hecheng Huaxue* **1998**, 6, (3), 324-327.
12. Bunce, S. C.; Dorsman, H. J.; Popp, F. D., Synthesis of  $\alpha,\beta$ -unsaturated cyclopropyl ketones and 3-cyclopropylpyrazolines. *J. Chem. Soc.* **1963**, 303-7.
13. Goodell, J. R.; Puig-Basagoiti, F.; Forshey, B. M.; Shi, P.-Y.; Ferguson, D. M., Identification

## Results

---

of compounds with anti-West Nile Virus activity. *Journal of medicinal chemistry* **2006**, 49, 2127-37.

14. Liu, W.; Shi, H.-M.; Jin, H.; Zhao, H.-Y.; Zhou, G.-P.; Wen, F.; Yu, Z.-Y.; Hou, T.-P., Design, synthesis and antifungal activity of a series of novel analogs based on diphenyl ketones. *Chemical biology & drug design* **2009**, 73, 661-7.

15. Falcao, d. F. L., Synthesis of nonnatural chalcones. Bol. Fac. Farm., Univ. Coimbra, Ed. Cient. **1968**, 28, 49-52.

16. Kim, Y. S.; Kumar, V.; Lee, S.; Iwai, A.; Neckers, L.; Malhotra, S. V.; Trepel, J. B., Methoxychalcone inhibitors of androgen receptor translocation and function. *Bioorganic & medicinal chemistry letters* **2012**, 22, 2105-9.

17. Chiaradia, L. D.; Martins, P. G. A.; Cordeiro, M. N. S.; Guido, R. V. C.; Ecco, G.; Andricopulo, A. D.; Yunes, R. A.; Vernal, J.; Nunes, R. J.; Terenzi, H., Synthesis, biological evaluation, and molecular modeling of chalcone derivatives as potent inhibitors of Mycobacterium tuberculosis protein tyrosine phosphatases (PtpA and PtpB). *Journal of medicinal chemistry* **2012**, 55, 390-402.

18. Heim, R.; Lucas, S.; Grombein, C. M.; Ries, C.; Schewe, K. E.; Negri, M.; Müller-Vieira, U.; Birk, B.; Hartmann, R. W., Overcoming Undesirable CYP1A2 Inhibition of Pyridyl-naphthalene-Type Aldosterone Synthase Inhibitors: Influence of Heteroaryl Derivatization on Potency and Selectivity. *Journal of medicinal chemistry* **2008**, 51, (16), 5064-5074.

## References of the manuscript

1. Newton, A. C. Protein kinase C: poised to signal. *Am J Physiol Endocrinol Metab* **2010**, 298, E395-402.

2. Moscat, J.; Diaz-Meco, M. T.; Wooten, M. W. Of the atypical PKCs, Par-4 and p62: recent understandings of the biology and pathology of a PB1-dominated complex. *Cell Death Differ* **2009**, 16, 1426-37.

3. Diaz-Meco, M. T.; Moscat, J. The atypical PKCs in inflammation: NF-kappaB and beyond. *Immunol Rev* **2012**, 246, 154-67.

4. Leitges, M.; Sanz, L.; Martin, P.; Duran, A.; Braun, U.; Garcia, J. F.; Camacho, F.; Diaz-Meco, M. T.; Rennert, P. D.; Moscat, J. Targeted disruption of the zetaPKC gene results in the impairment of the NF-kappaB pathway. *Mol Cell* **2001**, 8, 771-80.

## Results

---

5. Bandyopadhyay, G.; Standaert, M. L.; Sajan, M. P.; Kanoh, Y.; Miura, A.; Braun, U.; Kruse, F.; Leitges, M.; Farese, R. V. Protein kinase C-lambda knockout in embryonic stem cells and adipocytes impairs insulin-stimulated glucose transport. *Mol Endocrinol* **2004**, *18*, 373-83.
6. Martin, P.; Villares, R.; Rodriguez-Mascarenhas, S.; Zaballos, A.; Leitges, M.; Kovac, J.; Sizing, I.; Rennert, P.; Marquez, G.; Martinez, A. C.; Diaz-Meco, M. T.; Moscat, J. Control of T helper 2 cell function and allergic airway inflammation by PKCzeta. *Proc Natl Acad Sci U S A* **2005**, *102*, 9866-71.
7. Jaruga, B.; Hong, F.; Sun, R.; Radaeva, S.; Gao, B. Crucial role of IL-4/STAT6 in T cell-mediated hepatitis: up-regulating eotaxins and IL-5 and recruiting leukocytes. *J Immunol* **2003**, *171*, 3233-44.
8. Duran, A.; Rodriguez, A.; Martin, P.; Serrano, M.; Flores, J. M.; Leitges, M.; Diaz-Meco, M. T.; Moscat, J. Crosstalk between PKCzeta and the IL4/Stat6 pathway during T-cell-mediated hepatitis. *Embo J* **2004**, *23*, 4595-605.
9. Berra, E.; Diaz-Meco, M. T.; Lozano, J.; Frutos, S.; Municio, M. M.; Sanchez, P.; Sanz, L.; Moscat, J. Evidence for a role of MEK and MAPK during signal transduction by protein kinase C zeta. *Embo J* **1995**, *14*, 6157-63.
10. Moscat, J.; Diaz-Meco, M. T. The atypical protein kinase Cs. Functional specificity mediated by specific protein adapters. *EMBO Rep* **2000**, *1*, 399-403.
11. Martin, P.; Duran, A.; Minguet, S.; Gaspar, M. L.; Diaz-Meco, M. T.; Rennert, P.; Leitges, M.; Moscat, J. Role of zeta PKC in B-cell signaling and function. *Embo J* **2002**, *21*, 4049-57.
12. Karin, M.; Greten, F. R. NF-kappaB: linking inflammation and immunity to cancer development and progression. *Nat Rev Immunol* **2005**, *5*, 749-59.
13. Duran, A.; Diaz-Meco, M. T.; Moscat, J. Essential role of RelA Ser311 phosphorylation by zetaPKC in NF-kappaB transcriptional activation. *Embo J* **2003**, *22*, 3910-8.
14. Diaz-Meco, M. T.; Berra, E.; Municio, M. M.; Sanz, L.; Lozano, J.; Dominguez, I.; Diaz-Golpe, V.; Lain de Lera, M. T.; Alcamí, J.; Paya, C. V.; et al. A dominant negative protein kinase C zeta subspecies blocks NF-kappa B activation. *Mol Cell Biol* **1993**, *13*, 4770-5.
15. Folgueira, L.; McElhinny, J. A.; Bren, G. D.; MacMorran, W. S.; Diaz-Meco, M. T.; Moscat, J.; Paya, C. V. Protein kinase C-zeta mediates NF-kappa B activation in human immunodeficiency virus-infected monocytes. *J Virol* **1996**, *70*, 223-31.

## Results

---

16. Sontag, E.; Sontag, J. M.; Garcia, A. Protein phosphatase 2A is a critical regulator of protein kinase C zeta signaling targeted by SV40 small t to promote cell growth and NF-kappaB activation. *Embo J* **1997**, 16, 5662-71.
17. Anrather, J.; Csizmadia, V.; Soares, M. P.; Winkler, H. Regulation of NF-kappaB RelA phosphorylation and transcriptional activity by p21(ras) and protein kinase Czeta in primary endothelial cells. *J Biol Chem* **1999**, 274, 13594-603.
18. Martin, A. G.; San-Antonio, B.; Fresno, M. Regulation of nuclear factor kappa B transactivation. Implication of phosphatidylinositol 3-kinase and protein kinase C zeta in c-Rel activation by tumor necrosis factor alpha. *J Biol Chem* **2001**, 276, 15840-9.
19. LaVallie, E. R.; Chockalingam, P. S.; Collins-Racie, L. A.; Freeman, B. A.; Keohan, C. C.; Leitges, M.; Dorner, A. J.; Morris, E. A.; Majumdar, M. K.; Arai, M. Protein kinase Czeta is up-regulated in osteoarthritic cartilage and is required for activation of NF-kappaB by tumor necrosis factor and interleukin-1 in articular chondrocytes. *J Biol Chem* **2006**, 281, 24124-37.
20. Levy, D.; Kuo, A. J.; Chang, Y.; Schaefer, U.; Kitson, C.; Cheung, P.; Espejo, A.; Zee, B. M.; Liu, C. L.; Tangsombatvisit, S.; Tennen, R. I.; Kuo, A. Y.; Tanjing, S.; Cheung, R.; Chua, K. F.; Utz, P. J.; Shi, X.; Prinjha, R. K.; Lee, K.; Garcia, B. A.; Bedford, M. T.; Tarakhovsky, A.; Cheng, X.; Gozani, O. Lysine methylation of the NF-kappaB subunit RelA by SETD6 couples activity of the histone methyltransferase GLP at chromatin to tonic repression of NF-kappaB signaling. *Nat Immunol* **2011**, 12, 29-36.
21. Tiegs, G.; Hentschel, J.; Wendel, A. A T cell-dependent experimental liver injury in mice inducible by concanavalin A. *J Clin Invest* **1992**, 90, 196-203.
22. Lavoie, G.; Esteve, P. O.; Laulan, N. B.; Pradhan, S.; St-Pierre, Y. PKC isoforms interact with and phosphorylate DNMT1. *BMC Biol* **2011**, 9, 31.
23. Rangel-Salazar, R.; Wickstrom-Lindholm, M.; Aguilar-Salinas, C. A.; Alvarado-Caudillo, Y.; Dossing, K. B.; Esteller, M.; Labourier, E.; Lund, G.; Nielsen, F. C.; Rodriguez-Rios, D.; Solis-Martinez, M. O.; Wrobel, K.; Wrobel, K.; Zaina, S. Human native lipoprotein-induced de novo DNA methylation is associated with repression of inflammatory genes in THP-1 macrophages. *BMC Genomics* **2011**, 12, 582.
24. Murray, N. R.; Kalari, K. R.; Fields, A. P. Protein kinase Ciota expression and oncogenic signaling mechanisms in cancer. *J Cell Physiol* **2011**, 226, 879-87.
25. Sajan, M. P.; Nimal, S.; Mastorides, S.; Acevedo-Duncan, M.; Kahn, C. R.; Fields, A. P.; Braun, U.; Leitges, M.; Farese, R. V. Correction of metabolic abnormalities in a rodent model of

## Results

---

obesity, metabolic syndrome, and type 2 diabetes mellitus by inhibitors of hepatic protein kinase C- $\iota$ . *Metabolism* **2012**, 61, 459-69.

26. Standaert, M. L.; Galloway, L.; Karnam, P.; Bandyopadhyay, G.; Moscat, J.; Farese, R. V. Protein kinase C- $\zeta$  as a downstream effector of phosphatidylinositol 3-kinase during insulin stimulation in rat adipocytes. Potential role in glucose transport. *J Biol Chem* **1997**, 272, 30075-82.

27. Farese, R. V. Function and dysfunction of  $\alpha$ PKC isoforms for glucose transport in insulin-sensitive and insulin-resistant states. *Am J Physiol Endocrinol Metab* **2002**, 283, E1-11.

28. Farese, R. V.; Sajan, M. P. Metabolic functions of atypical protein kinase C: "good" and "bad" as defined by nutritional status. *Am J Physiol Endocrinol Metab* **2010**, 298, 385-394.

29. Mochly-Rosen, D.; Das, K.; Grimes, K. V. Protein kinase C, an elusive therapeutic target? *Nat Rev Drug Discov* **2012**, 11, 937-57.

30. Yuan, L.; Seo, J. S.; Kang, N. S.; Keinan, S.; Steele, S. E.; Michelotti, G. A.; Wetsel, W. C.; Beratan, D. N.; Gong, Y. D.; Lee, T. H.; Hong, J. Identification of 3-hydroxy-2-(3-hydroxyphenyl)-4H-1-benzopyran-4-ones as isoform-selective PKC- $\zeta$  inhibitors and potential therapeutics for psychostimulant abuse. *Mol Biosyst* 2009, 5, 927-30.

31. Wu, J.; Zhang, B.; Wu, M.; Li, H.; Niu, R.; Ying, G.; Zhang, N. Screening of a PKC  $\zeta$ -specific kinase inhibitor PKC $\zeta$ I257.3 which inhibits EGF-induced breast cancer cell chemotaxis. *Invest New Drugs* **2009**, 28, 268-75.

32. Trujillo, J. I.; Kiefer, J. R.; Huang, W.; Thorarensen, A.; Xing, L.; Caspers, N. L.; Day, J. E.; Mathis, K. J.; Kretzmer, K. K.; Reitz, B. A.; Weinberg, R. A.; Stegeman, R. A.; Wrightstone, A.; Christine, L.; Compton, R.; Li, X. 2-(6-Phenyl-1H-indazol-3-yl)-1H-benzo [d] imidazoles: Design and synthesis of a potent and isoform selective PKC- $\zeta$  inhibitor. *Bioorg Med Chem Lett* **2009**, 19, 908-911.

33. Kjaer, S.; Linch, M.; Purkiss, A.; Kostecky, B.; Knowles, P. P.; Rosse, C.; Riou, P.; Soudy, C.; Kaye, S.; Patel, B.; Soriano, E.; MurrayRust, J.; Barton, C.; Dillon, C.; Roffey, J.; Parker, P. J.; McDonald, N. Q. Adenosine-binding motif mimicry and cellular effects of a thieno[2,3-d]pyrimidine-based chemical inhibitor of atypical protein kinase C isoenzymes. *Biochem. J.* **2013**, 451, 329-342.

34. Titchenell, P. M.; Lin, C.-M.; Keil, J. M.; Sundstrom, J. M.; Smith, C. D.; Antonetti, D. A. Novel atypical PKC inhibitors prevent vascular endothelial growth factor-induced blood-retinal barrier dysfunction. *Biochem. J.* **2012**, 446, 455-467.

## Results

---

35. Titchenell, P. M.; Hollis, S. H. D.; Pons, J.-F.; Barber, A. J.; Jin, Y.; Antonetti, D. A. Synthesis and structure-activity relationships of 2-amino-3-carboxy-4-phenylthiophenes as novel atypical protein kinase C inhibitors. *Bioorg Med Chem Lett* **2013**, <http://dx.doi.org/10.1016/j.bmcl.2013.03.019>.
36. Lamba, V.; Ghosh, I. New directions in targeting protein kinases: focusing upon true allosteric and bivalent inhibitors. *Curr Pharm Des* **2012**, *18*, 2936-45.
37. Fröhner, W.; Lopez-Garcia, L. A.; Neimanis, S.; Weber, N.; Navratil, J.; Maurer, F.; Stroba, A.; Zhang, H.; Biondi, R. M.; Engel, M. 4-benzimidazolyl-3-phenylbutanoic acids as novel PIF-pocket-targeting allosteric inhibitors of protein kinase PKCzeta. *J Med Chem* **2011**, *54*, 6714-6723.
38. Engel, M.; Hindie, V.; Lopez-Garcia, L. A.; Stroba, A.; Schaeffer, F.; Adrian, I.; Imig, J.; Idrissova, L.; Nastainczyk, W.; Zeuzem, S.; Alzari, P. M.; Hartmann, R. W.; Piiper, A.; Biondi, R. M. Allosteric activation of the protein kinase PDK1 with low molecular weight compounds. *Embo J* **2006**, *25*, 5469-80.
39. Stroba, A.; Schaeffer, F.; Hindie, V.; Lopez-Garcia, L. A.; Adrian, I.; Fröhner, W.; Hartmann, R. W.; Biondi, R. M.; Engel, M. 3,5-diphenylpent-2-enoic acids as allosteric activators of the protein kinase PDK1: Structure-activity relationships and thermodynamic characterisation of binding as paradigms for PIF-binding pocket-targeting compounds. *J Med Chem* **2009**, *52*, 4683-4693.
40. Wilhelm, A.; Lopez-Garcia, L. A.; Busschots, K.; Froehner, W.; Maurer, F.; Boettcher, S.; Zhang, H.; Schulze, J. r. O.; Biondi, R. M.; Engel, M. 2-(3-Oxo-1,3-diphenylpropyl)malonic Acids as Potent Allosteric Ligands of the PIF Pocket of Phosphoinositide-Dependent Kinase-1: Development and Prodrug Concept. *Journal of Medicinal Chemistry* **2012**, *55*, 9817-9830.
41. Hindie, V.; Stroba, A.; Zhang, H.; Lopez-Garcia, L. A.; Idrissova, L.; Zeuzem, S.; Hirschberg, D.; Schaeffer, F.; Jorgensen, T. J.; Engel, M.; Alzari, P. M.; Biondi, R. M. Structure and allosteric effects of low-molecular-weight activators on the protein kinase PDK1. *Nat Chem Biol* **2009**, *5*, 758-64.
42. Stockman, B. J.; Kothe, M.; Kohls, D.; Weibley, L.; Connolly, B. J.; Sheils, A. L.; Cao, Q.; Cheng, A. C.; Yang, L.; Kamath, A. V.; Ding, Y. H.; Charlton, M. E. Identification of allosteric PIF-pocket ligands for PDK1 using NMR-based fragment screening and 1H-15N TROSY experiments. *Chem Biol Drug Des* **2009**, *73*, 179-88.
43. Huang, Y. R.; Katzenellenbogen, J. A. Regioselective Synthesis of Ligands for the Estrogen Receptor. *Org. Lett.* **2000**, *43*, 61-64.

## Results

---

44. Madsen, P.; Ling, A.; Plewe, M.; Sams, C. K.; Knudsen, L. B.; Sidelmann, U. G.; Ynddal, L.; Brand, C. L.; Andersen, B.; Murphy, D.; Teng, M.; Truesdale, L.; Kiel, D.; May, J.; Kuki, A.; Shi, S.; Johnson, M. D.; Teston, K. A.; Feng, J.; Lakis, J.; Anderes, K.; Gregor, V.; Lau, J. Optimization of Alkylidene Hydrazide Based Human Glucagon Receptor Antagonists. Discovery of the Highly Potent and Orally Available 3-Cyano-4-hydroxybenzoic Acid [1-(2,3,5,6-Tetramethylbenzyl)-1H-indol-4-ylmethylene]hydrazide. *Journal of Medicinal Chemistry* **2002**, *45*, 5755-5775.
45. Kirk, K. L. Fluorination in Medicinal Chemistry: Methods, Strategies, and Recent Developments. *Organic Process Research & Development* **2008**, *12*, 305-321.
46. Schmidtke, P.; Luque, F. J.; Murray, J. B.; Barril, X. Shielded Hydrogen Bonds as Structural Determinants of Binding Kinetics: Application in Drug Design. *J. Am. Chem. Soc.* **2011**, *133*, 18903-18910.
47. Sorme, P.; Arnoux, P.; Kahl-Knutsson, B.; Leffler, H.; Rini, J. M.; Nilsson, U. J. Structural and thermodynamic studies on cation- $\pi$  interactions in lectin-ligand complexes: high-affinity galectin-3 inhibitors through fine-tuning of an arginine-arene interaction. *J Am Chem Soc* **2005**, *127*, 1737-43.
48. Ebner, T.; Burchell, B. Substrate specificities of two stably expressed human liver UDP-glucuronosyltransferases of the UGT1 gene family. *Drug Metab. Dispos.* **1993**, *21*, 50-5.
49. Davis, M. I.; Hunt, J. P.; Herrgard, S.; Cicceri, P.; Wodicka, L. M.; Pallares, G.; Hocker, M.; Treiber, D. K.; Zarrinkar, P. P. Comprehensive analysis of kinase inhibitor selectivity. *Nat Biotechnol* **2011**, *29*, 1046-51.
50. Wagner, G.; Laufer, S. Small molecular anti-cytokine agents. *Med. Res. Rev.* **2006**, *26*, 1-62.
51. Zhu, J.; Huang, J.-W.; Tseng, P.-H.; Yang, Y.-T.; Fowble, J.; Shiau, C.-W.; Shaw, Y.-J.; Kulp, S. K.; Chen, C.-S. From the Cyclooxygenase-2 Inhibitor Celecoxib to a Novel Class of 3-Phosphoinositide-Dependent Protein Kinase-1 Inhibitors. *Cancer Res.* **2004**, *64*, 4309-4318.
52. Hansen, J. D.; Grina, J.; Newhouse, B.; Welch, M.; Topalov, G.; Littman, N.; Callejo, M.; Gloor, S.; Martinson, M.; Laird, E.; Brandhuber, B. J.; Vigers, G.; Morales, T.; Woessner, R.; Randolph, N.; Lyssikatos, J.; Olivero, A. Potent and selective pyrazole-based inhibitors of B-Raf kinase. *Bioorg. Med. Chem. Lett.* **2008**, *18*, 4692-4695.
53. Lopez-Garcia, L. A.; Schulze, J. O.; Fröhner, W.; Zhang, H.; Süß, E.; Weber, N.; Navratil, J.; Amon, S.; Hindie, V.; Zeuzem, S.; Jørgensen, T. J. D.; Alzari, P. M.; Neimanis, S.; Engel, M.; Biondi, R. M. Allosteric regulation of protein kinase PKC $\zeta$  by the N-terminal C1 domain and small compounds to the PIF-pocket. *Chem Biol* **2011**, *18*, 1463-1473.

## Results

---

54. Niesen, F. H.; Berglund, H.; Vedadi, M. The use of differential scanning fluorimetry to detect ligand interactions that promote protein stability. *Nat Protoc* **2007**, 2, 2212-21.
55. Davis, P. D.; Elliott, L. H.; Harris, W.; Hill, C. H.; Hurst, S. A.; Keech, E.; Kumar, M. K. H.; Lawton, G.; Nixon, J. S.; Wilkinson, S. E. Inhibitors of protein kinase C. 2. Substituted bisindolylmaleimides with improved potency and selectivity. *Journal of Medicinal Chemistry* **1992**, 35, 994-1001.
56. Nagashima, K.; Shumway, S. D.; Sathyanarayanan, S.; Chen, A. H.; Dolinski, B.; Xu, Y.; Keilhack, H.; Nguyen, T.; Wiznerowicz, M.; Li, L.; Lutterbach, B. A.; Chi, A.; Paweletz, C.; Allison, T.; Yan, Y.; Munshi, S. K.; Klippel, A.; Kraus, M.; Bobkova, E. V.; Deshmukh, S.; Xu, Z.; Mueller, U.; Szewczak, A. A.; Pan, B. S.; Richon, V.; Pollock, R.; Blume-Jensen, P.; Northrup, A.; Andersen, J. N. Genetic and pharmacological inhibition of PDK1 in cancer cells: characterization of a selective allosteric kinase inhibitor. *J Biol Chem* **2011**, 286, 6433-48.
57. Standaert, M. L.; Galloway, L.; Karnam, P.; Bandyopadhyay, G.; Moscat, J.; Farese, R. V. Protein kinase C-zeta as a downstream effector of phosphatidylinositol 3-kinase during insulin stimulation in rat adipocytes. Potential role in glucose transport. *J. Biol. Chem.* **1997**, 272, 30075-30082.
58. Limatola, C.; Schaap, D.; Moolenaar, W. H.; van, B. W. J. Phosphatidic acid activation of protein kinase C-zeta overexpressed in COS cells: comparison with other protein kinase C isoforms and other acidic lipids. *Biochem. J.* **1994**, 304, 1001-8.
59. Numazawa, S.; Ishikawa, M.; Yoshida, A.; Tanaka, S.; Yoshida, T. Atypical protein kinase C mediates activation of NF-E2-related factor 2 in response to oxidative stress. *Am. J. Physiol.* **2003**, 285, C334-C342.
60. Muller, G.; Ayoub, M.; Storz, P.; Rennecke, J.; Fabbro, D.; Pfizenmaier, K. PKC zeta is a molecular switch in signal transduction of TNF-alpha, bifunctionally regulated by ceramide and arachidonic acid. *Embo J* **1995**, 14, 1961-9.
61. Haas, T. L.; Emmerich, C. H.; Gerlach, B.; Schmukle, A. C.; Cordier, S. M.; Rieser, E.; Feltham, R.; Vince, J.; Warnken, U.; Wenger, T.; Koschny, R.; Komander, D.; Silke, J.; Walczak, H. Recruitment of the linear ubiquitin chain assembly complex stabilizes the TNF-R1 signaling complex and is required for TNF-mediated gene induction. *Mol Cell* **2009**, 36, 831-44.
62. Huang, X.; Chen, L.-Y.; Doerner, A. M.; Pan, W. W.; Smith, L.; Huang, S.; Papadimos, T. J.; Pan, Z. K. An Atypical Protein Kinase C (PKC $\zeta$ ) Plays a Critical Role in Lipopolysaccharide-Activated NF- $\kappa$ B in Human Peripheral Blood Monocytes and Macrophages. *The Journal of Immunology* **2009**, 182, 5810-5815.

## Results

---

63. Xie, Q. W.; Kashiwabara, Y.; Nathan, C. Role of transcription factor NF-kappa B/Rel in induction of nitric oxide synthase. *Journal of Biological Chemistry* **1994**, 269, 4705-4708.
64. Brouet, I.; Ohshima, H. Curcumin, an Anti-tumor Promoter and Anti-inflammatory Agent, Inhibits Induction of Nitric Oxide Synthase in Activated Macrophages. *Biochemical and Biophysical Research Communications* **1995**, 206, 533-540.
65. Green, L. C.; Wagner, D. A.; Glogowski, J.; Skipper, P. L.; Wishnok, J. S.; Tannenbaum, S. R. Analysis of nitrate, nitrite, and [15N]nitrate in biological fluids. *Analytical Biochemistry* **1982**, 126, 131-138.

### 3.2 Trisubstituted and Tetrasubstituted Pyrazolines as a Novel Class of Cell-growth Inhibitors in Tumor Cells with Wild Type p53

A major part of this chapter is submitted to the Journal of Bioorganic and Medicinal Chemistry

**Abstract:** Derivatives with scaffolds of 1,3,5-tri-substituted pyrazoline and 1,3,4,5-tetra-substituted pyrazoline were synthesized and tested for their inhibitory effects versus the p53<sup>+/+</sup> HCT116 and p53<sup>-/-</sup> H1299 human tumor cell lines. Several compounds were active against the two cell lines displaying IC<sub>50</sub> values in the low micromolar range with a clearly more pronounced effect on the p53<sup>+/+</sup> HCT116 cells. The compound class shows excellent developability due to the modular synthesis, allowing independent optimization of all three to four key substituents to improve the properties of the molecules.

#### Introduction

The pro-apoptotic p53 protein is a transcription factor that responds to various stress stimuli such as DNA damage and oxidative stress by increasing the expression of proteins involved in DNA repair, cell cycle arrest and induction of apoptosis.<sup>1</sup> Consistent with its role as a tumor-suppressor, p53 is deleted or mutated in approximately 50% of human cancers. In other tumors, p53 is retained in its wild type form, but its activity is effectively inhibited by the negative regulator murine double minute 2 (Mdm2). Mdm2, also known as E3 ubiquitin-protein ligase Mdm2, is a protein that is encoded by the *MDM2* gene in which the human homolog is sometimes referred to as Hdm2. Mdm2 serves to down regulate p53 levels by C-terminal ubiquitination and subsequent proteasomal degradation. In addition, Mdm2 has been shown to inhibit p53 transcriptional activity through direct binding to the p53 transactivation domain.<sup>2-4</sup> The interaction between Mdm2 and p53 involves a short helix formed by residues 13-29 of p53 and a hydrophobic cleft in Mdm2.

The realization that p53 most contributing residues to this interaction are Phe19, Trp23 and Leu26 stimulated the efforts to identify drug-like inhibitors of this protein-protein interaction. Such inhibitors are expected to release p53 from the negative control of Mdm2, and activate the apoptotic p53 pathway in tumors expressing wild type p53. However, tumors with mutated or deleted p53 are expected to be less responsive.<sup>5-7</sup> Such compounds may be useful for indications such as colorectal cancer chemoprevention or the treatment of precancerous conditions (e.g. adenomatous polyps) where p53 is functional but inhibited by Mdm2.

The prototypes for such class of inhibitors are imidazoline derivatives known as nutlins **I-III** (Figure 1). Structure activity relationships show that the *cis*-imidazoline represents a useful

## Results

scaffold to project functional groups similar to a helical peptide. Nutlins are tetrasubstituted imidazoline derivatives with two orthogonal halophenyls projecting in a non-coplanar style relative to the core ring, other substituents are an alkoxyphenyl substituent and a tertiary amide substituent. The alkoxyphenyl is directed towards the Phe19 pocket, one of the halo-phenyl group sits deeply in the Trp23 pocket while the other occupies the Leu26 pocket. Galatin and Abraham proposed a pharmacophore model based on the crystal structure of p53 peptide in complex with Mdm2 and several known non-peptidic small molecule inhibitors of Mdm2, with the three lipophilic groups at particular distances from each other.<sup>8</sup>

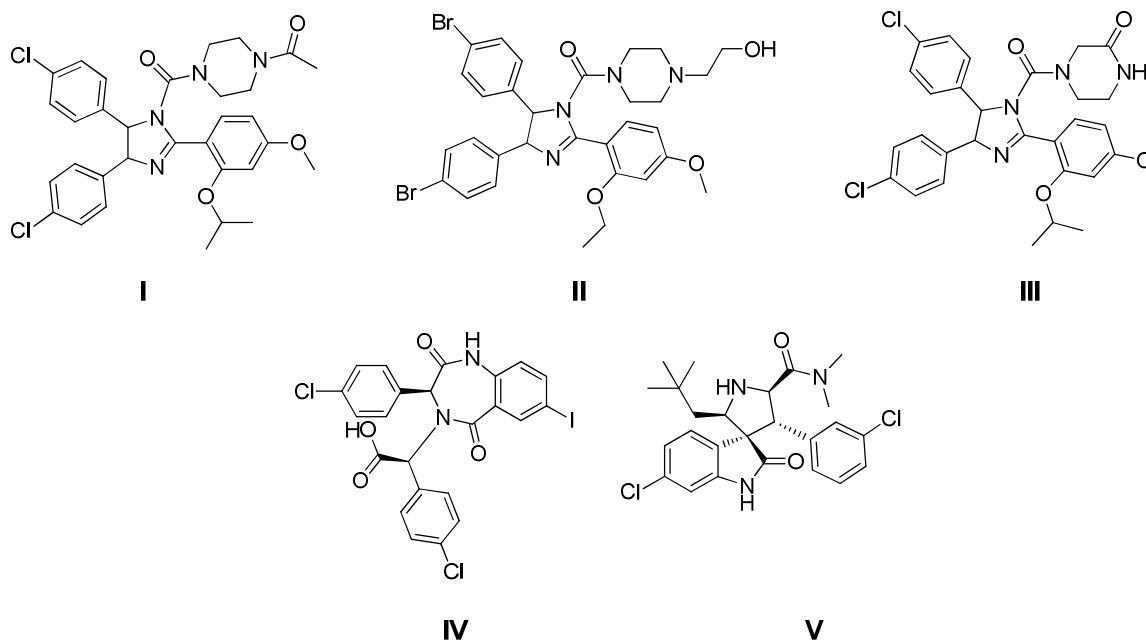


**Figure 1:** Previously reported Mdm-2 antagonists I-V.

Later, other structurally related compounds followed including the benzodiazepinedione **IV** and the spiroindole **V** (Figure1), all sharing at least two haloaryl groups projecting from a core diazepindione or pyrrolidine ring with nutlins.<sup>9-11</sup>

Although several of these inhibitors exhibited cellular activity, extensive optimization of the selectivity towards the Mdm2 binding pocket might be required, since a hydrophobic groove is characteristic of many “hot spots” at protein-protein interaction sites; bearing in mind that such hot spot binding pockets can possess a high conformational adaptivity and that hydrophobic contacts are not directional and thus less specific in their interactions. The chosen scaffolds for inhibitors should offer high synthetic flexibility to allow for the generation of a great variety of analogues during the optimization process.<sup>12</sup> Hence the search for additional rigid scaffolds appropriate to inhibit the Mdm2-p53 interaction and showing favorable synthetic tractability (good “developability”) is still ongoing.

## Results

---

In this report, we describe the design and synthesis of forty-six novel small organic molecules with core pyrazoline ring and two orthogonal dihalophenyl, and alkoxyphenyl or *tertiary*-butyl (**1-44**) substituent to mimic the potential three hydrophobic residues (Phe19, Trp23, and Leu26) of p53. Moreover two of the compounds contain an additional tertiary amide substituent (**45, 46**). As a first assay, the compounds were tested for their growth inhibitory activity against p53 wild-type (+/+) HCT116 human colorectal carcinoma and p53 null (-/-) H1299 human lung adenocarcinoma cell lines.

### Design of compounds

Our main objective was to develop a new class of potential p53-Mdm2 antagonists with an excellent synthetic tractability, thus providing the option to independently vary each key moiety for the optimization of potency, selectivity and pharmacokinetic properties. To this end, a synopsis of the hitherto published inhibitor classes led us to the design of the tri- and tetra-substituted pyrazoline derivatives.

Thus, three sets of pyrazolines were designed with a 1,3,5-trisubstituted pyrazoline scaffold. The 1<sup>st</sup> group is represented by compounds (**1-29**) in which the phenyls at positions 1 and 5 are mono-substituted with a chlorine atom and the 3-phenyl is mono- (**1-27**) or disubstituted (**28, 29**) with methoxy functions. The position of the chlorine atoms and the methoxy group(s) was varied in a systematic way to define the optimum substitution pattern that shows the best potency and selectivity. The dimethoxy substitution was made in a later stage in compounds **28** and **29** to test the effect of the 2<sup>nd</sup> methoxy group on the activity of compound **4**, the most potent growth inhibitor against the HCT116 tumor cell line in the series.

In the 2<sup>nd</sup> set of compounds (**30-35**) *t*-butyl group was used as a lipophilic substituent instead of the methoxyphenyl at position 3 of the pyrazoline. Besides, several lipophilic groups were employed at position 5 like naphthyl, biphenyl, 2,4-dichlorophenyl, 4-chlorophenyl and 4-bromophenyl. In the third set (**36-44**), haloaryl and carboaryls at positions 1 and 5 of pyrazoline were used similar to the first and second sets. However the 2-ethoxy phenyl part reported in nutlin-2 is used at position 3. In the last 2 compounds (**45-46**), we introduced a 4<sup>th</sup> substitution at position 4 of the pyrazoline with morpholinocarbonyl group to test the effect of introducing a tertiary amide on activity and to improve the water solubility.

To check the validity of our design, a three-dimensional overlay of the energy minimized forms of the 1,3,5-triphenylpyrazolinre scaffold (for which different substitution patterns are tried in compounds **1-29**) and compound **45** with nutlin-2 from PDB 1RV1 was done. It can be seen that all the substituents relevant to the binding of nutlin-2 to Mdm-2 overlapped well with the corresponding moieties of our compounds (Figure 2).

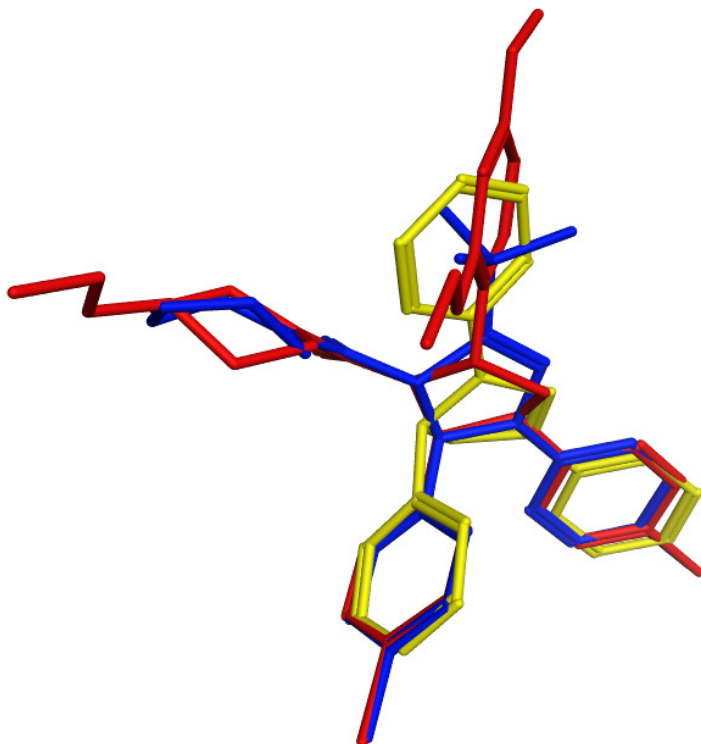


**Figure 2:** An overlay of the energy minimized forms the unsubstituted 1,3,5-triphenylpyrazoline scaffold (yellow) and compound 45 (blue) with nutlin-2 (red) from PDB 1RV1, showing spatial similarity. Energy minimization was done by MMFF94x forcefield and followed by automatic overlaying using MOE software.

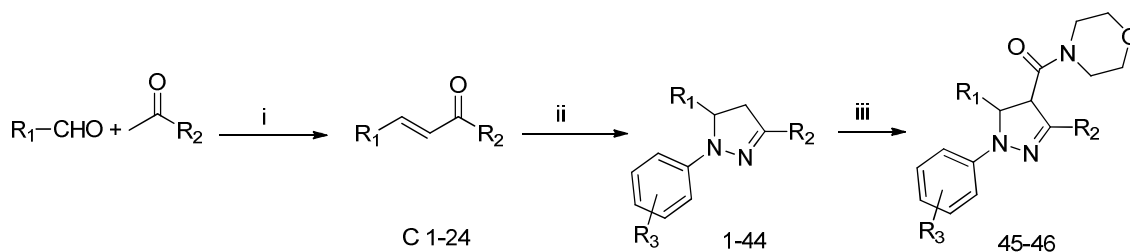
## Results and Discussion

### Chemistry

The synthesis of the desired pyrazolines was carried out in two steps. In the first step (Scheme 1), a Claisen-Schmidt condensation was carried out between aromatic aldehydes and pinacolone or acetophenone analogues, using 10% aq. KOH as a catalyst in methanol, in order to afford the required enones. In the second step, these enones were reacted to give the desired pyrazolines using the previously reported regioselective synthesis of 1,3,5-triarylpyrazolines.<sup>13</sup> This was accomplished via enone-arylhydrazine hydrochloride condensation reaction under an inert atmosphere using DMF as solvent while heating for 5 hours at 85°C. To introduce the morpholinocarbonyl group at position 4 of the respective pyrazoline derivative (**34**, **36**), deprotonation was carried out by LDA at -78°C to create the anion which reacted with morpholinecarbonyl chloride to give the desired product (Scheme 1).<sup>13</sup>

## Results

### Scheme 1:



Reagents and conditions: (i) 10%KOH, MeOH, ice cooling then room temperature, over night (ii) 1.5 equiv Ar-NH-NH<sub>2</sub>.HCl, DMF, 85 °C, 5h (iii) 1.5 equiv 4-morpholinecarbonylchloride, 1.5 equiv LDA, THF, -78 °C then room temperature, 20h

Compound #	C	R1	R2	R3
1	1	4-chlorophenyl	4-methoxyphenyl	2-chloro
2	1	4-chlorophenyl	4-methoxyphenyl	3-chloro
3	1	4-chlorophenyl	4-methoxyphenyl	4-chloro
4	2	3-chlorophenyl	4-methoxyphenyl	2-chloro
5	2	3-chlorophenyl	4-methoxyphenyl	3-chloro
6	2	3-chlorophenyl	4-methoxyphenyl	4-chloro
7	3	2-chlorophenyl	4-methoxyphenyl	2-chloro
8	3	2-chlorophenyl	4-methoxyphenyl	3-chloro
9	3	2-chlorophenyl	4-methoxyphenyl	4-chloro
10	4	4-chlorophenyl	3-methoxyphenyl	2-chloro
11	4	4-chlorophenyl	3-methoxyphenyl	3-chloro
12	4	4-chlorophenyl	3-methoxyphenyl	4-chloro
13	5	3-chlorophenyl	3-methoxyphenyl	2-chloro
14	5	3-chlorophenyl	3-methoxyphenyl	3-chloro
15	5	3-chlorophenyl	3-methoxyphenyl	4-chloro
16	6	2-chlorophenyl	3-methoxyphenyl	2-chloro
17	6	2-chlorophenyl	3-methoxyphenyl	3-chloro
18	6	2-chlorophenyl	3-methoxyphenyl	4-chloro
19	7	4-chlorophenyl	2-methoxyphenyl	2-chloro
20	7	4-chlorophenyl	2-methoxyphenyl	3-chloro
21	7	4-chlorophenyl	2-methoxyphenyl	4-chloro
22	8	3-chlorophenyl	2-methoxyphenyl	2-chloro
23	8	3-chlorophenyl	2-methoxyphenyl	3-chloro
24	8	3-chlorophenyl	2-methoxyphenyl	4-chloro
25	9	2-chlorophenyl	2-methoxyphenyl	2-chloro
26	9	2-chlorophenyl	2-methoxyphenyl	3-chloro
27	9	2-chlorophenyl	2-methoxyphenyl	4-chloro
28	10	3-chlorophenyl	3,4-dimethoxyphenyl	2-chloro
29	11	3-chlorophenyl	2,4-dimethoxyphenyl	2-chloro
30	12	naphthalen-2-yl	<i>t</i> -Bu	4-chloro
31	13	[1,1'-biphenyl]-4-yl	<i>t</i> -Bu	4-chloro
32	14	4-chlorophenyl	<i>t</i> -Bu	4-chloro
33	15	3,4-dichlorophenyl	<i>t</i> -Bu	4-chloro
34	16	4-bromophenyl	<i>t</i> -Bu	4-bromo

## Results

35	14	4-chlorophenyl	<i>t</i> -Bu	4-bromo
36	17	4-chlorophenyl	2-ethoxyphenyl	4-chloro
37	18	4-bromophenyl	2-ethoxyphenyl	4-bromo
38	19	5-bromothiophen-2-yl	2-ethoxyphenyl	4-bromo
39	17	4-chlorophenyl	2-ethoxyphenyl	4-bromo
40	20	naphthalen-2-yl	2-ethoxyphenyl	4-chloro
41	21	[1,1'-biphenyl]-4-yl	2-ethoxyphenyl	4-chloro
42	22	3,4-dichlorophenyl	2-ethoxyphenyl	4-chloro
43	23	2,4-dichlorophenyl	2-ethoxyphenyl	4-chloro
44	24	4-fluorophenyl	2-ethoxyphenyl	4-chloro
45	14	4-chlorophenyl	<i>t</i> -Bu	4-chloro
46	17	4-chlorophenyl	2-ethoxyphenyl	4-chloro

### Biological Activity

To evaluate whether our new scaffolds are active in cells and in addition show indications of the desired mechanism of action, we screened all of the synthesized pyrazolines for their ability to inhibit the growth of HCT116 and H1299 cell lines at 20  $\mu$ M (higher concentrations could not be used to avoid solubility problems of some compounds). IC<sub>50</sub> values were determined in concentration-response studies for compounds which showed more than 50 % inhibition in the single dose screen. H1299 is a human non-small cell lung carcinoma cell line derived from the lymph node; which has a homozygous partial deletion of the *TP53* gene and as a result, does not express the p53 protein. On the other hand, HCT116 cells are human colorectal carcinoma cells with wild type p53 that are widely used to study the effect of small molecule Mdm2 antagonists.

Nutlin-3 was used as a positive control to benchmark the activity of the new derivatives. Mdm2 antagonists are expected to show greater potency to inhibit the growth of HCT116 cells compared to H1299 cells, as was observed for nutlin-3 (showing IC<sub>50</sub> values of 1.6  $\mu$ M vs. 14.7  $\mu$ M, respectively). The results are shown in Table 1.

### Structure activity relationship

Generally, active cell-growth inhibitors showed preferential inhibition of HCT116 cells containing wild type p53 in a behavior analogous to nutlin-3 (compounds **4**, **16**, **22**, **23**, **30**, **33**, **35** and **45**). Compounds **32** and **46** were the only exceptions and were found to display almost equivalent growth inhibition in both tumor cell lines.

In the first set of compounds (**1-27**), the activity was sharply dependent on the halogen substitution pattern at the 1- and 5-phenyls and several clear relationships between structure and cell-growth inhibition could be observed for the most favorable substitutions.

## Results

---

**Table 1\*. Inhibition of HCT116 and H1299 cell lines**

Compound #	IC <sub>50</sub> HCT116 (μM)	IC <sub>50</sub> H1299 (μM)
1	ND	ND
2	ND	ND
3	ND	ND
4	1.5	7.2
5	ND	ND
6	ND	ND
7	ND	ND
8	ND	ND
9	ND	ND
10	ND	ND
11	ND	ND
12	ND	ND
13	ND	ND
14	ND	ND
15	18.5	ND
16	2.5	13.6
17	ND	ND
18	ND	ND
19	ND	ND
20	ND	ND
21	ND	ND
22	1.9	13.4
23	1.6	11.7
24	ND	ND
25	ND	ND
26	ND	ND
27	ND	ND
28	ND	ND
29	ND	ND
30	12.7	ND
31	ND	ND
32	17.3	19.3
33	5.3	14.8
34	ND	ND
35	4.3	19.4
36	ND	ND
37	ND	ND
38	ND	ND
39	ND	ND
40	ND	ND
41	ND	ND
42	ND	ND
43	ND	ND
44	ND	ND
45	3.5	14.2
46	8.0	8.4
Nutlin 3	1.6	14.7

\*Values are mean values of at least two experiments; standard deviation <10%.

## Results

---

At the 1-phenyl moiety, a chlorine substituent in *ortho* position was a consistent feature in three of the most potent growth inhibitors (**4**, **16** and **22**). Compound **23** the *meta*-chloro analogue of **22** showed comparable activities. On the other hand, none of the *para*-chloro derivatives showed significant activity. Similar to the 1-phenyl, substitution with 4-chloro at the phenyl ring in position 5 did not lead to active compounds, while shifting the chlorine to *meta* position was optimal for the activity, as demonstrated by 3 of the most potent member of the 1<sup>st</sup> set bearing a *meta*-chloro substituent at their 5-phenyl moiety (**4**, **22**, **23**). Nevertheless, *ortho*-chloro at the 1-phenyl could still give potent compounds (**16**).

Concerning the methoxy substitution at the 3-phenyl, it was tolerated at all positions with high potency whether *ortho* (compounds **22** and **23**), *meta* (compound **16**) or *para* (**4**) indicating that this moiety does not significantly affect potency. However, in compound **4**, the most potent growth inhibitor against both cell lines, introducing a second methoxy either at *meta* or *ortho* positions was deleterious to the activity as exemplified by compounds **28** and **29**.

For the second set of compounds, the 3-*t*-butyl derivatives, four out of the six analogues showed growth inhibitory activity, indicating that *t*-Bu group could act as a possible replacement for the methoxyphenyl group in the first set of compounds. However, none of the compounds were more potent than the triphenylpyrazolines in the first set. Compound **32** with bis-1,5-(4-chlorophenyl) moieties showed marginal activity towards both tumor cell lines. Replacement of the 4-chlorophenyl at position 5 of the pyrazoline in compound **32** by a 2-naphthyl substituent (compound **30**) caused a slight improvement in activity towards HCT116 cells only, while the biphenyl moiety in compound **31** seemed too bulky to be tolerated.

On the other hand, adding another chlorine at position 3 of the 5-phenyl (**33**) or replacing the 4-Cl at the 1-phenyl by 4-Br (**35**) caused a 3-4 fold increase in the inhibitory activity towards HCT116 cell line with slight or no improvement in the activity towards H1299 cell line. Surprisingly, replacement of the two chlorine atoms in compound **32** by bromine atoms was inferior for activity (**34**).

Unexpectedly, adapting the 2-ethoxyphenyl at the 3 position of the pyrazoline abolished the activity (compounds **36-44**). This negative result might be due to the sterical requirements of the ethoxy group that are not provided by the potential receptor pocket. Interestingly, introducing morpholinocarbonyl at position 4 of compound **36** (compound **46**) recovered some the potency on both cell lines equally. This might be due to a direct interaction achieved by the introduced group, or its effect on the relative orientation and conformation of the other substituents arising from the pyrazoline core. In addition, the morpholinocarbonyl group is expected to have a profound effect in enhancing the hydrophilic characteristics, which might improve the performance of the compound in the assay conditions. Similarly, the 4<sup>th</sup> substitution with

## Results

---

morpholinocarbonyl group in compound **32** (compound **45**) has increased the selectivity, with an improved potency by more than **4** fold against HCT116 cell line.

In summary, the 1,3,5-trisubstituted and 1,3,4,5-tetrasubstituted pyrazoline scaffolds yielded potent inhibitors of the colorectal cancer line HCT116 in the low micro molar range, showing a good SAR with clear dependence on the halogen substitution pattern at the 1- and 5-phenyl rings as described herein. Many compounds showed a preferential inhibition pattern similar to nutlin-3 when comparing HCT116 and H1299 cell lines, proposing Mdm2 as a potential molecular target. Thus, we tested whether the compounds were able to displace a fluorescence-labeled peptide (derived from p53) in a concentration-dependent manner from its complex with Mdm2 or MdmX, respectively. Successful displacement leads to a substantial decrease in fluorescence anisotropy reported as a relative value (%FA) in comparison to lithocholic acid as a positive control leading to a complete displacement of the fluorescence-labeled peptide (0 %FA).

Protein expression and purification, as well as the setup of the FP assay were performed as described recently.<sup>14</sup> To facilitate measurements despite solubility issues of various compounds, we have been using 10% v/v DMSO for all experiments. Under these conditions compounds used as positive controls did not indicate deviations from standard conditions. For none of the compounds identified as hits in cell lines a reduction to at least 50% FA was found when titrating from 5 $\mu$ M up to concentrations of 1mM. Among the compounds with inhibitory potency in cell lines, **4**, **15**, **16**, **22**, **23**, and **46** showed intrinsic fluorescence possibly interfering with the assay. Still, only for **16** an irregular FP curve was retrieved showing increase of fluorescence instead of the expected decrease. Compounds **30**, **32**, **33**, **35**, and **45** showed no intrinsic fluorescence, but also no decrease beyond 70% relative fluorescence anisotropy for both Mdm2 and MdmX. Of course, all these results can be biased by solubility issues of the compounds under the used assay conditions. However, clearly none of the compounds showed binding to Mdm2 or MdmX similar to the positive controls. Thus, it remains unclear through which mode of action the encouraging results in the cell lines can be explained. These results suggest that substantial modifications to improve polarity and solubility characteristics should be useful to elucidate our findings and might lead to new p53-Mdm2 antagonists.

## EXPERIMENTAL SECTION

### Chemistry

Solvents and reagents were obtained from commercial suppliers and used as received. A Bruker DRX 500 spectrometer was used to obtain <sup>1</sup>H NMR and <sup>13</sup>C NMR spectra. The chemical shifts are referenced to the residual protonated solvent signals or TMS was used as a reference. At least

## Results

---

95% purity in all the tested compounds (table 1) was obtained by means of HPLC coupled with mass spectrometry. Mass spectra (HPLC-ESI-MS) were obtained using a TSQ quantum (Thermo Electron Corporation) instrument prepared with a triple quadrupole mass detector (Thermo Finnigan) and an ESI source. All samples were inserted using an autosampler (Surveyor, Thermo Finnigan) by an injection volume of 10  $\mu$ L. The MS detection was determined using a source CID of 10 V and carried out at a spray voltage of 4.2 kV, a nitrogen sheath gas pressure of  $4.0 \times 10^5$  Pa, a capillary temperature of 400  $^{\circ}$ C, a capillary voltage of 35 V and an auxiliary gas pressure of  $1.0 \times 10^5$  Pa. The stationary phase used was an RP C18 NUCLEODUR 100-3 (125 X 3 mm) column (Macherey-Nagel). The solvent system consisted of water containing 0.1% TFA (A) and 0.1% TFA in acetonitrile (B). HPLC-Method: flow rate 400  $\mu$ L/min. The percentage of B started at an initial of 5%, was increased up to 100% during 16 min, kept at 100% for 2 min, and flushed back to 5% in 2 min. Melting points were determined using a Mettler FP1 melting point apparatus and are uncorrected.

### General procedure for enone synthesis.

To an ice-cooled solution of the appropriate ketone (10 mmol) in MeOH (50 mL), 10 % KOH aq. solution (30 ml) was added, followed by gradual addition of the corresponding aryl aldehyde (10 mmol). The mixture was left to attain room temperature and stirred overnight. The solid product was filtered and washed three times with MeOH/H<sub>2</sub>O mixture (5:3) and left to dry. In case of oily products the reaction mixture was extracted by CH<sub>2</sub>Cl<sub>2</sub> (4 x 20 mL) and the combined organic layers were washed with water, filtered over anhydrous MgSO<sub>4</sub>, evaporated under reduced pressure and used without further purification.

**(E)-3-(4-chlorophenyl)-1-(4-methoxyphenyl)prop-2-en-1-one (C1)**. Synthesized according to the general procedure for enone synthesis using 1-(4-methoxyphenyl) ethanone and 4-chlorobenzaldehyde; yellow solid; yield: 2.61 g (96 %); mp 125-126  $^{\circ}$ C.<sup>15</sup>

**(E)-3-(3-chlorophenyl)-1-(4-methoxyphenyl)prop-2-en-1-one (C2)**. Synthesized according to the general procedure for enone synthesis using 1-(4-methoxyphenyl) ethanone and 3-chlorobenzaldehyde; yellow solid; yield: 2.32 g (85 %); mp 97-99  $^{\circ}$ C.<sup>16</sup>

**(E)-3-(2-chlorophenyl)-1-(4-methoxyphenyl)prop-2-en-1-one (C3)**. Synthesized according to the general procedure for enone synthesis using 1-(4-methoxyphenyl)ethanone and 2-chlorobenzaldehyde; yellow solid; yield: 2.48 g (91 %); mp 79-80  $^{\circ}$ C.<sup>17</sup>

**(E)-3-(4-chlorophenyl)-1-(3-methoxyphenyl)prop-2-en-1-one (C4)**. Synthesized according to the general procedure for enone synthesis using 1-(3-methoxyphenyl)ethanone and 4-chlorobenzaldehyde; yellow oil; yield: 2.21 g (81 %).<sup>18</sup>

## Results

---

**(E)-3-(3-chlorophenyl)-1-(3-methoxyphenyl)prop-2-en-1-one (C5).** Synthesized according to the general procedure for enone synthesis using 1-(3-methoxyphenyl)ethanone and 3-chlorobenzaldehyde; yellow oil; yield: 2.4 g (88 %).<sup>19</sup>

**(E)-3-(2-chlorophenyl)-1-(3-methoxyphenyl)prop-2-en-1-one (C6).** Synthesized according to the general procedure for enone synthesis using 1-(3-methoxyphenyl)ethanone and 2-chlorobenzaldehyde; yellow solid; yield: 2.56 g (94 %); mp 117-117 °C.<sup>20</sup>

**(E)-3-(4-chlorophenyl)-1-(2-methoxyphenyl)prop-2-en-1-one (C7).** Synthesized according to the general procedure for enone synthesis using 1-(2-methoxyphenyl)ethanone and 4-chlorobenzaldehyde; yellow oil; yield: 2.51 g (92 %).<sup>21</sup>

**(E)-3-(3-chlorophenyl)-1-(2-methoxyphenyl)prop-2-en-1-one (C8).** Synthesized according to the general procedure for enone synthesis using 1-(2-methoxyphenyl)ethanone and 3-chlorobenzaldehyde; yellow solid; yield: 2.37 g (87 %); mp 96-98 °C; <sup>1</sup>H NMR (500 MHz, CDCl<sub>3</sub>) δ 7.48 (dd, *J* = 7.6, 1.8 Hz, 1H), 7.40 (dd, *J* = 8.8, 6.9 Hz, 2H), 7.33 (ddd, *J* = 8.4, 7.4, 1.8 Hz, 1H), 7.30 (dt, *J* = 7.1, 1.6 Hz, 1H), 7.25 – 7.16 (m, 3H), 6.90 – 6.87 (m, 1H), 6.85 (d, *J* = 15.8 Hz, 1H), 3.76 (s, 3H); <sup>13</sup>C NMR (125 MHz, CDCl<sub>3</sub>) δ 192.41, 158.24, 141.15, 137.08, 134.86, 133.16, 130.45, 130.08, 129.98, 129.01, 128.25, 127.93, 126.60, 120.82, 111.67, 55.79.

**(E)-3-(2-chlorophenyl)-1-(2-methoxyphenyl)prop-2-en-1-one (C9).** Synthesized according to the general procedure for enone synthesis using 1-(2-methoxyphenyl)ethanone and 2-chlorobenzaldehyde; yellow solid; yield: 2.29 g (84 %); mp 60-62 °C.<sup>22</sup>

**(E)-3-(3-chlorophenyl)-1-(3,4-dimethoxyphenyl)prop-2-en-1-one (C10).** Synthesized according to the general procedure for enone synthesis using 1-(3,4-dimethoxyphenyl)ethanone and 3-chlorobenzaldehyde; yellow solid; yield: 2.75 g (91 %); mp 110-111 °C; <sup>1</sup>H NMR (500 MHz, CDCl<sub>3</sub>) δ 7.60 (d, *J* = 15.6 Hz, 1H), 7.58 – 7.53 (m, 1H), 7.53 – 7.49 (m, 2H), 7.42 (d, *J* = 15.6 Hz, 1H), 7.37 (ddd, *J* = 6.4, 2.3, 1.5 Hz, 1H), 7.27 – 7.20 (m, 2H), 6.83 – 6.78 (m, 1H), 3.85 (d, *J* = 0.8 Hz, 6H); <sup>13</sup>C NMR (125 MHz, CDCl<sub>3</sub>) δ 188.12, 153.50, 149.36, 142.17, 136.95, 134.93, 131.06, 130.15, 130.11, 127.77, 126.73, 123.13, 122.91, 110.80, 110.01, 56.10, 56.06.

**(E)-3-(3-chlorophenyl)-1-(2,4-dimethoxyphenyl)prop-2-en-1-one (C11).** Synthesized according to the general procedure for enone synthesis using 1-(2,4-dimethoxyphenyl)ethanone and 3-chlorobenzaldehyde; yellow oil; yield: 2.66 g (88 %).<sup>23</sup>

**(E)-4,4-dimethyl-1-(naphthalen-2-yl)pent-1-en-3-one (C12).** Synthesized according to the general procedure for enone synthesis using pinacolone and 2-naphthaldehyde; yellow solid; yield: 2.24 g (94 %); mp 117-119 °C.<sup>24</sup>

## Results

---

**(E)-1-([1,1'-biphenyl]-4-yl)-4,4-dimethylpent-1-en-3-one (C13).** Synthesized according to the general procedure for enone synthesis using pinacolone and [1,1'-biphenyl]-4-carbaldehyde; yellow solid; yield: 2.3 g (87 %); mp 128-130 °C.<sup>25</sup>

**(E)-1-(4-chlorophenyl)-4,4-dimethylpent-1-en-3-one (C14).** Synthesized according to the general procedure for enone synthesis pinacolone and 4-chlorobenzaldehyde; white solid; yield: 2.11 g (95 %); mp 85-87 °C.<sup>26</sup>

**(E)-1-(3,4-dichlorophenyl)-4,4-dimethylpent-1-en-3-one (C15).** Synthesized according to the general procedure for enone synthesis using pinacolone and 3,4-dichlorobenzaldehyde; yellow solid; yield: 2.08 g (81 %); mp 94-96°C.<sup>27</sup>

**(E)-1-(4-bromophenyl)-4,4-dimethylpent-1-en-3-one (C16).** Synthesized according to the general procedure for enone synthesis using pinacolone and 4-bromobenzaldehyde; yellow solid; yield: 2.48 g (93 %); mp 102-103 °C.<sup>26</sup>

**(E)-3-(4-chlorophenyl)-1-(2-ethoxyphenyl)prop-2-en-1-one (C17).** Synthesized according to the general procedure for enone synthesis using 1-(2-ethoxyphenyl)ethanone and 4-chlorobenzaldehyde; yellow oil; yield: 2.32 g (81 %); <sup>1</sup>H NMR (500 MHz, CDCl<sub>3</sub>) δ 7.54 (dd, *J* = 7.6, 1.8 Hz, 1H), 7.45 (d, *J* = 15.9 Hz, 1H), 7.40 – 7.36 (m, 2H), 7.36 – 7.30 (m, 2H), 7.26 – 7.20 (m, 2H), 6.90 (td, *J* = 7.5, 0.9 Hz, 1H), 6.83 (dd, *J* = 11.9, 4.4 Hz, 1H), 4.00 (q, *J* = 7.0 Hz, 2H), 1.29 (t, *J* = 7.0 Hz, 3H); <sup>13</sup>C NMR (125 MHz, CDCl<sub>3</sub>) δ 192.33, 157.76, 140.79, 135.91, 133.83, 133.18, 130.63, 129.35, 129.14, 127.71, 120.77, 116.32, 112.62, 64.25, 14.84.

**(E)-3-(4-bromophenyl)-1-(2-ethoxyphenyl)prop-2-en-1-one (C18).** Synthesized according to the general procedure for enone synthesis using 1-(2-ethoxyphenyl)ethanone and 4-bromobenzaldehyde; yellow oil; yield: 2.84 g (86 %); <sup>1</sup>H NMR (500 MHz, CDCl<sub>3</sub>) δ 7.73 – 7.68 (m, 1H), 7.60 (d, *J* = 15.9 Hz, 1H), 7.57 – 7.53 (m, 3H), 7.51 – 7.45 (m, 3H), 7.06 (td, *J* = 7.5, 0.8 Hz, 1H), 6.99 (dd, *J* = 12.8, 6.3 Hz, 1H), 4.17 (q, *J* = 7.0 Hz, 2H), 1.45 (t, *J* = 7.0 Hz, 3H); <sup>13</sup>C NMR (125 MHz, CDCl<sub>3</sub>) δ 192.29, 157.77, 140.80, 134.25, 133.20, 132.09, 130.63, 129.57, 129.09, 127.79, 124.22, 120.76, 112.60, 64.23, 14.83.

**(E)-3-(5-bromothiophen-2-yl)-1-(2-ethoxyphenyl)prop-2-en-1-one (C19).** Synthesized according to the general procedure for enone synthesis using 1-(2-ethoxyphenyl)ethanone and 5-bromothiophene-2-carbaldehyde; yellow oil; yield: 3 g (89 %); <sup>1</sup>H NMR (500 MHz, CDCl<sub>3</sub>) δ 7.91 (dt, *J* = 4.2, 2.1 Hz, 1H), 7.87 (d, *J* = 15.4 Hz, 1H), 7.70 – 7.64 (m, 1H), 7.51 – 7.47 (m, 1H), 7.26 – 7.21 (m, 3H), 7.19 – 7.16 (m, 1H), 4.38 – 4.32 (m, 2H), 1.69 (t, *J* = 7.0 Hz, 3H); <sup>13</sup>C

## Results

---

NMR (125 MHz, CDCl<sub>3</sub>)  $\delta$  191.28, 157.94, 142.56, 133.71, 133.35, 131.62, 131.20, 130.79, 128.78, 126.56, 120.75, 115.53, 112.54, 64.25, 14.89.

**(E)-1-(2-ethoxyphenyl)-3-(naphthalen-2-yl)prop-2-en-1-one (C20).** Synthesized according to the general procedure for enone synthesis using 1-(2-ethoxyphenyl)ethanone and 2-naphthaldehyde; yellow solid; yield: 2.74 g (91 %); mp 89-91 °C.<sup>28</sup>

**(E)-3-([1,1'-biphenyl]-4-yl)-1-(2-ethoxyphenyl)prop-2-en-1-one (C21).** Synthesized according to the general procedure for enone synthesis using 1-(2-ethoxyphenyl)ethanone and [1,1'-biphenyl]-4-carbaldehyde; yellow solid; yield: 3.08 g (94 %); mp 98-99 °C; <sup>1</sup>H NMR (500 MHz, CDCl<sub>3</sub>)  $\delta$  7.48 – 7.45 (m, 3H), 7.44 (d, *J* = 2.4 Hz, 2H), 7.43 – 7.39 (m, 4H), 7.31 (d, *J* = 15.9 Hz, 1H), 7.27 – 7.21 (m, 2H), 7.15 (ddt, *J* = 5.1, 3.9, 1.9 Hz, 1H), 6.82 (td, *J* = 7.5, 0.9 Hz, 1H), 6.77 (d, *J* = 8.3 Hz, 1H), 3.94 (q, *J* = 7.0 Hz, 2H), 1.23 (t, *J* = 7.0 Hz, 3H); <sup>13</sup>C NMR (125 MHz, CDCl<sub>3</sub>)  $\delta$  192.69, 157.71, 142.86, 142.08, 140.23, 134.27, 132.97, 130.58, 129.43, 128.87, 128.77, 127.78, 127.52, 127.14, 127.01, 120.74, 112.65, 64.29, 14.87.

**(E)-3-(3,4-dichlorophenyl)-1-(2-ethoxyphenyl)prop-2-en-1-one (C22).** Synthesized according to the general procedure for enone synthesis using 1-(2-ethoxyphenyl)ethanone and 3,4-dichlorobenzaldehyde; yellow solid; yield: 2.53 g (79 %); mp 80-82 °C; <sup>1</sup>H NMR (500 MHz, CDCl<sub>3</sub>)  $\delta$  7.47 (dd, *J* = 7.7, 1.8 Hz, 1H), 7.44 (d, *J* = 2.0 Hz, 1H), 7.30 – 7.26 (m, 2H), 7.26 – 7.23 (m, 2H), 7.20 – 7.16 (m, 1H), 6.81 (ddd, *J* = 4.9, 3.3, 1.0 Hz, 1H), 6.78 – 6.75 (m, 1H), 3.93 (q, *J* = 7.0 Hz, 2H), 1.22 (t, *J* = 7.0 Hz, 3H); <sup>13</sup>C NMR (125 MHz, CDCl<sub>3</sub>)  $\delta$  191.87, 157.90, 139.16, 135.49, 133.83, 133.47, 133.19, 130.86, 130.74, 130.34, 129.63, 128.82, 127.20, 120.83, 112.61, 64.27, 14.85.

**(E)-3-(2,4-dichlorophenyl)-1-(2-ethoxyphenyl)prop-2-en-1-one (C23).** Synthesized according to the general procedure for enone synthesis using 1-(2-ethoxyphenyl)ethanone and 2,4-dichlorobenzaldehyde; yellow solid; yield: 2.79 g (87 %); mp 75-77 °C; <sup>1</sup>H NMR (500 MHz, CDCl<sub>3</sub>)  $\delta$  7.72 (d, *J* = 15.9 Hz, 1H), 7.45 (dt, *J* = 8.5, 4.3 Hz, 1H), 7.42 – 7.37 (m, 1H), 7.27 – 7.20 (m, 3H), 7.04 (dd, *J* = 8.3, 1.5 Hz, 1H), 6.84 – 6.78 (m, 1H), 6.74 (t, *J* = 9.5 Hz, 1H), 3.94 – 3.88 (m, 2H), 1.19 (t, *J* = 7.0 Hz, 3H); <sup>13</sup>C NMR (125 MHz, CDCl<sub>3</sub>)  $\delta$  192.12, 157.80, 136.75, 135.98, 135.90, 133.36, 132.21, 130.74, 130.04, 129.88, 128.88, 128.22, 127.47, 120.82, 112.57, 64.25, 14.84.

**(E)-1-(2-ethoxyphenyl)-3-(4-fluorophenyl)prop-2-en-1-one (C24).** Synthesized according to the general procedure for enone synthesis using 1-(2-ethoxyphenyl)ethanone and 4-fluorobenzaldehyde; yellow oil; yield: 2.51 g (93%); <sup>1</sup>H NMR (500 MHz, CDCl<sub>3</sub>)  $\delta$  7.82 (dt, *J* = 5.8, 2.9 Hz, 1H), 7.78 – 7.69 (m, 3H), 7.63 – 7.59 (m, 1H), 7.57 (d, *J* = 15.5 Hz, 1H), 7.27 – 7.21

## Results

---

(m, 2H), 7.21 – 7.16 (m, 1H), 7.14 (dd,  $J = 5.8, 2.5$  Hz, 1H), 4.29 (dd,  $J = 9.2, 4.8$  Hz, 2H), 1.58 (t,  $J = 7.0$  Hz, 3H).

### General procedure for pyrazoline synthesis.

A mixture of the enone derivative (2 mmol) and the corresponding phenylhydrazine hydrochloride (3 mmol) in 15 mL of anhydrous DMF was heated to 85 °C for 5 hours under argon atmosphere. The reaction solution was cooled to room temperature and partitioned between 50 mL of diethyl ether and 20 mL of water. The organic layer was separated and washed with three 20 mL-portions of water. The aqueous layers were combined and extracted with three 20 mL-portions of diethyl ether. The organic layers were combined, dried over anhydrous Na<sub>2</sub>SO<sub>4</sub> and concentrated in *vacuo*. The residue was purified using column chromatography or used in the next step without further purification.

### 1-(2-chlorophenyl)-5-(4-chlorophenyl)-3-(4-methoxyphenyl)-4,5-dihydro-1H-pyrazole (1).

The title compound was prepared by reaction of (*E*)-3-(4-chlorophenyl)-1-(4-methoxyphenyl)prop-2-en-1-one (**C1**) and 2-chlorophenylhydrazine hydrochloride according to the general procedure for pyrazoline synthesis; light brown solid; yield: 0.35 g (45%); mp 162–163 °C; <sup>1</sup>H NMR (500 MHz, CDCl<sub>3</sub>) δ 7.73 – 7.68 (m, 2H), 7.40 (dd,  $J = 12.5, 6.9$  Hz, 1H), 7.19 (dt,  $J = 9.4, 4.7$  Hz, 1H), 7.12 – 7.05 (m, 5H), 6.97 – 6.92 (m, 2H), 6.88 – 6.83 (m, 1H), 5.79 (dd,  $J = 11.3, 4.6$  Hz, 1H), 3.85 (s, 3H), 3.75 (dt,  $J = 28.6, 14.3$  Hz, 1H), 3.32 (dd,  $J = 16.8, 4.6$  Hz, 1H); <sup>13</sup>C NMR (125 MHz, CDCl<sub>3</sub>) δ 149.96, 142.94, 139.56, 133.39, 131.12, 130.22, 128.62, 128.14, 127.54, 127.09, 125.18, 124.59, 124.06, 123.54, 114.11, 65.51, 55.38, 42.64; MS (ESI):  $m/z = 397.05$  (M+H)<sup>+</sup>.

### 1-(3-chlorophenyl)-5-(4-chlorophenyl)-3-(4-methoxyphenyl)-4,5-dihydro-1H-pyrazole (2).

The title compound was prepared by reaction of (*E*)-3-(4-chlorophenyl)-1-(4-methoxyphenyl)prop-2-en-1-one (**C1**) and 3-chlorophenylhydrazine hydrochloride according to the general procedure for pyrazoline synthesis; brown solid; yield: 0.28 g (36%); mp 121–122 °C; <sup>1</sup>H NMR (500 MHz, CDCl<sub>3</sub>) δ 7.67 – 7.62 (m, 2H), 7.32 – 7.28 (m, 2H), 7.24 – 7.19 (m, 2H), 7.15 (t,  $J = 2.1$  Hz, 1H), 7.04 (t,  $J = 8.1$  Hz, 1H), 6.93 – 6.89 (m, 2H), 6.72 (dddd,  $J = 8.2, 4.6, 2.1, 0.8$  Hz, 2H), 5.17 (dd,  $J = 12.2, 6.7$  Hz, 1H), 3.85 – 3.76 (m, 4H), 3.07 (dd,  $J = 17.0, 6.7$  Hz, 1H); <sup>13</sup>C NMR (125 MHz, CDCl<sub>3</sub>) δ 160.50, 147.71, 145.82, 140.62, 134.82, 133.50, 129.88, 129.43, 127.43, 127.25, 124.90, 118.78, 114.11, 113.39, 110.99, 63.53, 55.36, 43.78; MS (ESI):  $m/z = 397.02$  (M+H)<sup>+</sup>.

**1,5-bis(4-chlorophenyl)-3-(4-methoxyphenyl)-4,5-dihydro-1H-pyrazole (3).** The title compound was prepared by reaction of (*E*)-3-(4-chlorophenyl)-1-(4-methoxyphenyl)prop-2-en-1-one (**C1**) and 4-chlorophenylhydrazine hydrochloride according to the general procedure for

## Results

---

pyrazoline synthesis; beige solid; yield: 0.4 g (51%); mp 111-112 °C; <sup>1</sup>H NMR (500 MHz, CDCl<sub>3</sub>) δ 7.67 – 7.60 (m, 2H), 7.30 – 7.26 (m, 2H), 7.20 (dd, *J* = 11.0, 7.2 Hz, 2H), 7.13 – 7.07 (m, 2H), 6.94 – 6.87 (m, 4H), 5.15 (dd, *J* = 12.1, 7.1 Hz, 1H), 3.84 – 3.75 (m, 4H), 3.07 (dd, *J* = 17.0, 7.1 Hz, 1H); <sup>13</sup>C NMR (125 MHz, CDCl<sub>3</sub>) δ 160.67, 147.63, 143.74, 140.95, 133.74, 130.22, 129.06, 127.58, 127.56, 125.27, 124.09, 114.64, 114.35, 64.09, 55.61, 44.08; MS (ESI): *m/z* = 397.01 (M+H)<sup>+</sup>.

### **1-(2-chlorophenyl)-5-(3-chlorophenyl)-3-(4-methoxyphenyl)-4,5-dihydro-1H-pyrazole (4).**

The title compound was prepared by reaction of (*E*)-3-(3-chlorophenyl)-1-(4-methoxyphenyl)prop-2-en-1-one (**C2**) and 2-chlorophenylhydrazine hydrochloride according to the general procedure for pyrazoline synthesis; yellow solid; yield: 0.37 g (47%); mp 130-131 °C; <sup>1</sup>H NMR (500 MHz, CDCl<sub>3</sub>) δ 7.73 – 7.65 (m, 2H), 7.41 (dt, *J* = 6.4, 3.2 Hz, 1H), 7.20 (dd, *J* = 8.0, 1.4 Hz, 1H), 7.16 (dd, *J* = 2.6, 1.4 Hz, 1H), 7.12 – 7.01 (m, 4H), 6.96 – 6.90 (m, 2H), 6.85 (ddd, *J* = 7.9, 7.5, 1.6 Hz, 1H), 5.76 (dd, *J* = 11.3, 4.8 Hz, 1H), 3.84 (s, 3H), 3.76 (dd, *J* = 16.8, 11.3 Hz, 1H), 3.32 (dd, *J* = 16.8, 4.8 Hz, 1H); <sup>13</sup>C NMR (125 MHz, CDCl<sub>3</sub>) δ 160.77, 150.19, 143.33, 143.14, 134.48, 130.02, 128.11, 127.82, 127.33, 127.14, 125.38, 125.14, 124.97, 124.36, 123.80, 114.41, 114.36, 65.94, 55.63, 42.93; MS (ESI): *m/z* = 397.06 (M+H)<sup>+</sup>.

### **1,5-bis(3-chlorophenyl)-3-(4-methoxyphenyl)-4,5-dihydro-1H-pyrazole (5).**

The title compound was prepared by reaction of (*E*)-3-(3-chlorophenyl)-1-(4-methoxyphenyl)prop-2-en-1-one (**C2**) and 3-chlorophenylhydrazine hydrochloride according to the general procedure for pyrazoline synthesis; brown solid; yield: 0.43 g (55%); mp 146-147 °C; <sup>1</sup>H NMR (500 MHz, CDCl<sub>3</sub>) δ 7.66 – 7.60 (m, 2H), 7.30 – 7.26 (m, 1H), 7.26 – 7.21 (m, 2H), 7.18 – 7.12 (m, 2H), 7.03 (t, *J* = 8.1 Hz, 1H), 6.93 – 6.86 (m, 2H), 6.71 (tdd, *J* = 8.6, 2.1, 0.8 Hz, 2H), 5.14 (dd, *J* = 12.2, 6.8 Hz, 1H), 3.85 – 3.79 (m, 4H), 3.08 (dd, *J* = 17.1, 6.8 Hz, 1H); <sup>13</sup>C NMR (125 MHz, CDCl<sub>3</sub>) δ 160.52, 147.71, 145.84, 144.28, 135.12, 134.84, 130.58, 129.90, 128.03, 127.45, 125.97, 124.85, 123.95, 118.85, 114.10, 113.41, 110.95, 63.67, 55.36, 43.78; MS (ESI): *m/z* = 397.05 (M+H)<sup>+</sup>.

### **5-(3-chlorophenyl)-1-(4-chlorophenyl)-3-(4-methoxyphenyl)-4,5-dihydro-1H-pyrazole (6).**

The title compound was prepared by reaction of (*E*)-3-(3-chlorophenyl)-1-(4-methoxyphenyl)prop-2-en-1-one (**C2**) and 4-chlorophenylhydrazine hydrochloride according to the general procedure for pyrazoline synthesis; brown solid; yield: 0.31 g (39%); mp 106-108 °C; <sup>1</sup>H NMR (500 MHz, CDCl<sub>3</sub>) δ, 7.68 – 7.61 (m, 2H), 7.35 – 7.29 (m, 2H), 7.27 – 7.24 (m, 1H), 7.17 (dt, *J* = 6.8, 1.9 Hz, 1H), 7.14 – 7.09 (m, 2H), 6.95 – 6.93 (m, 1H), 6.92 (q, *J* = 2.1 Hz, 2H), 6.91 – 6.90 (m, 1H), 5.14 (dd, *J* = 12.2, 7.2 Hz, 1H), 3.85 – 3.78 (m, 4H), 3.10 (dd, *J* = 17.1, 7.2 Hz, 1H); <sup>13</sup>C NMR (125 MHz, CDCl<sub>3</sub>) δ 160.44, 147.39, 144.38, 143.50, 135.10, 130.58, 129.28, 128.84, 128.00, 127.36, 126.06, 124.01, 123.89, 114.38, 114.11, 63.96, 55.37, 43.83; MS (ESI): *m/z* = 396.99 (M+H)<sup>+</sup>.

## Results

**1,5-bis(2-chlorophenyl)-3-(4-methoxyphenyl)-4,5-dihydro-1H-pyrazole (7).** The title compound was prepared by reaction of (*E*)-3-(2-chlorophenyl)-1-(4-methoxyphenyl)prop-2-en-1-one (**C3**) and 2-chlorophenylhydrazine hydrochloride according to the general procedure for pyrazoline synthesis; yellowish white solid; yield: 0.5 g (63%); mp 142-143 °C; <sup>1</sup>H NMR (500 MHz, CDCl<sub>3</sub>) δ 7.72 – 7.65 (m, 2H), 7.44 (dd, *J* = 8.2, 1.5 Hz, 1H), 7.32 (ddd, *J* = 6.9, 4.9, 1.9 Hz, 2H), 7.27 – 7.24 (m, 1H), 7.12 (dtdd, *J* = 14.7, 8.8, 7.4, 1.4 Hz, 3H), 6.93 – 6.86 (m, 3H), 6.15 (dd, *J* = 11.3, 6.4 Hz, 1H), 3.86 – 3.81 (m, 4H), 3.09 (dd, *J* = 16.6, 6.4 Hz, 1H); <sup>13</sup>C NMR (125 MHz, CDCl<sub>3</sub>) δ 160.49, 149.65, 142.87, 139.05, 132.08, 130.96, 129.66, 128.54, 127.91, 127.59, 127.10, 127.06, 125.19, 124.49, 123.40, 121.59, 114.04, 63.01, 55.36, 42.02; MS (ESI): *m/z* = 397.07 (M+H)<sup>+</sup>.

**5-(2-chlorophenyl)-1-(3-chlorophenyl)-3-(4-methoxyphenyl)-4,5-dihydro-1H-pyrazole (8).** The title compound was prepared by reaction of (*E*)-3-(2-chlorophenyl)-1-(4-methoxyphenyl)prop-2-en-1-one (**C3**) and 3-chlorophenylhydrazine hydrochloride according to the general procedure for pyrazoline synthesis; beige solid; yield: 0.23 g (29%); mp 148-149 °C; <sup>1</sup>H NMR (500 MHz, CDCl<sub>3</sub>) δ 7.76 – 7.71 (m, 2H), 7.51 (dddd, *J* = 6.9, 6.5, 1.2, 0.5 Hz, 1H), 7.31 – 7.20 (m, 4H), 7.11 (dt, *J* = 5.5, 4.8 Hz, 1H), 7.01 – 6.95 (m, 2H), 6.82 – 6.77 (m, 1H), 6.71 (ddd, *J* = 8.3, 2.2, 0.9 Hz, 1H), 5.65 (dd, *J* = 12.2, 6.4 Hz, 1H), 4.01 (dd, *J* = 17.2, 12.2 Hz, 1H), 3.89 (s, 3H), 3.11 (dd, *J* = 17.2, 6.4 Hz, 1H); <sup>13</sup>C NMR (125 MHz, CDCl<sub>3</sub>) δ 160.49, 148.10, 145.63, 138.76, 134.90, 131.79, 129.96, 129.94, 128.92, 127.66, 127.45, 127.18, 124.98, 118.68, 114.07, 113.23, 110.71, 60.96, 55.35, 42.28; MS (ESI): *m/z* = 397.07 (M+H)<sup>+</sup>.

**5-(2-chlorophenyl)-1-(4-chlorophenyl)-3-(4-methoxyphenyl)-4,5-dihydro-1H-pyrazole (9).** The title compound was prepared by reaction of (*E*)-3-(2-chlorophenyl)-1-(4-methoxyphenyl)prop-2-en-1-one (**C3**) and 4-chlorophenylhydrazine hydrochloride according to the general procedure for pyrazoline synthesis; yellow solid; yield: 0.35 g (44%); mp 149-151 °C; <sup>1</sup>H NMR (500 MHz, CDCl<sub>3</sub>) δ 7.67 – 7.63 (m, 1H), 7.45 – 7.43 (m, 1H), 7.28 – 7.24 (m, 2H), 7.23 – 7.16 (m, 2H), 7.15 – 7.10 (m, 2H), 7.01 – 6.96 (m, 1H), 6.93 – 6.86 (m, 3H), 5.57 (dd, *J* = 12.2, 6.7 Hz, 1H), 3.95 (dd, *J* = 17.1, 12.2 Hz, 1H), 3.83 (s, 3H), 3.03 (dd, *J* = 17.2, 6.7 Hz, 1H); MS (ESI): *m/z* = 397 (M+H)<sup>+</sup>.

**1-(2-chlorophenyl)-5-(4-chlorophenyl)-3-(3-methoxyphenyl)-4,5-dihydro-1H-pyrazole (10).** The title compound was prepared by reaction of (*E*)-3-(4-chlorophenyl)-1-(3-methoxyphenyl)prop-2-en-1-one (**C4**) and 2-chlorophenylhydrazine hydrochloride according to the general procedure for pyrazoline synthesis; brown solid; yield: 0.24 g (30%); mp 112-113 °C; <sup>1</sup>H NMR (500 MHz, CDCl<sub>3</sub>) δ 7.43 (dd, *J* = 8.1, 1.5 Hz, 1H), 7.39 (dd, *J* = 2.5, 1.5 Hz, 1H), 7.36 – 7.31 (m, 1H), 7.30 (dt, *J* = 7.6, 1.3 Hz, 1H), 7.21 (dd, *J* = 8.0, 1.4 Hz, 1H), 7.15 – 7.07 (m, 5H), 6.94 (ddd, *J* = 8.0, 2.6, 1.2 Hz, 1H), 6.89 (ddd, *J* = 7.9, 7.4, 1.6 Hz, 1H), 5.85 (dd, *J* = 11.5, 4.7 Hz, 1H), 3.87 (s, 3H), 3.79 (dd, *J* = 16.9, 11.5 Hz, 1H), 3.36 (dd, *J* = 16.9, 4.7 Hz, 1H); <sup>13</sup>C

## Results

---

NMR (125 MHz, CDCl<sub>3</sub>)  $\delta$  159.78, 149.77, 142.52, 139.37, 133.74, 133.46, 130.22, 129.63, 128.64, 128.10, 127.09, 124.66, 124.31, 123.74, 118.69, 115.23, 110.73, 65.62, 55.34, 42.45.; MS (ESI):  $m/z$  = 397.05 (M+H)<sup>+</sup>.

### **1-(3-chlorophenyl)-5-(4-chlorophenyl)-3-(3-methoxyphenyl)-4,5-dihydro-1H-pyrazole (11).**

The title compound was prepared by reaction of (*E*)-3-(4-chlorophenyl)-1-(3-methoxyphenyl)prop-2-en-1-one (**C4**) and 3-chlorophenylhydrazine hydrochloride according to the general procedure for pyrazoline synthesis; brown solid; yield: 0.46 g (58%); mp 91.6-93 °C; <sup>1</sup>H NMR (500 MHz, CDCl<sub>3</sub>)  $\delta$  7.27 – 7.22 (m, 4H), 7.17 (ddt, *J* = 9.0, 4.4, 3.2 Hz, 3H), 7.12 (t, *J* = 2.1 Hz, 1H), 6.99 (t, *J* = 8.1 Hz, 1H), 6.87 – 6.83 (m, 1H), 6.69 (dddd, *J* = 8.0, 5.9, 2.1, 0.9 Hz, 2H), 5.16 (dd, *J* = 12.3, 6.7 Hz, 1H), 3.81 (s, 3H), 3.77 (dd, *J* = 17.1, 12.3 Hz, 1H), 3.03 (dd, *J* = 17.1, 6.7 Hz, 1H); <sup>13</sup>C NMR (125 MHz, CDCl<sub>3</sub>)  $\delta$  160.00, 147.84, 145.65, 140.62, 135.08, 133.82, 133.71, 130.15, 129.88, 129.70, 127.43, 119.37, 118.83, 115.38, 113.76, 111.37, 111.03, 63.79, 55.60, 43.84; MS (ESI):  $m/z$  = 397.06 (M+H)<sup>+</sup>.

### **1,5-bis(4-chlorophenyl)-3-(3-methoxyphenyl)-4,5-dihydro-1H-pyrazole (12).**

The title compound was prepared by reaction of (*E*)-3-(4-chlorophenyl)-1-(3-methoxyphenyl)prop-2-en-1-one (**C4**) and 4-chlorophenylhydrazine hydrochloride according to the general procedure for pyrazoline synthesis; light brown solid; yield: 0.29 g (37%); 156-158 °C; <sup>1</sup>H NMR (500 MHz, CDCl<sub>3</sub>)  $\delta$  7.34 – 7.28 (m, 4H), 7.26 – 7.19 (m, 3H), 7.16 – 7.10 (m, 2H), 6.98 – 6.94 (m, 2H), 6.91 (ddd, *J* = 8.2, 2.6, 1.0 Hz, 1H), 5.22 (dd, *J* = 12.3, 7.0 Hz, 1H), 3.89 – 3.80 (m, 4H), 3.11 (dd, *J* = 17.1, 7.0 Hz, 1H); <sup>13</sup>C NMR (125 MHz, CDCl<sub>3</sub>)  $\delta$  160.05, 147.50, 143.35, 140.73, 133.86, 133.83, 129.88, 129.69, 129.10, 127.52, 124.47, 118.77, 115.27, 114.79, 111.04, 64.14, 55.59, 43.91; MS (ESI):  $m/z$  = 397.05 (M+H)<sup>+</sup>.

### **1-(2-chlorophenyl)-5-(3-chlorophenyl)-3-(3-methoxyphenyl)-4,5-dihydro-1H-pyrazole (13).**

The title compound was prepared by reaction of (*E*)-3-(3-chlorophenyl)-1-(3-methoxyphenyl)prop-2-en-1-one (**C5**) and 2-chlorophenylhydrazine hydrochloride according to the general procedure for pyrazoline synthesis; brown solid; yield: 0.41 g (52%); mp 99.8 °C; <sup>1</sup>H NMR (500 MHz, CDCl<sub>3</sub>)  $\delta$  7.57 (dd, *J* = 8.1, 1.5 Hz, 1H), 7.53 – 7.50 (m, 1H), 7.43 (ddd, *J* = 9.0, 7.7, 4.6 Hz, 2H), 7.35 (dt, *J* = 6.1, 3.1 Hz, 1H), 7.31 (s, 1H), 7.27 – 7.19 (m, 4H), 7.08 (ddd, *J* = 8.0, 2.6, 1.1 Hz, 1H), 7.03 (ddd, *J* = 8.9, 5.9, 1.6 Hz, 1H), 5.94 (dd, *J* = 11.5, 4.9 Hz, 1H), 4.01 (s, 3H), 3.93 (dd, *J* = 16.9, 11.5 Hz, 1H), 3.50 (dd, *J* = 16.9, 4.9 Hz, 1H); <sup>13</sup>C NMR (125 MHz, CDCl<sub>3</sub>)  $\delta$  159.82, 149.77, 142.90, 142.49, 134.28, 133.71, 130.30, 129.81, 129.63, 127.96, 127.09, 126.87, 124.88, 124.84, 124.39, 123.79, 118.74, 115.30, 110.80, 65.83, 55.37, 42.53; MS (ESI):  $m/z$  = 397.08 (M+H)<sup>+</sup>.

**1,5-bis(3-chlorophenyl)-3-(3-methoxyphenyl)-4,5-dihydro-1H-pyrazole (14).** The title compound was prepared by reaction of (*E*)-3-(3-chlorophenyl)-1-(3-methoxyphenyl)prop-2-en-

## Results

---

1-one (**C5**) and 3-chlorophenylhydrazine hydrochloride according to the general procedure for pyrazoline synthesis; beige solid; yield: 0.52 g (66%); mp 80-82 °C; <sup>1</sup>H NMR (500 MHz, CDCl<sub>3</sub>) δ 7.36 – 7.30 (m, 2H), 7.29 (dd, *J* = 4.9, 2.9 Hz, 2H), 7.27 – 7.25 (m, 2H), 7.19 (t, *J* = 2.1 Hz, 1H), 7.18 – 7.14 (m, 1H), 7.06 (t, *J* = 8.1 Hz, 1H), 6.94 – 6.89 (m, 1H), 6.79 – 6.71 (m, 2H), 5.21 (dd, *J* = 12.4, 6.7 Hz, 1H), 3.88 – 3.80 (m, 4H), 3.12 (dd, *J* = 17.2, 6.7 Hz, 1H); <sup>13</sup>C NMR (125 MHz, CDCl<sub>3</sub>) δ 159.80, 147.64, 145.46, 144.06, 135.18, 134.89, 133.45, 130.64, 129.95, 129.65, 128.14, 125.94, 123.92, 119.23, 118.65, 115.25, 113.57, 111.12, 110.83, 63.72, 55.39, 43.64; MS (ESI):*m/z* = 397.04 (M+H)<sup>+</sup>.

### **5-(3-chlorophenyl)-1-(4-chlorophenyl)-3-(3-methoxyphenyl)-4,5-dihydro-1H-pyrazole (15).**

The title compound was prepared by reaction of (*E*)-3-(3-chlorophenyl)-1-(3-methoxyphenyl)prop-2-en-1-one (**C5**) and 4-chlorophenylhydrazine hydrochloride according to the general procedure for pyrazoline synthesis; beige solid; yield: 0.21 g (27%); mp 137-139 °C; <sup>1</sup>H NMR (500 MHz, CDCl<sub>3</sub>) δ 7.28 (ddd, *J* = 8.0, 5.7, 2.9 Hz, 3H), 7.26 – 7.23 (m, 2H), 7.22 – 7.19 (m, 1H), 7.16 – 7.13 (m, 1H), 7.13 – 7.09 (m, 2H), 6.96 – 6.92 (m, 2H), 6.89 (ddd, *J* = 8.2, 2.6, 0.9 Hz, 1H), 5.18 (dd, *J* = 12.4, 7.1 Hz, 1H), 3.86 – 3.78 (m, 4H), 3.10 (dd, *J* = 17.1, 7.1 Hz, 1H); <sup>13</sup>C NMR (125 MHz, CDCl<sub>3</sub>) δ 159.80, 147.26, 144.15, 143.10, 135.15, 133.56, 130.61, 129.63, 128.88, 128.08, 126.02, 124.27, 123.96, 118.54, 115.08, 114.52, 110.78, 64.00, 55.34, 43.66; MS (ESI):*m/z* = 397 (M+H)<sup>+</sup>.

### **1,5-bis(2-chlorophenyl)-3-(3-methoxyphenyl)-4,5-dihydro-1H-pyrazole (16).**

The title compound was prepared by reaction of (*E*)-3-(2-chlorophenyl)-1-(3-methoxyphenyl)prop-2-en-1-one (**C6**) and 2-chlorophenylhydrazine hydrochloride according to the general procedure for pyrazoline synthesis; light brown solid; yield: 0.27 g (34%); mp 122-124 °C; <sup>1</sup>H NMR (500 MHz, CDCl<sub>3</sub>) δ 7.44 (dd, *J* = 8.2, 1.5 Hz, 1H), 7.32 (ddd, *J* = 9.2, 5.0, 1.4 Hz, 2H), 7.28 (tt, *J* = 4.2, 2.2 Hz, 2H), 7.26 – 7.23 (m, 2H), 7.16 – 7.05 (m, 3H), 6.91 – 6.85 (m, 2H), 6.20 (dd, *J* = 11.5, 6.5 Hz, 1H), 3.89 – 3.83 (m, 4H), 3.11 (dd, *J* = 16.7, 6.6 Hz, 1H); <sup>13</sup>C NMR (125 MHz, CDCl<sub>3</sub>) δ 159.77, 149.31, 142.44, 138.82, 133.83, 132.11, 130.98, 129.72, 129.56, 128.62, 127.89, 127.10, 127.08, 124.60, 123.67, 121.87, 118.73, 115.28, 110.76, 63.14, 55.35, 41.90; MS (ESI):*m/z* = 397.06 (M+H)<sup>+</sup>.

### **5-(2-chlorophenyl)-1-(3-chlorophenyl)-3-(3-methoxyphenyl)-4,5-dihydro-1H-pyrazole (17).**

The title compound was prepared by reaction of (*E*)-3-(2-chlorophenyl)-1-(3-methoxyphenyl)prop-2-en-1-one (**C6**) and 3-chlorophenylhydrazine hydrochloride according to the general procedure for pyrazoline synthesis; brown solid; yield: 0.38 g (47.5%); mp 153-154 °C; <sup>1</sup>H NMR (500 MHz, CDCl<sub>3</sub>) δ 7.52 (t, *J* = 7.4 Hz, 1H), 7.41 – 7.39 (m, 1H), 7.37 (t, *J* = 7.9 Hz, 1H), 7.34 – 7.28 (m, 2H), 7.28 – 7.26 (m, 1H), 7.24 (d, *J* = 4.2 Hz, 2H), 7.15 (dd, *J* = 14.0, 6.0 Hz, 1H), 7.00 – 6.94 (m, 1H), 6.87 – 6.81 (m, 1H), 6.77 – 6.72 (m, 1H), 5.71 (dd, *J* = 12.3, 6.3 Hz, 1H), 4.03 (dd, *J* = 17.3, 12.3 Hz, 1H), 3.94 (s, 3H), 3.13 (dd, *J* = 17.3, 6.3 Hz, 1H); <sup>13</sup>C

## Results

---

NMR (125 MHz, CDCl<sub>3</sub>)  $\delta$  159.79, 148.04, 145.28, 138.56, 134.94, 133.57, 131.77, 130.02, 129.98, 129.61, 129.01, 127.69, 127.12, 119.07, 118.66, 115.23, 113.40, 110.89, 110.78, 61.03, 55.38, 42.17; MS (ESI): $m/z$  = 397.04 (M+H)<sup>+</sup>.

### **5-(2-chlorophenyl)-1-(4-chlorophenyl)-3-(3-methoxyphenyl)-4,5-dihydro-1H-pyrazole (18).**

The title compound was prepared by reaction of (*E*)-3-(2-chlorophenyl)-1-(3-methoxyphenyl)prop-2-en-1-one (**C6**) and 4-chlorophenylhydrazine hydrochloride according to the general procedure for pyrazoline synthesis; brown solid; yield: 0.43 g (54%); mp 98-99 °C; <sup>1</sup>H NMR (500 MHz, CDCl<sub>3</sub>)  $\delta$  7.58 – 7.53 (m, 1H), 7.42 (dt, *J* = 4.2, 2.1 Hz, 1H), 7.40 (t, *J* = 7.9 Hz, 1H), 7.38 – 7.35 (m, 1H), 7.35 – 7.32 (m, 1H), 7.29 – 7.22 (m, 4H), 7.05 – 6.98 (m, 3H), 5.73 (dd, *J* = 12.4, 6.6 Hz, 1H), 4.07 (dd, *J* = 17.2, 12.4 Hz, 1H), 3.97 (s, 3H), 3.16 (dd, *J* = 17.2, 6.6 Hz, 1H); <sup>13</sup>C NMR (125 MHz, CDCl<sub>3</sub>)  $\delta$  160.04, 147.87, 143.16, 138.92, 133.93, 132.05, 130.25, 129.85, 129.23, 129.17, 127.92, 127.46, 124.32, 118.81, 115.33, 114.53, 110.98, 61.48, 55.60, 42.41; MS (ESI): $m/z$  = 397.02 (M+H)<sup>+</sup>.

### **1-(2-chlorophenyl)-5-(4-chlorophenyl)-3-(2-methoxyphenyl)-4,5-dihydro-1H-pyrazole (19).**

The title compound was prepared by reaction of (*E*)-3-(4-chlorophenyl)-1-(2-methoxyphenyl)prop-2-en-1-one (**C7**) and 2-chlorophenylhydrazine hydrochloride according to the general procedure for pyrazoline synthesis; beige solid; yield: 0.33 g (41%); mp 103-105 °C; <sup>1</sup>H NMR (500 MHz, DMSO)  $\delta$  7.82 (dd, *J* = 7.7, 1.8 Hz, 1H), 7.44 – 7.35 (m, 2H), 7.31 – 7.17 (m, 5H), 7.17 – 7.07 (m, 2H), 7.02 (td, *J* = 7.5, 1.1 Hz, 1H), 6.93 (ddd, *J* = 7.9, 7.3, 1.6 Hz, 1H), 5.76 (dd, *J* = 11.1, 5.6 Hz, 1H), 3.89 (dd, *J* = 17.8, 11.2 Hz, 1H), 3.82 (s, 3H), 3.38 (dd, *J* = 17.7, 5.6 Hz, 1H); MS (ESI): $m/z$  = 397.08 (M+H)<sup>+</sup>.

### **1-(3-chlorophenyl)-5-(4-chlorophenyl)-3-(2-methoxyphenyl)-4,5-dihydro-1H-pyrazole (20).**

The title compound was prepared by reaction of (*E*)-3-(4-chlorophenyl)-1-(2-methoxyphenyl)prop-2-en-1-one (**C7**) and 3-chlorophenylhydrazine hydrochloride according to the general procedure for pyrazoline synthesis; yellow solid; yield: 0.42 g (53%); mp 111-112 °C; <sup>1</sup>H NMR (500 MHz, CDCl<sub>3</sub>)  $\delta$  7.97 (td, *J* = 7.9, 1.7 Hz, 1H), 7.43 – 7.40 (m, 1H), 7.35 – 7.28 (m, 2H), 7.19 – 7.14 (m, 3H), 7.06 – 7.01 (m, 1H), 7.01 – 6.96 (m, 1H), 6.89 (dd, *J* = 8.3, 0.8 Hz, 1H), 6.74 – 6.68 (m, 1H), 6.66 – 6.61 (m, 1H), 5.56 (dd, *J* = 12.3, 6.5 Hz, 1H), 4.09 (dd, *J* = 18.2, 12.3 Hz, 1H), 3.80 (s, 3H), 3.21 (dd, *J* = 18.2, 6.5 Hz, 1H); <sup>13</sup>C NMR (125 MHz, CDCl<sub>3</sub>)  $\delta$  157.63, 148.11, 145.61, 139.06, 134.87, 131.77, 130.38, 129.89, 129.61, 128.76, 127.61, 121.50, 120.88, 118.70, 113.32, 111.53, 110.80, 61.06, 55.43, 45.24; MS (ESI):  $m/z$  = 397.07 (M+H)<sup>+</sup>.

**1,5-bis(4-chlorophenyl)-3-(2-methoxyphenyl)-4,5-dihydro-1H-pyrazole (21).** The title compound was prepared by reaction of (*E*)-3-(4-chlorophenyl)-1-(2-methoxyphenyl)prop-2-en-1-one (**C7**) and 4-chlorophenylhydrazine hydrochloride according to the general procedure for pyrazoline synthesis; yellow solid; yield: 0.48 g (61%); mp 159-160 °C; <sup>1</sup>H NMR (500 MHz,

## Results

---

$\text{CDCl}_3$ )  $\delta$  7.41 (dd,  $J = 8.2, 1.4$  Hz, 1H), 7.37 – 7.33 (m, 1H), 7.33 – 7.27 (m, 2H), 7.28 – 7.20 (m, 2H), 7.15 – 7.06 (m, 3H), 6.97 (tt,  $J = 7.6, 3.8$  Hz, 1H), 6.87 (ddd,  $J = 10.0, 8.8, 4.9$  Hz, 2H), 6.10 (dd,  $J = 11.3, 6.8$  Hz, 1H), 4.00 (dd,  $J = 17.5, 11.3$  Hz, 1H), 3.81 (s, 3H), 3.24 (dd,  $J = 17.5, 6.7$  Hz, 1H);  $^{13}\text{C}$  NMR (126 MHz,  $\text{CDCl}_3$ )  $\delta$  157.65, 149.69, 142.87, 139.26, 132.09, 130.91, 130.32, 129.00, 128.38, 127.96, 126.99, 124.71, 123.37, 121.53, 120.83, 63.21, 55.44, 44.91; MS (ESI):  $m/z = 397.06$  (M+H) $^+$ .

### **1-(2-chlorophenyl)-5-(3-chlorophenyl)-3-(2-methoxyphenyl)-4,5-dihydro-1H-pyrazole (22).**

The title compound was prepared by reaction of (*E*)-3-(3-chlorophenyl)-1-(2-methoxyphenyl)prop-2-en-1-one (**C8**) and 2-chlorophenylhydrazine hydrochloride according to the general procedure for pyrazoline synthesis; brown solid; yield: 0.35 g (44%); mp 117-119 °C;  $^1\text{H}$  NMR (500 MHz,  $\text{CDCl}_3$ )  $\delta$  7.37 – 7.29 (m, 3H), 7.27 – 7.23 (m, 2H), 7.19 – 7.15 (m, 1H), 7.14 – 7.10 (m, 2H), 7.00 (td,  $J = 7.7, 1.0$  Hz, 1H), 6.96 – 6.92 (m, 2H), 6.90 (d,  $J = 8.3$  Hz, 1H), 5.10 (dt,  $J = 22.0, 11.0$  Hz, 1H), 4.00 (dd,  $J = 18.1, 12.3$  Hz, 1H), 3.81 (s, 3H), 3.28 (dd,  $J = 18.1, 7.4$  Hz, 1H);  $^{13}\text{C}$  NMR (125 MHz,  $\text{CDCl}_3$ )  $\delta$  157.81, 147.70, 144.92, 143.76, 135.24, 130.72, 130.58, 129.43, 129.05, 128.07, 127.25, 126.66, 126.34, 124.29, 124.15, 121.71, 121.17, 114.73, 111.78, 64.47, 55.64, 47.12; MS (ESI):  $m/z = 397.06$  (M+H) $^+$ .

### **1,5-bis(3-chlorophenyl)-3-(2-methoxyphenyl)-4,5-dihydro-1H-pyrazole (23).**

The title compound was prepared by reaction of (*E*)-3-(3-chlorophenyl)-1-(2-methoxyphenyl)prop-2-en-1-one (**C8**) and 3-chlorophenylhydrazine hydrochloride according to the general procedure for pyrazoline synthesis; beige solid; yield: 0.2 g (25%); mp 126-127 °C  $^1\text{H}$  NMR (500 MHz,  $\text{CDCl}_3$ )  $\delta$  8.01 (dd,  $J = 7.8, 1.7$  Hz, 1H), 7.34 – 7.28 (m, 2H), 7.26 – 7.23 (m, 2H), 7.18 – 7.15 (m, 2H), 7.06 – 6.98 (m, 2H), 6.89 (dd,  $J = 8.3, 1.0$  Hz, 1H), 6.75 – 6.71 (m, 2H), 5.12 (dd,  $J = 12.3, 7.0$  Hz, 1H), 3.99 (dd,  $J = 18.1, 12.3$  Hz, 1H), 3.79 (s, 3H), 3.27 (dd,  $J = 18.1, 7.0$  Hz, 1H);  $^{13}\text{C}$  NMR (125 MHz,  $\text{CDCl}_3$ )  $\delta$  157.55, 147.78, 145.81, 144.55, 134.98, 134.78, 130.48, 130.43, 129.86, 128.86, 127.84, 125.97, 123.96, 121.28, 120.90, 118.82, 113.46, 111.47, 111.02, 63.85, 55.35, 46.82 ; MS (ESI):  $m/z = 397.07$  (M+H) $^+$ .

### **5-(3-chlorophenyl)-1-(4-chlorophenyl)-3-(2-methoxyphenyl)-4,5-dihydro-1H-pyrazole (24).**

The title compound was prepared by reaction of (*E*)-3-(3-chlorophenyl)-1-(2-methoxyphenyl)prop-2-en-1-one (**C8**) and 4-chlorophenylhydrazine hydrochloride according to the general procedure for pyrazoline synthesis; yellow solid; yield: 0.27 g (34%); mp 123-125 °C;  $^1\text{H}$  NMR (500 MHz,  $\text{CDCl}_3$ )  $\delta$  8.12 (dt,  $J = 5.6, 2.8$  Hz, 1H), 7.48 – 7.42 (m, 3H), 7.40 – 7.35 (m, 2H), 7.30 (ddd,  $J = 6.6, 3.9, 2.2$  Hz, 1H), 7.27 – 7.23 (m, 1H), 7.16 – 7.11 (m, 1H), 7.10 – 7.06 (m, 2H), 7.04 (dd,  $J = 8.4, 0.9$  Hz, 1H), 5.25 (dd,  $J = 12.3, 7.4$  Hz, 1H), 4.13 (dd,  $J = 18.1, 12.3$  Hz, 1H), 3.94 (s, 3H), 3.41 (dd,  $J = 18.1, 7.4$  Hz, 1H);  $^{13}\text{C}$  NMR (125 MHz,  $\text{CDCl}_3$ )  $\delta$  157.52, 147.43, 144.65, 143.47, 134.96, 130.47, 130.33, 129.18, 128.79, 127.81, 126.40, 124.02, 123.85, 121.40, 120.89, 114.44, 111.48, 64.17, 55.36, 46.85; MS (ESI):  $m/z = 397.06$  (M+H) $^+$ .

## Results

---

**1,5-bis(2-chlorophenyl)-3-(2-methoxyphenyl)-4,5-dihydro-1H-pyrazole (25).** The title compound was prepared by reaction of (*E*)-3-(2-chlorophenyl)-1-(2-methoxyphenyl)prop-2-en-1-one (**C9**) and 2-chlorophenylhydrazine hydrochloride according to the general procedure for pyrazoline synthesis; buff solid; yield: 0.3 g (38%); mp 138.5-139.5 °C; <sup>1</sup>H NMR (500 MHz, CDCl<sub>3</sub>) δ 8.10 (dd, *J* = 7.7, 1.7 Hz, 1H), 7.56 (dd, *J* = 8.2, 1.5 Hz, 1H), 7.52 – 7.42 (m, 3H), 7.42 – 7.37 (m, 1H), 7.30 – 7.20 (m, 3H), 7.15 – 7.09 (m, 1H), 7.02 (ddd, *J* = 9.7, 8.9, 4.9 Hz, 2H), 6.25 (dd, *J* = 11.3, 6.8 Hz, 1H), 4.15 (dd, *J* = 17.5, 11.3 Hz, 1H), 3.95 (s, 3H), 3.39 (dd, *J* = 17.5, 6.8 Hz, 1H); <sup>13</sup>C NMR (125 MHz, CDCl<sub>3</sub>) δ 157.62, 149.69, 142.85, 139.23, 132.07, 130.91, 130.31, 129.56, 128.98, 128.37, 127.94, 127.02, 126.99, 124.67, 123.35, 121.79, 121.48, 120.81, 111.41, 63.17, 55.40, 44.89. ; MS (ESI): *m/z* = 397.07 (M+H)<sup>+</sup>.

**5-(2-chlorophenyl)-1-(3-chlorophenyl)-3-(2-methoxyphenyl)-4,5-dihydro-1H-pyrazole (26).** The title compound was prepared by reaction of (*E*)-3-(2-chlorophenyl)-1-(2-methoxyphenyl)prop-2-en-1-one (**C9**) and 3-chlorophenylhydrazine hydrochloride according to the general procedure for pyrazoline synthesis; yellow solid; yield: 0.44 g (56%); mp 165-166 °C; <sup>1</sup>H NMR (500 MHz, CDCl<sub>3</sub>) δ 8.06 (dd, *J* = 7.8, 1.7 Hz, 1H), 7.49 (ddd, *J* = 7.6, 1.3, 0.6 Hz, 1H), 7.39 – 7.35 (m, 1H), 7.28 – 7.23 (m, 4H), 7.13 – 7.09 (m, 1H), 7.09 – 7.04 (m, 1H), 6.99 – 6.93 (m, 1H), 6.81 – 6.76 (m, 1H), 6.74 – 6.69 (m, 1H), 5.64 (dd, *J* = 12.3, 6.4 Hz, 1H), 4.16 (dd, *J* = 18.2, 12.3 Hz, 1H), 3.87 (s, 3H), 3.28 (dd, *J* = 18.2, 6.4 Hz, 1H); <sup>13</sup>C NMR (125 MHz, CDCl<sub>3</sub>) δ 157.59, 148.08, 145.55, 139.02, 134.84, 131.74, 130.37, 129.90, 129.87, 128.85, 128.74, 127.59, 127.20, 121.43, 120.85, 118.66, 113.27, 111.47, 110.75, 61.00, 55.40, 45.22; MS (ESI):*m/z* = 397.07 (M+H)<sup>+</sup>.

**5-(2-chlorophenyl)-1-(4-chlorophenyl)-3-(2-methoxyphenyl)-4,5-dihydro-1H-pyrazole (27).** The title compound was prepared by reaction of (*E*)-3-(2-chlorophenyl)-1-(2-methoxyphenyl)prop-2-en-1-one (**C9**) and 4-chlorophenylhydrazine hydrochloride according to the general procedure for pyrazoline synthesis; beige solid; yield: 0.37 g (46%); mp 173-175 °C; <sup>1</sup>H NMR (500 MHz, CDCl<sub>3</sub>) δ 7.92 (dd, *J* = 7.8, 1.7 Hz, 1H), 7.29 – 7.22 (m, 3H), 7.22 – 7.13 (m, 2H), 7.07 – 7.02 (m, 2H), 6.97 – 6.92 (m, 1H), 6.92 – 6.81 (m, 3H), 5.08 (dd, *J* = 12.2, 7.3 Hz, 1H), 3.93 (dd, *J* = 18.0, 12.2 Hz, 1H), 3.75 (s, 3H), 3.21 (dd, *J* = 18.0, 7.3 Hz, 1H); <sup>13</sup>C NMR (125 MHz, CDCl<sub>3</sub>) δ 157.55, 147.44, 143.49, 140.98, 133.30, 130.30, 130.06, 129.00, 128.77, 127.33, 126.49, 123.84, 121.50, 120.99, 114.48, 111.53, 111.30, 64.06, 55.53, 46.87; MS (ESI):*m/z* = 397.06 (M+H)<sup>+</sup>.

**1-(2-chlorophenyl)-5-(3-chlorophenyl)-3-(3,4-dimethoxyphenyl)-4,5-dihydro-1H-pyrazole (28).** The title compound was prepared by reaction of (*E*)-3-(3-chlorophenyl)-1-(3,4-dimethoxyphenyl)prop-2-en-1-one (**C10**) and 2-chlorophenylhydrazine hydrochloride according to the general procedure for pyrazoline synthesis; beige solid; yield: 0.32 g (37%); mp 118-119 °C; <sup>1</sup>H NMR (500 MHz, CDCl<sub>3</sub>) δ 7.66 (d, *J* = 2.0 Hz, 1H), 7.57 (dt, *J* = 8.3, 1.7 Hz, 1H), 7.35

## Results

---

(dd,  $J = 8.0, 1.5$  Hz, 1H), 7.33 – 7.29 (m, 1H), 7.28 – 7.17 (m, 5H), 7.04 – 6.99 (m, 2H), 5.90 (dd,  $J = 11.4, 4.8$  Hz, 1H), 4.10 (s, 3H), 4.06 (s, 3H), 3.92 (dd,  $J = 16.8, 11.4$  Hz, 1H), 3.49 (dd,  $J = 16.8, 4.8$  Hz, 1H);  $^{13}\text{C}$  NMR (125 MHz,  $\text{CDCl}_3$ )  $\delta$  150.32, 150.07, 149.27, 143.01, 142.78, 134.23, 130.25, 129.77, 127.88, 127.06, 126.88, 125.38, 124.90, 124.26, 123.69, 119.45, 110.70, 108.43, 103.76, 65.77, 56.00, 55.96, 42.60; MS (ESI):  $m/z = 426.96$  (M+H) $^+$ .

**1-(2-chlorophenyl)-5-(3-chlorophenyl)-3-(2,4-dimethoxyphenyl)-4,5-dihydro-1H-pyrazole (29).** The title compound was prepared by reaction of (*E*)-3-(3-chlorophenyl)-1-(2,4-dimethoxyphenyl)prop-2-en-1-one (**C11**) and 2-chlorophenylhydrazine hydrochloride according to the general procedure for pyrazoline synthesis; beige solid; yield: 0.40 g (47%); mp 154-156 °C;  $^1\text{H}$  NMR (500 MHz,  $\text{CDCl}_3$ )  $\delta$  8.02 (t,  $J = 8.5$  Hz, 1H), 7.40 – 7.37 (m, 1H), 7.36 – 7.29 (m, 2H), 7.27 – 7.22 (m, 2H), 7.12 (t,  $J = 8.1$  Hz, 1H), 6.82 – 6.77 (m, 2H), 6.65 (dd,  $J = 8.7, 2.4$  Hz, 1H), 6.53 (d,  $J = 2.4$  Hz, 1H), 5.17 (dd,  $J = 12.2, 7.0$  Hz, 1H), 4.04 (dd,  $J = 18.0, 12.2$  Hz, 1H), 3.92 (s, 3H), 3.87 (s, 3H), 3.33 (dd,  $J = 18.1, 7.1$  Hz, 1H);  $^{13}\text{C}$  NMR (125 MHz,  $\text{CDCl}_3$ )  $\delta$  161.91, 158.85, 147.84, 146.11, 144.74, 134.97, 134.76, 130.45, 129.87, 129.83, 127.79, 126.01, 124.01, 118.57, 114.28, 113.38, 110.94, 105.51, 98.66, 63.77, 55.46, 55.37, 46.85; MS (ESI):  $m/z = 427.10$  (M+H) $^+$ .

**3-(*tert*-butyl)-1-(4-chlorophenyl)-5-(naphthalen-2-yl)-4,5-dihydro-1H-pyrazole (30).** The title compound was prepared by reaction of (*E*)-4,4-dimethyl-1-(naphthalen-2-yl)pent-1-en-3-one (**C12**) and 4-chlorophenylhydrazine hydrochloride according to the general procedure for pyrazoline synthesis; off-white solid; yield: 0.46 g (63%); mp 126-127 °C;  $^1\text{H}$  NMR (500 MHz,  $\text{CDCl}_3$ )  $\delta$  7.84 – 7.77 (m, 3H), 7.73 (d,  $J = 6.9$  Hz, 1H), 7.50 – 7.42 (m, 2H), 7.37 (dd,  $J = 8.5, 1.8$  Hz, 1H), 7.06 – 7.01 (m, 2H), 6.92 – 6.87 (m, 2H), 5.11 (dd,  $J = 11.8, 8.0$  Hz, 1H), 3.53 (dd,  $J = 17.3, 11.8$  Hz, 1H), 2.80 (dt,  $J = 37.9, 19.0$  Hz, 1H), 1.23 (s, 9H);  $^{13}\text{C}$  NMR (125 MHz,  $\text{CDCl}_3$ )  $\delta$  159.44, 144.93, 140.06, 133.53, 132.88, 129.24, 128.64, 127.85, 127.75, 126.38, 125.97, 124.58, 123.78, 123.33, 114.40, 65.26, 43.26, 33.89, 28.25; MS (ESI):  $m/z = 363.22$  (M+H) $^+$ .

**5-([1,1'-biphenyl]-4-yl)-3-(*tert*-butyl)-1-(4-chlorophenyl)-4,5-dihydro-1H-pyrazole (31).** The title compound was prepared by reaction of (*E*)-1-([1,1'-biphenyl]-4-yl)-4,4-dimethylpent-1-en-3-one (**C13**) and 4-chlorophenylhydrazine hydrochloride according to the general procedure for pyrazoline synthesis; beige solid; yield: 0.45 g (58%); mp 139.5-141 °C;  $^1\text{H}$  NMR (500 MHz,  $\text{CDCl}_3$ )  $\delta$  7.56 (ddd,  $J = 8.2, 5.1, 1.6$  Hz, 4H), 7.46 – 7.38 (m, 2H), 7.37 – 7.28 (m, 3H), 7.11 – 7.03 (m, 2H), 6.92 – 6.84 (m, 2H), 4.99 (dd,  $J = 11.7, 7.9$  Hz, 1H), 3.48 (dd,  $J = 17.3, 11.8$  Hz, 1H), 2.79 (dd,  $J = 17.3, 7.9$  Hz, 1H), 1.23 (s, 9H);  $^{13}\text{C}$  NMR (125 MHz,  $\text{CDCl}_3$ )  $\delta$  159.34, 144.82, 141.64, 140.59, 140.45, 128.76, 128.64, 127.81, 127.34, 127.01, 126.26, 123.27, 114.37, 64.72, 43.27, 33.84, 28.24; MS (ESI):  $m/z = 389.21$  (M+H) $^+$ .

## Results

---

**3-(*tert*-butyl)-1,5-bis(4-chlorophenyl)-4,5-dihydro-1*H*-pyrazole (32).** The title compound was prepared by reaction of (*E*)-1-(4-chlorophenyl)-4,4-dimethylpent-1-en-3-one (**C14**) and 4-chlorophenylhydrazine hydrochloride according to the general procedure for pyrazoline synthesis. white solid; yield: 0.34 g (49.5%); mp 85.3-87 °C; <sup>1</sup>H NMR (500 MHz, CDCl<sub>3</sub>) δ 7.33 – 7.28 (m, 2H), 7.21 – 7.17 (m, 2H), 7.10 – 7.05 (m, 2H), 6.85 – 6.80 (m, 2H), 4.94 (dd, *J* = 11.7, 7.6 Hz, 1H), 3.46 (dd, *J* = 17.2, 11.7 Hz, 1H), 2.71 (dd, *J* = 17.2, 7.6 Hz, 1H), 1.21 (s, 9H); <sup>13</sup>C NMR (125 MHz, CDCl<sub>3</sub>) δ 159.25, 144.53, 141.07, 133.26, 129.29, 128.68, 127.24, 123.48, 114.33, 64.28, 43.14, 33.82, 28.20; MS (ESI): *m/z* = 347.16 (M+H)<sup>+</sup>.

**3-(*tert*-butyl)-1-(4-chlorophenyl)-5-(3,4-dichlorophenyl)-4,5-dihydro-1*H*-pyrazole (33).** The title compound was prepared by reaction of (*E*)-1-(3,4-dichlorophenyl)-4,4-dimethylpent-1-en-3-one (**C15**) and 4-chlorophenylhydrazine hydrochloride according to the general procedure for pyrazoline synthesis; yellow solid; yield: 0.54 g (71%); mp 86-87 °C; <sup>1</sup>H NMR (500 MHz, CDCl<sub>3</sub>) δ 7.42 – 7.35 (m, 2H), 7.12 – 7.04 (m, 3H), 6.85 – 6.77 (m, 2H), 4.90 (dd, *J* = 11.8, 7.7 Hz, 1H), 3.46 (dd, *J* = 17.3, 11.8 Hz, 1H), 2.70 (dd, *J* = 17.3, 7.7 Hz, 1H), 1.21 (s, 9H); <sup>13</sup>C NMR (125 MHz, CDCl<sub>3</sub>) δ 159.31, 144.41, 142.90, 133.25, 131.60, 131.19, 128.78, 127.88, 125.17, 123.83, 114.38, 63.96, 43.08, 33.85, 28.19; MS (ESI): *m/z* = 381.03 (M+H)<sup>+</sup>.

**1,5-bis(4-bromophenyl)-3-(*tert*-butyl)-4,5-dihydro-1*H*-pyrazole (34).** The title compound was prepared by reaction of (*E*)-1-(4-bromophenyl)-4,4-dimethylpent-1-en-3-one (**C16**) and 4-bromophenylhydrazine hydrochloride according to the general procedure for pyrazoline synthesis; beige solid; yield: 0.42 g (48%); mp 132.5-133.5 °C; <sup>1</sup>H NMR (500 MHz, CDCl<sub>3</sub>) δ 7.47 – 7.42 (m, 2H), 7.22 – 7.17 (m, 2H), 7.14 – 7.10 (m, 2H), 6.79 – 6.73 (m, 2H), 4.92 (dd, *J* = 11.8, 7.5 Hz, 1H), 3.45 (dd, *J* = 17.3, 11.8 Hz, 1H), 2.70 (dd, *J* = 17.3, 7.5 Hz, 1H), 1.20 (s, 9H); <sup>13</sup>C NMR (125 MHz, CDCl<sub>3</sub>) δ 159.31, 144.84, 141.53, 132.26, 131.57, 127.56, 121.34, 114.78, 110.64, 64.16, 43.08, 33.83, 28.19; MS (ESI): *m/z* = 436.99 (M+H)<sup>+</sup>.

**1-(4-bromophenyl)-3-(*tert*-butyl)-5-(4-chlorophenyl)-4,5-dihydro-1*H*-pyrazole (35).** The title compound was prepared by reaction of (*E*)-1-(4-chlorophenyl)-4,4-dimethylpent-1-en-3-one (**C14**) and 4-bromophenylhydrazine hydrochloride according to the general procedure for pyrazoline synthesis; light brown solid; yield: 0.46 g (59%); mp 132-134 °C; <sup>1</sup>H NMR (500 MHz, CDCl<sub>3</sub>) δ 7.30 – 7.26 (m, 2H), 7.21 – 7.13 (m, 4H), 6.78 – 6.72 (m, 2H), 4.92 (dd, *J* = 11.7, 7.5 Hz, 1H), 3.44 (dd, *J* = 17.3, 11.8 Hz, 1H), 2.69 (dd, *J* = 17.3, 7.5 Hz, 1H), 1.19 (s, 9H); <sup>13</sup>C NMR (125 MHz, CDCl<sub>3</sub>) δ 159.33, 144.87, 141.01, 133.29, 131.58, 129.32, 127.23, 114.79, 110.73, 64.12, 43.14, 33.85, 28.21; MS (ESI): *m/z* = 392.10 (M)<sup>+</sup>.

**1,5-bis(4-chlorophenyl)-3-(2-ethoxyphenyl)-4,5-dihydro-1*H*-pyrazole (36).** The title compound was prepared by reaction of (*E*)-3-(4-chlorophenyl)-1-(2-ethoxyphenyl)prop-2-en-1-one (**C17**) and 4-chlorophenylhydrazine hydrochloride according to the general procedure for

## Results

---

pyrazoline synthesis; greenish yellow solid ; yield: 0.54 g (66%); mp 107-109 °C; <sup>1</sup>H NMR (500 MHz, CDCl<sub>3</sub>) δ 7.30 – 7.21 (m, 4H), 7.20 – 7.15 (m, 2H), 7.09 – 7.02 (m, 2H), 6.96 – 6.86 (m, 3H), 6.83 (d, *J* = 8.3 Hz, 1H), 5.09 (dd, *J* = 12.2, 6.9 Hz, 1H), 4.03 – 3.92 (m, 3H), 3.23 (dd, *J* = 17.9, 6.9 Hz, 1H), 1.32 (t, *J* = 6.9 Hz, 3H); <sup>13</sup>C NMR (125 MHz, CDCl<sub>3</sub>) δ 156.91, 147.52, 143.45, 140.94, 133.29, 130.25, 129.28, 128.82, 127.35, 126.41, 123.77, 121.60, 120.76, 114.42, 112.28, 63.96, 63.87, 46.85, 14.80; MS (ESI): *m/z* = 411.06 (M+H)<sup>+</sup>.

**1,5-bis(4-bromophenyl)-3-(2-ethoxyphenyl)-4,5-dihydro-1H-pyrazole (37).** The title compound was prepared by reaction of (*E*)-3-(4-bromophenyl)-1-(2-ethoxyphenyl)prop-2-en-1-one (**C18**) and 4-bromophenyldiazine hydrochloride according to the general procedure for pyrazoline synthesis; beige solid; yield: 0.54 g (54%); mp 164.5-166 °C; <sup>1</sup>H NMR (500 MHz, CDCl<sub>3</sub>) δ 7.96 (dd, *J* = 7.8, 1.7 Hz, 1H), 7.51 – 7.43 (m, 2H), 7.30 (ddt, *J* = 8.4, 5.3, 1.7 Hz, 1H), 7.27 – 7.23 (m, 2H), 7.20 – 7.11 (m, 3H), 6.99 (tt, *J* = 4.9, 2.4 Hz, 1H), 6.92 – 6.86 (m, 2H), 5.18 – 5.07 (m, 1H), 4.12 – 3.97 (m, 3H), 3.29 (dd, *J* = 17.9, 6.9 Hz, 1H), 1.38 (t, *J* = 7.0 Hz, 2H); <sup>13</sup>C NMR (125 MHz, CDCl<sub>3</sub>) δ 156.66, 147.35, 143.54, 141.15, 131.98, 130.04, 128.57, 128.47, 127.43, 126.38, 121.29, 120.51, 114.63, 110.80, 109.68, 63.73, 63.62, 46.54, 14.71; MS (ESI): *m/z* = 501.01 (M+H)<sup>+</sup>.

**1-(4-bromophenyl)-5-(5-bromothiophen-2-yl)-3-(2-ethoxyphenyl)-4,5-dihydro-1H-pyrazole (38).** The title compound was prepared by reaction of (*E*)-3-(5-bromothiophen-2-yl)-1-(2-ethoxyphenyl)prop-2-en-1-one (**C19**) and 4-bromophenyldiazine hydrochloride according to the general procedure for pyrazoline synthesis; beige solid; yield: 0.44 g (43%); mp 144-145 °C; <sup>1</sup>H NMR (500 MHz, CDCl<sub>3</sub>) δ 7.93 (dd, *J* = 7.8, 1.7 Hz, 1H), 7.31 – 7.25 (m, 3H), 7.02 – 6.96 (m, 3H), 6.86 (dd, *J* = 13.2, 5.8 Hz, 2H), 6.73 (dd, *J* = 3.8, 0.6 Hz, 1H), 5.33 (dd, *J* = 11.6, 6.3 Hz, 1H), 4.08 – 4.01 (m, 2H), 3.95 (dd, *J* = 17.8, 11.6 Hz, 1H), 3.43 (dd, *J* = 17.8, 6.4 Hz, 1H), 1.39 (t, *J* = 7.0 Hz, 3H); <sup>13</sup>C NMR (125 MHz, CDCl<sub>3</sub>) δ 156.98, 148.33, 147.30, 143.98, 132.26, 131.70, 130.49, 129.62, 128.92, 127.39, 124.58, 120.79, 115.44, 112.24, 111.74, 63.91, 60.64, 46.94, 14.84; MS (ESI): *m/z* = 506.79 (M+H)<sup>+</sup>.

**1-(4-bromophenyl)-5-(4-chlorophenyl)-3-(2-ethoxyphenyl)-4,5-dihydro-1H-pyrazole. (39)** The title compound was prepared by reaction of (*E*)-3-(4-chlorophenyl)-1-(2-ethoxyphenyl)prop-2-en-1-one (**C17**) and 4-bromophenyldiazine hydrochloride according to the general procedure for pyrazoline synthesis; beige solid; yield: 0.47 g (52%); mp 150-152 °C; <sup>1</sup>H NMR (500 MHz, CDCl<sub>3</sub>) δ 7.99 – 7.94 (m, 1H), 7.54 – 7.46 (m, 2H), 7.36 – 7.19 (m, 6H), 6.93 – 6.85 (m, 3H), 5.15 (dd, *J* = 12.2, 6.8 Hz, 1H), 4.10 – 3.98 (m, 3H), 3.29 (dd, *J* = 18.0, 6.8 Hz, 1H), 1.38 (t, *J* = 7.0 Hz, 3H) ; MS (ESI): *m/z* = 457.12 (M+H)<sup>+</sup>.

**1-(4-chlorophenyl)-3-(2-ethoxyphenyl)-5-(naphthalen-2-yl)-4,5-dihydro-1H-pyrazole (40).** The title compound was prepared by reaction of (*E*)-1-(2-ethoxyphenyl)-3-(naphthalen-2-

## Results

yl)prop-2-en-1-one (**C20**) and 4-chlorophenylhydrazine hydrochloride according to the general procedure for pyrazoline synthesis; yellow solid; yield: 0.37 g (43%); mp 164-165 °C; <sup>1</sup>H NMR (500 MHz, CDCl<sub>3</sub>) δ 8.05 – 7.99 (m, 1H), 7.85 – 7.74 (m, 4H), 7.50 – 7.44 (m, 2H), 7.43 (dd, *J* = 8.5, 1.8 Hz, 1H), 7.32 – 7.25 (m, 1H), 7.10 – 7.05 (m, 2H), 7.05 – 6.96 (m, 3H), 6.88 (dd, *J* = 8.3, 0.6 Hz, 1H), 5.33 (dd, *J* = 12.2, 7.4 Hz, 1H), 4.13 – 3.97 (m, 3H), 3.40 (dd, *J* = 18.0, 7.4 Hz, 1H), 1.35 (t, *J* = 7.0 Hz, 3H); <sup>13</sup>C NMR (125 MHz, CDCl<sub>3</sub>) δ 156.94, 147.61, 143.82, 139.95, 133.50, 132.92, 130.15, 129.28, 128.87, 128.71, 127.86, 127.76, 126.35, 125.95, 124.73, 123.88, 123.61, 121.78, 120.75, 114.50, 112.31, 64.95, 63.88, 46.99, 14.79; MS (ESI): *m/z* = 427.05 (M+H)<sup>+</sup>.

**5-([1,1'-biphenyl]-4-yl)-1-(4-chlorophenyl)-3-(2-ethoxyphenyl)-4,5-dihydro-1H-pyrazole (41).** The title compound was prepared by reaction of (*E*)-3-([1,1'-biphenyl]-4-yl)-1-(2-ethoxyphenyl)prop-2-en-1-one (**C21**) and 4-chlorophenylhydrazine hydrochloride according to the general procedure for pyrazoline synthesis; brown solid; yield: 0.52 g (57%); mp 191-192 °C; <sup>1</sup>H NMR (500 MHz, CDCl<sub>3</sub>) δ 7.98 (s, 1H), 7.58 (d, *J* = 24.3 Hz, 4H), 7.49 – 7.18 (m, 6H), 7.10 (dd, *J* = 18.8, 14.3 Hz, 2H), 7.01 (dd, *J* = 7.9, 3.5 Hz, 3H), 6.88 (s, 1H), 5.21-5.17 (m, 1H), 4.04-3.98 (m, 3H), 3.36 (dd, *J* = 12.8, 5.0 Hz, 1H), 1.38 (t, *J* = 7.0 Hz, 3H); MS (ESI): *m/z* = 453.18 (M+H)<sup>+</sup>.

**1-(4-chlorophenyl)-5-(3,4-dichlorophenyl)-3-(2-ethoxyphenyl)-4,5-dihydro-1H-pyrazole (42).** The title compound was prepared by reaction of (*E*)-3-(3,4-dichlorophenyl)-1-(2-ethoxyphenyl)prop-2-en-1-one (**C22**) and 4-chlorophenylhydrazine hydrochloride according to the general procedure for pyrazoline synthesis; yellow solid; yield: 0.65 g (73%); mp 170-171 °C; <sup>1</sup>H NMR (500 MHz, CDCl<sub>3</sub>) δ 8.08 (dd, *J* = 7.8, 1.7 Hz, 1H), 7.54 – 7.49 (m, 2H), 7.45 – 7.39 (m, 1H), 7.28 – 7.22 (m, 3H), 7.11 (tt, *J* = 7.4, 2.9 Hz, 1H), 7.08 – 7.03 (m, 2H), 7.01 (dd, *J* = 8.3, 0.7 Hz, 1H), 5.23 (dd, *J* = 12.2, 6.9 Hz, 1H), 4.22 – 4.06 (m, 3H), 3.41 (dd, *J* = 18.0, 7.0 Hz, 1H), 1.51 (t, *J* = 7.0 Hz, 3H); <sup>13</sup>C NMR (125 MHz, CDCl<sub>3</sub>) δ 156.91, 147.55, 143.31, 142.81, 133.20, 131.62, 131.18, 130.40, 129.27, 128.87, 128.85, 127.98, 126.33, 125.30, 124.06, 121.35, 120.78, 114.43, 112.26, 63.88, 63.59, 46.78, 14.81; MS (ESI): *m/z* = 445.05 (M+H)<sup>+</sup>.

**1-(4-chlorophenyl)-5-(2,4-dichlorophenyl)-3-(2-ethoxyphenyl)-4,5-dihydro-1H-pyrazole (43).** The title compound was prepared by reaction of (*E*)-3-(2,4-dichlorophenyl)-1-(2-ethoxyphenyl)prop-2-en-1-one (**C23**) and 4-chlorophenylhydrazine hydrochloride according to the general procedure for pyrazoline synthesis; yellow solid; yield: 0.55 g (61%); mp 162-163 °C; <sup>1</sup>H NMR (500 MHz, CDCl<sub>3</sub>) δ 7.97 (dd, *J* = 7.8, 1.8 Hz, 1H), 7.50 – 7.45 (m, 1H), 7.34 – 7.24 (m, 2H), 7.20 – 7.08 (m, 3H), 6.99 (td, *J* = 7.7, 1.1 Hz, 1H), 6.93 – 6.86 (m, 3H), 5.51 (dd, *J* = 12.2, 6.4 Hz, 1H), 4.24 – 3.96 (m, 3H), 3.24 (dd, *J* = 18.1, 6.5 Hz, 1H), 1.41 (t, *J* = 7.0 Hz, 3H); <sup>13</sup>C NMR (125 MHz, CDCl<sub>3</sub>) δ 156.95, 147.93, 143.05, 137.75, 133.83, 132.48, 130.37, 129.07, 128.93, 128.77, 128.35, 127.87, 123.90, 121.44, 120.75, 114.16, 112.32, 63.92, 60.86, 45.22, 14.76; MS (ESI): *m/z* = 445.06 (M+H)<sup>+</sup>.

## Results

---

### **1-(4-chlorophenyl)-3-(2-ethoxyphenyl)-5-(4-fluorophenyl)-4,5-dihydro-1H-pyrazole (44).**

The title compound was prepared by reaction of (*E*)-1-(2-ethoxyphenyl)-3-(4-fluorophenyl)prop-2-en-1-one (**C24**) and 4-chlorophenylhydrazine hydrochloride according to the general procedure for pyrazoline synthesis; yellow solid; yield: 0.36 g (46%); mp 112-114 °C; <sup>1</sup>H NMR (500 MHz, CDCl<sub>3</sub>) δ 7.50 – 7.37 (m, 4H), 7.27 – 7.22 (m, 2H), 7.21 – 7.12 (m, 3H), 7.12 – 7.07 (m, 2H), 7.03 (dd, *J* = 8.3, 0.7 Hz, 1H), 5.31 (dd, *J* = 12.1, 6.9 Hz, 1H), 4.22 – 4.11 (m, 3H), 3.43 (dd, *J* = 17.9, 6.9 Hz, 1H), 1.52 (t, *J* = 7.0 Hz, 3H); MS (ESI): *m/z* = 395.12 (M+H)<sup>+</sup>.

### **(3-(*tert*-butyl)-1,5-bis(4-chlorophenyl)-4,5-dihydro-1H-pyrazol-4-yl)(morpholino)methanone (45).**

To a three-necked flask containing 20 mL of dry THF, a 0.75 mL of lithium diisopropylamide (LDA), 2M solution in THF/*n*-heptane/ethylbenzene was added under argon atmosphere, followed by a solution of 347 mg (1 mmol) of 3-(*tert*-butyl)-1,5-bis(4-chlorophenyl)-4,5-dihydro-1H-pyrazole (**32**) in 10 mL of THF *via* a syringe at -78 °C. The mixture was stirred for 1h. Afterward, 4-morpholinecarbonyl chloride (0.175 mL, 1.5 mmol) was added to the solution, the resulting mixture was stirred at -78 °C for 30 min, then left to attain room temperature and stirred for 20h. The reaction was quenched with 10 mL of brine, the aqueous layer was separated and extracted with two 10 mL- portions of CH<sub>2</sub>Cl<sub>2</sub>, the combined organic layer was dried over MgSO<sub>4</sub> and concentrated in *vacuo*. The residue was purified by CC (CH<sub>2</sub>Cl<sub>2</sub>/hexane, 5:1) to afford (**45**); white solid; yield : 0.29 g (63%); mp 170-171 °C; <sup>1</sup>H NMR (500 MHz, DMSO) δ 7.41 (d, *J* = 8.4 Hz, 2H), 7.23 (d, *J* = 8.4 Hz, 2H), 7.13 (d, *J* = 8.9 Hz, 2H), 6.81 (d, *J* = 8.9 Hz, 2H), 5.28 (s, 1H), 4.31 (s, 1H), 3.71 – 3.42 (m, 8H), 1.15 (s, 9H); MS (ESI): *m/z* = 460.19 (M+H)<sup>+</sup>.

### **(1,5-bis(4-chlorophenyl)-3-(2-ethoxyphenyl)-4,5-dihydro-1H-pyrazol-4 -yl) (morpholino)methanone (46) .**

The title compound is obtained using the same procedure applied for the previous compound **45** using 1,5-bis(4-chlorophenyl)-3-(2-ethoxyphenyl)-4,5-dihydro-1H-pyrazole (**36**). The product was obtained as white solid; yield : 0.40 g (76%); mp 180-181 °C; <sup>1</sup>H NMR (500 MHz, CDCl<sub>3</sub>) δ 7.60 (dd, *J* = 7.6, 1.7 Hz, 1H), 7.28 – 7.23 (m, 3H), 7.22 – 7.18 (m, 2H), 7.03 – 6.97 (m, 2H), 6.94 (td, *J* = 7.5, 1.0 Hz, 1H), 6.87 – 6.80 (m, 2H), 6.81 – 6.74 (m, 1H), 5.39 (d, *J* = 6.0 Hz, 1H), 4.64 (d, *J* = 6.0 Hz, 1H), 3.95 – 3.88 (m, 2H), 3.64 – 3.46 (m, 2H), 3.37 – 3.23 (m, 3H), 3.23 – 3.04 (m, 2H), 2.80 – 2.71 (m, 1H), 1.12 (t, *J* = 7.0 Hz, 3H); MS (ESI): *m/z* = 522.05 (M+H)<sup>+</sup>.

## Cell Culture

Cancer cell lines cultured included wild type p53 cell line (HCT-116) and a p53 null cell line (H1299) and were obtained from the American Type Culture Collection (ATCC). Both cell

## Results

---

lines were cultured in a 37°C humidified incubator with 5% CO<sub>2</sub> with the same medium (RPMI-1640 supplemented with 5% fetal bovine serum), and passaged twice weekly. Only cultures exhibiting greater than 95% viability were used in growth inhibition experiments (determined by trypan blue exclusion).

### Growth Inhibition Assay:

Cells were seeded in 96-well tissue culture-treated assay plates at a density of  $1.5 \times 10^4$  cells/cm<sup>2</sup>, then allowed to attach overnight before addition of experimental compounds. Compounds were dissolved in DMSO, then diluted to the final concentration indicated so as to ensure that DMSO concentration is less than 0.2%. After treatment with either a single screening concentration or a titration series of concentrations of compounds, cells were incubated for an additional 72 h. Relative cell growth was determined by addition of Promega CellTiter Glo luciferase-based assay of ATP content. The resultant luminescence was measured, and each data set was analyzed using DMSO (vehicle control) as a baseline value for growth inhibition. GraphPad Prism software was used to develop dose-response curves and IC<sub>50</sub> values for active compounds.

### References

1. Lane, D.P. *Nature* **1992**, 358, 15-16.
2. Linares, L. K.; Scheffner, M. *FEBS Lett.* **2003**, 554, 73-6.
3. Bhatt, P.; d'Avout, C.; Kane, N. S.; Borowiec, J. A.; Saxena, A. *FEBS J.* **2012**, 279, 370-83.
4. Vassilev, L. T.; Vu, B. T.; Graves, B.; Carvajal, D.; Podlaski, F.; Filipovic, Z.; Kong, N.; Kammlott, U.; Lukacs, C.; Klein, C.; Fotouhi, N.; Liu, E. A. *Science* **2004**, 303, 844-848.
5. Kallen, J.; Goepfert, A.; Blechschmidt, A.; Izaac, A.; Geiser, M.; Tavares, G.; Ramage, P.; Furet, P.; Masuya, K.; Lisztwan, J. *J Biol Chem.* **2009**, 284, 8812-21.
6. Ma, B., Pan, Y.; Gunasekaran, K.; Keskin, O.; Venkataraghavan, R. B.; Levine, A. J.; Nussinov, R. *Phys Biol.* **2005**, 2, :S56-66.
7. Chene, P. *Nat. Rev. Cancer* **2003**, 3, 102-109.
8. Galatin, P. S.; Abraham, D. J. *J Med Chem.* **2004**, 47, 4163-5.
9. Millard, M.; Pathania, D.; Grande F; Xu, S; Neamati, N. *Curr Pharm Des.* **2011**, 17, 536-59.
10. Mohammad, R. M.; Wu, J.; Azmi, A.S.; Aboukameel, A.; Sosin, A.; Wu, S.; Yang, D.; Wang, S.; Al-Katib, A. M. *Mol Cancer.* **2009**, 8, 115.
11. Grasberger, B. L.; Lu, T.; Schubert, C.; Parks, D. J.; Carver, T. E.; Koblisch, H. K.; Cummings, M. D.; LaFrance, L. V.; Milkiewicz, K. L.; Calvo, R. R.; Maguire, D.; Lattanze, J.; Franks, C. F.; Zhao, S.; Ramachandren, K.; Bylebyl, G. R.; Zhang, M.; Manthey, C.L.; Petrella, E. C.; Pantoliano, M. W.; Deckman, I. C.; Spurlino, J. C.; Maroney, A. C.; Tomczuk, B. E.; Molloy, C. J.; Bone, R. F. *J Med Chem.* **2005**, 48, 909-12.

## Results

---

12. Kozakov, D.; Hall, D. R.; Chuang, G.-Y.; Cencic, R.; Brenke, R.; Grove, L. E.; Beglov, D.; Pelletier, J.; Whitty, A.; Vajda, S. *Proc. Natl. Acad. Sci. U. S. A.* **2011**, 108, (33), 13528-13533, S13528/1-S13528/26.
13. Huang, Y. R.; Katzenellenbogen, J. A. *Org. Lett.* **2000**, 43, 61-64.
14. Vogel, S. M., Bauer, M. R.; Joerger, A. C.; Wilcken, R.; Brandt, T.; Veprintsev, D. B.; Rutherford, T. J.; Fersht, A. R.; Boeckler, F. M. *Proc. Natl. Acad. Sci. U. S. A.* **2012**, 109, 16906-10.
15. Chimenti, F.; Fioravanti, R.; Bolasco, A.; Chimenti, P.; Secci, D.; Rossi, F.; Yanez, M.; Orallo, F.; Ortuso, F.; Alcaro, S. *J. Med. Chem.* **2009**, 52, (9), 2818-2824.
16. Rao, M. L. N.; Venkatesh, V.; Jadhav, D. N. *J. Organomet. Chem.* **2008**, 693, (15), 2494-2498.
17. Wu, J.; Li, J.; Cai, Y.; Pan, Y.; Ye, F.; Zhang, Y.; Zhao, Y.; Yang, S.; Li, X.; Liang, G. *J. Med. Chem.* **2011**, 54, (23), 8110-8123.
18. Sivakumar, P. M.; Ganesan, S.; Veluchamy, P.; Doble, M. *Chem. Biol. Drug Des.* **2010**, 76, (5), 407-411.
19. Beaupere, D.; Uzan, R.; Doucet, J. P., *C. R. Acad. Sci., Ser. C* **1974**, 278, (3), 187-9.
20. Zhao, P.-L.; Liu, C.-L.; Huang, W.; Wang, Y.-Z.; Yang, G.-F. *J. Agric. Food Chem.* **2007**, 55, (14), 5697-5700.
21. Hajra, S.; Bar, S.; Sinha, D.; Maji, B. *J. Org. Chem.* **2008**, 73, (11), 4320-4322.
22. Liu, X.; Go, M.-L. *Bioorg. Med. Chem.* **2006**, 14, (1), 153-163.
23. Cohen, F. E.; McKerrow, J. H.; Kenyon, G. L.; Li, Z.; Chen, X.; Gong, B.; Li, R. US5739170A, **1998**.
24. Choudary, B. M.; Mahendar, K.; Kantam, M. L.; Ranganath, K. V. S.; Athar, T. *Adv. Synth. Catal.* 2006, 348, (14), 1977-1985.
25. Ma, S.-Y.; Davis, R. A. US5691363A, **1997**.
26. Unterhalt, B.; Koehler, H.; Reinhold, H. J. *Arch. Pharm. (Weinheim, Ger.)* **1978**, 311, (7), 604-8.
27. Dimmock, J. R.; Kirkpatrick, D. L.; Webb, N. G.; Cross, B. M. *J. Pharm. Sci.* **1982**, 71, (9), 1000-7.
28. Erker, T.; Brunhofer, G.; Jaeger, U.; Vanura, K.; Dirsch, V.; Heiss, E. WO2012013725A1, **2012**

## 4 Discussion, Conclusion and Outlook

The main aim of this thesis was to develop PKC $\zeta$  potent and isoform selective inhibitors through targeting the PIF pocket on the kinase catalytic domain as described in chapter 3.1. The development strategy was based on the previously reported PKC $\zeta$  moderate allosteric inhibitors 4-benzimidazolyl-3-phenylbutanoic acids which were proven to target the PIF pocket. As shown in Figure 16, cell and cell free potency optimization was intended through:

- 1) Rigidification of the three flexible bonds connecting the two aryls.
- 2) Replacement of the essential carboxylate function, which can impair cellular permeability, by another HBA function to improve the permeability characteristics.

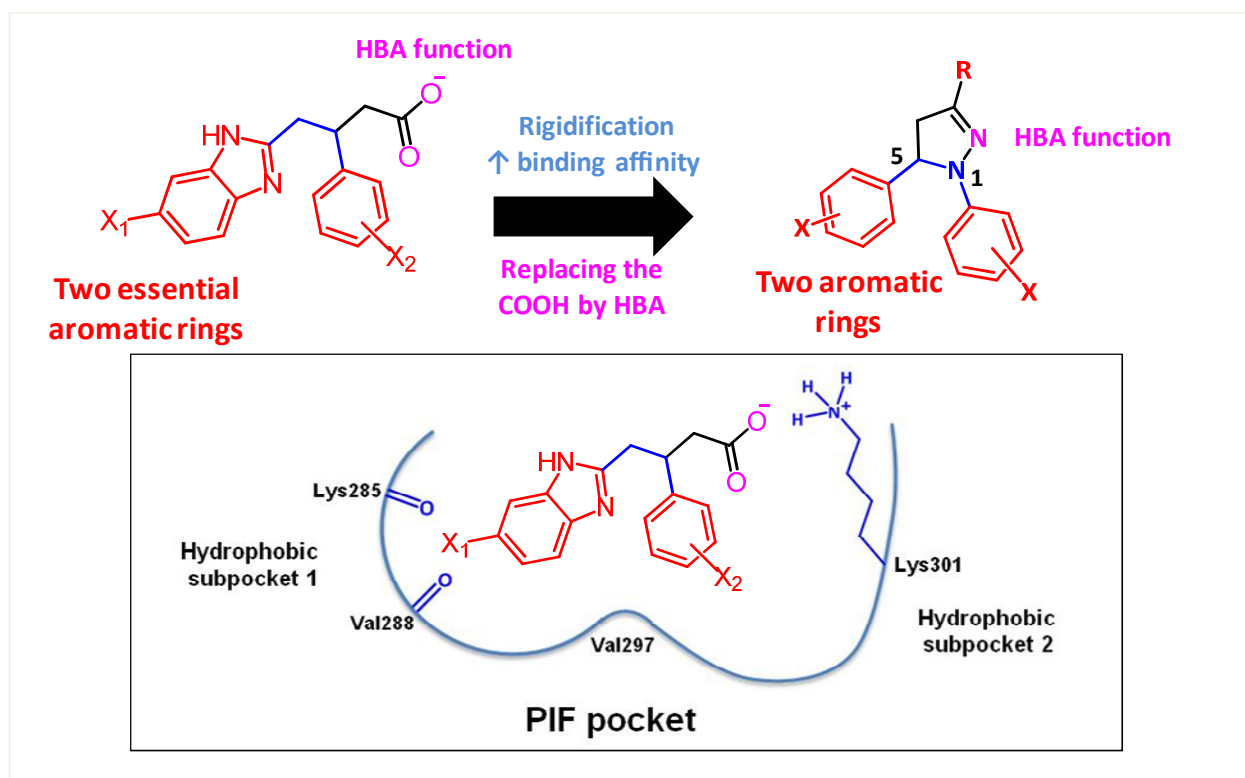


Figure 16: The optimization strategy adapted starting from the previously reported 4-benzimidazolyl-3-phenylbutanoic acids, based on the PIF pocket structure as proposed from the closely related PKC $\zeta$  crystal structure.

The two requirements were found to be satisfied by using the pyrazoline scaffold which supplies the 1- and 5- phenyls to presumably interact with the two mostly hydrophobic PIF subpockets, in a similar way to the two aryls from the previous scaffold, as shown in the lower part of Figure 16. In addition, the imine nitrogen was assumed to replace the carboxylate in its

## Discussion, Conclusion and Outlook

interaction with Lys301. The substituent at position three of the pyrazoline was expected to be solvent exposed, yet, it can be utilized to improve pharmacokinetic characteristics, with a possible interaction with Lys301, as can be seen in figure 16.

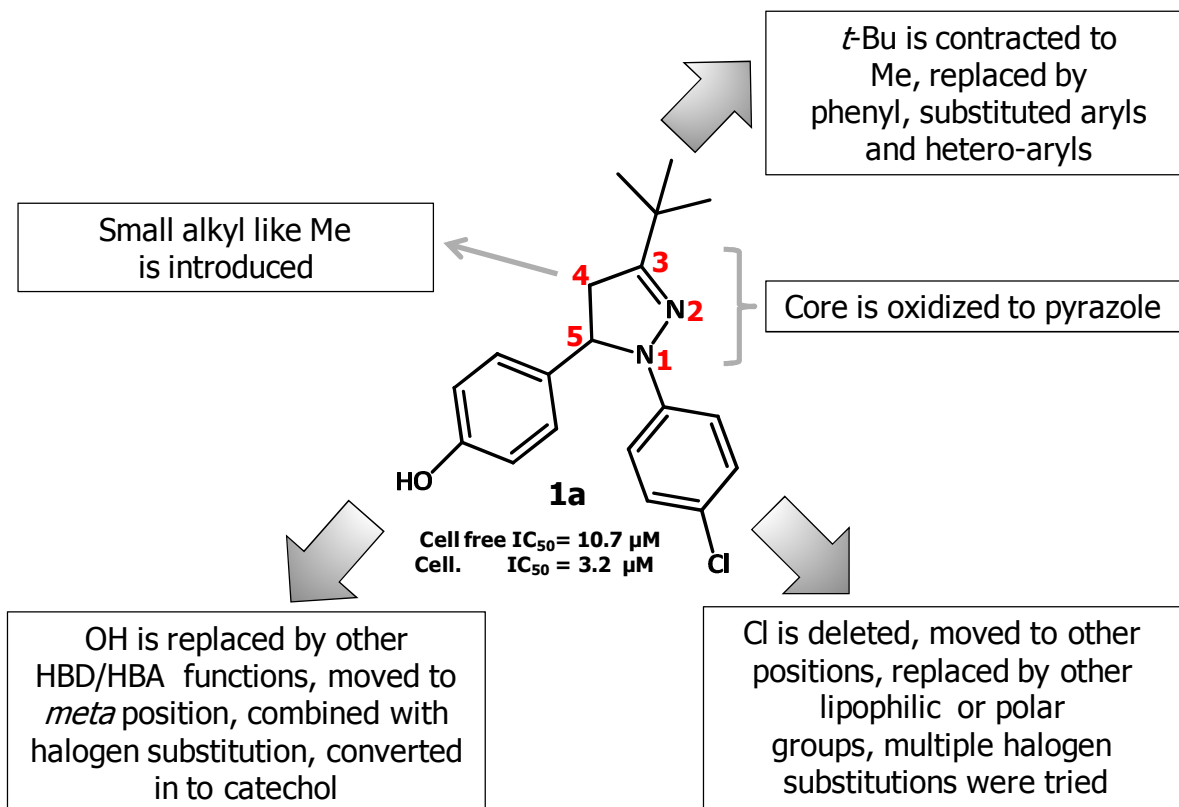


Figure 17: Structure of the hit compound **1a** and different modifications adapted. The pyrazoline scaffold is rich in modifiable sites; at positions 1, 3, 4, and 5, in addition to the possibility of oxidation to the planar pyrazole.

The first pyrazolines synthesized were bearing a halogen substitution at both the 1- and 5-phenyls similar to the previously reported inhibitors, as this was expected to suit the nature of two mostly hydrophobic PIF-subpockets; however, this did not lead to active compounds. It was then hypothesized that substituting the 5-phenyl with a hydroxyl group to interact as a HBD with one of the two backbone carbonyls in subpocket 1 (shown in figure 16) can improve the binding affinity. This successfully led to the hit compound **1a** with a cell free IC<sub>50</sub> of 10.7 μM and 3.2 μM in the reporter gene assay in U937 cells (Figure 17). Several modifications were done to optimize both the cell and cell free potencies of the hit compound **1a** as shown in Figure 17.

The optimization process led to many potent compounds with an IC<sub>50</sub> of less than 0.1 μM in the cell free assay and a submicromolar IC<sub>50</sub> in U937 cells. The phenolic OH at the 5-phenyl

## Discussion, Conclusion and Outlook

was found to be an essential irreplaceable feature in all active compounds in both types of assays.

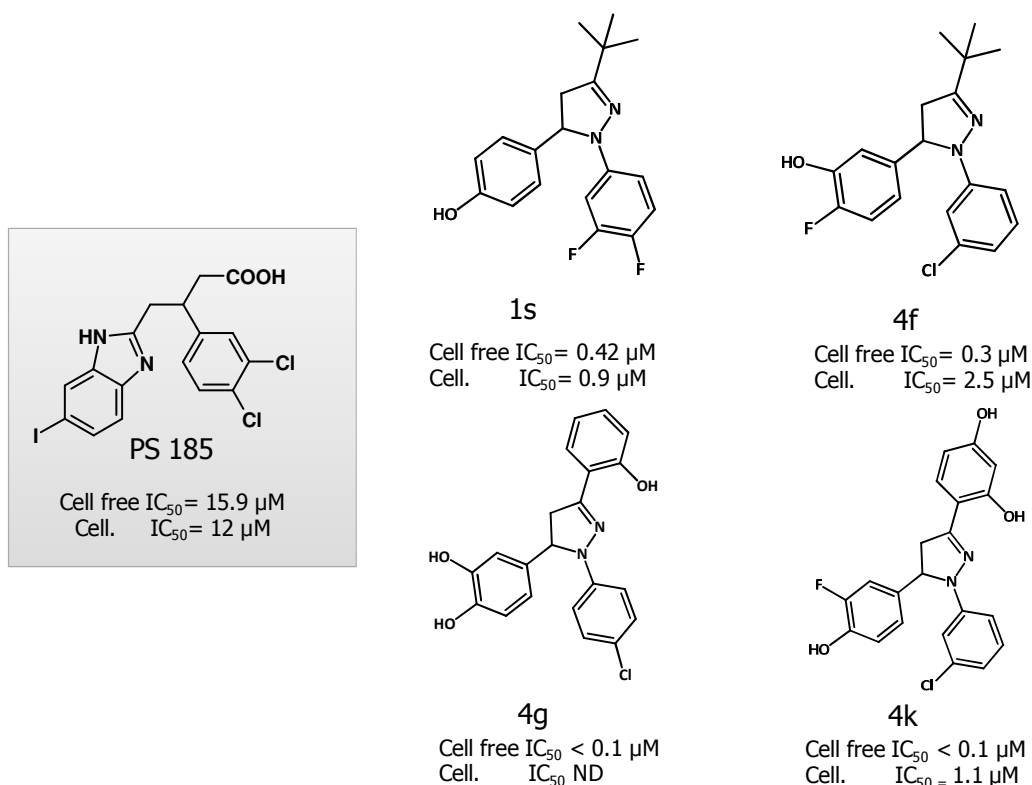


Figure 18: The most active compounds as PKC $\zeta$  inhibitors from the pyrazoline series. PS185 is the most active compound from the previously reported 4-benzimidazolyl-3-phenylbutanoic acids. The IC<sub>50</sub> values for the cell free and U937 cell assays are shown. ND: not determined.

The most active compounds obtained in the new series are shown in Figure 18, where their IC<sub>50</sub> values are displayed in comparison with PS185, the most potent compound from the previously reported butanoic acid inhibitors. As can be observed, one order of magnitude improvement was achieved in the cell assay results compared with the previous inhibitors; however, this fold of improvement was not as high as that observed in the cell free assay, which is most probably due to non-specific protein binding inside the cells. A conclusion which is augmented by the observation that adding serum albumin to the cell assay medium dramatically reduced compounds' potency when compared to serum albumin free conditions, especially with compounds having plain phenyl or heteroaryl at position three of the pyrazoline. To overcome this, we have just started a second phase of development to have compounds with increased polarity and improved physicochemical characteristics in which more drug-like moieties like imidazole, triazole and thiazole are adapted at the highly tolerant 3-position of the pyrazoline

## **Discussion, Conclusion and Outlook**

---

ring. This is also important for testing the compounds using *in vivo* disease models, where solubility and a suitable logP range are limiting factors for successful results.

The improved potency and selectivity for PKC $\zeta$  vs. the whole PKC family and related kinases makes the discovered and optimized compounds good pharmacological tools to further study PKC $\zeta$  as drug target, as well as studying the possible therapeutic applications together with the probable side effects resulting from its inhibition.

The inhibition of PKC $\zeta$  can launch a field of treatment of many important diseases including bronchial asthma, hepatitis, autoimmune diseases and B cell lymphomas; however the exact indication of the developed inhibitors is still under investigation using the suitable disease models. To aid in the attempts of investigation, we currently started validation experiments using real time PCR to analyze the effect of some potent compounds like compound **4f** on cytokines expression. The preliminary data in hand showed that **4f** down regulated the expression of several cytokines and chemokine receptors in U937 cells which have been differentiated into monocytes.

On the other hand, the involvement of PKC $\zeta$  in many important cellular responses in different tissues can limit the medicinal use of the developed inhibitors as a result of the possible side effects. However, if side effects are proven, tissue specific drug delivery may overcome the problem, for instance, using inhalation dosage forms for treatment of bronchial asthma or adapting certain structural modifications for selective tissue uptake.

All the synthesized pyrazolines were obtained as racemates, the poor resolution on the chiral column hindered the study of enantio-selectivity in the inhibitors' interaction with the PIF pocket, which makes the design of enantio-selective synthesis in the next step of development an important requirement to study such effect.

The three dimensional shape of the tri-substituted pyrazoline scaffold suggested that it can also fit into other surface pockets like the Mdm2 pocket, to disrupt its interaction with p53, as was discussed in chapter 3.2. The pyrazoline scaffold seemed to represent an ideal protein-protein interaction inhibitor scaffold, useful to generate ligands for surface protein interaction pockets which normally accommodate two adjacent lipophilic residues like aromatic rings of Phe, Tyr or Trp, or lipophilic side chains of Leu for example. The scaffold might mimic the correct positioning of the respective aromatic rings or lipophilic side chains when they are either protruding from a short  $\alpha$ -helix with the usual 2-3 residues spacers (like p53) or from loops with two amino acid residues as spacer like in the case of the HM peptide (FXXF). The suitability of the tri- and tetra-substituted pyrazoline scaffolds as Mdm2 inhibitor was also suggested by the structure overlay of the designed inhibitors with nutlin-2 from its crystal structure with Mdm2.

## **Discussion, Conclusion and Outlook**

---

Although some of the synthesized compounds were able to show potent and preferential growth inhibition against HCT116 cells with wild-type p53 vs. H1299 cells which lack p53 expression, in a comparable behavior to nulin-3, the promising hits failed to displace a fluorescence-labeled peptide from its complex with Mdm2 on verifying the binding to Mdm2. The lack of activity in the latter assay was attributed to many reasons including solubility problems and compounds' native fluorescence. This finding suggests that further modifications are required to improve polarity and solubility characteristics, and highlights the need to optimize the assay conditions.

# 5 References

1. Krauss, G. Biochemistry of Signal Transduction and Regulation. 4<sup>th</sup> ed.; 2008.
2. Bruce Alberts, A. J., Julian Lewis, Martin Raff, Keith Roberts and Peter Walter. Molecular Biology of the Cell. 4<sup>th</sup> ed.; 2002.
3. Johnson, L. N.; Lewis, R. J. Structural Basis for Control by Phosphorylation. *Chemical Reviews* **2001**, 101, 2209-2242.
4. Johnson, L. N. Protein kinase inhibitors: contributions from structure to clinical compounds. *Q. Rev. Biophys.* **2009**, 42, 1-40.
5. Eswaran, J.; Knapp, S. Insights into protein kinase regulation and inhibition by large scale structural comparison. *Biochim. Biophys. Acta, Proteins Proteomics* **2010**, 1804, 429-432.
6. Pearce, L. R.; Komander, D.; Alessi, D. R. The nuts and bolts of AGC protein kinases. *Nat Rev Mol Cell Biol* **2010**, 11, 9-22.
7. Jura, N.; Zhang, X.; Endres, Nicholas F.; Seeliger, Markus A.; Schindler, T.; Kuriyan, J. Catalytic Control in the EGF Receptor and Its Connection to General Kinase Regulatory Mechanisms. *Molecular Cell* **2011**, 42, 9-22.
8. Steinberg, S. F. Structural basis of protein kinase C isoform function. *Physiol. Rev.* **2008**, 88, 1341-1378.
9. Diaz-Meco, M. T.; Moscat, J. The atypical PKCs in inflammation: NF-kappaB and beyond. *Immunol Rev* **2012**, 246, 154-67.
10. Hirai, T.; Chida, K. Protein Kinase C $\zeta$ ; (PKC $\zeta$ ): Activation Mechanisms and Cellular Functions. *The Journal of Biochemistry* **2003**, 133, 1-7.
11. Newton, A. C. Regulation of the ABC kinases by phosphorylation: protein kinase C as a paradigm. *Biochem. J.* **2003**, 370, 361-371.
12. Le Good, J. A.; Ziegler, W. H.; Parekh, D. B.; Alessi, D. R.; Cohen, P.; Parker, P. J. Protein Kinase C Isoforms Controlled by Phosphoinositide 3-Kinase Through the Protein Kinase PDK1. *Science* **1998**, 281, 2042-2045.
13. Biondi, R. M.; Cheung, P. C.; Casamayor, A.; Deak, M.; Currie, R. A.; Alessi, D. R. Identification of a pocket in the PDK1 kinase domain that interacts with PIF and the C-terminal residues of PKA. *Embo J* **2000**, 19, 979-88.
14. Balendran, A.; Biondi, R. M.; Cheung, P. C.; Casamayor, A.; Deak, M.; Alessi, D. R. A 3-phosphoinositide-dependent protein kinase-1 (PDK1) docking site is required for the

## References

---

- phosphorylation of protein kinase C $\zeta$  (PKC $\zeta$ ) and PKC-related kinase 2 by PDK1. *J Biol Chem* **2000**, 275, 20806-13.
15. Newton, A. C. Protein kinase C: poised to signal. *Am J Physiol Endocrinol Metab* **2010**, 298, E395-402.
16. Díaz-Meco, M. T.; Municio, M. M.; Frutos, S.; Sanchez, P.; Lozano, J.; Sanz, L.; Moscat, J. The Product of par-4, a Gene Induced during Apoptosis, Interacts Selectively with the Atypical Isoforms of Protein Kinase C. *Cell* **1996**, 86, 777-786.
17. Moscat, J.; Diaz-Meco, M. T. The atypical protein kinase Cs. Functional specificity mediated by specific protein adapters. *EMBO Rep* **2000**, 1, 399-403.
18. Ohno, S. Intercellular junctions and cellular polarity: the PAR-aPKC complex, a conserved core cassette playing fundamental roles in cell polarity. *Current Opinion in Cell Biology* **2001**, 13, 641-648.
19. Sanchez, P.; De Carcer, G.; Sandoval, I. V.; Moscat, J.; Diaz-Meco, M. a. T. Localization of Atypical Protein Kinase C Isoforms into Lysosome-Targeted Endosomes through Interaction with p62. *Molecular and Cellular Biology* **1998**, 18, 3069-3080.
20. Moscat, J.; Diaz-Meco, M. T. p62 at the Crossroads of Autophagy, Apoptosis, and Cancer. *Cell* **2009**, 137, 1001-1004.
21. Karin, M.; Greten, F. R. NF- $\kappa$ B: linking inflammation and immunity to cancer development and progression. *Nat. Rev. Immunol.* **2005**, 5, 749-759.
22. Gilmore, T. D. Introduction to NF-kappaB: players, pathways, perspectives. *Oncogene* **2006**, 25, 6680-4.
23. Leitges, M.; Sanz, L.; Martin, P.; Duran, A.; Braun, U.; Garcia, J. F.; Camacho, F.; Diaz-Meco, M. T.; Rennert, P. D.; Moscat, J. Targeted disruption of the zetaPKC gene results in the impairment of the NF-kappaB pathway. *Mol Cell* **2001**, 8, 771-80.
24. Moscat, J.; Diaz-Meco, M. T. Fine tuning NF- $\kappa$ B: new openings for PKC $\zeta$ . *Nat. Immunol.* **2011**, 12, 12-14.
25. Levy, D.; Kuo, A. J.; Chang, Y.; Schaefer, U.; Kitson, C.; Cheung, P.; Espejo, A.; Zee, B. M.; Liu, C. L.; Tangsombatvisit, S.; Tennen, R. I.; Kuo, A. Y.; Tanjing, S.; Cheung, R.; Chua, K. F.; Utz, P. J.; Shi, X.; Prinjha, R. K.; Lee, K.; Garcia, B. A.; Bedford, M. T.; Tarakhovsky, A.; Cheng, X.; Gozani, O. Lysine methylation of the NF-kappaB subunit RelA by SETD6 couples activity of the histone methyltransferase GLP at chromatin to tonic repression of NF-kappaB signaling. *Nat Immunol* **2011**, 12, 29-36.
26. Martin, P.; Duran, A.; Minguet, S.; Gaspar, M. L.; Diaz-Meco, M. T.; Rennert, P.; Leitges, M.; Moscat, J. Role of zeta PKC in B-cell signaling and function. *Embo J* **2002**, 21, 4049-57.

## References

---

27. Martin, P.; Villares, R.; Rodriguez-Mascarenhas, S.; Zaballos, A.; Leitges, M.; Kovac, J.; Sizing, I.; Rennert, P.; Marquez, G.; Martinez, A. C.; Diaz-Meco, M. T.; Moscat, J. Control of T helper 2 cell function and allergic airway inflammation by PKCzeta. *Proc Natl Acad Sci U S A* **2005**, *102*, 9866-71.
28. Duran, A.; Rodriguez, A.; Martin, P.; Serrano, M.; Flores, J. M.; Leitges, M.; Diaz-Meco, M. T.; Moscat, J. Crosstalk between PKCzeta and the IL4/Stat6 pathway during T-cell-mediated hepatitis. *Embo J* **2004**, *23*, 4595-605.
29. Umetsu, D. T.; DeKruyff, R. H. The regulation of allergy and asthma. *Immunol. Rev.* **2006**, *212*, 238-255.
30. Umetsu, D. T.; McIntire, J. J.; Akbari, O.; Macaubas, C.; DeKruyff, R. H. Asthma: an epidemic of dysregulated immunity. *Nat. Immunol.* **2002**, *3*, 715-720.
31. Martin, P.; Moscat, J. Th1/Th2 differentiation and B cell function by the atypical PKCs and their regulators. *Frontiers in Immunology* **2012**, *3*.
32. Do, J.-S.; Park, K.-S.; Seo, H.-J.; Kim, J.-H.; Hwang, J.-K.; Song, E.-J.; Nam, S.-Y. Therapeutic target validation of protein kinase C (PKC)- $\zeta$  for asthma using a mouse model. *Int. J. Mol. Med.* **2009**, *23*, 561-566.
33. Morin, C.; Fortin, S.; Rousseau, E. Bronchial inflammation induced PKC $\zeta$  over-expression: involvement in mechanical properties of airway smooth muscle. *Can. J. Physiol. Pharmacol.* **2012**, *90*, 261-269.
34. Langlois, A.; Chouinard, F.; Flamand, N.; Ferland, C.; Rola-Pleszczynski, M.; Laviolette, M. Crucial implication of protein kinase C (PKC)- $\delta$ , PKC $\zeta$ , ERK-1/2, and p38 MAPK in migration of human asthmatic eosinophils. *J. Leukocyte Biol.* **2009**, *85*, 656-663.
35. Yao, H.; Hwang, J.-w.; Moscat, J.; Diaz-Meco, M. T.; Leitges, M.; Kishore, N.; Li, X.; Rahman, I. Protein Kinase Czeta Mediates Cigarette Smoke/Aldehyde- and Lipopolysaccharide-induced Lung Inflammation and Histone Modifications. *Journal of Biological Chemistry* **285**, 5405-5416.
36. Moscat, J.; Rennert, P.; Diaz-Meco, M. T. PKC $\zeta$  at the crossroad of NF- $\kappa$ B and Jak1/Stat6 signaling pathways. *Cell Death Differ.* **2006**, *13*, 702-711.
37. Jaruga, B.; Hong, F.; Sun, R.; Radaeva, S.; Gao, B. Crucial role of IL-4/STAT6 in T cell-mediated hepatitis: up-regulating eotaxins and IL-5 and recruiting leukocytes. *J Immunol* **2003**, *171*, 3233-44.
38. Liu, Y.; Wang, B.; Wang, J.; Wan, W.; Sun, R.; Zhao, Y.; Zhang, N. Down-regulation of PKC $\zeta$  expression inhibits chemotaxis signal transduction in human lung cancer cells. *Lung Cancer* **2009**, *63*, 210-218.

## References

---

39. Sun, R.; Gao, P.; Chen, L.; Ma, D.; Wang, J.; Oppenheim, J. J.; Zhang, N. Protein Kinase Czeta Is Required for Epidermal Growth Factor-Induced Chemotaxis of Human Breast Cancer Cells. *Cancer Research* **2005**, *65*, 1433-1441.
40. Guo, H.; Gu, F.; Li, W.; Zhang, B.; Niu, R.; Fu, L.; Zhang, N.; Ma, Y. Reduction of protein kinase C  $\zeta$  inhibits migration and invasion of human glioblastoma cells. *J. Neurochem.* **2009**, *109*, 203-213.
41. Cohen, E. E. W.; Lingen, M. W.; Zhu, B.; Zhu, H.; Straza, M. W.; Pierce, C.; Martin, L. E.; Rosner, M. R. Protein Kinase Czeta Mediates Epidermal Growth Factor-Induced Growth of Head and Neck Tumor Cells by Regulating Mitogen-Activated Protein Kinase. *Cancer Research* **2006**, *66*, 6296-6303.
42. Datta, K.; Li, J.; Bhattacharya, R.; Gasparian, L.; Wang, E.; Mukhopadhyay, D. Protein Kinase Czeta Transactivates Hypoxia-Inducible Factor  $\alpha$  by Promoting Its Association with p300 in Renal Cancer. *Cancer Research* **2004**, *64*, 456-462.
43. Rimessi, A.; Zecchini, E.; Siviero, R.; Giorgi, C.; Leo, S.; Rizzuto, R.; Pinton, P. The selective inhibition of nuclear PKC $\zeta$  restores the effectiveness of chemotherapeutic agents in chemoresistant cells. *Cell Cycle* **2012**, *11*, 1040-1048.
44. Filomenko, R.; Poirson-Bichat, F.; Billerey, C.; Belon, J.-P.; Garrido, C.; Solary, E.; Bettaieb, A. Atypical Protein Kinase Czeta as a Target for Chemosensitization of Tumor Cells. *Cancer Research* **2002**, *62*, 1815-1821.
45. Leseux, L.; Laurent, G.; Laurent, C.; Rigo, M.; Blanc, A.; Olive, D.; Bezombes, C. PKC $\zeta$ -mTOR pathway: a new target for rituximab therapy in follicular lymphoma. *Blood* **2008**, *111*, 285-291.
46. Cecconi, D.; Zamo, A.; Bianchi, E.; Parisi, A.; Barbi, S.; Milli, A.; Rinalducci, S.; Rosenwald, A.; Hartmann, E.; Zolla, L.; Chilosì, M. Signal transduction pathways of mantle cell lymphoma: a phosphoproteome-based study. *Proteomics* **2008**, *8*, 4495-506.
47. Bogoyevitch, M. A.; Fairlie, D. P. A new paradigm for protein kinase inhibition: blocking phosphorylation without directly targeting ATP binding. *Drug Discovery Today* **2007**, *12*, 622-633.
48. Fabbro, D.; Cowan-Jacob, S. W.; Möbitz, H.; Martiny-Baron, G. *Targeting Cancer with Small-Molecular-Weight Kinase Inhibitors*. Springer: Heidelberg, 2012; Vol. 795, p 1-34.
49. Grunwald, V.; Heinzer, H.; Fiedler, W. Managing side effects of angiogenesis inhibitors in renal cell carcinoma. *Onkologie* **2007**, *30*, 519-24.
50. Wolter, P.; Stefan, C.; Decallonne, B.; Dumez, H.; Bex, M.; Carmeliet, P.; Schoffski, P. The clinical implications of sunitinib-induced hypothyroidism: a prospective evaluation. *Br J Cancer* **2008**, *99*, 448-54.

## References

---

51. Liu, Y.; Gray, N. S. Rational design of inhibitors that bind to inactive kinase conformations. *Nat Chem Biol* **2006**, *2*, 358-64.
52. Fischer, P. M. The design of drug candidate molecules as selective inhibitors of therapeutically relevant protein kinases. *Curr. Med. Chem.* **2004**, *11*, 1563-1583.
53. Engel, M. The PIF pocket of AGC kinases: a target site for allosteric modulators and protein-protein interaction inhibitors. In *Protein-Protein Interactions in Drug Discovery*, Doemling, A., Ed. Wiley-VCH: Weinheim, 2012; pp 187-223.
54. Huang, X.; Shipps, G. W.; Cheng, C. C.; Spacciapoli, P.; Zhang, X.; McCoy, M. A.; Wyss, D. F.; Yang, X.; Achab, A.; Soucy, K.; Montavon, D. K.; Murphy, D. M.; Whitehurst, C. E. Discovery and Hit-to-Lead Optimization of Non-ATP Competitive MK2 (MAPKAPK2) Inhibitors. *ACS Med. Chem. Lett.* **2011**, *2*, 632-637.
55. Gould, C. M.; Antal, C. E.; Reyes, G.; Kunkel, M. T.; Adams, R. A.; Ziyar, A.; Riveros, T.; Newton, A. C. Active site inhibitors protect protein kinase C from dephosphorylation and stabilize its mature form. *J Biol Chem* **2011**, *286*, 28922-30.
56. Okuzumi, T.; Fiedler, D.; Zhang, C.; Gray, D. C.; Aizenstein, B.; Hoffman, R.; Shokat, K. M. Inhibitor hijacking of Akt activation. *Nat Chem Biol* **2009**, *5*, 484-93.
57. Knighton, D. R.; Zheng, J. H.; Ten Eyck, L. F.; Ashford, V. A.; Xuong, N. H.; Taylor, S. S.; Sowadski, J. M. Crystal structure of the catalytic subunit of cyclic adenosine monophosphate-dependent protein kinase. *Science* **1991**, *253*, 407-14.
58. Engel, M.; Hindie, V.; Lopez-Garcia, L. A.; Stroba, A.; Schaeffer, F.; Adrian, I.; Imig, J.; Idrissova, L.; Nastainczyk, W.; Zeuzem, S.; Alzari, P. M.; Hartmann, R. W.; Piiper, A.; Biondi, R. M. Allosteric activation of the protein kinase PDK1 with low molecular weight compounds. *Embo J* **2006**, *25*, 5469-80.
59. Biondi, R. M.; Kieloch, A.; Currie, R. A.; Deak, M.; Alessi, D. R. The PIF-binding pocket in PDK1 is essential for activation of S6K and SGK, but not PKB. *Embo J* **2001**, *20*, 4380-90.
60. Biondi, R. M.; Komander, D.; Thomas, C. C.; Lizcano, J. M.; Deak, M.; Alessi, D. R.; van Aalten, D. M. High resolution crystal structure of the human PDK1 catalytic domain defines the regulatory phosphopeptide docking site. *Embo J* **2002**, *21*, 4219-28.
61. Frodin, M.; Antal, T. L.; Dummler, B. A.; Jensen, C. J.; Deak, M.; Gammeltoft, S.; Biondi, R. M. A phosphoserine/threonine-binding pocket in AGC kinases and PDK1 mediates activation by hydrophobic motif phosphorylation. *Embo J* **2002**, *21*, 5396-407.
62. Grodsky, N.; Li, Y.; Bouzida, D.; Love, R.; Jensen, J.; Nodes, B.; Nonomiya, J.; Grant, S. Structure of the catalytic domain of human protein kinase C beta II complexed with a bisindolylmaleimide inhibitor. *Biochemistry* **2006**, *45*, 13970-13981.
63. Hindie, V.; Stroba, A.; Zhang, H.; Lopez-Garcia, L. A.; Idrissova, L.; Zeuzem, S.; Hirschberg, D.; Schaeffer, F.; Jorgensen, T. J.; Engel, M.; Alzari, P. M.; Biondi, R. M. Structure

## References

---

and allosteric effects of low-molecular-weight activators on the protein kinase PDK1. *Nat Chem Biol* **2009**, *5*, 758-64.

64. Nagashima, K.; Shumway, S. D.; Sathyanarayanan, S.; Chen, A. H.; Dolinski, B.; Xu, Y.; Keilhack, H.; Nguyen, T.; Wiznerowicz, M.; Li, L.; Lutterbach, B. A.; Chi, A.; Paweletz, C.; Allison, T.; Yan, Y.; Munshi, S. K.; Klippel, A.; Kraus, M.; Bobkova, E. V.; Deshmukh, S.; Xu, Z.; Mueller, U.; Szewczak, A. A.; Pan, B. S.; Richon, V.; Pollock, R.; Blume-Jensen, P.; Northrup, A.; Andersen, J. N. Genetic and pharmacological inhibition of PDK1 in cancer cells: characterization of a selective allosteric kinase inhibitor. *J Biol Chem* **2011**, *286*, 6433-48.

65. Yang, J.; Cron, P.; Thompson, V.; Good, V. M.; Hess, D.; Hemmings, B. A.; Barford, D. Molecular mechanism for the regulation of protein kinase B/Akt by hydrophobic motif phosphorylation. *Mol Cell* **2002**, *9*, 1227-40.

66. Huang, X.; Begley, M.; Morgenstern, K. A.; Gu, Y.; Rose, P.; Zhao, H.; Zhu, X. Crystal structure of an inactive Akt2 kinase domain. *Structure* **2003**, *11*, 21-30.

67. Smith, K. J.; Carter, P. S.; Bridges, A.; Horrocks, P.; Lewis, C.; Pettman, G.; Clarke, A.; Brown, M.; Hughes, J.; Wilkinson, M.; Bax, B.; Reith, A. The structure of MSK1 reveals a novel autoinhibitory conformation for a dual kinase protein. *Structure* **2004**, *12*, 1067-77.

68. Malakhova, M.; Kurinov, I.; Liu, K.; Zheng, D.; D'Angelo, I.; Shim, J. H.; Steinman, V.; Bode, A. M.; Dong, Z. Structural diversity of the active N-terminal kinase domain of p90 ribosomal S6 kinase 2. *PLoS One* **2009**, *4*, e8044.

69. Stroba, A.; Schaeffer, F.; Hindie, V.; Lopez-Garcia, L. A.; Adrian, I.; Fröhner, W.; Hartmann, R. W.; Biondi, R. M.; Engel, M. 3,5-diphenylpent-2-enoic acids as allosteric activators of the protein kinase PDK1: Structure-activity relationships and thermodynamic characterisation of binding as paradigms for PIF-binding pocket-targeting compounds. *J Med Chem* **2009**, *52*, 4683-4693.

70. Wilhelm, A.; Lopez-Garcia, L. A.; Busschots, K.; Froehner, W.; Maurer, F.; Boettcher, S.; Zhang, H.; Schulze, J. r. O.; Biondi, R. M.; Engel, M. 2-(3-Oxo-1,3-diphenylpropyl)malonic Acids as Potent Allosteric Ligands of the PIF Pocket of Phosphoinositide-Dependent Kinase-1: Development and Prodrug Concept. *Journal of Medicinal Chemistry* **2012**, *55*, 9817-9830.

71. Lopez-Garcia, L. A.; Schulze, J. O.; Fröhner, W.; Zhang, H.; Süß, E.; Weber, N.; Navratil, J.; Amon, S.; Hindie, V.; Zeuzem, S.; Jørgensen, T. J. D.; Alzari, P. M.; Neimanis, S.; Engel, M.; Biondi, R. M. Allosteric regulation of protein kinase PKCzeta by the N-terminal C1 domain and small compounds to the PIF-pocket. *Chem Biol* **2011**, *18*, 1463-1473.

72. Fröhner, W.; Lopez-Garcia, L. A.; Neimanis, S.; Weber, N.; Navratil, J.; Maurer, F.; Stroba, A.; Zhang, H.; Biondi, R. M.; Engel, M. 4-benzimidazolyl-3-phenylbutanoic acids as novel PIF-pocket-targeting allosteric inhibitors of protein kinase PKCzeta. *J Med Chem* **2011**, *54*, 6714-6723.

## References

---

73. Wei, L.; Gao, X.; Warne, R.; Hao, X.; Bussiere, D.; Gu, X. J.; Uno, T.; Liu, Y. Design and synthesis of benzoazepin-2-one analogs as allosteric binders targeting the PIF pocket of PDK1. *Bioorg Med Chem Lett* **2010**, *20*, 3897-902.
74. Knight, Z. A.; Shokat, K. M. Features of selective kinase inhibitors. *Chem Biol* **2005**, *12*, 621-37.
75. Yuan, L.; Seo, J. S.; Kang, N. S.; Keinan, S.; Steele, S. E.; Michelotti, G. A.; Wetsel, W. C.; Beratan, D. N.; Gong, Y. D.; Lee, T. H.; Hong, J. Identification of 3-hydroxy-2-(3-hydroxyphenyl)-4H-1-benzopyran-4-ones as isoform-selective PKC-zeta inhibitors and potential therapeutics for psychostimulant abuse. *Mol Biosyst* **2009**, *5*, 927-30.
76. Wu, J.; Zhang, B.; Wu, M.; Li, H.; Niu, R.; Ying, G.; Zhang, N. Screening of a PKC zeta-specific kinase inhibitor PKCzI257.3 which inhibits EGF-induced breast cancer cell chemotaxis. *Invest New Drugs* **2009**, *28*, 268-75.
77. Trujillo, J. I.; Kiefer, J. R.; Huang, W.; Thorarensen, A.; Xing, L.; Caspers, N. L.; Day, J. E.; Mathis, K. J.; Kretzmer, K. K.; Reitz, B. A.; Weinberg, R. A.; Stegeman, R. A.; Wrightstone, A.; Christine, L.; Compton, R.; Li, X. 2-(6-Phenyl-1H-indazol-3-yl)-1H-benzo [d] imidazoles: Design and synthesis of a potent and isoform selective PKC-zeta inhibitor. *Bioorg Med Chem Lett* **2009**, *19*, 908-911.
78. Kjaer, S.; Linch, M.; Purkiss, A.; Kostecky, B.; Knowles, P. P.; Rosse, C.; Riou, P.; Soudy, C.; Kaye, S.; Patel, B.; Soriano, E.; MurrayRust, J.; Barton, C.; Dillon, C.; Roffey, J.; Parker, P. J.; McDonald, N. Q. Adenosine-binding motif mimicry and cellular effects of a thieno[2,3-d]pyrimidine-based chemical inhibitor of atypical protein kinase C isoenzymes. *Biochem. J.* **2013**, *451*, 329-342.
79. Titchenell, P. M.; Hollis Showalter, H. D.; Pons, J.-F. o.; Barber, A. J.; Jin, Y.; Antonetti, D. A. Synthesis and structure-activity relationships of 2-amino-3-carboxy-4-phenylthiophenes as novel atypical protein kinase C inhibitors. *Bioorganic & Medicinal Chemistry Letters* **2013**, *23*, 3034-3038.
80. Titchenell, P. M.; Lin, C.-M.; Keil, J. M.; Sundstrom, J. M.; Smith, C. D.; Antonetti, D. A. Novel atypical PKC inhibitors prevent vascular endothelial growth factor-induced blood-retinal barrier dysfunction. *Biochem. J.* **2012**, *446*, 455-467.
81. Teodoro, J. G.; Evans, S. K.; Green, M. R. Inhibition of tumor angiogenesis by p53: a new role for the guardian of the genome. *J Mol Med (Berl)* **2007**, *85*, 1175-86.
82. Vousden, K. H.; Lu, X. Live or let die: the cell's response to p53. *Nat Rev Cancer* **2002**, *2*, 594-604.
83. Fridman, J. S.; Lowe, S. W. Control of apoptosis by p53. *Oncogene* **2003**, *22*, 9030-40.
84. Feki, A.; Irminger-Finger, I. Mutational spectrum of p53 mutations in primary breast and ovarian tumors. *Crit Rev Oncol Hematol* **2004**, *52*, 103-16.

## References

---

85. Freedman, D. A.; Wu, L.; Levine, A. J. Functions of the MDM2 oncoprotein. *Cell Mol Life Sci* **1999**, *55*, 96-107.
86. Juven-Gershon, T.; Oren, M. Mdm2: the ups and downs. *Mol Med* **1999**, *5*, 71-83.
87. Rayburn, E.; Zhang, R.; He, J.; Wang, H. MDM2 and human malignancies: expression, clinical pathology, prognostic markers, and implications for chemotherapy. *Curr Cancer Drug Targets* **2005**, *5*, 27-41.
88. Momand, J.; Jung, D.; Wilczynski, S.; Niland, J. The MDM2 gene amplification database. *Nucleic Acids Res* **1998**, *26*, 3453-9.
89. Kussie, P. H.; Gorina, S.; Marechal, V.; Elenbaas, B.; Moreau, J.; Levine, A. J.; Pavletich, N. P. Structure of the MDM2 oncoprotein bound to the p53 tumor suppressor transactivation domain. *Science* **1996**, *274*, 948-53.
90. Wang, S.; Zhao, Y.; Bernard, D.; Aguilar, A.; Kumar, S. Targeting the MDM2-p53 protein-protein interaction for new cancer therapeutics. In *Top. Med. Chem.*, Springer: 2012; Vol. 8, pp 57-80.
91. Patrick, G. *An introduction to medicinal Chemistry*. 4<sup>th</sup> ed.; Oxford University Press: 2009.
92. Vassilev, L. T.; Vu, B. T.; Graves, B.; Carvajal, D.; Podlaski, F.; Filipovic, Z.; Kong, N.; Kammlott, U.; Lukacs, C.; Klein, C.; Fotouhi, N.; Liu, E. A. In Vivo Activation of the p53 Pathway by Small-Molecule Antagonists of MDM2. *Science (Washington, DC, U. S.)* **2004**, *303*, 844-848.
93. Shin, J.-S.; Ha, J.-H.; He, F.; Muto, Y.; Ryu, K.-S.; Yoon, H. S.; Kang, S.; Park, S. G.; Park, B. C.; Choi, S.-U.; Chi, S.-W. Structural insights into the dual-targeting mechanism of Nutlin-3. *Biochemical and Biophysical Research Communications* **2012**, *420*, 48-53.
94. Grasberger, B. L.; Lu, T.; Schubert, C.; Parks, D. J.; Carver, T. E.; Koblisch, H. K.; Cummings, M. D.; LaFrance, L. V.; Milkiewicz, K. L.; Calvo, R. R.; Maguire, D.; Lattanze, J.; Franks, C. F.; Zhao, S.; Ramachandren, K.; Bylebyl, G. R.; Zhang, M.; Manthey, C. L.; Petrella, E. C.; Pantoliano, M. W.; Deckman, I. C.; Spurlino, J. C.; Maroney, A. C.; Tomczuk, B. E.; Molloy, C. J.; Bone, R. F. Discovery and Cocrystal Structure of Benzodiazepinedione HDM2 Antagonists That Activate p53 in Cells. *J. Med. Chem.* **2005**, *48*, 909-912.
95. Ding, K.; Lu, Y.; Nikolovska-Coleska, Z.; Qiu, S.; Ding, Y.; Gao, W.; Stuckey, J.; Krajewski, K.; Roller, P. P.; Tomita, Y.; Parrish, D. A.; Deschamps, J. R.; Wang, S. Structure-Based Design of Potent Non-Peptide MDM2 Inhibitors. *J. Am. Chem. Soc.* **2005**, *127*, 10130-10131.
96. Ding, K.; Lu, Y.; Nikolovska-Coleska, Z.; Wang, G.; Qiu, S.; Shangary, S.; Gao, W.; Qin, D.; Stuckey, J.; Krajewski, K.; Roller, P. P.; Wang, S. Structure-Based Design of Spirooxindoles as Potent, Specific Small-Molecule Inhibitors of the MDM2-p53 Interaction. *J. Med. Chem.* **2006**, *49*, 3432-3435.

## References

---

97. Yu, S.; Qin, D.; Shangary, S.; Chen, J.; Wang, G.; Ding, K.; McEachern, D.; Qiu, S.; Nikolovska-Coleska, Z.; Miller, R.; Kang, S.; Yang, D.; Wang, S. Potent and orally active small-molecule inhibitors of the MDM2-p53 interaction. *J Med Chem* **2009**, *52*, 7970-3.